frontiers | Research Topics

Dietary patterns and oxidative stress: implications for obesity, T2D, and cancer management

Edited by
Qingyu Wang, Dongxian Guan and Yixuan Li

Published in
Frontiers in Nutrition

ISSN 1664-8714
ISBN 978-2-8325-7421-8
DOI 10.3389/978-2-8325-7421-8

Generative AI statement
Any alternative text (Alt text) provided alongside figures in the articles in this ebook has been generated by Frontiers with the support of artificial intelligence and reasonable efforts have been made to ensure accuracy, including review by the authors wherever possible. If you identify any issues, please contact us.

About Frontiers

Frontiers is more than just an open access publisher of scholarly articles: it is a pioneering approach to the world of academia, radically improving the way scholarly research is managed. The grand vision of Frontiers is a world where all people have an equal opportunity to seek, share and generate knowledge. Frontiers provides immediate and permanent online open access to all its publications, but this alone is not enough to realize our grand goals.

Frontiers journal series

The Frontiers journal series is a multi-tier and interdisciplinary set of open-access, online journals, promising a paradigm shift from the current review, selection and dissemination processes in academic publishing. All Frontiers journals are driven by researchers for researchers; therefore, they constitute a service to the scholarly community. At the same time, the *Frontiers journal series* operates on a revolutionary invention, the tiered publishing system, initially addressing specific communities of scholars, and gradually climbing up to broader public understanding, thus serving the interests of the lay society, too.

Dedication to quality

Each Frontiers article is a landmark of the highest quality, thanks to genuinely collaborative interactions between authors and review editors, who include some of the world's best academicians. Research must be certified by peers before entering a stream of knowledge that may eventually reach the public - and shape society; therefore, Frontiers only applies the most rigorous and unbiased reviews. Frontiers revolutionizes research publishing by freely delivering the most outstanding research, evaluated with no bias from both the academic and social point of view. By applying the most advanced information technologies, Frontiers is catapulting scholarly publishing into a new generation.

What are Frontiers Research Topics?

Frontiers Research Topics are very popular trademarks of the *Frontiers journals series*: they are collections of at least ten articles, all centered on a particular subject. With their unique mix of varied contributions from Original Research to Review Articles, Frontiers Research Topics unify the most influential researchers, the latest key findings and historical advances in a hot research area.

Find out more on how to host your own Frontiers Research Topic or contribute to one as an author by contacting the Frontiers editorial office: frontiersin.org/about/contact

Dietary patterns and oxidative stress: implications for obesity, T2D, and cancer management

Topic editors

Qingyu Wang — Capital Medical University, China

Dongxian Guan — Boston Children's Hospital, Harvard Medical School, United States

Yixuan Li — China Agricultural University, China

Citation

Wang, Q., Guan, D., Li, Y., eds. (2026). *Dietary patterns and oxidative stress: implications for obesity, T2D, and cancer management*. Lausanne: Frontiers Media SA. doi: 10.3389/978-2-8325-7421-8

Table of contents

05 Editorial: Dietary patterns and oxidative stress: implications for obesity, T2D, and cancer management
Qingyu Wang, Yixuan Li and Dongxian Guan

07 Diverse associations between pancreatic intra-, inter-lobular fat and the development of type 2 diabetes in overweight or obese patients
Lihui Wang, Yinghao Li, Renfeng Li, Jinwen Luan, Kaiming Cao, Tiancheng Liu, Haiyang Hu, Shanshan Chen, Le Bu, Longhua Liu, Hongzhi Wang and Qing Lu

20 Heat-killed *Bifidobacterium longum* BBMN68 and inulin protect against high-fat diet-induced obesity by modulating gut microbiota
Siyuan Sun, Qi Zhang, Dongdong Li, Hongliang Li, Hairan Ma, Xiuying Wu, Yixuan Li, Pengjie Wang, Rong Liu, Haihong Feng, Yongxiang Zhang, Yue Sang, Bing Fang and Ran Wang

32 Effect of synbiotic supplementation on obesity and gut microbiota in obese adults: a double-blind randomized controlled trial
Xiaokang Niu, Qi Zhang, Julong Liu, Yuyang Zhao, Nan Shang, Shusen Li, Yinghua Liu, Wei Xiong, Erna Sun, Yong Zhang, Hongfeng Zhao, Yixuan Li, Pengjie Wang, Bing Fang, Liang Zhao, Juan Chen, Fuqing Wang, Guofang Pang, Chenyuan Wang, Jingjing He and Ran Wang

43 Association of oxidative balance score with all-cause and cardiovascular mortality in overweight and obese
Shuxin Ying, Hongyan Ding, Yanjin Chen and Su Zheng

55 The energy model of insulin resistance: A unifying theory linking seed oils to metabolic disease and cancer
Catherine Shanahan

68 Systematic analysis of the burden of chronic kidney disease due to type 2 diabetes attributable to dietary risks based on the global burden of disease study 2021
Yanli Hou, Lingzhi Qin, Xuting Jin, Jiajia Ren, Jiamei Li, Xiaoling Zhang, Jingjing Zhang, Ruohan Li, Ya Gao, Xiaochuang Wang and Gang Wang

79 Frailty and GLIM-defined malnutrition contribute to poor clinical outcomes in older adult inpatients in the general surgery department
Chengyu Liu, Liru Chen, Peng Liu, Lei Li, Bo Cheng, Jingyong Xu, Hongyuan Cui and Mingwei Zhu

87 Association of dietary inflammatory index and oxidative balance score with all-cause and cardiovascular mortality in US non-diabetic adults
YuNan Han, Lin Li, YongXiang Wang and Wen Fan

98 Utilizing nutrition-related biomarkers to develop a nutrition-related aging clock for the chinese demographic
Ya-Qing Ma, Ya-Min Dang, Lv-Tao Zeng, Xin Gao, Si-Jia Li, Li-Qun Zhang, Jin Li, Xiao-Yang Zhou, Shan-Shan Ren, Hong-Lei Liu, Ruo-Mei Qi, Jing Pang, Ju Cui, Tie-Mei Zhang and Jian-Ping Cai

113 Iron status and dietary iron intake in relation to overweight/obesity in U.S. adults: a nationwide population-based study
Yuanyuan Lin, Yexin Chen, Jiangteng Liu, Minghao Li, Ying Tang, Jinxi Zhao and Yaofu Zhang

122 Low expression of SOD and PRX4 as indicators of poor prognosis and systemic inflammation in colorectal cancer
Sanghyun An, Hye Youn Kwon, Kwangmin Kim, Soo-Ki Kim, Cheol Su Kim, Bora Kim, Hyejin Do and Youngwan Kim

frontiers | Frontiers in Nutrition

TYPE Editorial
PUBLISHED 12 January 2026
DOI 10.3389/fnut.2025.1758019

OPEN ACCESS

EDITED AND REVIEWED BY
Barbara R. Cardoso,
Monash University, Australia

*CORRESPONDENCE
Qingyu Wang
daisyqingyu@outlook.com

RECEIVED 01 December 2025
REVISED 10 December 2025
ACCEPTED 16 December 2025
PUBLISHED 12 January 2026

CITATION
Wang Q, Li Y and Guan D (2026) Editorial: Dietary patterns and oxidative stress: implications for obesity, T2D, and cancer management. *Front. Nutr.* 12:1758019. doi: 10.3389/fnut.2025.1758019

Editorial: Dietary patterns and oxidative stress: implications for obesity, T2D, and cancer management

Qingyu Wang[1]*, Yixuan Li[2] and Dongxian Guan[3]

[1]Medical Research Center, Beijing Chaoyang Hospital, Capital Medical University, Beijing, China, [2]Key Laboratory of Functional Dairy, Department of Nutrition and Health, China Agricultural University, Beijing, China, [3]Institute of Modern Biology, Nanjing University, Nanjing, China

KEYWORDS

calorie restriction, cancer, high calorie, metabolic disease, ROS

Editorial on the Research Topic
Dietary patterns and oxidative stress: implications for obesity, T2D, and cancer management

Understanding how dietary patterns modulate internal oxidative stress is becoming increasingly important for explaining the rising global burden of metabolic diseases, including obesity, type 2 diabetes (T2D), and cancer. Excessive caloric intake has been shown to promote the generation of reactive oxygen species (ROS), which in turn drive chronic inflammation, metabolic dysfunction, and oxidative cellular injury. Thus, high-calorie dietary patterns and the oxidative stress they induce contribute to numerous pathological processes, including tumor initiation and progression (1, 2), insulin resistance (3), β-cell dysfunction (4), and obesity-related tissue impairment (5). However, evidence regarding which specific dietary components and molecular pathways exacerbate or alleviate oxidative injury remains limited (6). To address this gap, this Research Topic presents studies that elucidate the mechanistic links between dietary exposures, oxidative stress, inflammation, and chronic disease risk, while also highlighting emerging biomarkers and potential intervention strategies.

Calorie excess, nutrient imbalance, and Western dietary habits elevate the production of ROS. Two complementary studies by Han et al. and Ying et al. examine the impact of diet-derived inflammatory and oxidative indices on mortality risk. Han et al. demonstrate that higher Dietary Inflammatory Index scores are significantly associated with increased all-cause and cardiovascular mortality in non-diabetic adults, whereas higher Dietary Oxidative Balance Scores are associated with lower mortality risk. Ying et al. extend these insights to overweight and obese populations and report that elevated oxidative balance scores correlate with reduced all-cause and cardiovascular mortality in these groups. A global perspective is provided by Hou et al., who quantify the burden of T2D-related chronic kidney disease (CKD) attributable to dietary risks using data from the Global Burden of Disease (GBD) 2021 study. Their analysis shows that diets low in fruits, whole grains, and vegetables and diets high in processed meats are major contributors to the burden of T2D-related CKD. Taken together, these findings highlight the value of dietary indices that capture inflammatory and oxidative potential as tools for predicting chronic disease risk.

It has become increasingly clear that our diets influence far more than caloric intake. The interplay between micronutrients and metabolic homeostasis is highlighted by Lin et al., who report that the risks of overweight and obesity are inversely associated with serum iron levels, transferrin saturation, and dietary iron intake. Their findings suggest that iron status may shape energy metabolism, adipocyte function, and inflammatory processes. Dietary intake also modulates gut microbiome composition, and both probiotics and prebiotics have attracted considerable attention. Niu et al. demonstrate that a pre-screened synbiotic combination containing *Bifidobacterium animalis* subsp. *lactis* MN-Gup, galacto-oligosaccharides, and xylo-oligosaccharides reduce body fat, LDL cholesterol, and waist circumference, while promoting beneficial gut bacteria and bile acid profiles. Sun et al. show that heat-killed *B. longum* BBMN68 combined with inulin improves lipid metabolism and increases short-chain fatty acids in high-fat diet–induced obese rats, supporting a post-biotic approach to oxidative and metabolic regulation. Collectively, these interventions emphasize that microbiota-directed therapies might modulate oxidative stress indirectly through intestinal metabolites, bile acid signaling, and the maintenance of gut barrier integrity.

High oxidative status has long been recognized as a contributing factor in cancer progression. An et al. demonstrate that low tumor expression of key antioxidant enzymes in colorectal cancer, particularly SOD and PRX4, is associated with distant metastasis, systemic inflammation, poor differentiation, and reduced survival. These findings reinforce the concept that diminished endogenous antioxidant capacity may accelerate tumor progression. This work also highlights the potential value of tissue-based antioxidant markers as prognostic tools that could complement existing clinical assessments.

Overall, the studies in this Research Topic advance our understanding of how dietary patterns, micronutrient status, gut microbiota, and inflammatory burden intersect with oxidative stress to influence the development and progression of obesity, T2D, and cancer. They also strengthen the evidence that oxidative stress is not just a downstream consequence of poor metabolic health but also an important mediator linking dietary exposures with chronic disease outcomes.

Author contributions

QW: Writing – review & editing, Writing – original draft. YL: Writing – review & editing. DG: Writing – review & editing.

Conflict of interest

The author(s) declared that this work was conducted in the absence of any commercial or financial relationships that could be construed as a potential conflict of interest.

Generative AI statement

The author(s) declared that generative AI was not used in the creation of this manuscript.

Any alternative text (alt text) provided alongside figures in this article has been generated by Frontiers with the support of artificial intelligence and reasonable efforts have been made to ensure accuracy, including review by the authors wherever possible. If you identify any issues, please contact us.

Publisher's note

References

1. Glorieux C, Liu S, Trachootham D, Huang P. Targeting ROS in cancer: rationale and strategies. *Nat Rev Drug Discov.* (2024) 23:583–606. doi: 10.1038/s41573-024-00979-4

2. Singh R, Manna PP. Reactive oxygen species in cancer progression and its role in therapeutics. *Explor Med.* (2022) 3:43–57. doi: 10.37349/emed.2022.00073

3. Dandona P, Ghanim H, Chaudhuri A, Dhindsa S, Kim SS. Macronutrient intake induces oxidative and inflammatory stress: potential relevance to atherosclerosis and insulin resistance. *Exp Mol Med.* (2010) 42:245–53. doi: 10.3858/emm.2010.42.4.033

4. Zhao Y, Wang QY, Zeng LT, Wang JJ, Liu Z, Fan GQ, et al. Long-term high-fat high-fructose diet induces type 2 diabetes in rats through oxidative stress. *Nutrients.* (2022) 14:2181. doi: 10.3390/nu14112181

5. Han CY. Roles of reactive oxygen species on insulin resistance in adipose tissue. *Diabetes Metab J.* (2016) 40:272–9. doi: 10.4093/dmj.2016.40.4.272

6. Jomova K, Raptova R, Alomar SY, Alwasel SH, Nepovimova E, Kuca K, et al. Reactive oxygen species, toxicity, oxidative stress, and antioxidants: chronic diseases and aging. *Arch Toxicol.* (2023) 97:2499–574. doi: 10.1007/s00204-023-03562-9

frontiers | Frontiers in Nutrition

TYPE Original Research
PUBLISHED 03 July 2024
DOI 10.3389/fnut.2024.1421032

OPEN ACCESS

EDITED BY
Qingyu Wang,
Beijing Hospital, China

REVIEWED BY
Guoyu Wu,
Guangdong Pharmaceutical University, China
Jing Luo,
Nanjing Agricultural University, China
Ibrahim AlZaim,
Aarhus University, Denmark

*CORRESPONDENCE
Longhua Liu
✉ liulonghua@sus.edu.cn
Hongzhi Wang
✉ hzwang@phy.ecnu.edu.cn
Qing Lu
✉ Drluqingsjtu@163.com

†These authors have contributed equally to this work

RECEIVED 21 April 2024
ACCEPTED 24 June 2024
PUBLISHED 03 July 2024

CITATION
Wang L, Li Y, Li R, Luan J, Cao K, Liu T, Hu H, Chen S, Bu L, Liu L, Wang H and Lu Q (2024) Diverse associations between pancreatic intra-, inter-lobular fat and the development of type 2 diabetes in overweight or obese patients.
Front. Nutr. 11:1421032.
doi: 10.3389/fnut.2024.1421032

Diverse associations between pancreatic intra-, inter-lobular fat and the development of type 2 diabetes in overweight or obese patients

Lihui Wang[1†], Yinghao Li[2†], Renfeng Li[1†], Jinwen Luan[3], Kaiming Cao[1], Tiancheng Liu[1], Haiyang Hu[1], Shanshan Chen[4], Le Bu[5], Longhua Liu[3]*, Hongzhi Wang[2]* and Qing Lu[1]*

[1]Department of Radiology, Shanghai East Hospital, Tongji University, Shanghai, China, [2]Physics Department & Shanghai Key Laboratory of Magnetic Resonance, School of Physics and Electronic Science, East China Normal University, Shanghai, China, [3]School of Exercise and Health, Shanghai University of Sport, Shanghai, China, [4]College of Medical Imaging, Shanghai University of Medicine and Health Science, Shanghai, China, [5]Department of Endocrinology and Metabolism, Shanghai Tenth People's Hospital, Medicine School of Tongji University, Shanghai, China

Pancreatic fat is associated with obesity and type 2 diabetes mellitus (T2DM); however, the relationship between different types of pancreatic fat and diabetes status remains unclear. Therefore, we aimed to determine the potential of different types of pancreatic fat accumulation as a risk factor for T2DM in overweight or obese patients. In total, 104 overweight or obese patients were recruited from January 2020 to December 2022. The patients were divided into three groups: normal glucose tolerance (NGT), impaired fasting glucose or glucose tolerance (IFG/IGT), and T2DM. mDixon magnetic resonance imaging (MRI) was used to detect pancreatic fat in all three groups of patients. The pancreatic head fat (PHF), body fat (PBF), and tail fat (PTF) in the IFG/IGT group were 21, 20, and 31% more than those in the NGT group, respectively. PHF, PBF, and PTF were positively associated with glucose metabolic dysfunction markers in the NGT group, and inter-lobular fat volume (IFV) was positively associated with these markers in the IFG/IGT group. The areas under the receiver operating characteristic curves for PHF, PBF, and PTF (used to evaluate their diagnostic potential for glucose metabolic dysfunction) were 0.73, 0.73, and 0.78, respectively, while those for total pancreatic volume (TPV), pancreatic parenchymal volume, IFV, and IFV/TPV were 0.67, 0.67, 0.66, and 0.66, respectively. These results indicate that intra-lobular pancreatic fat, including PHF, PTF, and PBF, may be a potential independent risk factor for the development of T2DM. Additionally, IFV exacerbates glucose metabolic dysfunction. Intra-lobular pancreatic fat indices were better than IFV for the diagnosis of glucose metabolic dysfunction.

KEYWORDS

obesity, T2DM, mDixon MRI, pancreas fat quantification, intra-lobular fat, inter-lobular fat

1 Introduction

Worldwide, over 1.9 billion adults are overweight, of which more than 650 million are obese, based on data from the World Health Organization. Obesity, characterized by excessive fat accumulation, is a strong risk factor for many metabolic diseases such as type 2 diabetes mellitus (T2DM), hypertension, and cardiovascular diseases (1, 2). Both hyperplasia (adipogenesis) and hypertrophy contribute to excessive fat accumulation in adipose tissue (3). As a key nutrition-responsive metabolic tissue, adipose tissue stores lipids and secretes different adipokines to regulate whole-body lipid and glucose metabolism, which are strongly associated with metabolic diseases (4–6). Healthy or functional adipose tissue helps to protect from metabolic dysfunctions, while dysfunctional adipose tissue may exacerbate it by different mechanism such as lipotoxicity and secreted proinflammatory adipokines (7).

Adipose tissue is mainly divided into white adipose tissue (WAT) and brown adipose tissue (BAT). WAT can be located in different regions, including subcutaneous white adipose tissue (sWAT), visceral white adipose tissue (vWAT) and other locations including the bone marrow, underline the skin and surrounding the heart (7). Compared with sWAT, the fat mass of vWAT has a stronger positive correlation with the occurrence of metabolic diseases, including T2DM (8, 9). During overweight and obesity, WAT could be highly remodeled including increased adipocyte size, changed secret pattern, cell composition and induced hypoxia and inflammation within adipose tissue (7, 10). Hypoxia within the adipose tissue induced by decreasing adipose tissue blood flow and vascular rarefaction might result in adipocyte death and further macrophage infiltration as well as endothelial dysfunction (10). In addition to enlarged adipose tissue, ectopic fat can also infiltrate other metabolic organs, such as the liver and pancreas, resulting in fatty liver and pancreas disease, respectively (11). Fatty liver disease is strongly associated with insulin resistance and T2DM (12). Lifestyle interventions or certain drug treatments for T2DM, such as thiazolidinediones, can also alleviate fatty liver disease, and vice versa (13). Hypercaloric diets, with high saturated fat and glucose levels, can gradually overburden adipocytes with excessive lipolysis, resulting in an elevated flow of free fatty acids and triglyceride synthesis in the liver (13, 14). Lipid intermediates, such as diacylglycerols, could inhibit insulin signaling pathways by impairing insulin receptor substrate 2 (IRS2) phosphorylation as well as elevating the PKC pathway in the liver resulting in insulin resistance (15). Although the role of fatty liver disease in T2DM has been well studied, the potential relationship between fatty pancreas disease and glucose metabolism has not, despite growing interest.

The pancreas contains two distinct components: the exocrine pancreas, including acinar and ductal cells; and the endocrine pancreas, including islets of Langerhans (16). The exocrine pancreas plays a critical role in digesting carbohydrates, fats, and proteins by secreting digestive enzymes, such as amylases, lipases, and proteinases; while the endocrine pancreas regulates glucose homeostasis by secreting insulin (β cells), glucagon (λ cells), etc. (17, 18). Insulin plays a central role in the downregulation of blood glucose, whereas glucagon upregulates blood glucose. Pancreatic fat has been shown to associations with many different factors such as metabolic syndromes, metabolic dysfunction-associated steatotic liver disease (MASLD) and age etc. (18). Ectopic fat accumulation in the pancreas is associated with obesity and related metabolic diseases such as T2DM (19). Increased body mass index (BMI) and obesity are positively associated with fatty pancreas independent of sex and age, and pancreatic fat is negatively associated with insulin secretion (20). Ectopic fat can be deposited in different parts of the pancreas, including the islets of Langerhans, acinar cells, and inter-lobular stroma (21). Intra-lobular fat in endocrine cells (such as β cells) and acinar cells was shown to contribute to the occurrence of T2DM; hence, decreased intra-lobular fat may help alleviate T2DM (22–24). Inter-lobular fat is usually present during acute pancreatitis; however, it may also be involved in the development of T2DM by stimulating inflammation (25). Both oxidative cell stress and proinflammatory adipokines (such as leptin, adipsin, and resistin) can stimulate local inflammation and further insulin resistance, T2DM and related atherosclerosis (6, 26–28). However, it remains to be determined whether there are similar or different associations between pancreatic intra-, inter-lobular fat and the development of T2DM.

Many methods have been developed to detect fat accumulation in the pancreas, such as: histology, ultrasonography, computed tomography (CT), and magnetic resonance imaging (MRI) (18). While histology is not practical in routine hospital investigations, due to its invasiveness, non-invasive methods are important for pancreatic fat quantification. Ultrasonography is relatively cheap and widely available; however, it has limited use due to unestablished objective standards and unsatisfactory sensitivity and specificity due to investigator bias (29). CT is relatively expensive, requires the intravenous injection of radioactive tracers, and involves radioactive exposure, making it unsuitable for longitudinal fat quantification studies (30). Hence, MRI is commonly used for fat quantification because it does not involve the risk of ionizing radiation and has the advantages of high soft tissue resolution, multiparameter and multisequence scanning, and high repeatability. Multi-echo Dixon (mDixon MRI), a novel MRI technology that enables reliable and highly reproducible pancreatic fat quantification, is widely used (31). Similar to regular magnetic resonance spectroscopy (MRS) and histology, the measurement of proton density fat fraction (PDFF) using mDixon MRI is very accurate and reproducible and is also considered the gold standard (32). Its overall correlation coefficient was 0.999 for repeated scans at different locations, field strengths, and vendors (32). Using advanced mDixon MRI, some studies have documented that elevated BMI, age, and metabolic syndrome are

Abbreviations: T2DM, Type 2 diabetes; mDixon MRI, Multi-echo Dixon; WHR, Waist-hip circumference ratio; NGT, Normal glucose tolerance; IFG/IGT, Impaired fasting glucose or glucose tolerance; sWAT, Subcutaneous white adipose tissue; vWAT, Visceral white adipose tissue; oDI, Oral disposition index; IGI, Insulinogenic index; HOMA-β, Homeostasis model assessment-β; HOMA-IR, Homeostasis model assessment of insulin resistance; AUCCP/AUCGLU, Area under curve of C peptide/area under curve of glucose; AUCINS/AUCGLU, Area under curve of insulin/ area under curve of glucose; AUCCP.0–120, Area under curve of C peptide 0–120 min; AUCINS.0–120, Area under curve of insulin 0–120 min; AUCGLU.0–120, Area under curve of glucose 0–120 min; GA, Glycated albumin; CPE, C-peptide estimation; FINS, Fasting insulin; PINS, Plasma insulin; FBG, Fasting blood glucose; PBG, Plasma blood glucose; IL-10, Interleukin-10; TNF- α, Tumor necrosis factor; CRP, C-reactive protein; LPa, Lipoprotein a; ApoE, Apolipoprotein E; ApoB, Apolipoprotein B; ApoA, Apolipoprotein A; TG, Triglyceride; FFA, Free fatty acid; TC, Total cholesterol; LDL-c, Low-density lipoprotein cholesterol; HDL-c, High-density lipoprotein cholesterol; GGT, Gamma glutamyl transpeptidase; AST, Aspartate aminotransferase; ALT, Alanine aminotransferase.

positively associated with pancreatic fat accumulation (18). However, whether pancreatic fat accumulation is an independent risk factor for the development of T2DM has not been comprehensively studied. Therefore, in this study we aimed to determine the potential of different types of pancreatic fat accumulation as a risk factor for T2DM in overweight or obese patients.

2 Methods

2.1 Participants

A total of 265 hospitalized overweight or obese patients who underwent MRI using the mDixon technique were initially recruited for this cross-sectional study. All participants were enrolled in three individual cohort studies conducted at our hospital from January 2020 to December 2022 (Figure 1). The inclusion criteria were: age between 18 and 69 years, a BMI of 24 kg/m^2 or more, complete medical history and laboratory examination, and no contraindications for MRI. The exclusion criteria were: any form of pancreatic disease, including inflammation, tumor, or autoimmune disease; other endocrine and metabolic diseases, such as type 1 diabetes, hypothyroidism, Cushing's syndrome, and pituitary dysfunction; incomplete images or image artifacts; and absence of a complete laboratory examination. Based on these criteria, 104 patients were included in the study (Figure 1).

2.2 Anthropometry and metabolite assays

The heights and weights of all participants were measured and recorded using standardized and calibrated scales and stadiometers. BMI was calculated as body weight (kg) divided by height squared (m^2). Waist circumference (WC) was measured midway between the lowest rib and iliac crest in the horizontal plane. Hip circumference (HC) was measured at the level of maximum hip extension. The waist-hip circumference ratio (WHR) was calculated as WC divided by HC.

2.3 Biochemical examination

All participants underwent routine biochemical tests after fasting overnight for at least 10 h. These tests included: liver function tests [alanine transaminase (ALT), aspartate transaminase (AST), and gamma glutamyl-transferase (GGT)], lipid panel tests [total cholesterol (TC), triglyceride (TG), high-density lipoprotein cholesterol (HDL-c), low-density lipoprotein cholesterol (LDL-c), lipoprotein a (LPa), apolipoprotein E (ApoE), apolipoprotein B (ApoB), apolipoprotein A (ApoA), and free fatty acid (FFA)], inflammatory factors and amylase [white blood count (WBC), C-reactive protein (CRP), pancreatic amylase, interleukin (IL)-1β, IL-6, IL-8, IL-10, and tissue necrosis factor (TNF)-α], thyroid function

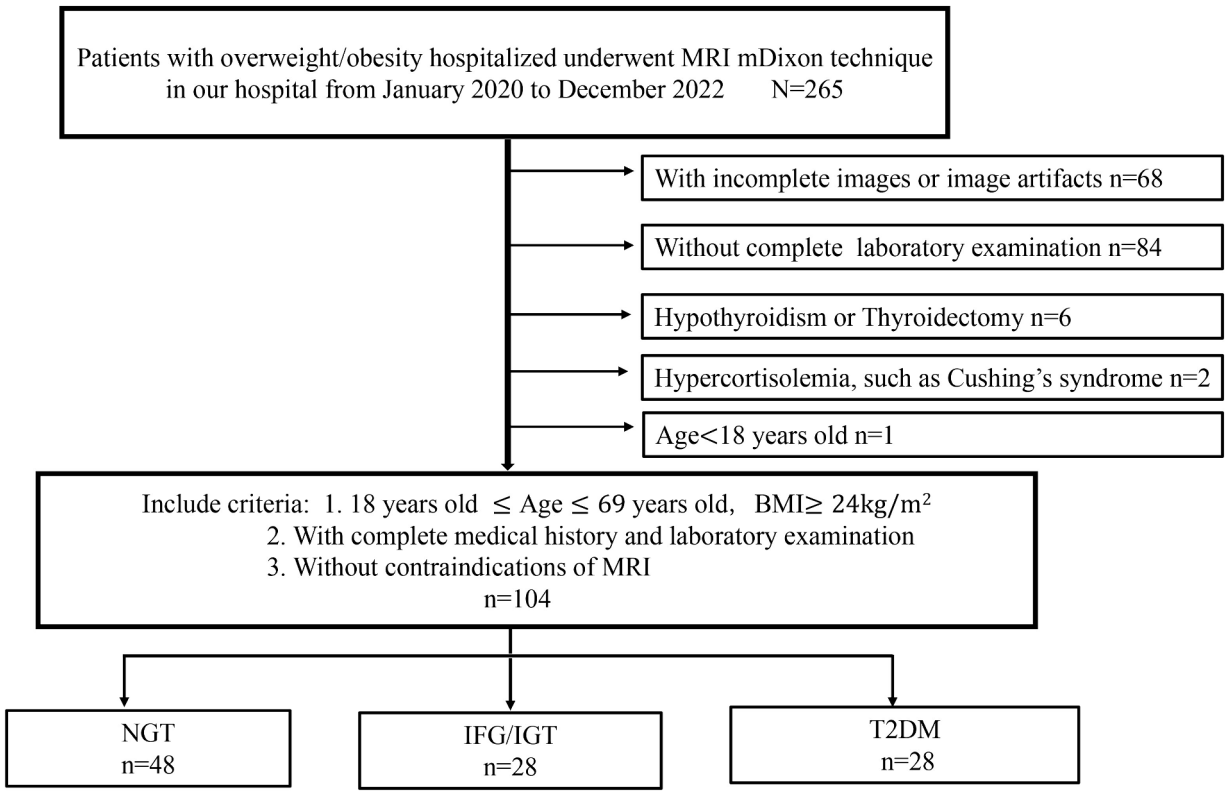

FIGURE 1
Flow chart of participant selection for this study. A total of 265 hospitalized overweight or obese patients who underwent MRI using the mDixon technique were initially recruited for this study. Sixty eight patients are with incomplete images or image artifacts, 84 patients are without complete laboratory examination, six patients are hypothyroidism or thyroidectomy, two patients are hypercortisolemia and one is under 18 years old. Finally, 104 patients were included in this study and divided into three groups: NGT (n = 48), IFG/IGT (n = 28), T2DM (n = 28).

tests [thyroid-stimulating hormone (TSH), free T3 (FT3), and free T4 (FT4)], and adrenocortical function and uric acid (UA) (cortisol, UA).

2.4 Oral glucose tolerance test and calculations

All participants underwent a 75 g oral glucose tolerance test (OGTT) after overnight fasting. Venous blood samples were drawn at 0, 30, 60, and 120 min to measure the plasma glucose, serum insulin, and C-peptide concentrations. Fasting blood glucose (FBG) levels were measured using the glucose oxidase method, and serum insulin and C-peptide levels were estimated using the chemiluminescence method. Hemoglobin A1c (HbA1c) levels were measured using high-performance liquid chromatography.

The calculation formulas for clinical assessment of insulin sensitivity and β-cell function were as follows: homeostasis model assessment of insulin resistance (HOMA-IR) = FBG [mg/dL] × fasting insulin (FINS) [μIU/mL]/22.5; Matsuda index = 10,000/(FBG [mg/dL] × FINS [μIU/mL] × mean glucose [mg/dL] × mean insulin [μIU/mL])$^{1/2}$; homeostasis model assessment of beta-cell function (HOMA-β) = 20 × FINS [μIU/mL]/(FBG-3.5) [mg/dL]; insulinogenic index (IGI) = Δ insulin (INS)0–30/Δ glucose (GLU) 0–30 = (INS30 - INS0) [μIU/mL]/ (GLU30 - GLU0) [mg/dL], where INSx and GLUx represent insulin and glucose values at time x min during the OGTT, respectively; Area under the curve of plasma insulin (AUCINS) 0 ~ 120 [min*μIU/mL]/area under the curve of plasma glucose (AUCGLU) 0 ~ 120 [min*mg/dL], wherein AUCGLU 0 ~ 120 and AUCINS 0 ~ 120, which were calculated using the trapezoid rule, represented the areas under the curve of plasma glucose and insulin secretion rates during the OGTT from 0 to 120 min, respectively; and oral Disposition Index (oDI) = IGI/FINS.

2.5 Separation and quantification of pancreatic fat, vWAT, and sWAT

A 3.0 T MRI system (Ingenia, Philips Healthcare, Best, Netherlands) was used for the MRI examinations. Abdominal MRI examinations for all participants were performed after at least 10 h of fasting in the supine position. The modified Dixon (mDixon MRI) Quant sequence was applied for the quantitative assessment of visceral fat disposition in all three groups of patients: normal glucose tolerance (NGT), impaired fasting glucose or glucose tolerance (IFG/IGT), and T2DM. This modified 6- echoes Dixon sequence included a repetition time of 15 ms, 6 echoes time = TE1/ΔTE 1.15 ms/1.15 ms, flip angle of 3°, matrix size of 188 × 155, field of view of 320 mm, and slice thickness of 3 mm (33). Three-dimensional axial images were captured from the diaphragmatic dome to the pelvic floor during a single breath-hold. After the acquisition, multislice two-dimensional axial images were reconstructed, and five maps, including water, fat, fat fraction, R2*, and T2*, were automatically generated. Using a post-processing workstation (Philips Intellispace; Philips Healthcare, Best, The Netherlands), pancreatic PDFF was measured in the pancreatic intralobular fat by manually placing an approximate ROI of 1 cm^2 within the head, body, and tail of the pancreas (34). The ROI sizes were selected according to the total extent of the organ or tissue of interest (34). All ROIs were placed to avoid major vessels, ducts, collection systems, and imaging artifacts (35). The pancreatic head, body, and tail diameters were determined as previously described (36). The cross-sectional area of sWAT and vWAT were quantified using the generated fat maps mentioned above. The two-dimensional fat area was multiplied by the slice thickness, followed by all slice levels added to calculate the volumes of sWAT and vWAT.

The inter-lobular fat in the pancreatic region was quantified using mDixon method and U-Net deep learning network model based on previously established methods (37–39). Generally, a grade-connected U-Net deep learning network model was used for pancreatic fat segmentation (38). The U-Net network is constructed based on Fully Convolutional Network with encoder-decoder structure (39). The encoder part is sampled by several convolution-pooling processes of the input image, while the decoder section uses dehumination and feature stitching to achieve a more feature layer of the field of vision, improves the network's attention to edge features, and improves the segmentation performance of the model. This study uses the grade-connected nnU-Net network with automated image pre-processing and training parameters. In the image pre-processing stage, it automatically sets up cutting, re-sampling, rotation and other standardized processes according to sample information. In the training, we use learning rate attenuation to improve the network learning ability. During the post-processing process, keep the maximum connected domain to generate dividing images based on prior knowledge. In fat-fraction images, inter-lobular fat showed a high-signal-intensity area in the pancreas, comparable to subcutaneous fat. After preprocessing with denoising, enhancement, and image calibration, the image was divided into two areas using a threshold method: fat and non-fat areas. During the postprocessing stage, isolated noise points, filled holes, and connected broken areas were used to obtain more accurate segmentation results. Segmentation of pancreatic inter-lobular fat was performed using a threshold of 60% signal intensity (36). Representative images show the whole pancreas, the inter-lobular fat, and also dissect the pancreatic intra-lobular fat, including three different parts (head, body, and tail) as: total pancreatic volume (TPV), pancreatic parenchymal volume (PPV), inter-lobular fat volume (IFV), the ratio of inter-lobular fat volume to total pancreatic volume (IFV/TPV), pancreatic head fat (PHF), pancreatic body fat (PBF), and pancreatic tail fat (PTF) (Figure 2A).

2.6 Statistical analysis

SPSS version 25.0 (SPSS Inc., Chicago, IL, United States) was used for all statistical analyses. Normal distribution of data was tested using the Kolmogorov–Smirnov test. For the analysis of seven different pancreatic indexes in three groups (NGT, IFG/IGT, T2DM), data are presented as means ± standard deviations, and significant analysis was based on the one-way ANOVA. Correlation studies in all three models (unadjusted, Model 1, and Model 2) were performed using Spearman's correlation coefficients. To avoid the confounding effects of age, BMI, and WHR, adjusted Model 1 was applied to study the correlation of pancreatic indices with glucose metabolism, inflammation, and liver function indices in the three groups. Furthermore, to avoid masking by liver dysfunction, Model 2 was adjusted for age, BMI, WHR, ALT, AST, and GGT.

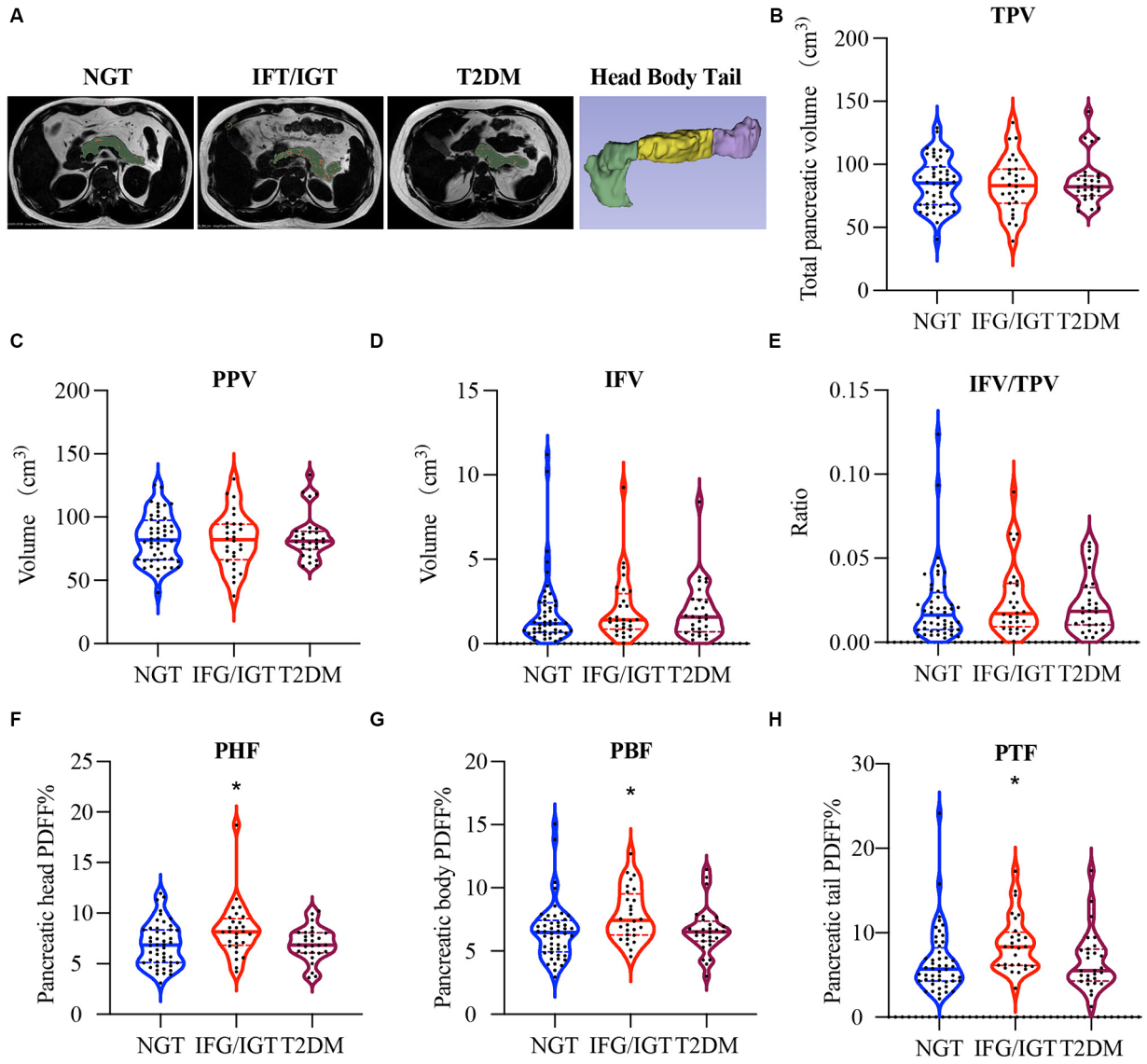

FIGURE 2
More pancreatic fat in IFG/IGT than NGT patients. **(A)** Representative images of intra-lobular fat, including pancreas head, body, and tail dissection and inter-lobular fat in participants with different glucose metabolic statuses. Pancreatic parenchyma including intra-lobular fat is shown in green, inter-lobular pancreatic fat is shown in red. **(B–H)** Violin plots for **(B)** total pancreas volume (TPV), **(C)** pancreatic parenchymal volume (PPV), **(D)** inter-lobular fat volume (IFV), **(E)** the ratio of inter-lobular fat volume to total pancreatic volume (IFV/TPV), **(F)** pancreatic head fat (PHF), **(G)** pancreatic body fat (PBF), and **(H)** pancreatic tail fat (PTF). NGT, normal glucose tolerance; IFG/IGT, impaired fasting glucose or glucose tolerance; T2DM, type 2 diabetes mellitus. *$p < 0.05$, one way ANOVA.

3 Results

3.1 Clinical characteristics of the patient groups

To investigate the potential roles of pancreatic fat in T2DM, 104 overweight/obese patients were divided into three groups: 48 patients in the NGT group, 28 in the IFG/IGT group, and 28 in the T2DM group based on the WHO-recommended criteria (40). There were no significant differences in age, BMI, WHR, sWAT, or vWAT among the three groups (Table 1). Regarding the glucose metabolism index, oDI, IGI, and HOMA-β were gradually decreased during the developing of diabetes; while HbA1c, GA, PBG at 0.5, 1, 2, and 3 h were significantly increased for both IFG/IGT and T2DM groups compared with the NGT group. However, the insulin levels at the 2, and 3 h time points were higher in the IFG/IGT group than in the NGT group, but much lower in the T2DM group than in the NGT group at 0.5 h and 1 h time points. Regarding inflammation status, no significant differences existed among the groups for IL-10, IL-8, IL6, IL-1β, TNF-α, and CRP. Furthermore, no significant changes in lipid metabolism were observed for TG, TC, LDL-c, HDL-c, ApoA, ApoB, or ApoE among the groups. However, the LPa was lower in the T2DM group than in the NGT group. Liver dysfunction worsened during the course of diabetes, as indicated by GGT, AST, and ALT levels. There were no significant differences in ACTH, UA, TSH, FT3, and FT4 levels among the three groups (Table 1).

TABLE 1 Clinical characteristics for NGT, IFG/IGT, and T2DM patients.

	Total $n = 104$	NGT $n = 48$	IFG/IGT $n = 28$	T2DM $n = 28$	p value
Gender (male, female)	(57, 37)	(31, 17)	(14, 14)	(22, 6)	0.0826
Age, yrs	36.49 ± 11.62	34.23 ± 11.27	39.04 ± 10.32	37.82 ± 13.03	0.172
BMI, kg/m^2	33.45 ± 5.89	34.47 ± 7.11	32.84 ± 3.6	32.3 ± 5.25	0.505
WHR	0.95 ± 0.1	0.96 ± 0.1	0.94 ± 0.1	0.97 ± 0.1	0.691
sWAT, cm^3	4011.75 ± 1903.39	4275.05 ± 2249.22	3975.94 ± 1446.23	3596.18 ± 1618.35	0.326
vWAT, cm^3	2628.31 ± 1165.61	2525.07 ± 1246.15	2529.52 ± 1182.37	2904.07 ± 986.84	0.346
Glucose metabolism index					
oDI	0.08 ± 0.07	0.12 ± 0.08	0.08 ± 0.06*	0.03 ± 0.03$^{\#\#\#}$	<0.001
IGI	1.16 ± 0.98	1.56 ± 1.03	1.22 ± 0.82	0.42 ± 0.49$^{\#\#\#}$	<0.001
Matsuda. index	424.9 ± 32.26	430.61 ± 27.03	421.95 ± 35.44	418.07 ± 36.41	0.226
HOMA-β	257.41 ± 234.36	302.9 ± 241.48	270.83 ± 249.21	166.02 ± 182.75$^{\#\#}$	0.045
HOMA-IR	4.58 ± 4.33	3.32 ± 2.55	4.02 ± 2.56	7.28 ± 6.56$^{\#\#}$	0.002
AUCCP/AUCGLU	1.18 ± 0.54	1.43 ± 0.5	1.27 ± 0.36	0.66 ± 0.38$^{\#\#\#}$	<0.001
AUCINS/AUCGLU	10.8 ± 6.66	12.94 ± 5.84	12.09 ± 6.59	5.85 ± 5.58$^{\#\#\#}$	<0.001
AUCCP.0–120	1200.63 ± 487.16	1290.01 ± 471.47	1357.94 ± 385.56	887.71 ± 478.56$^{\#\#\#}$	<0.001
AUCINS.0–120	10968.9 ± 6737.33	11662.12 ± 5747.67	12887.6 ± 7040.84	7861.84 ± 7169.18$^{\#}$	0.011
AUCGLU.0–120	1084.89 ± 316.99	896.57 ± 113.64	1066.52 ± 108.83***	1426.1 ± 406.03$^{\#\#\#}$	<0.001
HbA1C, %	6.17 ± 1.86	5.4 ± 0.34	5.55 ± 0.51	8.19 ± 2.73$^{\#\#\#}$	<0.001
GA, %	13.88 ± 5.75	11.75 ± 1.48	12.47 ± 1.05*	19.3 ± 9.33$^{\#\#\#}$	<0.001
CPE (0 h), ng/mL	3.76 ± 1.79	3.69 ± 1.68	4.04 ± 2.05	3.62 ± 1.73	0.646
CPE2 (0.5 h), ng/mL	9.3 ± 4.22	10.98 ± 4.09	9.79 ± 3.24	5.89 ± 3.39$^{\#\#\#}$	<0.001
CPE3 (1 h), ng/mL	11.78 ± 4.65	13.32 ± 4.01	12.7 ± 3.79	8.16 ± 4.66$^{\#\#\#}$	<0.001
CPE4 (2 h), ng/mL	12.11 ± 4.57	11.81 ± 4.13	14.4 ± 4.22*	10.33 ± 4.81	0.003
CPE5 (3 h), ng/mL	8.52 ± 3.72	7.24 ± 3.41	10.05 ± 4.14**	9.16 ± 3.07$^{\#}$	0.004
FINS, μIU/mL	18.22 ± 15.23	15.6 ± 11.73	17.87 ± 11.12	23.05 ± 22.04	0.120
0.5 h PINS, μIU/mL	93.9 ± 63.74	112.56 ± 61.2	101.3 ± 65.21	53.74 ± 48.76$^{\#\#\#}$	<0.001
1 h PINS, μIU/mL	111.97 ± 69.14	125.44 ± 61.05	126.07 ± 71.77	73.89 ± 67.66$^{\#\#}$	0.003
2 h PINS, μIU/mL	99.71 ± 73.83	86.49 ± 54.47	130.24 ± 79.07*	91.85 ± 89.63	0.034
3 h PINS, μIU/mL	50.54 ± 49.62	32.15 ± 30.03	65.7 ± 57.16**	66.83 ± 58.67$^{\#\#}$	<0.001
FBG, mmol/L	5.48 ± 1.93	4.74 ± 0.55	4.96 ± 0.79	7.26 ± 2.91$^{\#\#\#}$	<0.001
0.5 h PBG, mmol/L	9.01 ± 2.11	8.21 ± 1.3	8.94 ± 1.28*	10.5 ± 3.03$^{\#\#\#}$	<0.001
1 h PBG, mmol/L	10.25 ± 3.06	8.52 ± 1.63	10.19 ± 1.82***	13.4 ± 3.54$^{\#\#\#}$	<0.001
2 h PBG, mmol/L	9.27 ± 4.34	6.53 ± 0.78	8.84 ± 0.99***	14.41 ± 5.36$^{\#\#\#}$	<0.001
3 h PBG, mmol/L	6.76 ± 3.85	4.84 ± 1.05	5.97 ± 1.55**	10.99 ± 5.26$^{\#\#\#}$	<0.001
Inflammation factors					
IL-10	5.06 ± 0.34	5.07 ± 0.33	5.1 ± 0.5	5 ± 0.01	0.591
IL-8	89.82 ± 103.12	91.03 ± 116.52	93.72 ± 97.05	83.99 ± 89.34	0.945
IL-6	3.48 ± 1.67	3.82 ± 2.07	2.81 ± 0.95*	3.63 ± 1.35	0.059
IL-1β	6.87 ± 4.28	6.76 ± 4.35	6.5 ± 3.24	7.43 ± 5.13	0.743
TNF-α	7.88 ± 3.83	7.83 ± 4.82	7.58 ± 3.51	8.24 ± 2.04	0.834
CRP	2.75 ± 3.65	2.92 ± 4.01	1.95 ± 3.06	3.22 ± 3.51	0.471
Lipid metabolism index					
LPa	168.71 ± 264.29	193.61 ± 201.23	186.51 ± 411.94	107.15 ± 133.68$^{\#}$	0.385
ApoE	17.76 ± 24.48	16.67 ± 22.18	9.71 ± 12.37	27.99 ± 33.45	0.095

(Continued)

TABLE 1 (Continued)

	Total $n = 104$	NGT $n = 48$	IFG/IGT $n = 28$	T2DM $n = 28$	p value
ApoB	1.09 ± 0.24	1.06 ± 0.25	1.11 ± 0.24	1.11 ± 0.23	0.635
ApoA	1.21 ± 0.19	1.2 ± 0.19	1.26 ± 0.18	1.16 ± 0.2	0.193
TG	2.2 ± 1.51	1.98 ± 1.43	2.05 ± 1.02	2.75 ± 1.92	0.082
FFA	0.61 ± 0.25	0.54 ± 0.24	0.64 ± 0.27	0.69 ± 0.24$^{\#}$	0.034
CHOL	5.16 ± 1.12	5.08 ± 1.11	5.12 ± 0.89	5.32 ± 1.36	0.670
LDL-C	3.2 ± 0.83	3.14 ± 0.85	3.17 ± 0.81	3.32 ± 0.83	0.641
HDL-C	1.1 ± 0.21	1.11 ± 0.23	1.13 ± 0.19	1.05 ± 0.21	0.352
Liver function index					
GGT	50.07 ± 50.73	41.27 ± 35.45	52.04 ± 67.87	63.67 ± 51.99	0.181
AST	31.25 ± 26.28	24.73 ± 20.36	26.54 ± 11.27	47.74 ± 37.99$^{\#\#}$	0.004
ALT	48.85 ± 59.95	35.75 ± 38.13	39.25 ± 30.67	82.11 ± 94.5$^{\#}$	0.009
Others					
Cortisol	278.39 ± 106.68	293.24 ± 106.47	249.45 ± 111.51	284.41 ± 100.11	0.266
ACTH	33.09 ± 17.6	33.57 ± 19.3	26.73 ± 11.15	37.95 ± 18.3	0.080
UA	437.25 ± 121.87	437.34 ± 136.06	421.25 ± 114.44	454.31 ± 103.02	0.614
TSH	2.38 ± 1.22	2.34 ± 1.07	2.38 ± 1.07	2.45 ± 1.62	0.940
FT3	5.19 ± 0.72	5.28 ± 0.7	5.04 ± 0.64	5.2 ± 0.84	0.419
FT4	15.15 ± 3.14	15.38 ± 3.33	14.97 ± 3.02	14.94 ± 3.05	0.817

Data were presented as mean ± SD, $^{*}p < 0.05$, $^{**}p < 0.01$, $^{***}p < 0.001$ in the IFG/IGT vs NGT group; $^{\#}p < 0.05$, $^{\#\#}p < 0.01$, $^{\#\#\#}p < 0.001$ in the T2DM vs NGT group based on one-way ANOVA after Bonferroni correction.

NGT, normal glucose tolerance; IFG/IGT, impaired fasting glucose or glucose tolerance; T2DM, type 2 diabetes; WHR, Waist-hip circumference ratio; sWAT, subcutaneous white adipose tissue; vWAT, visceral white adipose tissue; oDI, oral Disposition Index; IGI, insulinogenic index; HOMA-β, homeostasis model assessment-β; HOMA-IR, homeostasis model assessment of insulin resistance; AUCCP/AUCGLU, Area under curve of C peptide/ area under curve of glucose; AUCINS/AUCGLU, Area under curve of insulin/ area under curve of glucose; AUCCP.0–120, area under curve of C peptide 0–120 min; AUCINS.0–120, area under curve of insulin 0–120 min; AUCGLU.0-120:area under curve of glucose 0–120 min; GA, glycated albumin; CPE:C peptide estimation; FINS, fasting insulin; PINS, plasma insulin; FBG, fasting blood glucose; PBG, plasma blood glucose; IL-10, interleukin-10; TNF-α, tumor necrosis factor-α; CRP, C-reactive protein; LPa, lipoprotein a; ApoE, apolipoprotein E; ApoB, apolipoprotein B; ApoA, apolipoprotein A; TG, triglyceride; FFA, free fatty acid; CHOL, cholesterol; LDL-c, low-density lipoprotein cholesterol; HDL-c, high-density lipoprotein cholesterol; GGT, gamma glutamyltranspeptidase; AST, aspartate aminotransferase; ALT, alanine aminotransferase; ACTH, adrenocorticotropic hormone; UA, uric acid; TSH, thyroid stimulating hormone; FT3, free triiodothyronine; FT4, free thyroxine.

3.2 More pancreatic fat in patients with IFG/IGT than NGT

There were no significant differences in TPV (Figure 2B), PPV (Figure 2C), IFV (Figure 2D), and IFV/TPV (Figure 2E) among all three groups of patients. Interestingly, the PHF in the IFG/IGT group was 21% higher than that in the NGT group, whereas the PHF in the T2DM group was comparable to that in the NGT group (Figure 2F). Similarly, PBF and PTF in the IFG/IGT group were 20 and 31% more than those in the NGT group, respectively; whereas there were no significant differences between the NGT and T2DM group (Figures 2G,H).

3.3 Distinct correlation between pancreatic fat and metabolic indexes

To study which parts of pancreatic fat are severe risk factors for T2DM, all seven pancreatic indices including TPV, PPV, IFV, IFV/TPV, PHF, PBF, and PTF were correlated with the anthropometric, glucose metabolism, inflammation, and liver function indexes in the three groups (Figure 3). We found that age was positively associated with IFV/TPV in the IFG/IGT group; however, there was no significant association with other pancreatic indices. BMI and vWAT were strongly and positively correlated with all pancreatic indices in most combinations, particularly in the NGT and IFG/IGT groups. For the glucose metabolism index, both TPV and PPV were positively associated with glucose metabolic dysfunction markers such as HOMA-β, HOMA-IR, AUCCP/AUCGLU, AUCCP.0–120, and C-peptide estimation (CPE) (0 h) in the NGT and IFG/IGT groups, but not in the T2DM group. Intriguingly, there was a positive association between IFV and glucose metabolic dysfunction markers such as HOMA-IR, HbA1C, CPE4 (2 h), FINS, and 2 h FINS in the IFG/IGT group, but not in the NGT or T2DM groups. In contrast, PHF, PBF, and PTF were significantly positively associated with glucose metabolic dysfunction markers, including HbA1c, CPE4 (1 h), and 1 h PINS in the NGT group but not in the IFG/IGT or T2DM groups (Figure 3). Furthermore, PHF, PBF, and PTF were positively associated with inflammation marker such as IL-6 and CRP in the IFG/IGT group (Figure 3). It is worth noting that TPV, PPV, and IFV were positively associated with liver dysfunction markers including GGT and ALT especially in the NGT group, which may cofound these associations.

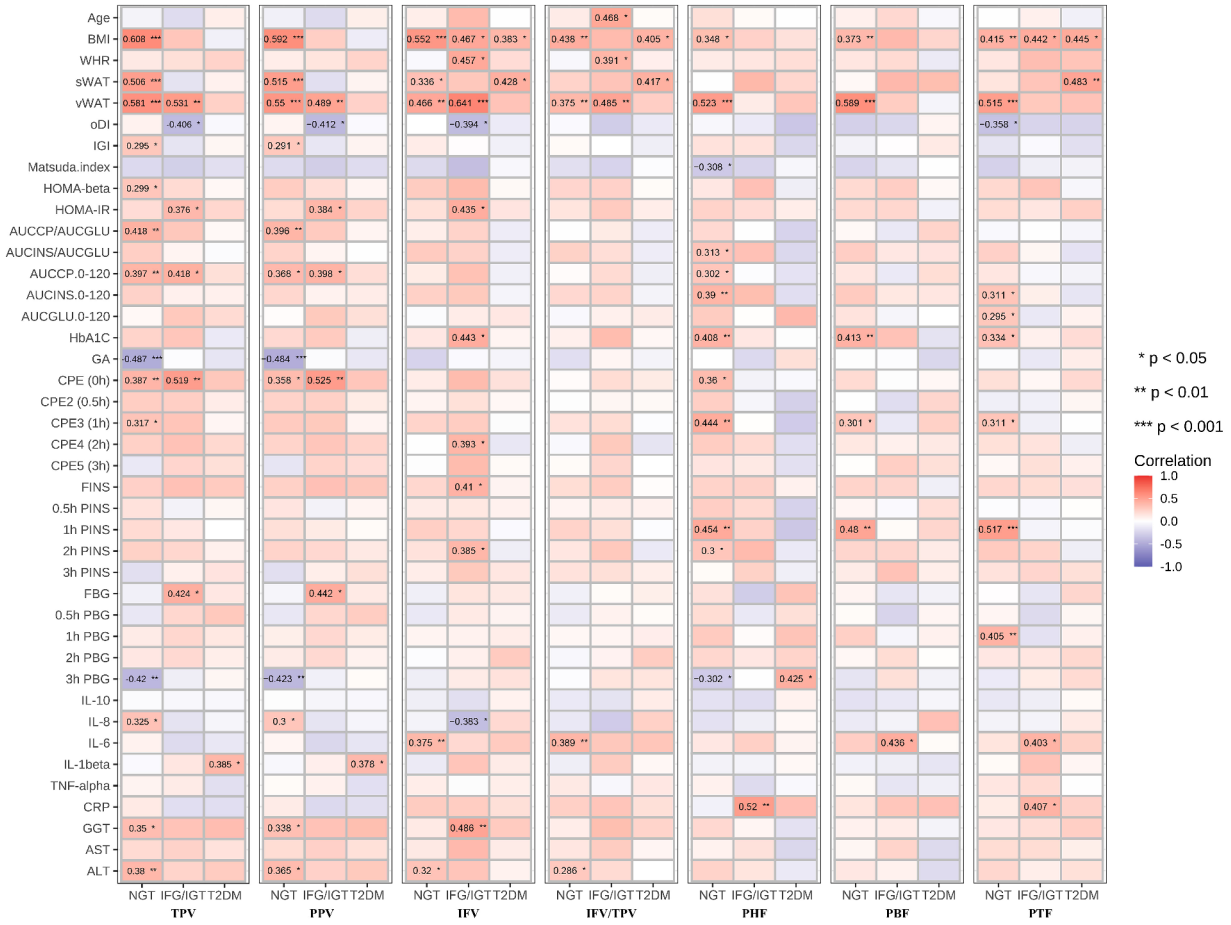

FIGURE 3
Correlation map between all seven pancreatic indexes with clinical indexes in the three groups. The seven pancreatic indexes are including TPV, PPV, IFV, IFV/TPV, PHF, PBF, and PTF. The clinical indexes are including Age, BMI, WHR, sWAT, vWAT, oDI, IGI, Matsuda. Index, HOMA-beta, HOMA-IR, AUCCP/AUCGLU, AUCINS/AUCGLU, AUCCP.0–120, AUCINS 0–120, AUCGLU0-120, HbA1C, GA, CPE (0 h), CPE2 (0.5 h), CPE3 (1 h), CPE4 (2 h), CPE5 (3 h), FINS, 0.5 h FINS, 1 h FINS, 2 h FINS, 3 h FINS, FBG, 0.5 h FBG, 1 h FBG, 2 h FBG, 3 h FBG, IL-10, IL-8, IL-6, IL-1beta, TNF-alpha, CRP, GGT, AST, ALT. These three groups are NGT, IFG/IGT, T2DM. *$p < 0.05$, **$p < 0.01$, ***$p < 0.001$, *t*-test.

3.4 Inter-lobular fat exacerbated glucose metabolic dysfunction

To avoid the confounding effects of age, BMI, and WHR, an adjusted Model 1 applied to study the correlation of pancreatic indices with glucose metabolism, inflammation, and liver function indices in the three groups independent of age, BMI and WHR (Figure 4). It shows that PHF, PBF, and PTF were negatively associated with sWAT, but significantly positively associated with vWAT in the NGT group. In addition, IFV and IFV/IPV were positively correlated with glucose metabolic dysfunction markers but negatively associated with the Matsuda index in the IFG/IGT group, which was consistent with the unadjusted model. Similar to the unadjusted model, PHF, PBF, and PTF were positively associated with glucose metabolic dysfunction markers including HbA1c and 1 h PINS in the NGT group; however, no significant association between PFs (PHF, PBF, and PTF) and glucose metabolic dysfunction was observed in both the IFG/IGT and T2DM groups. Both IFV and IFV/IPV were positively associated with the IL-6 and CRP levels in the NGT group. PHF and PTF were also positively correlated with the inflammatory marker CRP in the IFG/IGT and T2DM groups, indicating that inflammatory markers may be risk factors for the development of diabetes (Figure 4). Meanwhile, the liver dysfunction markers GGT, AST, and ALT were significantly positively associated with IFV in the IFG/IGT group, but not in the NGT or T2DM groups, which may indicate a correlation between IFV and glucose metabolic dysfunction markers.

3.5 PHF and PBF were glucose metabolism dysfunction markers independent of liver dysfunction

To avoid masking by liver dysfunction, Model 2 was adjusted for age, BMI, WHR, ALT, AST, and GGT. Consistent with the unadjusted or adjusted Model 1, PHF, PBF, and PTF were positively associated with glucose metabolic dysfunction markers in the NGT group, whereas PHF and PBF were positively associated with glucose metabolic dysfunction markers in the IFG/IGT group. Consistent with the unadjusted model and Model 1, IFV was also positively associated with glucose metabolic dysfunction markers in the IFG/IGT group in adjusted Model 2. Furthermore, PHF and PTF were negatively associated with oDI and IGI but positively correlated with 3 h PBG in

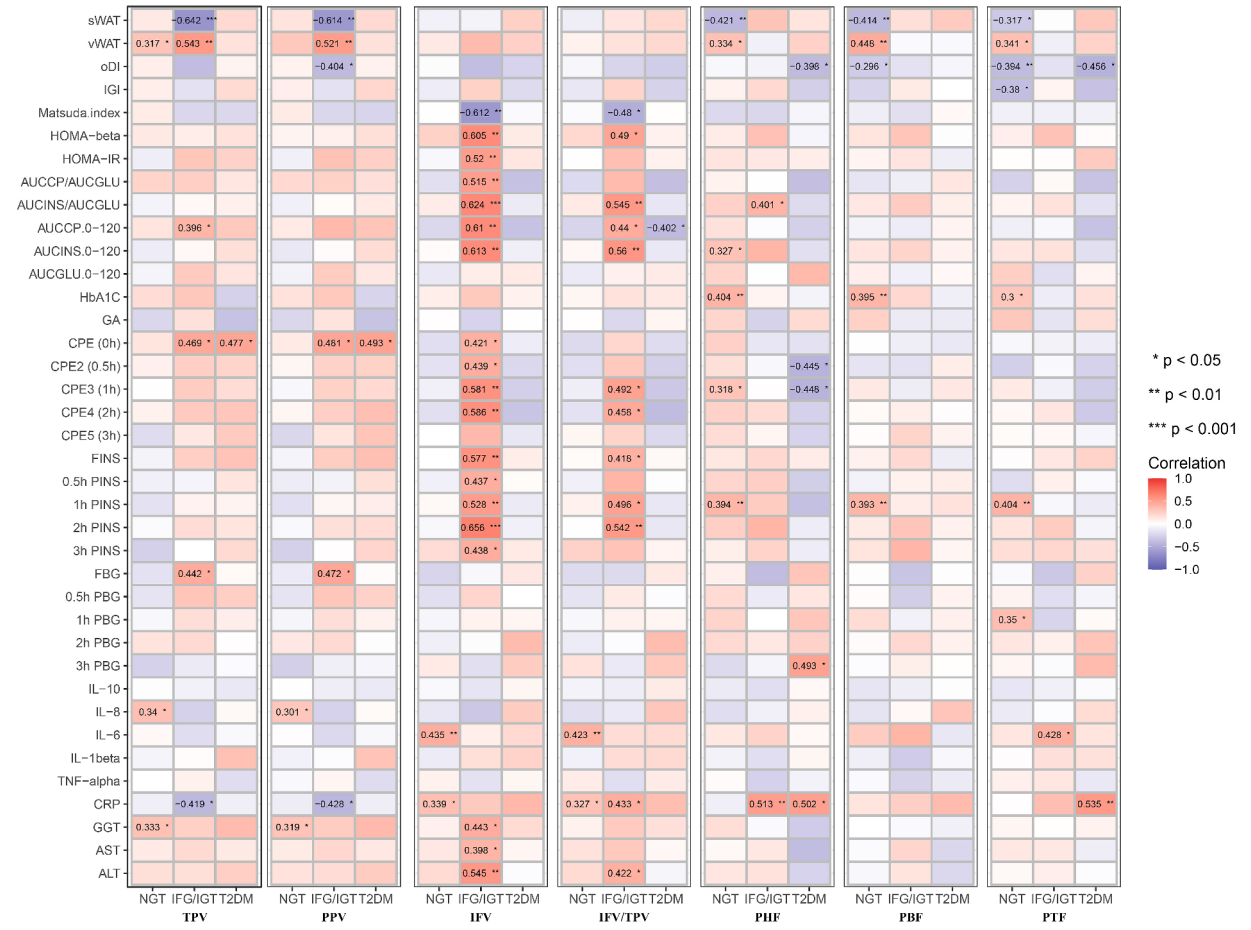

FIGURE 4
Correlation map between all seven pancreatic indexes with clinical indexes in the three groups after adjusting with age, BMI, WHR. These pancreatic indexes, clinical indexes and groups are the same as in Figure 3. BMI, body mass index; WHR, waist-hip ratio. *$p < 0.05$, **$p < 0.01$, ***$p < 0.001$, *t*-test.

the T2DM group. Interestingly, in Model 2, both PHF and PBF were positively associated with the glucose metabolic dysfunction index including HOMA-β and AUCINS/AUCGLU in IFG/IGT group, which indicated that PHF and PBF accumulation may be independent risk factors for insulin resistance (Figure 5).

3.6 Pancreatic intra-lobular fat was a better index than inter-lobular fat for glucose metabolic dysfunction

To study whether pancreatic indices could be applied for the early diagnosis of glucose metabolic dysfunction, both the NGT and IFG/IGT groups were used logistic regression study and evaluated by using receiver operating characteristic (ROC) curves. The area under the ROC curve (AUC) for the combination of age, BMI, and WHR was 0.64 ($p = 0.0429$) (Figure 6A), and for the combination of age, BMI, WHR, ALT, AST, and GGT was 0.66 ($p = 0.0189$) (Figure 6B), indicating that it was not sufficient to diagnose glucose metabolic dysfunction if only indices including age, BMI, WHR, ALT, AST, and GGT were included. Each of the seven pancreatic indices was combined with age, BMI, WHR, ALT, AST, and GGT to test their potential for the early diagnosis of glucose metabolic dysfunction. TPV, PPV, IFV, and IFV/TPV did not significantly improve the AUC, with values of 0.67 ($p = 0.0168$), 0.67 ($p = 0.0168$), 0.66 ($p = 0.0175$), and 0.66 ($p = 0.0175$), respectively (Figures 6C–F). In contrast, pancreatic intra-lobular fat, including PHF, PBF, and PTF, significantly improved the early diagnosis of glucose metabolic dysfunction, with AUCs of 0.73 ($p = 0.0011$), 0.73 ($p = 0.0007$), and 0.78 ($p < 0.0001$, respectively) (Figures 6G–I). These data indicate that pancreatic intra-lobular fat, including PHF, PBF, and PTF, is a better index for the diagnosis of glucose metabolic dysfunction than inter-lobular fat.

4 Discussion

In this study, 104 overweight or obese patients were recruited to investigate the roles of different types of the pancreatic fat in the development of T2DM using mDixon MRI. Glucose metabolism indices could distinguish between the NGT, IFG/IGT, and T2DM groups. PHF, PBF, and PTF levels were significantly higher in the IFG/IGT group than in the NGT group. Furthermore, regarding the correlation between pancreatic fat and the glucose metabolic index, PHF, PBF, and PTF were positively associated with glucose metabolic dysfunction markers in the NGT group in all three correlation models; whereas IFV showed a strong positive correlation with glucose

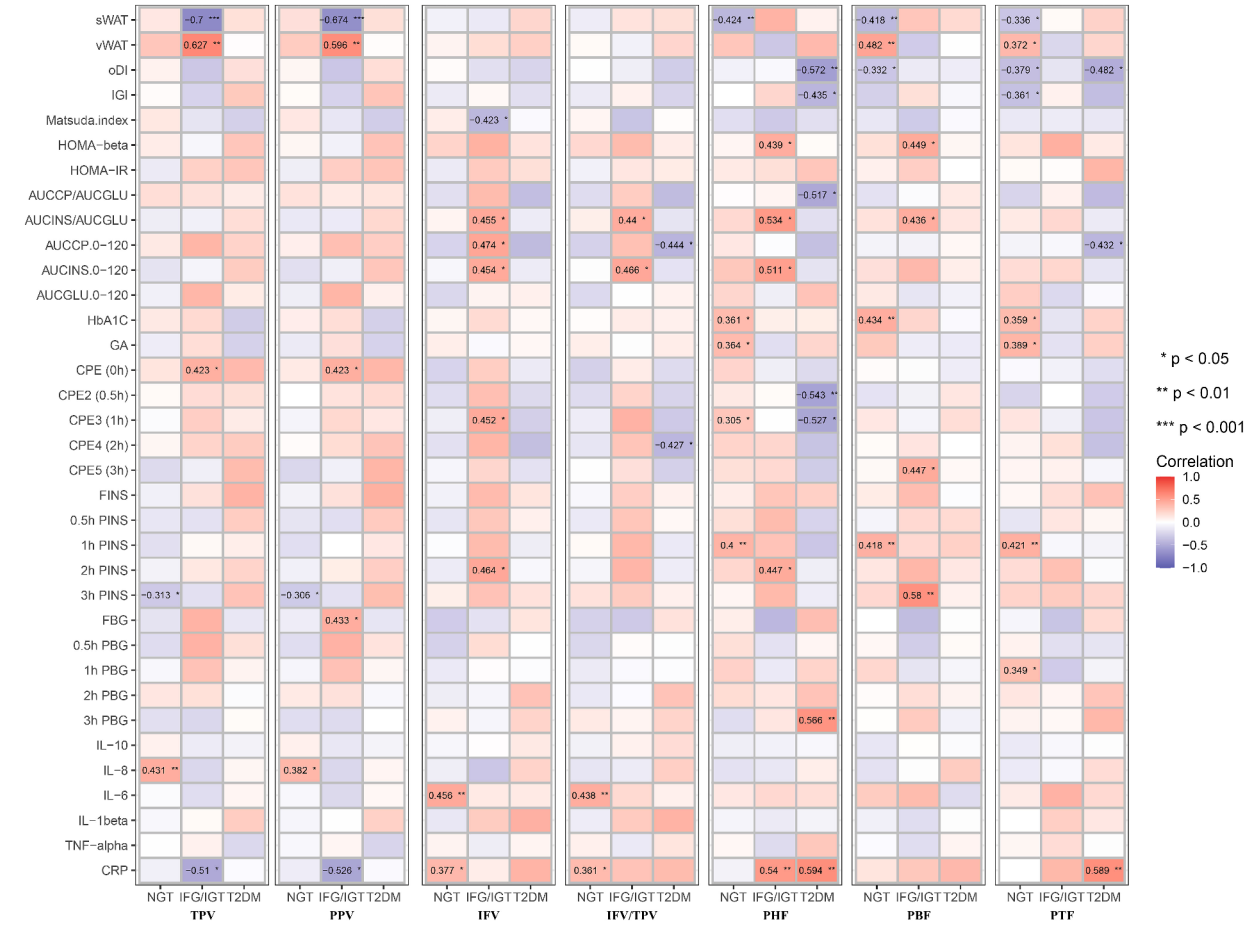

FIGURE 5
Correlation map between all seven pancreatic indexes with clinical indexes in the three groups after adjusting with age, BMI, WHR, GGT, AST, and ALT. These pancreatic indexes, clinical indexes and groups are the same as in Figure 3. BMI, body mass index; WHR, waist-hip circumference ratio; GGT, gamma glutamyl transpeptidase; AST, aspartate aminotransferase; ALT, alanine aminotransferase. *$p < 0.05$, **$p < 0.01$, ***$p < 0.001$, *t*-test.

metabolic dysfunction markers in the IFG/IGT group, but not in the NGT group. After adjusting for age, BMI, WHR, and ALT, AST, and GGT levels, both PHF and PBF levels were positively associated with glucose metabolic dysfunction in the NGT and IFG/IGT groups. These results strongly indicate that PHF and PBF may be independent risk factors for early stage T2DM, and that IFV exacerbates glucose metabolic dysfunction. Furthermore, the ROC showed that PHF, PBF, and PTF were better indices than inter-lobular fat in the diagnosis of glucose metabolic dysfunction. To the best of our knowledge, this is the first study to distinguish the distinct roles of PHF, PBF, PTF, and IFV in different stages of T2DM in overweight and obese Asian patients.

mDixon MRI is suitable for quantifying different parts of pancreatic fat in overweight or obese patients. As a noninvasive method for detecting pancreatic fat, ultrasonography is not suitable for distinguishing the different parts of pancreatic fat, including PHF, PBF, PTF, and IFV, especially in overweight or obese patients. Due to ectopic fat, it is difficult to get satisfactory images using ultrasonography (29). Although CT is much more sensitive than ultrasonography, ionizing radiation limits its widespread use for pancreatic fat quantification (41). Recently, mDixon MRI has become widely used for quantifying pancreatic fat because of its reliable reproducibility and safety. Dixon images are highly correlated with CT images in pancreatic fat quantification (41, 42). In this cross-sectional study, mDixon MRI was used to measure different parts of pancreatic fat in overweight and obese patients, saving them from the ionizing radiation of CT scanning, but with similar sensitivity. To maintain the randomness of this study, radiologists were blinded to all other clinical indices of the patients and used mDixon MRI to measure the different parts of the pancreatic fat using a well-established protocol (34). All data were analyzed by two different researchers and the results were no significant difference between two different researchers using paired-*t* test.

Both inter- and intra-lobular fat accumulation in the pancreas disturb normal pancreatic function, including glucose metabolism. The endocrine pancreas plays a critical role in regulating glucose homeostasis mainly by secreting insulin (β cells) and glucagon (λ cells) (17, 18). Ectopic fat accumulation may result in the secretion of proinflammatory adipokines to stimulate inflammation, which exacerbates insulin resistance and related metabolic diseases (6, 43). In this study, PHF was positively associated with glucose metabolic dysfunction markers in the IFG/IGT group, as well as strongly positively correlated with the inflammatory marker CRP. Both IFV

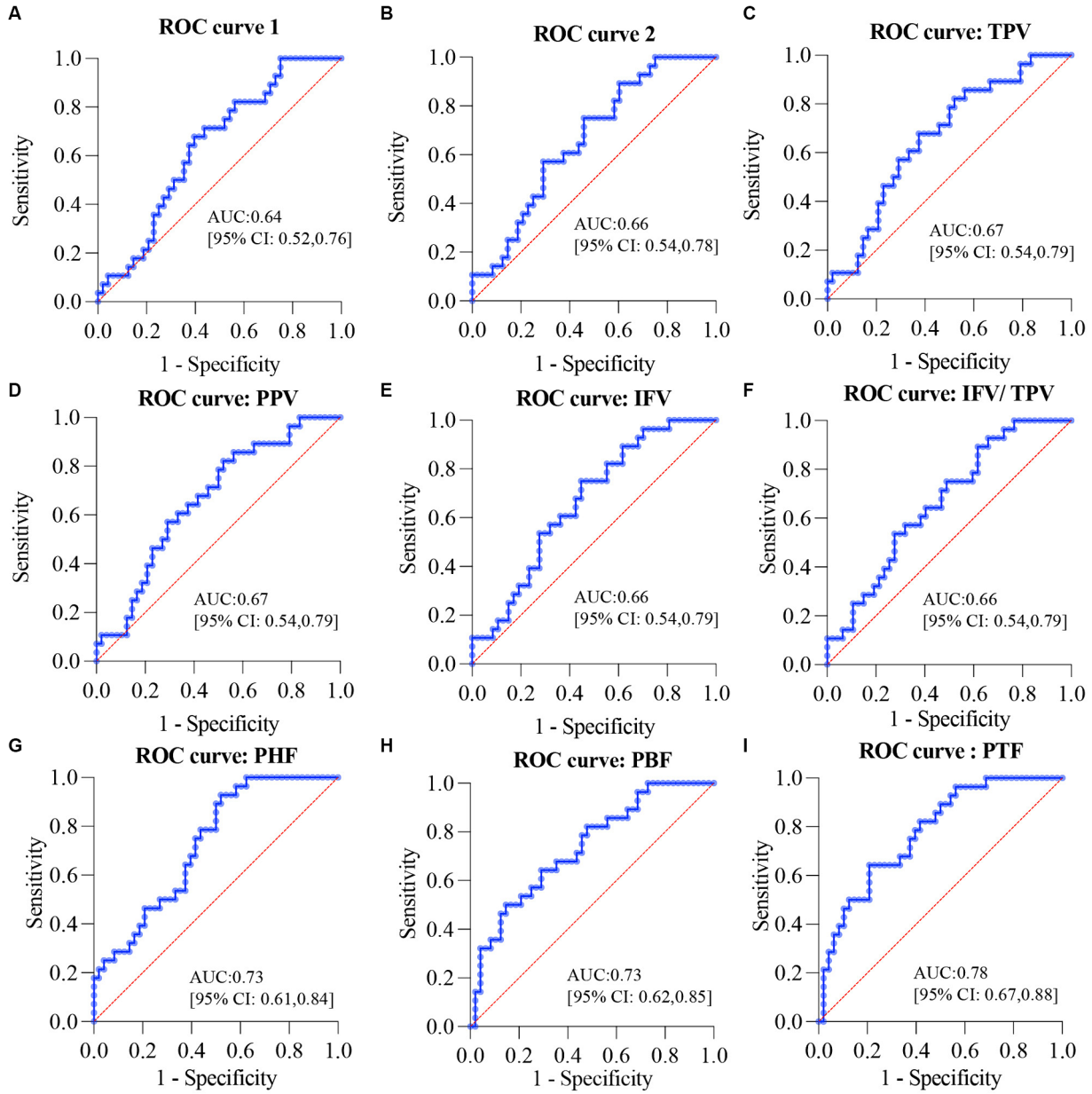

FIGURE 6
ROC curves for the diagnosis of glucose metabolic dysfunction in overweight or obese patients. **(A)** ROC curve for the combination of age, BMI, and WHR. **(B)** ROC curve for the combination of age, BMI, WHR, ALT, AST, and GGT. **(C)** ROC curve for the combination of TPV, age, BMI, WHR, ALT, AST, and GGT. **(D)** ROC curve for the combination of PPV, age, BMI, WHR, ALT, AST, and GGT. **(E)** ROC curve for the combination of IFV, age, BMI, WHR, ALT, AST, and GGT. **(F)** ROC curve for the combination of IFV/TPV, age, BMI, WHR, ALT, AST, and GGT. **(G)** ROC curve for the combination of PHF, age, BMI, WHR, ALT, AST, and GGT. **(H)** ROC curve for the combination of PBF, age, BMI, WHR, ALT, AST, and GGT. **(I)** ROC curve for the combination of PTF, age, BMI, WHR, ALT, AST, and GGT. ROC, receiver operating characteristic; BMI, body mass index; WHR, waist-hip circumference ratio; GGT, gamma glutamyl transpeptidase; AST, aspartate aminotransferase; ALT, alanine aminotransferase; TPV, total pancreas volume; PPV, pancreatic parenchymal volume; IFV, inter-lobular fat volume; IFV/TPV, the ratio of inter-lobular fat volume to total pancreatic volume; PHF, pancreatic head fat; PBF, pancreatic body fat; PTF, pancreatic tail fat.

and IFV/TPV were positively associated with the inflammation markers IL-6 and CRP in the NGT group (Figure 5).

Being overweight or obese is usually strongly associated with fatty liver disease. Liver dysfunction, especially insulin resistance, is one of the key characteristics of T2DM (44, 45). Although both fatty liver and pancreas are associated with the incidence of T2DM, a study showed that fatty pancreas was an independent risk factor for diabetes in a 10-year prospective cohort study (46). Another study showed that the hazard ratio for T2DM was 3.38 for pancreatic fat in 146 patients with T2DM over 6 years of follow-up. It also showed that pancreatic fat was negatively associated with insulin secretion in participants with prediabetes but not with a metabolomic pattern (47). And another study recruited 132 T2DM patients and investigated the potential association between pancreatic fat with T2DM using CT which found that pancreatic fat was a potential predictor of beta cell dysfunction as well as T2DM (48). However, these previous studies did not

distinguish the potential heterogeneous roles of different parts of pancreatic fat in glucose metabolic dysfunction. After adjusting for the liver dysfunction markers ALT, AST, and GGT in Model 2, PHF, PBF, and PTF were still positively associated with glucose metabolic dysfunction, especially in the NGT and IFG/IGT groups; whereas IFV was significantly associated with glucose metabolic dysfunction mainly in the IFG/IGT group, but not in the NGT group (Figure 5).

Inflammation played roles in the development of obesity related T2DM. Previous cross-sectional and prospective studies have indicated that CRP, IL6, IL8, IL1β, and TNFα are predictive biomarkers for T2DM (49, 50). During obese, the enlarge adipose tissue and liver could release pro-inflammation cytokines such as IL6, TNFα, and CRP to blood (49). Excessive glucose and lipids could stress pancreatic β cells and insulin responsive tissues including liver, adipose tissue and muscle which lead to overproduce cytokines. The NF-κB and JNK pathway was involved in inflammation induced insulin resistance and T2DM development (51, 52). Here, we found that Both IFV and IFV/TPV were positively associated with the inflammation markers IL-6 and CRP in the NGT group, and CRP was also positively associated with PHF in both IFG/IGT and T2DM group (Figure 5).

This study had certain limitation due to the limited ethnic origin of the participants. All the participants were from China, which may limit the generalizability of our findings. Future studies should involve patients with diverse ethnic backgrounds to validate if our findings are generalizable.

In conclusion, this study dissected the potential role of different types of pancreatic fat in overweight or obese patients with distinct diabetic status using mDixon MRI. Pancreatic fat, including PHF, PBF, and PTF, was shown to be a potential independent risk factor for the progression of diabetes, whereas IFV exacerbated glucose metabolic dysfunction. Pancreatic intra-lobular fat, including PHF, PBF, and PTF, may be a better index for the diagnosis of glucose metabolic dysfunction than inter-lobular fat. Hence, the detection of fat in different parts of the pancreas, including PHF, PBF, PTF, and IFV, may facilitate the early diagnosis of metabolic dysfunction, allow early intervention, and enable the evaluation of certain treatments on glucose metabolic dysfunction. Future studies should evaluate the roles of different types of pancreatic fat in other populations.

Data availability statement

The original contributions presented in the study are included in the article/supplementary material, further inquiries can be directed to the corresponding authors.

Ethics statement

The studies involving humans were approved by Medical Ethics Committee of Shanghai East Hospital. The studies were conducted in accordance with the local legislation and institutional requirements. The participants provided their written informed consent to participate in this study.

Author contributions

LW: Investigation, Writing – original draft, Data curation, Formal analysis, Writing – review & editing. YL: Investigation, Data curation, Writing – original draft. RL: Investigation, Data curation, Software, Validation, Writing – original draft. JL: Formal analysis, Visualization, Writing – review & editing. KC: Methodology, Validation, Writing – review & editing. TL: Investigation, Writing – review & editing. HH: Investigation, Writing – review & editing. SC: Validation, Writing – review & editing. LB: Methodology, Writing – review & editing. LL: Funding acquisition, Investigation, Writing – review & editing. HW: Conceptualization, Investigation, Supervision, Writing – review & editing. QL: Conceptualization, Funding acquisition, Project administration, Supervision, Writing – review & editing.

Funding

The author(s) declare that financial support was received for the research, authorship, and/or publication of this article. This work was supported by the Shanghai Municipal Health Commission (NO: 202340212), Shanghai East Hospital Special Research Fund (NO: DFRC2023015) and the Shanghai Higher Education Young Teachers Training Funding Program (A2-0213-22-0058-5).

Acknowledgments

We would like to thank Editage (www.editage.com) for their writing support on the manuscript.

Conflict of interest

The authors declare that the research was conducted in the absence of any commercial or financial relationships that could be construed as a potential conflict of interest.

Publisher's note

References

1. Kahn SE, Hull RL, Utzschneider KM. Mechanisms linking obesity to insulin resistance and type 2 diabetes. *Nature*. (2006) 444:840–6. doi: 10.1038/nature05482

2. Powell-Wiley TM, Poirier P, Burke LE, Després JP, Gordon-Larsen P, Lavie CJ, et al. Obesity and cardiovascular disease: a scientific statement from the American Heart Association. *Circulation*. (2021) 143:e984–e1010. doi: 10.1161/CIR.0000000000000973

3. Wang QA, Tao C, Gupta RK, Scherer PE. Tracking adipogenesis during white adipose tissue development, expansion and regeneration. *Nat Med*. (2013) 19:1338–44. doi: 10.1038/nm.3324

4. Cohen P, Spiegelman BM. Cell biology of fat storage. *Mol Biol Cell*. (2016) 27:2523–7. doi: 10.1091/mbc.E15-10-0749

5. Caesar R, Manieri M, Kelder T, Boekschoten M, Evelo C, Müller M, et al. A combined transcriptomics and lipidomics analysis of subcutaneous, epididymal and mesenteric adipose tissue reveals marked functional differences. *PLoS One*. (2010) 5:e11525. doi: 10.1371/journal.pone.0011525

6. Liu L, Shi Z, Ji X, Zhang W, Luan J, Zahr T, et al. Adipokines, adiposity, and atherosclerosis. *Cell Mol Life Sci*. (2022) 79:272. doi: 10.1007/s00018-022-04286-2

7. Hagberg CE, Spalding KL. White adipocyte dysfunction and obesity-associated pathologies in humans. *Nat Rev Mol Cell Biol*. (2024) 25:270–89. doi: 10.1038/s41580-023-00680-1

8. Bjorndal B, Burri L, Staalesen V, Skorve J, Berge RK. Different adipose depots: their role in the development of metabolic syndrome and mitochondrial response to hypolipidemic agents. *J Obes*. (2011) 2011:490650. doi: 10.1155/2011/490650

9. Wajchenberg BL. Subcutaneous and visceral adipose tissue: their relation to the metabolic syndrome. *Endocr Rev*. (2000) 21:697–738. doi: 10.1210/edrv.21.6.0415

10. AlZaim I, de Rooij L, Sheikh BN, Borgeson E, Kalucka J. The evolving functions of the vasculature in regulating adipose tissue biology in health and obesity. *Nat Rev Endocrinol*. (2023) 19:691–707. doi: 10.1038/s41574-023-00893-6

11. Gerst F, Wagner R, Kaiser G, Panse M, Heni M, Machann J, et al. Metabolic crosstalk between fatty pancreas and fatty liver: effects on local inflammation and insulin secretion. *Diabetologia*. (2017) 60:2240–51. doi: 10.1007/s00125-017-4385-1

12. Tanase DM, Gosav EM, Costea CF, Ciocoiu M, Lacatusu CM, Maranduca MA, et al. The intricate relationship between type 2 diabetes mellitus (T2DM), insulin resistance (IR), and nonalcoholic fatty liver disease (NAFLD). *J Diabetes Res*. (2020) 2020:3920196–16. doi: 10.1155/2020/3920196

13. Dewidar B, Kahl S, Pafili K, Roden M. Metabolic liver disease in diabetes - from mechanisms to clinical trials. *Metabolism*. (2020) 111S:154299. doi: 10.1016/j.metabol.2020.154299

14. Tilg H, Moschen AR, Roden M. NAFLD and diabetes mellitus. *Nat Rev Gastroenterol Hepatol*. (2017) 14:32–42. doi: 10.1038/nrgastro.2016.147

15. Samuel VT, Liu ZX, Qu X, Elder BD, Bilz S, Befroy D, et al. Mechanism of hepatic insulin resistance in non-alcoholic fatty liver disease. *J Biol Chem*. (2004) 279:32345–53. doi: 10.1074/jbc.M313478200

16. Zhou Q, Melton DA. Pancreas regeneration. *Nature*. (2018) 557:351–8. doi: 10.1038/s41586-018-0088-0

17. Campbell JE, Newgard CB. Mechanisms controlling pancreatic islet cell function in insulin secretion. *Nat Rev Mol Cell Biol*. (2021) 22:142–58. doi: 10.1038/s41580-020-00317-7

18. Wagner R, Eckstein SS, Yamazaki H, Gerst F, Machann J, Jaghutriz BA, et al. Metabolic implications of pancreatic fat accumulation. *Nat Rev Endocrinol*. (2022) 18:43–54. doi: 10.1038/s41574-021-00573-3

19. Filippatos TD, Alexakis K, Mavrikaki V, Mikhailidis DP. Nonalcoholic fatty pancreas disease: role in metabolic syndrome, "prediabetes," diabetes and atherosclerosis. *Dig Dis Sci*. (2022) 67:26–41. doi: 10.1007/s10620-021-06824-7

20. Heni M, Machann J, Staiger H, Schwenzer NF, Peter A, Schick F, et al. Pancreatic fat is negatively associated with insulin secretion in individuals with impaired fasting glucose and/or impaired glucose tolerance: a nuclear magnetic resonance study. *Diabetes Metab Res Rev*. (2010) 26:200–5. doi: 10.1002/dmrr.1073

21. Petrov MS, Taylor R. Intra-pancreatic fat deposition: bringing hidden fat to the fore. *Nat Rev Gastroenterol Hepatol*. (2022) 19:153–68. doi: 10.1038/s41575-021-00551-0

22. White MG, Shaw JA, Taylor R. Type 2 diabetes: the pathologic basis of reversible beta-cell dysfunction. *Diabetes Care*. (2016) 39:2080–8. doi: 10.2337/dc16-0619

23. Singh RG, Yoon HD, Poppitt SD, Plank LD, Petrov MS. Ectopic fat accumulation in the pancreas and its biomarkers: a systematic review and meta-analysis. *Diabetes Metab Res Rev*. (2017) 33:e2918. doi: 10.1002/dmrr.2918

24. al-Mrabeh A, Hollingsworth KG, Shaw JAM, McConnachie A, Sattar N, Lean MEJ, et al. 2-year remission of type 2 diabetes and pancreas morphology: a post-hoc analysis of the DiRECT open-label, cluster-randomised trial. *Lancet Diabetes Endocrinol*. (2020) 8:939–48. doi: 10.1016/S2213-8587(20)30303-X

25. Gillies NA, Pendharkar SA, Singh RG, Asrani VM, Petrov MS. Lipid metabolism in patients with chronic hyperglycemia after an episode of acute pancreatitis. *Diabetes Metab Syndr*. (2017) 11:S233–41. doi: 10.1016/j.dsx.2016.12.037

26. Sakai NS, Taylor SA, Chouhan MD. Obesity, metabolic disease and the pancreas-quantitative imaging of pancreatic fat. *Br J Radiol*. (2018) 91:20180267. doi: 10.1259/bjr.20180267

27. Ren Y, Zhao H, Yin C, Lan X, Wu L, du X, et al. Adipokines, Hepatokines and Myokines: focus on their role and molecular mechanisms in adipose tissue inflammation. *Front Endocrinol (Lausanne)*. (2022) 13:873699. doi: 10.3389/fendo.2022.873699

28. Shi Z, Wang L, Luan J, Yin L, Ji X, Zhang W, et al. Exercise promotes bone marrow microenvironment by inhibiting Adipsin in diet-induced male obese mice. *Nutrients*. (2022) 15:19. doi: 10.3390/nu15010019

29. Lindsell DR. Ultrasound imaging of pancreas and biliary tract. *Lancet*. (1990) 335:390–3. doi: 10.1016/0140-6736(90)90217-s

30. Cypess AM, Haft CR, Laughlin MR, Hu HH. Brown fat in humans: consensus points and experimental guidelines. *Cell Metab*. (2014) 20:408–15. doi: 10.1016/j.cmet.2014.07.025

31. Sarma MK, Saucedo A, Darwin CH, Felker ER, Umachandran K, Kohanghadosh D, et al. Noninvasive assessment of abdominal adipose tissues and quantification of hepatic and pancreatic fat fractions in type 2 diabetes mellitus. *Magn Reson Imaging*. (2020) 72:95–102. doi: 10.1016/j.mri.2020.07.001

32. Bray TJ, Chouhan MD, Punwani S, Bainbridge A, Hall-Craggs MA. Fat fraction mapping using magnetic resonance imaging: insight into pathophysiology. *Br J Radiol*. (2018) 91:20170344. doi: 10.1259/bjr.20170344

33. Liu B, Xu J, Jin Y, Su W, Zhang X, Qiao Y, et al. Advantages of 3-dimensional measurements for supraspinatus intramuscular fatty evaluation in patients with medium to massive rotator cuff tears: comparison with a single sagittal slice. *Am J Sports Med*. (2022) 50:699–707. doi: 10.1177/03635465211068854

34. Oguz SH, İdilman I, Helvaci N, Guzelce EC, Eyupoglu D, Karcaaltincaba M, et al. Tissue fat quantification by magnetic resonance imaging: proton density fat fraction in polycystic ovary syndrome. *Reprod Biomed Online*. (2020) 41:329–34. doi: 10.1016/j.rbmo.2020.04.024

35. Tang A, Desai A, Hamilton G, Wolfson T, Gamst A, Lam J, et al. Accuracy of MR imaging-estimated proton density fat fraction for classification of dichotomized histologic steatosis grades in nonalcoholic fatty liver disease. *Radiology*. (2015) 274:416–25. doi: 10.1148/radiol.14140754

36. Desouza SV, Yoon HD, Singh RG, Petrov MS. Quantitative determination of pancreas size using anatomical landmarks and its clinical relevance: a systematic literature review. *Clin Anat*. (2018) 31:913–26. doi: 10.1002/ca.23217

37. Livingstone RS, Begovatz P, Kahl S, Nowotny B, Straßburger K, Giani G, et al. Initial clinical application of modified Dixon with flexible echo times: hepatic and pancreatic fat assessments in comparison with (1)H MRS. *MAGMA*. (2014) 27:397–405. doi: 10.1007/s10334-013-0421-4

38. Ronneberger OFP, Brox T. *MICCAI: Medical Image Computing and Computer-Assisted Intervention. 18th international conference, Munich, Germany, October 5–9. 2015, Proceedings, Part II*. Springer International Publishing (2015). p. 234–241.

39. Long JSE, Darrell T. *Proceedings of the IEEE conference on computer vision and pattern recognition*. Boston (2015). p. 3431–3440.

40. Alberti KG, Zimmet PZ. Definition, diagnosis and classification of diabetes mellitus and its complications. Part 1: diagnosis and classification of diabetes mellitus provisional report of a WHO consultation. *Diabet Med*. (1998) 15:539–53. doi: 10.1002/(SICI)1096-9136(199807)15:7<539::AID-DIA668>3.0.CO;2-S

41. Tanabe M, Higashi M, Tanabe M, Kawano Y, Inoue A, Narikiyo K, et al. Automated whole-volume measurement of CT fat fraction of the pancreas: correlation with Dixon MR imaging. *Br J Radiol*. (2023) 96:20220937. doi: 10.1259/bjr.20220937

42. Yao WJ, Guo Z, Wang L, Li K, Saba L, Guglielmi G, et al. Pancreas fat quantification with quantitative CT: an MRI correlation analysis. *Clin Radiol*. (2020) 75:397.e1. doi: 10.1016/j.crad.2019.12.017

43. Fantuzzi G. Adipose tissue, adipokines, and inflammation. *J Allergy Clin Immunol*. (2005) 115:911–919: quiz 920. doi: 10.1016/j.jaci.2005.02.023

44. Tilg H, Adolph TE, Dudek M, Knolle P. Non-alcoholic fatty liver disease: the interplay between metabolism, microbes and immunity. *Nat Metab*. (2021) 3:1596–607. doi: 10.1038/s42255-021-00501-9

45. Ferguson D, Finck BN. Emerging therapeutic approaches for the treatment of NAFLD and type 2 diabetes mellitus. *Nat Rev Endocrinol*. (2021) 17:484–95. doi: 10.1038/s41574-021-00507-z

46. Chan TT, Tse YK, Lui RNS, Wong GLH, Chim AML, Kong APS, et al. Fatty pancreas is independently associated with subsequent diabetes mellitus development: a 10-year prospective cohort study. *Clin Gastroenterol Hepatol*. (2022) 20:2014-2022 e2014. doi: 10.1016/j.cgh.2021.09.027

47. Jaghutriz BA, Wagner R, Heni M, Lehmann R, Machann J, Stefan N, et al. Metabolomic characteristics of fatty pancreas. *Exp Clin Endocrinol Diabetes*. (2020) 128:804–10. doi: 10.1055/a-0896-8671

48. Fukase A, Fukui T, Sasamori H, Hiromura M, Terasaki M, Mori Y, et al. Pancreatic fat accumulation evaluated by multidetector computed tomography in patients with type 2 diabetes. *J Diabetes Investig*. (2020) 11:1188–96. doi: 10.1111/jdi.13243

49. Donath MY, Shoelson SE. Type 2 diabetes as an inflammatory disease. *Nat Rev Immunol*. (2011) 11:98–107. doi: 10.1038/nri2925

50. Sater MS, AlDehaini DMB, Malalla ZHA, Ali ME, Giha HA. Plasma IL-6, TREM1, uPAR, and IL6/IL8 biomarkers increment further witnessing the chronic inflammation in type 2 diabetes. *Horm Mol Biol Clin Investig*. (2023) 44:259–69. doi: 10.1515/hmbci-2022-0103

51. Cai D, Yuan M, Frantz DF, Melendez PA, Hansen L, Lee J, et al. Local and systemic insulin resistance resulting from hepatic activation of IKK-beta and NF-kappaB. *Nat Med*. (2005) 11:183–90. doi: 10.1038/nm1166

52. de Baat A, Trinh B, Ellingsgaard H, Donath MY. Physiological role of cytokines in the regulation of mammalian metabolism. *Trends Immunol*. (2023) 44:613–27. doi: 10.1016/j.it.2023.06.002

frontiers | Frontiers in Nutrition

TYPE Original Research
PUBLISHED 14 August 2024
DOI 10.3389/fnut.2024.1406070

OPEN ACCESS

EDITED BY
Abraham Wall-Medrano,
Universidad Autónoma de Ciudad Juárez, Mexico

REVIEWED BY
Lourdes Santiago López,
National Council of Science and Technology (CONACYT), Mexico
Gihyeon Kim,
Genome and Company, Republic of Korea

*CORRESPONDENCE
Ran Wang
✉ wangran@cau.edu.cn
Bing Fang
✉ bingfang@cau.edu.cn

†These authors have contributed equally to this work and share first authorship

RECEIVED 24 March 2024
ACCEPTED 30 July 2024
PUBLISHED 14 August 2024

CITATION
Sun S, Zhang Q, Li D, Li H, Ma H, Wu X, Li Y, Wang P, Liu R, Feng H, Zhang Y, Sang Y, Fang B and Wang R (2024) Heat-killed *Bifidobacterium longum* BBMN68 and inulin protect against high-fat diet-induced obesity by modulating gut microbiota. *Front. Nutr.* 11:1406070. doi: 10.3389/fnut.2024.1406070

Heat-killed *Bifidobacterium longum* BBMN68 and inulin protect against high-fat diet-induced obesity by modulating gut microbiota

Siyuan Sun[1†], Qi Zhang[1†], Dongdong Li[1,2†], Hongliang Li[2,3], Hairan Ma[3], Xiuying Wu[3], Yixuan Li[1], Pengjie Wang[1], Rong Liu[1], Haihong Feng[4], Yongxiang Zhang[5], Yue Sang[4], Bing Fang[1]* and Ran Wang[1]*

[1]Key Laboratory of Functional Dairy, Department of Nutrition and Health, China Agricultural University, Beijing, China, [2]Inner Mongolia Mengniu Dairy (Group) Co., Ltd., Hohhot, Inner Mongolia, China, [3]Mengniu Hi-Tech Dairy (Beijing) Co., Ltd., Beijing, China, [4]Research Center for Probiotics, China Agricultural University, Beijing, China, [5]College of Food Science and Engineering, Gansu Agricultural University, Lanzhou, China

Introduction: Obesity, a pervasive global epidemic, has heightened susceptibility to chronic ailments and diminished the overall life expectancy on a global scale. Probiotics and inulin (IN) have been documented to mitigate obesity by exerting an influence on the composition of the gut microbiota. Whether heat-killed *Bifidobacterium longum* BBMN68 (MN68) and IN have an anti-obesity effect remains to be investigated.

Methods: In this study, Wistar rats were fed a high-fat diet (HFD), and orally administered heat-killed MN68 (2×10^{11} CFU/kg) and/or inulin (0.25 kg/kg) for 12 weeks. Histological analysis, serology analysis and 16S rRNA gene sequencing were performed.

Results: Heat-killed MN68 + IN treatment showed an enhanced effect on preventing weight gain, diminishing fat accumulation, and regulating lipid metabolism, compared to either heat-killed MN68 treatment or inulin treatment. Gut microbiota results showed that heat-killed MN68 + IN treatment significantly increased the relative abundance of *Bacteroidota*, *Oscillospira*, *Intestinimonas*, *Christensenella*, and *Candidatus_Stoquefichus*, and reduced the relative abundance of *Enterococcus*. Furthermore, heat-killed MN68 + IN significantly increased the SCFA levels, which were correlated with changes in the gut microbiota.

Discussion: This research provides support for the application of heat-killed MN68 and IN in the treatment of obesity, and highlights the combination of heat-killed BBMN68 and IN as functional food ingredients.

KEYWORDS

***Bifidobacterium longum* BBMN68, inulin, obesity, gut microbiota, heat-killed**

1 Introduction

The prevalence of obesity has become a serious health concern globally. Obesity, specifically excess lipid accumulation, substantially increases the risk of several diseases like type 2 diabetes, cardiovascular disease, and cancers (1). Fat reduction surgery, physical exercises, and drugs are commonly used to prevent obesity. However, all of these treatment have their inherent drawbacks: fat reduction surgeries are expensive and carry risks such as infection, bleeding, and regaining weight; physical exercises seems challengeable due to time constraints and lack of time effectiveness; drugs have several side effects, including drug dependence, abdominal pain, and abdominal distension (2). In recent decades, it has been established that gut microbiota dysbiosis is causally linked to the onset of obesity. Studies have shown that the gut microbiota participates in the decomposition and synthesis of fat through different mechanisms (3). Hence, there is an imminent requirement to discern safe and efficacious natural products for averting obesity through the modulation of gut microbiota.

Postbiotics are suitable candidates for preventing chronic disease, which is currently a very interesting topic (4). Compared with living bacteria, postbiotics possess no risk of bacteria translocation and are easy to standardize (5). Moreover, recent studies have shown that heat-killed or fragmented *lactobacillus* strains (such as CP1563, Lr263, and HK L-137) can ameliorate obesity-induced metabolic abnormalities or adipose tissue inflammation (6–8). Postbiotics contribute to obesity prevention through several mechanisms, including the enhancement of intestinal permeability, modulation of the gut microbiota and its metabolites (such as short-chain fatty acids, SCFAs) (8), and the regulation of hormone levels in the intestine to exert control over energy metabolism (9). Consequently, leveraging postbiotics stands as a promising strategy in the prevention of obesity.

Inulin is widely regarded as one of the most effective and frequently employed prebiotics for the modulation of gut microbiota (10). Studies have shown that inulin treatment leads to gut microbiota remodeling and the SCFAs increase in obese mice, which enhances the expression of angiopoietin-like protein 4 (ANGPTL4) and regulates lipid metabolism (11). Similar research revealed that inulin protects against obesity by nourishing gut microbiota to restore IL-22-mediated enterocyte function in mice going on a high-fat diet (HFD) (11, 12). In a placebo-controlled randomized trial, researchers found that oligofructose-enriched inulin selectively altered the gut microbiota and significantly reduced weight z score, body fat percentage, and serum IL-6 levels in overweight or obese children (13). It has also been shown that the incorporation of *Lactobacillus acidophilus* and inulin can improve lipid metabolism and biochemical parameters in mice with HFD (14). Nevertheless, the impact of combining inulin with heat-killed probiotics for the prevention of obesity remains unexplored.

Bifidobacterium longum BBMN68 (MN68) was isolated from the centenarian feces in Bama, China. It exerts beneficial effects like improving immunity and maintaining the integrity of the gut barrier (15). Previous studies have also explored the bile tolerance and adhesion mechanism of BBMN68, which indicates that MN68 could be used as probiotics for improving body immunity, reducing allergic responses, and enhancing the intestinal digestion function (16, 17). In this study, an HFD-induced obese rat model was established to determine if heat-killed MN68 and inulin could prevent obesity, and 16S rRNA gene sequencing method was used to analyze the gut microbiota. We aim to provide a theoretical basis for the combined use of heat-killed MN68 and inulin as natural food ingredients for preventing obesity.

2 Materials and methods

2.1 Animals and diets

Specific pathogen-free (SPF) male Wistar rats (4–5 weeks old) were obtained from Vital River Laboratory Animal Technology Co Ltd., Beijing, China. Sterilized water and standard rodent chow (Beijing University Health Science Center, Beijing, China) were provided *ad libitum* throughout the experiment. All procedures involving animals were conducted by the Guidelines in the Care and Use of Animals. The study was reviewed and approved by the Animal Studies Committee of the Health Science Center, Institute of Medicinal Plant Development, Chinese Academy of Medical Sciences, Beijing, China (Approval number: PONY-2021-FL-58).

The rats were maintained in a temperature-controlled environment (22°C ± 2°C) with a light–dark cycle alternating between 12 h of light and 12 h of darkness. For establishing the obesity prevention model, 36 rats were equally divided into six groups. After acclimatizing the rats with the basal diet for 1 week in individual cages, the rats were fed test diets for 12 weeks. The control group (two groups of rats) received physiological saline, where one control group was fed the normal diet (3.85 gm%), and the second control group was fed the high-fat diet (4.73 gm%, Table 1). The remaining four groups fed on the fat-rich diet received pasteurized yogurt alone, inulin and heat-killed BBMN68 supplements alone, and a combination of inulin and heat-killed BBMN68 supplements, respectively. All components were administered via oral gavage (1 mL/rat) every day for 12 weeks, and the experimental outline was shown in Figure 1A. The body fat rate and lean meat percentage were measured by small animal magnetic resonance imaging (MRI) system-permanent magnet MRI NM21-060H-I (Suzhou Niumag Analytical Instrument Co., Ltd., China), and the fecal samples were collected before the rats were euthanized and stored at −80°C for further use.

2.2 Preparation of the test samples

BBMN68 was cultured in De Man, Rogosa, and Sharpe (MRS) broth supplemented with 2% maltose for 24 h. After repeated culturing, BBMN68 was centrifuged at 5000 rpm for 10 min. The pellet was then dissolved in phosphate buffered solution (PBS), and BBMN68 was autoclaved at 121°C for 15 min. After BBMN68 was heat-killed and inactivated, they were powdered and mixed with pasteurized yogurt. The pasteurized yogurt was an excipient for probiotic samples. To prevent the influence of pasteurized yogurt, a pasteurized yogurt control (PY) group was also established. In the IN group, inulin supplements were added to make the final concentration of 0.25 g/mL and in the MN68 group, 2×10^8 CFU/mL heat-inactivated BBMN68 was used. In the MN68 + IN group, the same concentrations of inulin and heat-killed BBMN68 were used.

TABLE 1 Composition of normal diet and high-fat diet for rats.

	High-fat diet (Batch No. SYHF45)		Normal diet (Batch No. SYC50H)	
	gm%	kcal%	gm%	kcal%
Protein	23.7	20	19.2	20
Carbohydrate	41.4	35	67.3	70
Fat	23.6	45	4.3	10
Kcal/gm	4.73		3.85	
Ingredient	gm	kcal	gm	kcal
Casein	200	800	200	800
L-Cystine	2	12	3	12
Corn Starch	72.8	291	452.2	1808.8
Maltodextrin	100	400	75	300
Sucrose	172.8	691	172.8	691
Cellulose	50	0	50	0
Soybean Oil	25	225	25	225
Lard	177.5	1,598	20	180
Mineral Mix S10026	10	0	10	0
DiCalcium Carbonate	13	0	13	0
Calcium Carbonate	5.5	0	5.5	0
Potassium Citrate, $1H_2O$	16.5	0	16.5	0
Vitamin Mix V10001	10	40	10	40
Choline Bitartrate	2	0	2	0
FD&C Yellow Dye #5	0	0	0.04	0
FD&C Red Dye #40	0	0	0.01	0
FD&C Blue Dye #1	0.05	0	0	0
Total	858.15	4,057	1055.05	4,057

The unit of "gm" is the short name of "gram".

2.3 Analysis of biochemical parameters in serum

After 12 weeks, blood samples were collected from the abdominal aorta after rats were fasted overnight, and then centrifuged at 1000 × *g* for 15 min to isolate the serum, which were stored at −80°C for further use. Lipid metabolism indexes in serum including fasting plasma glucose (FPG), fasting insulin (FINS), total cholesterol (TC), triglyceride (TG), high-density lipoprotein-cholesterol (HDL-C), and low-density lipoprotein-cholesterol (LDL-C) were determined by HITACHI Automatic Analyzer 3100. The concentrations of leptin, adiponectin, lipopolysaccharide (LPS), interleukin (IL)-10, IL-1β, IL-6, IL-4, IL-10, tumor necrosis factor-α (TNF-α), and interferon-γ (IFN-γ) were measured by using commercially available enzyme-linked immunosorbent assay (ELISA) kits [Multisciences (Lianke) Biotech, Co., Ltd., Hangzhou, China].

2.4 Histological analysis

The epididymal adipose tissues were fixed in 4% paraformaldehyde and embedded in paraffin. The paraffin-embedded sections were stained using hematoxylin and eosin (H&E). The histopathology of liver tissues and epididymal adipocyte was visualized using an optical microscope (Leica DM6 B). The number and the area of the adipocytes were calculated using ImageJ 1.52v software (Wayne Rasband, National Institutes of Health, USA).

2.5 SCFAs analysis

Acetate, propionate, and butyrate concentrations were measured as described previously (18). Briefly, 25 mg of fecal sample was mixed with 500 μL of purified water containing 0.5% phosphoric acid, and the samples were ground at freezing temperature. The samples were placed in centrifuge tubes and treated with ultrasonic sound for 10 min at an ultrasonic power of 1,000 watts, followed by centrifugation at 13,000 × *g* for 15 min. Next, 200 μL of n-butanol (10 μg/mL 2-ethylbutyric acid as the internal standard) was added to the 200 μL supernatant for extraction and vortexed for 10 s. The samples were then treated using ultrasonic sound at 4°C for 10 min and centrifuged at 13000 × *g* for 5 min. The supernatant was collected and filtered through a 0.22 μm membrane. The concentration of SCFAs was measured using a gas chromatographic-mass spectrometer 8890B-7000D (GC–MS, Agilent J&W Scientific, Folsom, CA, USA) equipped with the HP-FFAP column (30 m × 0.25 mm × 0.25 μm, Agilent Technologies, Inc., Santa Clara, CA, USA). The temperature of the splitless injector was 250°C, the injection volume was 1 μL, and

the carrier gas used was nitrogen. The temperature program of the GC oven was set as follows: starting at 80°C for 5 min, increased by 20°C/min to 120°C for 2 min, increased by 5°C/min to 160°C for 8 min, and maintained at 220°C for 3 min. The temperature of the electron impact ion source was 230°C, and the electron energy was 70 eV. The MassHunter software v10.0.707.0 (Agilent, USA) was used to analyze and calculate the final concentrations of different SCFAs.

2.6 16S rRNA sequencing and gut microbiota analysis

DNA extracted from the fecal samples of mice was amplified, and 16S rDNA sequencing was performed. The primers were designed for the variable V3–V4 regions and a PCR instrument (ABI GeneAmp® 9700 type) was performed to amplify DNA fragments of samples. Each experiment was carried out in triplicate. The amplified PCR products were mixed and resolved on 2% agarose gel. The AxyPrepDNA gel extraction kit (AXYGEN company) was used to extract PCR products, diluted with Tris–HCl, and the PCR products were quantified using QuantiFluor™ -ST blue fluorescence quantification system (Promega, Wisconsin, United States). The Miseq library was built using TruSeq™ DNA Sample Prep Kit (Illumina), and PCR products were sequenced using the Illumina platform. The sequencing data is accessible at the link http://www.ncbi.nlm.nih.gov/bioproject/911911 with BioProject ID: PRJNA911911.

For downstream analysis, quality control of paired-end raw sequencing reads was performed using Fastp (version 0.19.6). Merging of the reads was conducted using Flash (version 1.2.11) as follows: (1) Bases with quality scores below 20 were trimmed from the end of reads using a sliding window of 50 bp, discarding reads shorter than 50 bp and those containing ambiguous bases (N); (2) Paired-end reads were merged based on overlap, with a minimum overlap length of 10 bp; (3) The maximum allowable mismatch ratio in the overlap region was set to 0.2, with non-conforming sequences being filtered out; and (4) Sequences were demultiplexed and reoriented according to barcodes and primers, with no mismatches allowed in barcodes and up to two mismatches allowed in primers. Normalization was achieved by rarefying all sample sequences to the same reads for subsequent analyses. For taxonomic profiling, the RDP classifier[1] was used to align sequences against the Silva 16S rRNA gene database (v138) with a confidence threshold of 70%. All reads were clustered into the operational taxonomic units (OTUs) using Usearch (version 7.1), which are defined by a 97% identity threshold of the 16S rRNA sequences. For the bioinformatics analysis, Majorbio Cloud (Majorbio Bio-Pharm Technology Co., Ltd., Shanghai, China), a web-based free platform, was used to perform the Wilcoxon rank-sum test and to construct Spearman Correlation Heatmap and the Linear discriminant analysis effect size (LEfSe) plot.

2.7 Statistical analysis

All data are represented as mean (M) ± standard deviation (SD). The data on body weight, fat accumulation, and serum levels were analyzed using one-way ANOVA with LSD test. SPSS statistics 26 was used for statistical analysis, and $p < 0.05$ was considered statistically significant.

3 Results

3.1 MN68 + IN treatment effectively reduces obesity-related parameters in obese rats

After 12 weeks of administering supplements via oral gavage, a significant reduction in the body weight of rats in the MN68 and IN group was observed compared to the HFD and IN group; the weight gain in rats from MN68, IN, and MN68 + IN group was all significantly less compared to the HFD group ($p < 0.05$) (Figures 1A,B). Regarding body composition, the body fat mass in the MN68 + IN group was significantly less ($p < 0.05$) than those in both the HFD and PY groups. No significant difference in the percentage of lean mass was found between the MN68 + IN group and the HFD group (Figure 1C). Significant reductions in both epididymal and perirenal adipose weight were observed in the IN and MN68 + IN groups compared to the HFD and PY groups (Figure 1D). There were no significant differences in the food intake among the HFD groups (Figure 1E). The rats in the IN and MN68 groups showed less obesity extent compared to the rats in the HFD group. Therefore, the combination of heat-killed MN68 and inulin showed a favorable delayed process of obesity induced by a high-fat diet.

3.2 MN68 + IN treatment changes liver and adipose histology and regulates the lipid metabolism indexes

The histopathological changes in both epididymal adipose tissues and liver tissues were observed under the microscope (Figures 2A,B). The H&E staining morphological analysis revealed that the liver and adipose tissue cells in the ND group were normal and orderly. Compared to the ND group, the liver tissue of the HFD group showed slight hepatocyte degeneration and lipid droplet infiltration. The liver lesions of IN, MN68, and MN68 + IN groups were reduced, and the number of lipid vacuoles was reduced. The outline of adipose tissue cells in the HFD group was larger than that in the ND group, and the arrangement was looser. The volume of adipocytes in IN, MN68, and MN68 + IN groups was smaller and the cell arrangement was tighter compared with the HFD group. The size of the adipocytes was measured, and the results showed that the size of adipocytes in the MN68, IN, and MN68 + IN group was significantly less ($p < 0.05$) compared to the HFD group (Figures 2C,D).

Serum lipid metabolism indexes including TC, TG, HDL-C, and LDL-C were detected in the six experimental groups. Compared to the ND group, HFD treatment significantly increased the serum TC, TG, and LDL-C levels, and significantly decreased the HDL-C level ($p < 0.05$, Figures 2E,F). There were no obvious differences in the serum levels of the four lipid metabolism indexes among the HFD group and the PY group. After MN68 treatment for 12 weeks, the serum TC and LDL-C were significantly decreased ($p < 0.05$), and there was no significant change in the TG levels between the HFD and MN68 groups ($p > 0.05$). Compared to the HFD group, a significant

1 http://rdp.cme.msu.edu/, version 2.13.

10.3389/fnut.2024.1406070

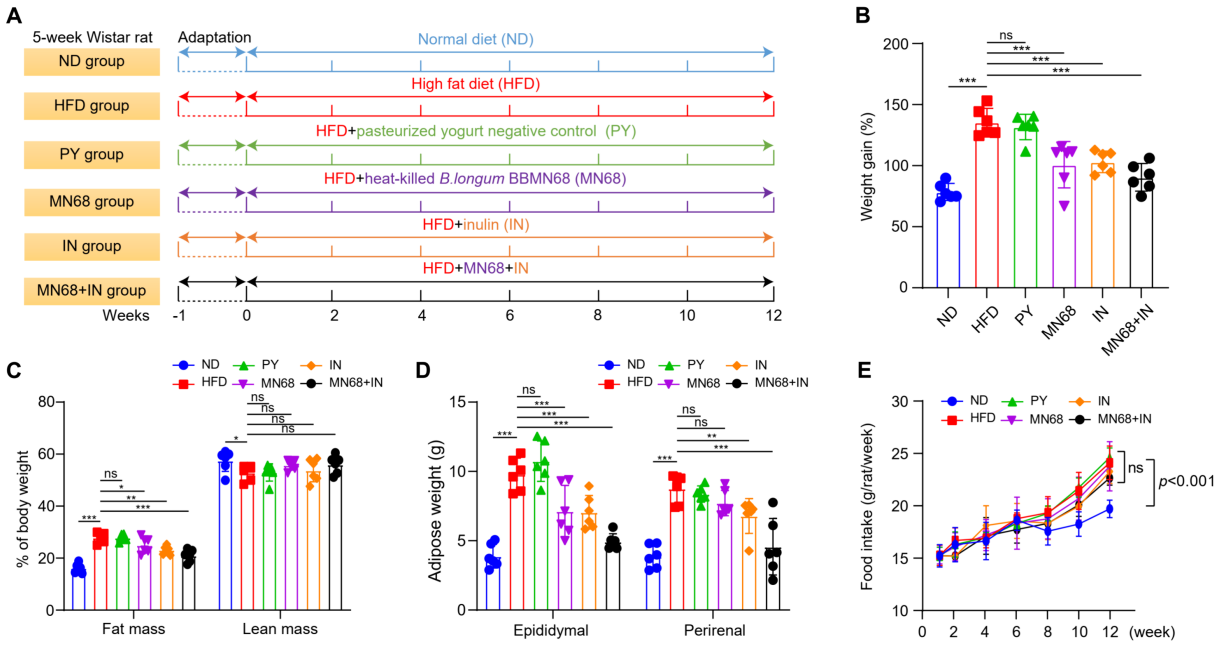

FIGURE 1
Heat-killed MN68 and inulin reduce body weight and fat accumulation in HFD-induced obesity rats. Experimental workflow in rats **(A)**. Body weight gain after 12 weeks **(B)**. Fat mass and lean mass percentage of body weight **(C)**. Total white fat weight from different organs **(D)**. Food intake **(E)**. Rats were divided into six groups (per group $n = 6$): ND, normal diet; HFD, high-fat diet; PY, pasteurized yogurt treatment; IN, pasteurized yogurt with inulin treatment; MN68, pasteurized yogurt with BBMN68 treatment; MN68 + IN, pasteurized yogurt with both inulin and BBMN68 treatment. Data were presented as the means (M) ± standard deviation (SD). p values were determined by a one-way ANOVA with LSD test. *$p < 0.05$; **$p < 0.01$, ***$p < 0.001$.

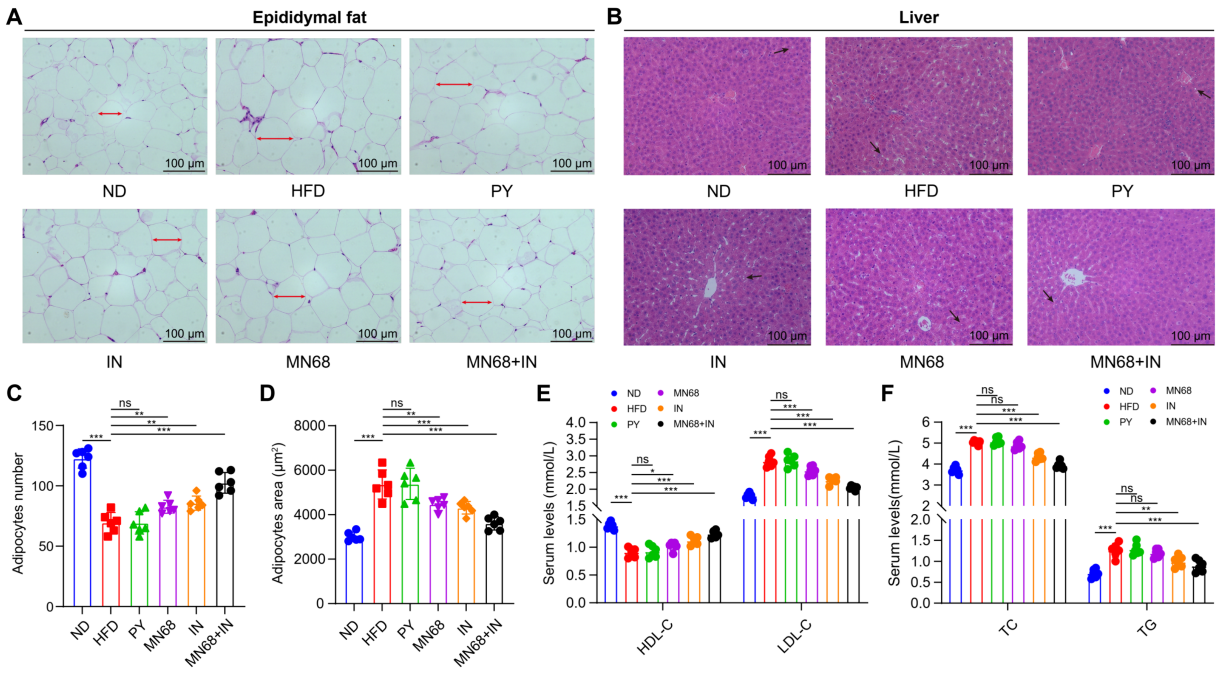

FIGURE 2
Heat-killed MN68 and inulin improve serum lipid metabolism indexes, and liver and adipose tissue morphology in HFD-induced obesity rats. H&E staining of epididymal fat tissue **(A)** and liver tissue **(B)**. Epididymal adipose cell measurement indexes include adipocyte number **(C)** and adipocyte area **(D)**. Lipid metabolism indexes in serum include TC (total cholesterol), TG (triglyceride), HDL-C (high-density lipoprotein-cholesterol), and LDL-C (low-density lipoprotein-cholesterol) **(E,F)**. Rats were divided into six groups (per group $n = 6$): ND, normal diet; HFD, high-fat diet; PY, pasteurized yogurt treatment; IN, pasteurized yogurt with inulin treatment; MN68, pasteurized yogurt with BBMN68 treatment; MN68 + IN, pasteurized yogurt with both inulin and BBMN68 treatment. Data were presented as the means (M) ± standard deviation (SD). p values were determined by a one-way ANOVA with LSD test. *$p < 0.05$; **$p < 0.01$, ***$p < 0.001$.

TABLE 2 Heat-killed MN68 and inulin regulate serum biochemical parameters and insulin resistance in HFD-induced obesity rats.

Serum biochemical parameters	Groups					
	ND	HFD	PY	MN68	IN	MN68 + IN
Leptin (ng/mL)	1.996 ± 0.235^{a}	2.077 ± 0.454^{a}	2.176 ± 0.344^{a}	1.992 ± 0.185^{a}	2.101 ± 0.239^{a}	2.270 ± 0.243^{a}
Adiponectin (μg/mL)	14.304 ± 1.372^{a}	11.415 ± 1.701^{b}	11.883 ± 0.957^{b}	12.478 ± 1.222^{b}	12.589 ± 0.909^{b}	12.119 ± 1.109^{b}
LPS (EU/mL)	0.299 ± 0.038^{d}	0.599 ± 0.060^{a}	0.613 ± 0.058^{a}	0.505 ± 0.043^{b}	0.472 ± 0.047^{bc}	0.407 ± 0.076^{c}
IL-1β (pg/mL)	34.285 ± 2.216^{d}	70.255 ± 5.749^{a}	69.689 ± 4.735^{a}	60.276 ± 6.600^{b}	53.142 ± 6.976^{c}	48.935 ± 7.352^{c}
IL-6 (pg/mL)	18.905 ± 1.221^{b}	26.077 ± 4.029^{a}	25.658 ± 4.908^{a}	25.200 ± 3.355^{a}	28.823 ± 4.223^{a}	26.572 ± 2.264^{a}
TNF-α (pg/ml)	0.764 ± 0.078^{b}	0.920 ± 0.069^{a}	0.918 ± 0.140^{a}	0.860 ± 0.102^{ab}	0.827 ± 0.117^{ab}	0.862 ± 0.098^{ab}
IFN-γ (pg/mL)	19.657 ± 3.291^{d}	40.160 ± 3.896^{a}	38.669 ± 3.819^{a}	29.485 ± 4.622^{b}	26.844 ± 2.715^{bc}	23.236 ± 2.008^{cd}
IL-4 (pg/mL)	2.988 ± 0.282^{a}	2.704 ± 0.224^{c}	2.711 ± 0.235^{c}	2.751 ± 0.227^{c}	2.774 ± 0.223^{c}	2.855 ± 0.309^{b}
IL-10 (pg/mL)	7.712 ± 0.413^{a}	4.963 ± 0.443^{d}	4.809 ± 0.454^{d}	5.059 ± 0.544^{d}	6.011 ± 0.561^{c}	6.866 ± 0.394^{b}
FPG (mmol/L)	5.610 ± 0.084^{c}	6.755 ± 0.117^{a}	6.653 ± 0.102^{ab}	6.687 ± 0.126^{ab}	6.570 ± 0.184^{b}	6.558 ± 0.113^{b}
FINS (μU/mL)	2.845 ± 0.055^{b}	3.062 ± 0.069^{a}	3.055 ± 0.095^{a}	3.043 ± 0.065^{a}	3.008 ± 0.066^{a}	3.010 ± 0.047^{a}
HOMA-IR	0.710 ± 0.020^{c}	0.922 ± 0.026^{a}	0.903 ± 0.027^{ab}	0.905 ± 0.034^{ab}	0.878 ± 0.026^{b}	0.877 ± 0.024^{b}

Rats were divided into six groups (per group $n = 6$): ND, normal diet; HFD, high-fat diet; PY, pasteurized yogurt treatment; IN, pasteurized yogurt with inulin treatment; MN68, pasteurized yogurt with BBMN68 treatment; MN68 + IN, pasteurized yogurt with both inulin and BBMN68 treatment. Data were presented as the means (M) ± standard deviation (SD). p values were determined by a one-way ANOVA with LSD test, and different lowercase letters (e.g., a, b, c) indicate significant differences, $p < 0.05$. LPS, lipopolysaccharide; IL, interleukin; TNF-α, tumor necrosis factor-α; IFN-γ, interferon-γ; FPG, fasting plasma glucose; FINS, fasting insulin; HOMA-IR, homeostasis model assessment of insulin resistance; HOMA-IR was calculated by FPG (mmol/L) × FINS (μU/mL)/22.5.

decrease ($p < 0.05$) in TC, TG, and LDL-C concentrations was observed in the IN, and MN68 + IN groups, with the MN68 + IN group having the most significant effect. Thus, these results demonstrate that Heat-killed MN68 and inulin improve serum lipid metabolism indexes, and liver and adipose tissue morphology in HFD-induced obesity rats, and their combination has a better effect.

To analyze the influence of heat-killed MN68 and inulin on serum biochemical parameters in HFD-induced obesity rats, serum leptin, adiponectin, LPS, and inflammatory factors levels were detected among the six groups. As shown in Table 2, rats in the HFD group were significantly changed compared to the ND group. Heat-killed MN68 + IN had significantly effect on reducing the LPS, IL-1β, and IFN-γ levels, and lifting the IL-4 and IL-10 levels. Nevertheless, heat-killed MN68 and inulin had no significant effect on the serum leptin, adiponectin, IL-6, and TNF-α levels. Moreover, serum FPG, FINS, and HOMA-IR levels were compared to explore the effect of heat-killed MN68 and inulin on insulin resistance in HFD-induced obesity rats. Compared to the ND group, a significant increase in FPG and FINS concentrations were observed in the HFD group ($p < 0.05$). MN68 + IN treatment significantly decreased the FPG and HOMA-IR levels, but there was no significant difference in the FINS level compared to the HFD group.

3.3 MN68 + IN treatment regulates the gut microbiota composition

3.3.1 Diversity of gut microbiota

16S rDNA sequencing was performed to explore the microbial diversity in the fecal samples of rats in different groups after 12 weeks of oral gavage. The abundance of α-diversity, including *Sobs*, and *Shannon* indexes of the microbiota of rats in the ND group, was significantly higher compared to the other groups (Figures 3A,B). However, no significant differences in the abundance of α-diversity were observed in other groups. Principal coordinate analysis revealed a significant difference ($p = 0.001$) in the composition of the gut microbiota in all groups (Figure 3C). The dots of the ND group were departed from other groups while the dots of the MN68 + IN groups were departed from the HFD group (Figure 3D). Venn diagrams show that the OTU number of the ND group was much more than other groups (Figure 3E).

3.3.2 The composition of the microbial community at the phylum and genus level

As for the phyla microbiota, *Bacteroidota* and *Firmicutes* were the two main phyla among the six groups (Figures 4A,B). The abundance of *Bacteroidota* in the MN68 + IN group was significantly higher ($p < 0.05$) than those in the HFD and PY groups with the abundance of *Firmicutes* showing the opposite trend. Relative abundances at the genus level were shown in Figure 4C, and different abundances were found among the six groups. Excluding the genera categorized as "no-rank" and "unclassified," the 10 genera exhibiting the highest relative abundance include *Blautia*, *Colidextribacter*, *Ruminococcus_torques_group*, *Bacteroides*, *Lachnoclostridium*, *Lachnospiraceae_UCG-010, Ruminococcus_gauvreauii_group*, *Lachnospiraceae_NK4A136_group*, *Flavonifractor*, *Marvinbryantia*, and *Lactobacillus* (Figure 4C). The *LEfSe* analysis showed that *Blautia*, and *Faecalitalea* were significantly enriched in the MN68 group, and *Akkermansia*, *Bifidobacterium*, and *Lactococcus* were enriched in the IN group (Figure 4D). As for the MN68 + IN group, the genera *Oscillospira*, *Intestinimonas, Christensenella,* and *Candidatus_Stoquefichus* were significantly enriched.

3.3.3 MN68 + IN treatment modulates SCFA-related gut microbiota and increases SCFA production

Spearman correlation analysis was performed to study the correlation of the SCFA and the distribution of genera in fecal microbiota in all mice, and the results are shown in Figure 5A. The genera *Ruminococcus, Roseburia, Lactobacillus,* and *Bacteroides* were found to have a positive correlation with all acetate, propionate, and butyrate concentration. The concentrations of acetate, propionate, and butyrate were measured (Figure 5B). The results showed a significant

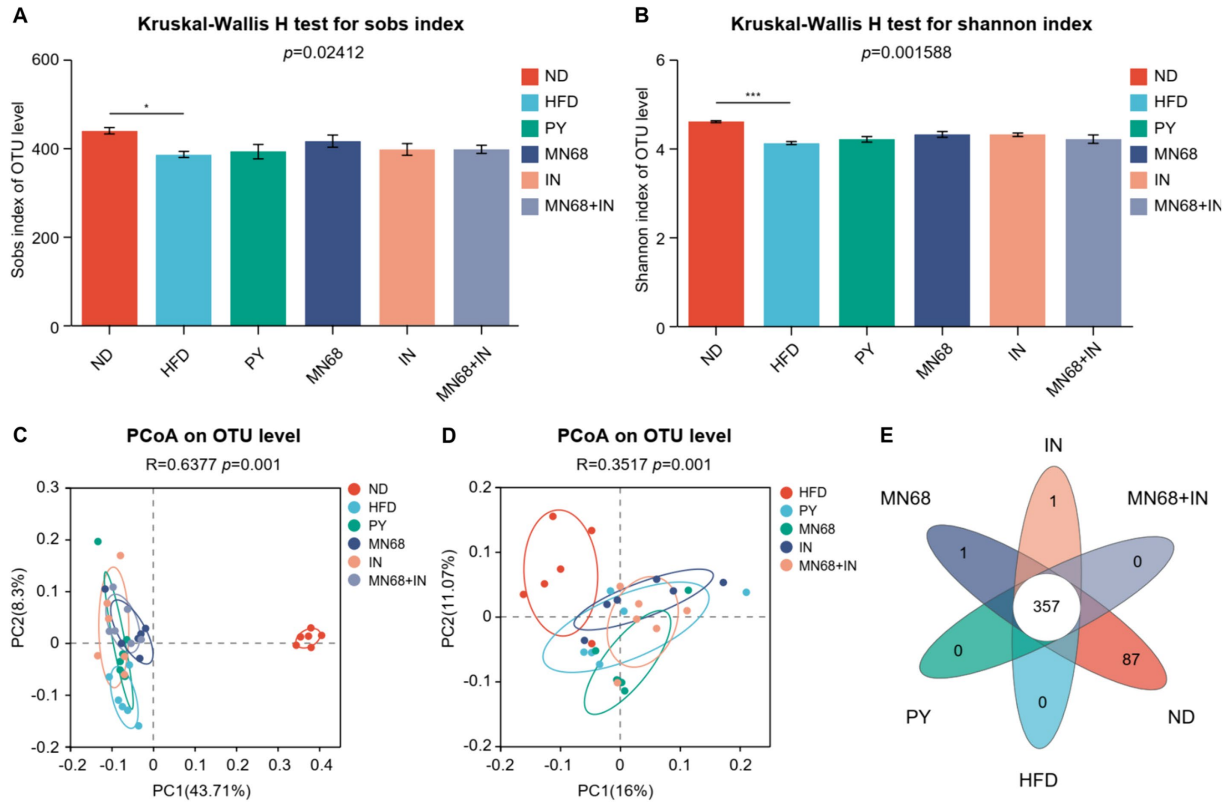

FIGURE 3
Heat-killed MN68 and inulin alter the gut microbiota diversity in HFD-induced obesity rats. Sobs **(A)** and Shannon **(B)** indexes of α-diversity. PCoA plot of β-diversity based on the OTU among groups **(C,D)**. Venn diagram with the overlapping area showing the shared OTUs among groups **(E)**. Rats were divided into six groups (per group $n = 6$): ND, normal diet; HFD, high-fat diet; PY, pasteurized yogurt treatment; IN, pasteurized yogurt with inulin treatment; MN68, pasteurized yogurt with BBMN68 treatment; MN68 + IN, pasteurized yogurt with both inulin and BBMN68 treatment. Data were presented as the means (M) ± standard deviation (SD). *p* values were determined by a one-way ANOVA with the Kruskal-Wallis test. $^{*}p < 0.05$; $^{**}p < 0.01$; $^{***}p < 0.001$.

increase ($p < 0.05$) in the levels of acetate, propionate, and butyrate in rats in the MN68 + IN group compared to the rats supplemented heat-killed MN68 or inulin alone, which tended to recover the original concentrations of SCFAs in the gut of rats in the ND group.

4 Discussion

The prevalence of obesity is high globally, so there is an urgent need to explore new effective methods to prevent and treat obesity. Mounting evidence has demonstrated that gut microbiota plays a key role in obesity development (19), and novel therapeutic approaches, such as the use of probiotics, prebiotics, and postbiotics, could aid in preventing obesity (20). Previous studies have shown that *Bifidobacterium longum* BBMN68 improves intestinal functions and immunity (15, 21). However, the potential of heat-killed BBMN68 as a postbiotic is yet to be explored. Moreover, yogurt is redefined as a carrier for probiotic food and could benefit individuals who are obese by regulating their appetite and improving intestinal barrier function as well as lipid profiles (22). However, the function of pasteurized yogurt, an ideal matrix for delivering nonviable bacteria, is still unknown. Therefore, in this study, we have determined the effect of oral administration of pasteurized yogurt containing heat-killed BBMN68 and inulin on obesity prevention using the HFD-induced Wistar rat model.

For the successful establishment of the HFD-induced obesity model, the average weight of animals in the HFD group should be 20% higher compared to the ND group (23). In our study, the average weights of rats in the ND and HFD groups were 422.12 g and 568.68 g, respectively, thus indicating that the obesity model was successfully established. HFD increases lipids in the body, which are then deposited on the white adipose tissues like epididymal adipose tissue (18). We analyzed the weight gain in rats in different groups, and the results demonstrated that the weight gain in the rats in the MN68 + IN group was significantly less, and the rats were relatively slimmer compared to the HFD and PY groups. Furthermore, a significant reduction in weight gain, fat body rate, epididymal fat weight, and adipocyte size was observed in the rats in the MN68 + IN group compared to the IN group and the MN68 group. This indicates that MN68 + IN could effectively alleviate and prevent obesity. Together, these results show that heat-killed BBMN68 and inulin have an enhanced effect on preventing obesity.

Leptin and adiponectin are the key adipokines secreted by the adipocytes. Leptin resistance is characterized by high levels of leptin in serum, typically observed in patients with nutritional obesity (24). Furthermore, the diet of these patients is rich in glucose and fat, thereby increasing the level of adiponectin in serum (25). Our results

10.3389/fnut.2024.1406070

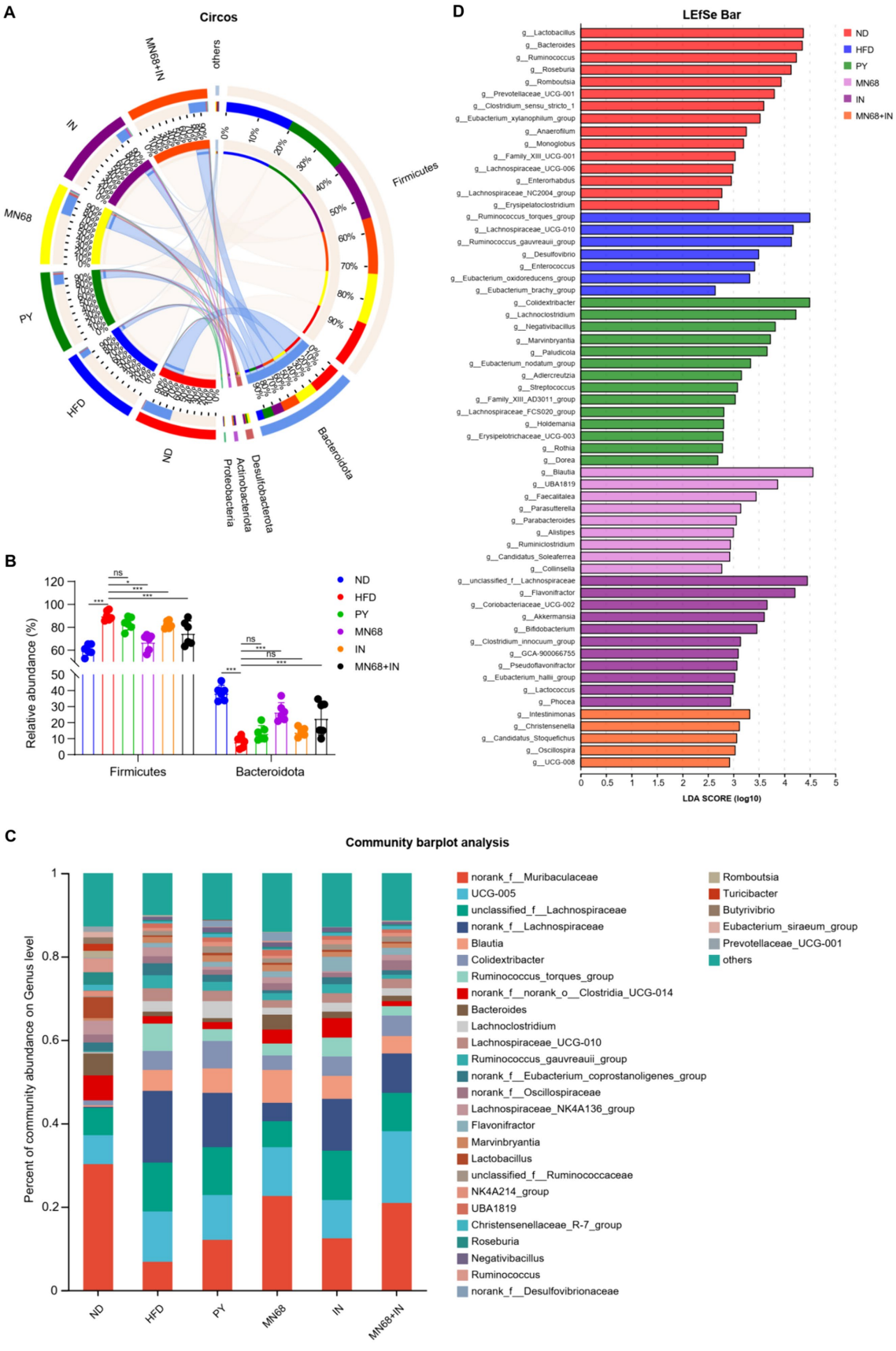

FIGURE 4
Heat-killed MN68 and inulin change the gut microbiota composition on phylum and genus levels in HFD-induced obesity rats. **(A)** Circos graph of the phyla microbiota among the six groups. **(B)** Relative abundance of *Bacteroidota* and *Firmicutes*. **(C)** Microbiota composition at the genus level.

(Continued)

FIGURE 4 (Continued)
(D) *LEfSe* analysis among the six groups. Rats were divided into six groups (per group $n = 6$): ND, normal diet; HFD, high-fat diet; PY, pasteurized yogurt treatment; IN, pasteurized yogurt with inulin treatment; MN68, pasteurized yogurt with BBMN68 treatment; MN68 + IN, pasteurized yogurt with both inulin and BBMN68 treatment. Data were presented as the means (M) ± standard deviation (SD). p values were determined by a one-way ANOVA with Kruskal-Wallis test and Wilcoxon rank-sum test. *$p < 0.05$; **$p < 0.01$, ***$p < 0.001$.

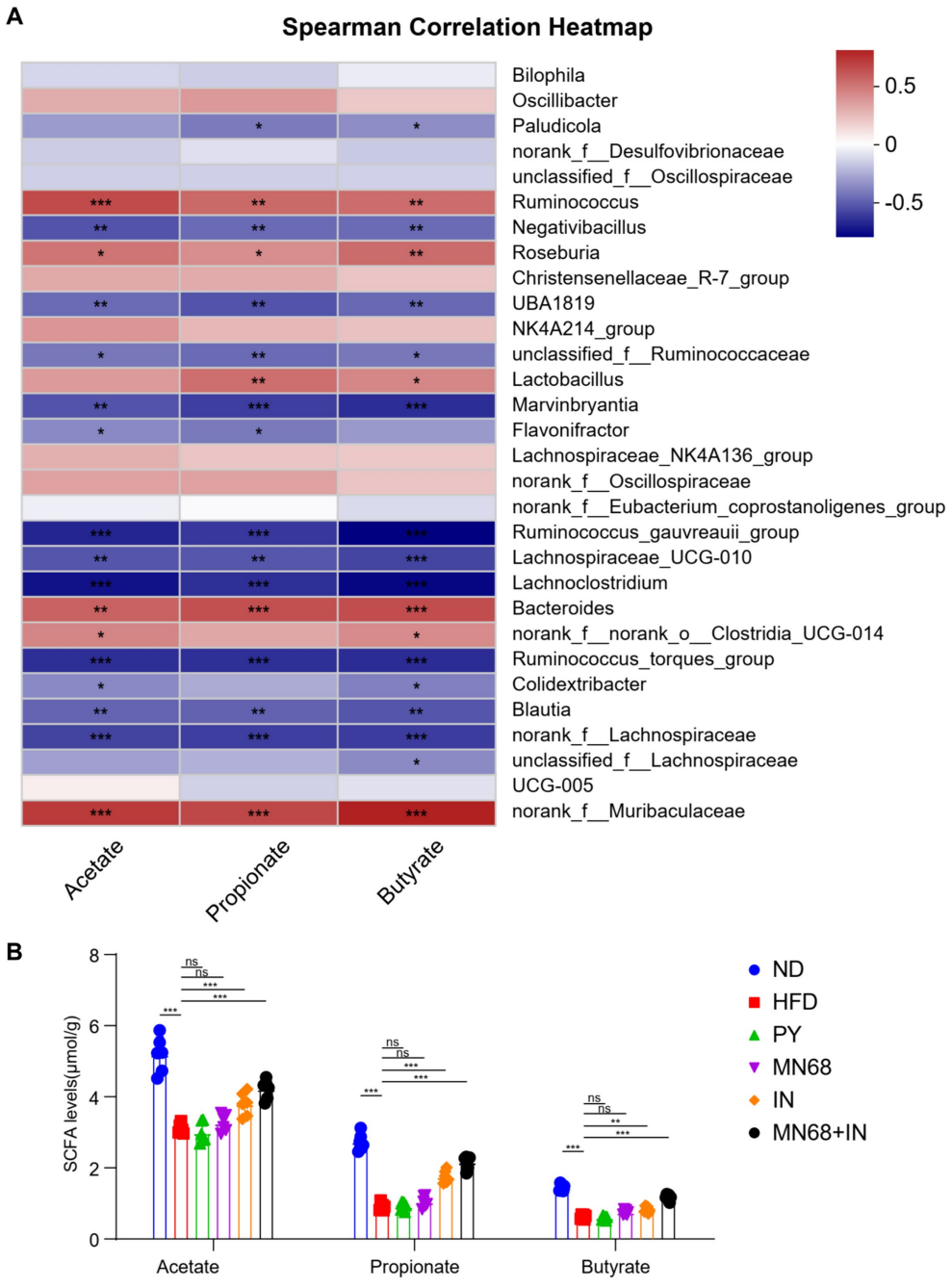

FIGURE 5
Heat-killed MN68 and inulin increase the SCFA level by regulating gut microbiota composition in HFD-induced obesity rats and regulating the relative expression of obesity-related genes. **(A)** Spearman correlation heatmap between gut microbiota and SCFA level. Red indicates a positive correlation coefficient, while blue indicates a negative correlation coefficient. **(B)** SCFA level among the six groups. Rats were divided into six groups (per group $n = 6$): ND, normal diet; HFD, high-fat diet; PY, pasteurized yogurt treatment; IN, pasteurized yogurt with inulin treatment; MN68, pasteurized yogurt with BBMN68 treatment; MN68 + IN, pasteurized yogurt with both inulin and BBMN68 treatment. Data were presented as the means (M) ± standard deviation (SD). p values were determined by a one-way ANOVA with LSD test and Wilcoxon rank-sum test. *$p < 0.05$; **$p < 0.01$, ***$p < 0.001$.

revealed an increased level of leptin and a decreased level of adiponectin in the rats in the HFD group, but there was no significant difference among the treatment groups. The same trend can also be found in the plasma glucose and insulin concentrations, indicating that the lipid-related hormone level is moderately altered in treatment groups.

In most cases, obesity can trigger a series of inflammatory reactions. IFN-γ is a pro-inflammatory cytokine, and the reduction in IFN-γ levels improves metabolic outcomes in obesity (26). IL-10 is an anti-inflammatory cytokine that could prevent diet-induced obesity and suppress inflammatory responses (27). LPS is derived from gram-negative bacteria and can induce inflammatory responses in the host. An increase in LPS levels is directly associated with increased intestinal permeability (28). Our findings indicate a reduction in levels of LPS, IL-1β, and IFN-γ in groups administrated by pasteurized yogurt, coupled with an increase in IL-4 and IL-10 levels. This suggests that pasteurized yogurt has the potential to mitigate inflammation and contribute to the preservation of the gut barrier integrity in the host.

We performed 16S rDNA sequencing to determine the composition of gut microbiota in rats. The heat-killed BBMN68 and inulin could not significantly reverse the richness of the gut microbiota of HFD-fed rats. *LEfSe* analysis revealed that the SCFA-producing genera, *Roseburia* (29), *Romboutsia* (30), and *Eubacterium xylanophilum* (31) were enriched in the ND group. Furthermore, in the IN group, the genera enriched were negatively related to obesity like *Akkermansia* (32) and *Flavonifractor* (33) while in the MN68 + IN group, SCFA-producing genera *Intestinimonas* (34), *Oscillospira* (35) were also enriched. Overall, the combination of heat-killed BBMN68 and inulin increases the abundance of SCFA-producing bacteria in the gut microbiota, which increases the level of SCFAs in the body.

A study has shown that *Roseburia* cocultured with *Akkermansia* uses mucin to produce SCFAs (36), which enhances MUC2 expression in intestinal epithelial cells and increases mucus production (37). In addition, *Blautia* produces bacteriocins to inhibit pathogenic bacteria from colonizing the intestine (38). Our results revealed that beneficial bacteria like *Blautia* were enriched in the MN68 group. The proportion of SCFA-producing bacteria *Intestinimonas* and *Oscillospira* as well as negatively obese-associated genera *Christensenella* (39) were higher in the MN68 + IN groups compared to all HFD-induced groups. *Candidatus_Stoquefichus*, which is more abundant in THE MN68 + IN group, has shown to be negatively related to gut inflammation (40). These results suggested that the combination of heat-killed BBMN68 and inulin could modulate the gut microbiota and promote the growth of SCFA-producing bacteria.

Acetate and propionate can inhibit fat accumulation in adipose tissue via G protein-coupled receptor 43/free fatty acid receptor 2 (GPR43/FFAR2) (41). Cpt1 is a rate-limiting enzyme for the mitochondrial fatty acid β-oxidation. The dietary SCFA supplementation increases the expression of *Cpt1* in adipose tissue, which is associated with GPR43 signaling (42). A study has shown that the inactivated *Lactobacillus acidophilus* and mixed prebiotics increase the concentration of acetate and propionate in feces (43). Our results showed that the concentration of SCFA was significantly higher in the MN68 + IN group compared to the HFD group. Researchers have documented the anti-inflammatory properties of SCFAs, which encompass the suppression of pro-inflammatory cytokine synthesis and the mitigation of oxidative stress within the organism (44, 45). In congruence with these findings, our results reveal that groups exhibiting elevated SCFA levels, such as the MN68 + IN group, have decreased levels of pro-inflammatory cytokines (LPS, IL-1β, and IFN-γ) and heightened levels of anti-inflammatory cytokines (IL-4 and IL-10). These outcomes suggest that MN68 + IN treatment holds potential for ameliorating oxidative stress. Collectively, our findings indicate that heat-killed BBMN68 and inulin may augment SCFA synthesis and inhibit adipose tissue lipid deposition, thereby contributing to the prevention of obesity.

Recently, more advanced sequencing techniques have emerged. For example, ASV (Amplicon Sequence Variant) analysis offers improved resolution, error detection, and data utilization in identifying species (46) compared to OTU analysis. As a result, such method can be utilized in future studies to achieve more precise taxonomical analysis. A multi-omics integrated analysis can also be employed to identify specific pathways that are pivotal in the suppression of obesity.

5 Conclusion

The co-administration of heat-killed BBMN68 and inulin demonstrates efficacy in mitigating obesity development in Wistar rats. The treatment not only attenuates weight gain but also reduces the body fat rate and the size of adipocytes. Furthermore, the co-administration of heat-killed BBMN68 and inulin promotes the enrichment of SCFA-producing bacteria, such as the genera *Intestinimonas* and *Oscillospira*. The heightened abundance of these bacteria contributes to an increased concentration of SCFAs, mitigating inflammation and preventing weight gain. Our study provides an alternative approach to obesity prevention and highlights the potential of utilizing the combination of heat-killed BBMN68 and inulin as functional food ingredients, showing promise in improving obesity. Future studies can focus on exploring more physiological functions of heat-killed BBMN68 in different models or clinical cases.

Data availability statement

The datasets presented in this study can be found in online repositories. The names of the repository/repositories and accession number(s) can be found at: https://www.ncbi.nlm.nih.gov/, PRJNA911911.

Ethics statement

The animal study was approved by the Ethics Committee of Pony Testing Group Co., Ltd. The study was conducted in accordance with the local legislation and institutional requirements.

Author contributions

SS: Conceptualization, Project administration, Writing – original draft. QZ: Conceptualization, Project administration, Writing – original draft. DL: Conceptualization, Project administration, Writing – original draft. HL: Methodology, Writing – original draft. HM: Methodology, Writing – original draft. XW: Project administration, Writing – original draft. YL: Supervision, Writing – original draft. PW: Supervision, Writing – original draft. RL: Supervision, Writing – original draft. HF: Project administration, Writing – original draft. YZ: Validation, Writing – original draft. YS: Validation, Writing – original draft. BF: Supervision, Writing – original draft. RW: Writing – review & editing.

Funding

The author(s) declare financial support was received for the research, authorship, and/or publication of this article. This research was financially supported by the National Key R&D Program of China (grant number 2021YFD1600204).

Acknowledgments

The spelling, grammar, sentence structure, and terminology of our manuscript were edited by Bullet Edits Limited.

Conflict of interest

DL and HL were employed by Inner Mongolia Mengniu Dairy (Group) Co., Ltd., China. HL, HM and XW were employed by Mengniu Hi-Tech Dairy (Beijing) Co., Ltd., China.

The remaining authors declare that the research was conducted in the absence of any commercial or financial relationships that could be construed as a potential conflict of interest.

Publisher's note

All claims expressed in this article are solely those of the authors and do not necessarily represent those of their affiliated organizations, or those of the publisher, the editors and the reviewers. Any product that may be evaluated in this article, or claim that may be made by its manufacturer, is not guaranteed or endorsed by the publisher.

Supplementary material

The Supplementary material for this article can be found online at: https://www.frontiersin.org/articles/10.3389/fnut.2024.1406070/full#supplementary-material

References

1. Bluher M. Obesity: global epidemiology and pathogenesis. *Nat Rev Endocrinol*. (2019) 15:288–98. doi: 10.1038/s41574-019-0176-8

2. Franz MJ, Van Wormer JJ, Crain AL, Boucher JL, Histon T, Caplan W, et al. Weight-loss outcomes: a systematic review and meta-analysis of weight-loss clinical trials with a minimum 1-year follow-up. *J Am Diet Assoc*. (2007) 107:1755–67. doi: 10.1016/j.jada.2007.07.017

3. Sun L, Ma L, Ma Y, Zhang F, Zhao C, Nie Y. Insights into the role of gut microbiota in obesity: pathogenesis, mechanisms, and therapeutic perspectives. *Protein Cell*. (2018) 9:397–403. doi: 10.1007/s13238-018-0546-3

4. Salminen S, Collado MC, Endo A, Hill C, Lebeer S, Quigley EMM, et al. The International Scientific Association of Probiotics and Prebiotics (ISAPP) consensus statement on the definition and scope of postbiotics. *Nat Rev Gastroenterol Hepatol*. (2021) 18:649–67. doi: 10.1038/s41575-021-00440-6

5. Homayouni Rad A, Aghebati Maleki L, Samadi Kafil H, Fathi Zavoshti H, Abbasi A. Postbiotics as novel health-promoting ingredients in functional foods. *Health Promot Perspect*. (2020) 10:3–4. doi: 10.15171/hpp.2020.02

6. Nakamura F, Ishida Y, Sawada D, Ashida N, Sugawara T, Sakai M, et al. Fragmented lactic acid bacterial cells activate peroxisome proliferator-activated receptors and ameliorate dyslipidemia in obese mice. *J Agric Food Chem*. (2016) 64:2549–59. doi: 10.1021/acs.jafc.5b05827

7. Hsieh FC, Lan CC, Huang TY, Chen KW, Chai CY, Chen WT, et al. Heat-killed and live *Lactobacillus reuteri* GMNL-263 exhibit similar effects on improving metabolic functions in high-fat diet-induced obese rats. *Food Funct*. (2016) 7:2374–88. doi: 10.1039/C5FO01396H

8. Yoshitake R, Hirose Y, Murosaki S, Matsuzaki G. Heat-killed *Lactobacillus plantarum* L-137 attenuates obesity and associated metabolic abnormalities in C57BL/6 J mice on a high-fat diet. *Biosci Microbiota Food Health*. (2021) 40:84–91. doi: 10.12938/bmfh.2020-040

9. Chambers ES, Viardot A, Psichas A, Morrison DJ, Murphy KG, Zac-Varghese SE, et al. Effects of targeted delivery of propionate to the human colon on appetite regulation, body weight maintenance and adiposity in overweight adults. *Gut*. (2015) 64:1744–54. doi: 10.1136/gutjnl-2014-307913

10. Li T, Zhang Y, Song J, Chen L, Du M, Mao X. Yogurt enriched with inulin ameliorated reproductive functions and regulated gut microbiota in dehydroepiandrosterone-induced polycystic ovary syndrome mice. *Nutrients*. (2022) 14:279. doi: 10.3390/nu14020279

11. Zou J, Chassaing B, Singh V, Pellizzon M, Ricci M, Fythe MD, et al. Fiber-mediated nourishment of gut microbiota protects against diet-induced obesity by restoring IL-22-mediated colonic health. *Cell Host Microbe*. (2018) 23:41–53.e4. doi: 10.1016/j.chom.2017.11.003

12. Guo J, Zhang M, Wang H, Li N, Lu Z, Li L, et al. Gut microbiota and short chain fatty acids partially mediate the beneficial effects of inulin on metabolic disorders in obese ob/ob mice. *J Food Biochem*. (2022) 46:e14063. doi: 10.1111/jfbc.14063

13. Nicolucci AC, Hume MP, Martinez I, Mayengbam S, Walter J, Reimer RA. Prebiotics reduce body fat and alter intestinal microbiota in children who are overweight or with obesity. *Gastroenterology*. (2017) 153:711–22. doi: 10.1053/j.gastro.2017.05.055

14. Rangel-Torres BE, Garcia-Montoya IA, Rodriguez-Tadeo A, Jimenez-Vega F. The symbiosis between Lactobacillus acidophilus and inulin: metabolic benefits in an obese murine model. *Probiotics Antimicrob Proteins*. (2022) 16:26–34. doi: 10.1007/s12602-022-10012-y

15. Yang H, Liu A, Zhang M, Ibrahim SA, Pang Z, Leng X, et al. Oral administration of live Bifidobacterium substrains isolated from centenarians enhances intestinal function in mice. *Curr Microbiol*. (2009) 59:439–45. doi: 10.1007/s00284-009-9457-0

16. Xiong Y, Zhai Z, Lei Y, Xiao B, Hao Y. A novel major pilin subunit protein fimM is involved in adhesion of bifidobacterium longum BBMN68 to intestinal epithelial cells. *Front Microbiol*. (2020) 11:590435. doi: 10.3389/fmicb.2020.590435

17. Xu Q, Zhai Z, An H, Yang Y, Yin J, Wang G, et al. The MarR family regulator BmrR is involved in bile tolerance of *Bifidobacterium longum* BBMN68 via controlling the expression of an ABC transporter. *Appl Environ Microbiol*. (2019) 85:e02453-18. doi: 10.1128/AEM.02453-18

18. Cao Q, Liu L, Hu Y, Jiang N, Wang Y, Chen J, et al. Irradiation of carotid baroreceptor with low-intensity pulsed ultrasound exerts different metabolic protection in perirenal, epididymal white adipose tissue and interscapular brown adipose tissue of obese rats. *FASEB J*. (2020) 34:15431–47. doi: 10.1096/fj.202001550R

19. Gomes AC, Hoffmann C, Mota JF. The human gut microbiota: metabolism and perspective in obesity. *Gut Microbes*. (2018) 9:308–25. doi: 10.1080/19490976.2018.1465157

20. Cuevas-Sierra A, Ramos-Lopez O, Riezu-Boj JI, Milagro FI, Martinez JA. Diet, gut microbiota, and obesity: links with host genetics and epigenetics and potential applications. *Adv Nutr*. (2019) 10:S17–30. doi: 10.1093/advances/nmy078

21. Yang HY, Liu SL, Ibrahim SA, Zhao L, Jiang JL, Sun WF, et al. Oral administration of live Bifidobacterium substrains isolated from healthy centenarians enhanced immune function in BALB/c mice. *Nutr Res*. (2009) 29:281–9. doi: 10.1016/j.nutres.2009.03.010

22. Hill C, Guarner F, Reid G, Gibson GR, Merenstein DJ, Pot B, et al. Expert consensus document. The International Scientific Association for Probiotics and Prebiotics consensus statement on the scope and appropriate use of the term probiotic. *Nat Rev Gastroenterol Hepatol*. (2014) 11:506–14. doi: 10.1038/nrgastro.2014.66

23. Hariri N, Thibault L. High-fat diet-induced obesity in animal models. *Nutr Res Rev*. (2010) 23:270–99. doi: 10.1017/S0954422410000168

24. Pan H, Guo J, Su Z. Advances in understanding the interrelations between leptin resistance and obesity. *Physiol Behav*. (2014) 130:157–69. doi: 10.1016/j.physbeh.2014.04.003

25. Moreno-Fernandez S, Garces-Rimon M, Vera G, Astier J, Landrier JF, Miguel M. High fat/high glucose diet induces metabolic syndrome in an experimental rat model. *Nutrients*. (2018) 10:1502. doi: 10.3390/nu10101502

26. Strissel KJ, DeFuria J, Shaul ME, Bennett G, Greenberg AS, Obin MS. T-cell recruitment and Th1 polarization in adipose tissue during diet-induced obesity in C57BL/6 mice. *Obesity (Silver Spring)*. (2010) 18:1918–25. doi: 10.1038/oby.2010.1

27. Hong EG, Ko HJ, Cho YR, Kim HJ, Ma Z, Yu TY, et al. Interleukin-10 prevents diet-induced insulin resistance by attenuating macrophage and cytokine response in skeletal muscle. *Diabetes*. (2009) 58:2525–35. doi: 10.2337/db08-1261

28. Saad MJ, Santos A, Prada PO. Linking gut microbiota and inflammation to obesity and insulin resistance. *Physiology*. (2016) 31:283–93. doi: 10.1152/physiol.00041.2015

29. Reichardt N, Duncan SH, Young P, Belenguer A, McWilliam Leitch C, Scott KP, et al. Phylogenetic distribution of three pathways for propionate production within the human gut microbiota. *ISME J*. (2014) 8:1323–35. doi: 10.1038/ismej.2014.14

30. Ye X, Liu Y, Hu J, Gao Y, Ma Y, Wen D. Chlorogenic acid-induced gut microbiota improves metabolic endotoxemia. *Front Endocrinol*. (2021) 12:762691. doi: 10.3389/fendo.2021.762691

31. Wei J, Zhao Y, Zhou C, Zhao Q, Zhong H, Zhu X, et al. Dietary polysaccharide from *Enteromorpha clathrata* attenuates obesity and increases the intestinal abundance of butyrate-producing bacterium, eubacterium xylanophilum, in mice fed a high-fat diet. *Polymers*. (2021) 13:3286. doi: 10.3390/polym13193286

32. Cani PD, de Vos WM. Next-generation beneficial microbes: the case of *Akkermansia muciniphila*. *Front Microbiol*. (2017) 8:1765. doi: 10.3389/fmicb.2017.01765

33. Manca C, Lacroix S, Perusse F, Flamand N, Chagnon Y, Drapeau V, et al. Oral capsaicinoid administration alters the plasma endocannabinoidome and fecal microbiota of reproductive-aged women living with overweight and obesity. *Biomedicines*. (2021) 9:1246. doi: 10.3390/biomedicines9091246

34. Klaring K, Hanske L, Bui N, Charrier C, Blaut M, Haller D, et al. Intestinimonas butyriciproducens gen. nov., sp. nov., a butyrate-producing bacterium from the mouse intestine. *Int J Syst Evol Microbiol*. (2013) 63:4606–12. doi: 10.1099/ijs.0.051441-0

35. Hu Y, Xu J, Sheng Y, Liu J, Li H, Guo M, et al. Pleurotus ostreatus ameliorates obesity by modulating the gut microbiota in obese mice induced by high-fat diet. *Nutrients*. (2022) 14:1868. doi: 10.3390/nu14091868

36. Pichler MJ, Yamada C, Shuoker B, Alvarez-Silva C, Gotoh A, Leth ML, et al. Butyrate producing colonic *Clostridiales metabolise* human milk oligosaccharides and cross feed on mucin via conserved pathways. *Nat Commun*. (2020) 11:3285. doi: 10.1038/s41467-020-17075-x

37. Paone P, Cani PD. Mucus barrier, mucins and gut microbiota: the expected slimy partners? *Gut*. (2020) 69:2232–43. doi: 10.1136/gutjnl-2020-322260

38. Liu X, Mao B, Gu J, Wu J, Cui S, Wang G, et al. Blautia-a new functional genus with potential probiotic properties? *Gut Microbes*. (2021) 13:1–23. doi: 10.1080/19490976.2021.1903826

39. Singh TP, Natraj BH. Next-generation probiotics: a promising approach towards designing personalized medicine. *Crit Rev Microbiol*. (2021) 47:479–98. doi: 10.1080/1040841X.2021.1902940

40. Yang X, He Z, Hu R, Yan J, Zhang Q, Li B, et al. Dietary beta-carotene on postpartum uterine recovery in mice: crosstalk between gut microbiota and inflammation. *Front Immunol*. (2021) 12:744425. doi: 10.3389/fimmu.2021.744425

41. Kimura I, Ozawa K, Inoue D, Imamura T, Kimura K, Maeda T, et al. The gut microbiota suppresses insulin-mediated fat accumulation via the short-chain fatty acid receptor GPR43. *Nat Commun*. (2013) 4:1829. doi: 10.1038/ncomms2852

42. Lu Y, Fan C, Li P, Lu Y, Chang X, Qi K. Short chain fatty acids prevent high-fat-diet-induced obesity in mice by regulating G protein-coupled receptors and gut microbiota. *Sci Rep*. (2016) 6:37589. doi: 10.1038/srep37589

43. Panasevich MR, Daristotle L, Quesnell R, Reinhart GA, Frantz NZ. Altered fecal microbiota, IgA, and fermentative end-products in adult dogs fed prebiotics and a nonviable *Lactobacillus acidophilus*. *J Anim Sci*. (2021) 99:skab347. doi: 10.1093/jas/skab347

44. Lucas S, Omata Y, Hofmann J, Bottcher M, Iljazovic A, Sarter K, et al. Short-chain fatty acids regulate systemic bone mass and protect from pathological bone loss. *Nat Commun*. (2018) 9:55. doi: 10.1038/s41467-017-02490-4

45. Medawar E, Beyer F, Thieleking R, Haange SB, Rolle-Kampczyk U, Reinicke M, et al. Prebiotic diet changes neural correlates of food decision-making in overweight adults: a randomised controlled within-subject cross-over trial. *Gut*. (2024) 73:298–310. doi: 10.1136/gutjnl-2023-330365

46. Jeske JT, Gallert C. Microbiome analysis via OTU and ASV-based pipelines-a comparative interpretation of ecological data in WWTP systems. *Bioengineering*. (2022) 9:146. doi: 10.3390/bioengineering9040146

frontiers | Frontiers in Nutrition

TYPE Clinical Trial
PUBLISHED 27 November 2024
DOI 10.3389/fnut.2024.1510318

OPEN ACCESS

EDITED BY
Xiaolong Ji,
Zhengzhou University of Light Industry, China

REVIEWED BY
Junhua Xie,
Nanchang University, China
Jiajia Song,
Southwest University, China

*CORRESPONDENCE
Chenyuan Wang
✉ wangchenyuan@mengniu.cn
Jingjing He
✉ hejingjing89@cau.edu.cn
Ran Wang
✉ wangran@cau.edu.cn

†These authors have contributed equally to this work

Received 12 October 2024
ACCEPTED 15 November 2024
PUBLISHED 27 November 2024

CITATION
Niu X, Zhang Q, Liu J, Zhao Y, Shang N, Li S, Liu Y, Xiong W, Sun E, Zhang Y, Zhao H, Li Y, Wang P, Fang B, Zhao L, Chen J, Wang F, Pang G, Wang C, He J and Wang R (2024) Effect of synbiotic supplementation on obesity and gut microbiota in obese adults: a double-blind randomized controlled trial. *Front. Nutr.* 11:1510318. doi: 10.3389/fnut.2024.1510318

Effect of synbiotic supplementation on obesity and gut microbiota in obese adults: a double-blind randomized controlled trial

Xiaokang Niu[1†], Qi Zhang[2†], Julong Liu[3†], Yuyang Zhao[1], Nan Shang[1], Shusen Li[3], Yinghua Liu[4], Wei Xiong[5], Erna Sun[3], Yong Zhang[4], Hongfeng Zhao[3], Yixuan Li[1], Pengjie Wang[1], Bing Fang[2], Liang Zhao[2], Juan Chen[1], Fuqing Wang[6], Guofang Pang[7], Chenyuan Wang[3]*, Jingjing He[2]* and Ran Wang[1]*

[1]Key Laboratory of Functional Dairy, Co-Constructed by Ministry of Education and Beijing Government, Department of Nutrition and Health, China Agricultural University, Beijing, China, [2]Research Center for Probiotics, China Agricultural University, Beijing, China, [3]Mengniu Hi-Tech Dairy Product Beijing Co., Ltd., Beijing, China, [4]Department of Nutrition, The First Medical Center of Chinese PLA General Hospital, Beijing, China, [5]Food Laboratory of Zhongyuan, Luohe, China, [6]Tibet Tianhong Science and Technology Co., Ltd., Lhasa, China, [7]Chinese Academy of Inspection and Quarantine, Beijing, China

Background: Synbiotics, combining specific probiotics and selected prebiotics, may benefit health issues like obesity, but evidence remains inconsistent.

Objective: This study aimed to verify the effect of a pre-screened synbiotics combination [containing *Bifidobacterium animalis* subsp. *lactis* MN-Gup (MN-Gup), galacto-oligosaccharides (GOS) and xylo-oligosaccharides (XOS)] on obesity in the population.

Methods: In a randomized, double-blind, placebo-controlled trial, 80 individuals with obesity consumed daily synbiotics (containing MN-Gup 1×10^{11} CFU/day, GOS 0.7 g/day, and XOS 0.7 g/day) or placebo for 12 weeks. Body composition, blood lipids, serum hormone, bile acids, and gut microbiota were measured pre-and post-intervention.

Results: Synbiotics supplementation significantly decreased body fat percentage, waist, and serum low-density lipoprotein cholesterol (LDL-C), increased peptide YY, cholecystokinin, oxyntomodulin, GSH (glutathione peroxidase) in individuals with obesity. Additionally, synbiotic supplementation led to an enrichment of beneficial bacteria and bile acids chenodeoxycholic acid (CDCA). *Bifidobacterium* and *Romboutsia* were significantly positively correlated with CDCA. A more favorable effect was observed in individuals with obesity and abnormal LDL-C compared to those without dyslipidemia.

Conclusion: Twelve-week synbiotics intervention reduced body fat percentage, waist, and serum LDL-C, especially in individuals with obesity and abnormal LDL-C. The possible mechanisms may be related to changes in gut microbiota, bile acids and gut hormones.

Clinical trial registration: Chictr.org.cn, identifier ChiCTR2200064156.

KEYWORDS

Bifidobacterium animalis subsp. *lactis* MN-Gup, synbiotics, obesity, gut microbiota, randomized controlled trial

1 Introduction

Obesity represents a serious global public health challenge, with its prevalence escalating rapidly over the past five decades, affecting approximately 700 million adults worldwide (1). Due to excessive fat accumulation, obesity is strongly associated with dyslipidemia, hypertension and cardiovascular diseases (2). There are currently various ways to alleviate obesity, such as drug intervention, surgical intervention, etc., but these methods have their own limitations, such as high side effects and high risks. Therefore, safe and effective ways to alleviate obesity are of great significance and need to be found.

Probiotics have garnered significant attention in the application of relieving obesity due to their potential in regulating gut microbiota and its metabolites (3–7). Research has shown that certain beneficial bacteria can modify bile acid composition (8). Additionally, secondary bile acids have been shown to active Takeda G protein-coupled receptor 5 (TGR5), thereby promoting the proliferation of intestinal epithelial cells (9), which subsequently secrete hormones such as peptide YY (PYY), cholecystokinin (CCK), oxyntomodulin (OXM), and human angiopoietin-like protein 4 (ANGPTL4) (10–12), all of which have been supported to possess the potential of inhibiting fat synthesis (13–15).

Prebiotics are organic substances that are not digested and absorbed by the host, but can selectively promote the proliferation of some bacteria in human gut, thereby improving the health of the host (16, 17). Besides, they can also increase the survival rate of probiotics in the gastrointestinal tract (18). The synergistic combinations of probiotics and prebiotics, known as synbiotics, are hypothesized to exert a more potent impact compared to individual probiotics and prebiotics (19). Prebiotics such as inulin, fructo-oligosaccharides (FOS), galacto-oligosaccharides (GOS), xylo-oligosaccharides (XOS), and polydextrose are commonly combined with probiotics to form synbiotics, aiming to enhance their effects (20–23). However, the efficacy of different synbiotics in improving obesity varies. For instance, a combination of *Lactobacillus acidophilus*, *Bifidobacterium lactis*, *Bifidobacterium longum*, and *Bifidobacterium bifidum* and GOS was found to regulate gut microbiota and reduce weight in individuals with obesity (24). Synbiotics containing *Bifidobacterium lactis* UBBLa-70 and FOS not only improved body composition but also regulated glucose and lipid metabolism (25). Conversely, another study showed that the synbiotics comprising *Lactobacillus acidophilus*, *Bifidobacterium lactis*, *Bifidobacterium longum*, and *Bifidobacterium bifidum* and GOS did not exhibit statistically significant differences in body composition (24).

Given that the primary objective of incorporating prebiotics in synbiotics is to selectively enhance the proliferation of probiotics, the formulation combining probiotics and prebiotics holds significant importance. The variability observed in the effect of synbiotics on ameliorating obesity could potentially be attributed to whether a pre-screening process for the combination of probiotics and prebiotics was conducted. Our previous *in vitro* pre-screening experiments have demonstrated that GOS and XOS exhibit significant potential in promoting the proliferation of *Bifidobacterium animalis* subsp. *lactis* MN-Gup (MN-Gup, which is from BaMa longevity village, Guangxi, China, CGMCC No. 15578), rendering them suitable for synergistic combining to form synbiotics combination (26). Furthermore, our subsequent animal experiments have revealed that MN-Gup-based synbiotics possessed promising capabilities in significantly alleviating obesity in mice (26). This study aimed to investigate the effect of synbiotics (MN-Gup-GOS-XOS, containing MN-Gup, GOS and XOS) on improving obesity-related indicators and gut microbiota through a randomized controlled trial involving individuals with obesity.

2 Methods

2.1 Study design

A randomized, double-blind, placebo-controlled trial was designed to investigate the effects of synbiotics on alleviating obesity in individuals with obesity in Beijing, China, and was performed between November 2022 and February 2023. The study was approved by the Institutional Review Board of China Agricultural University Ethics Committee (CAUHR-20220903, registered on September 23, 2022). Written informed permission was acquired from each individual.

2.2 Inclusion and exclusion criteria

Inclusion criteria: (1) aged 18–45 years; and (2) body mass index (BMI) $\geq$28 kg/m^2 or body fat percentage for males >25%, females >30%.

Exclusion criteria: (1) secondary obesity caused by diseases (e.g., hypothalamic obesity, pituitary obesity, thyroid obesity, adrenal obesity, or pancreatic obesity); or (2) in pregnancy or lactation; or (3) suffering from severe gastrointestinal diseases (i.e., ulcers, bleeding, obstruction, tumors, etc.); or (4) with a history of other serious disorders (i.e., diseases of heart, liver, kidney, brain, hematopoietic system, mental, tumors, etc.); or (5) taking weight-loss pills, antibiotics, proton pump inhibitors, H_2 receptor antagonists, laxatives, antidiarrheal drugs, antibacterial agents, and hormones within 4 weeks; or (6) had taken probiotics within 1 month before the study; (7) participated in other clinical trials within 3 months.

2.3 Randomization and blinding

The randomization process was conducted by a research assistant who was not involved in the study. Randomization was performed using the Pocock and Simon minimization dynamic randomization method, incorporating baseline data (age, gender, BMI, and body fat percentage) to ensure balanced allocation across intervention groups at baseline participants were randomly assigned (1:1) to the synbiotic group and placebo group. Researchers and participants were blinded to intervention assignments until the study was completed.

2.4 Intervention and procedures

Prior to the study, participants were recruited via the internet and were subjected to age, gender, body composition, disease status, and drug use for screening. This study included a 2-week run-in period and a 12-week intervention period (Supplementary Figure S1). Throughout the run-in period, the participants were strictly prohibited from consuming foods containing probiotics (such as probiotic powder, probiotic yogurt, etc.). During the intervention period, everyone was instructed to consume a sachet of synbiotics (containing MN-Gup 1×10^{11} CFU/day, GOS 0.7 g/day, and XOS 0.7 g/day) or a sachet of placebo (maltodextrin powder without probiotics and prebiotic) once daily after either lunch or dinner for a duration of 12 weeks. The synbiotics and placebo utilized in this study were provided by Mengniu Hi-Tech Dairy Product Beijing Co., Ltd. Participants were requested to maintain their regular diet and exercise routine and were instructed to refrain from taking any other probiotics or probiotic-containing dietary supplements. Any adverse events or discomfort experienced by the participants were to be noted down in their diaries. Blood and fecal samples were collected and body composition were detected before and after intervention, respectively.

2.5 Primary outcomes

Primary outcomes are BMI and body fat percentage (body fat mass/weight), which were measured using the Inbody 770 body composition tester (Biospace Shanghai Co., Ltd., China).

2.6 Exploratory outcomes

2.6.1 Body composition measurement

Soft lean mass of subjects was measured using the Inbody 770 body composition tester (Biospace Shanghai Co., Ltd., China). Waist circumference and hip circumference (cm) were measured using a flexible tape.

2.6.2 Blood sample collection and blood index measurement

Blood samples were collected via venipuncture following an overnight fasting period both before and after the intervention. Subsequently, serum was collected by centrifugation to quantify blood lipids, serum hormones, bile acids, as well as markers of liver and kidney function.

Total cholesterol (TC), triglycerides (TG), low-density lipoprotein cholesterol (LDL-C), and high-density lipoprotein cholesterol (HDL-C) were measured using Elabscience ELISA kits (Elabscience Biotechnology Co., Ltd., China). Hormone indicators including peptide YY (PYY), cholecystokinin (CCK), oxyntomodulin (OXM), angiopoietin like protein 4 (ANGPTL4), GSH (glutathione peroxidase), T-AOC (total antioxidant capacity) of serum were measured using Meimian ELISA kits (Jiangsu Meimian industrial Co., Ltd., China), according to the manufacturer's instructions. Serum uric acid (UA), creatinine (CR), urea (UR), aspartate aminotransferase (AST), and alanine aminotransferase (ALT), as the safety indicators, were measured using COIBO ELISA kits (Shanghai COIBO Biotechnology Co., Ltd., China).

2.7 Dietary information measurement

A dietary questionnaire was employed to assess the individuals' dietary information for three consecutive days, both before and after the intervention. Subjects were given written and verbal instructions on how to maintain a complete food record with sufficient detail for analysis. If information was incomplete, the staff contacted the individual to confirm details of the foods consumed. Energy, carbohydrate, fat, and protein intake were computed using the food exchange method (27).

2.8 Serum bile acid measurement

Fasting plasma samples were obtained via venipuncture and serum was collected by centrifugation. Serum bile acids were measured refers to the previous research method using Agilent ultra-high-performance liquid chromatography-mass spectrometry (UHPLC-MS) [Agilent Technologies (China) Co., Ltd., China], and is modified (28). The specific steps are as follows: 50 μL serum and 200 μL internal standard solution [consisting of lithocholic acid (LCA)-D4, DCA-D4, and glycochenodeoxycholic acid (GCDCA)-D4 in methanol] were added to a 1.5 mL centrifuge tube. After vortex oscillation (Haimen Kylin-Bell Lab Instruments Co., Ltd., China) and centrifugation [Eppendorf (Shanghai) International Trade Co., Ltd., China] at 4°C for 30 s, 200 μL supernatant was transferred to a new 1.5 mL centrifuge tube. Then 200 μL ultrapure water was added for freeze drying using Sihuan freeze dryer (Beijing Sihuan Qihang Technology Co., Ltd., Beijing) and the residue is redissolved in 160 μL ultra-pure water. The dissolved sample was centrifuged at 12,000 r/min for 5 min, and the supernatant was transferred to a liquid injection bottle for HPLC analysis. The chromatographic column is the ZORBAX RRHD C18 column of the Agilent 1290LC system (50 mm × 2.1 mm, 1.8 μm) [Agilent Technologies (China) Co., Ltd., China]. The mobile phase elution procedure was as follows: 0–3 min: 35–50% methanol, 3–7.5 min: 50–75% methanol, 7.5–12 min: 75–100% methanol, 12–14 min: 100% methanol. The injection volume, flow rate, and the column temperature were 2 μL, 0.4 mL/min, and 30°C, respectively. Mass spectrum conditions: spray voltage: 4,500 V, nitrogen temperature: 350°C, flow rate: 11 L/min, capillary voltage: 4,000 V in positive ion mode and 3,500 V in negative ion mode.

2.9 Gut microbiota measurement

Fresh fecal samples were collected at baseline and after 12 weeks of intervention, and were collected and stored in sterile retention bottles. The samples were promptly placed on ice, transported to the laboratory within 1 h, and then frozen at −80°C for future use. Gut microbiota analysis of fresh feces was completed by Shanghai Majorbio Bio-pharm Technology Co., Ltd. (Shanghai, China). Fecal samples were taken out from-80°C for thawing until they restored to room temperature. Fecal DNA were extracted according to the requirements of the kit [E.Z.N.A.® SoilDNA, Annoron (Beijing) Biotechnology Co., Ltd., China]. Nanodrop micro spectrophotometer [Thermo Fisher Scientific (China) Co., Ltd., China] was used for DNA quality inspection. The hypervariable region V3–V4 of the bacterial 16S rRNA gene was amplified with primer pairs 338F (5′-ACTCCTACGGGAGGCAGCAG-3′) and 806R (5′-GGAC TACHVGGGTWTCTAAT-3′). Sequencing was performed using the

Miseq PE 300/NovaSeq PE 250 platform (Illumina, United States). Pathway information was obtained according to the KEGG database while the abundance of each functional category was calculated according to OTU abundance (29).

2.10 Statistical analysis

The sample size was estimated according to Stenman et al. (23) with the results of the change of body fat percentage and 39 subjects per group were needed with an α-error of 0.05 and β-error of 0.20. Considering the dropout rate, 40 individuals were planned to be recruited into each group.

Intent to treatment set (ITT) was used for analysis in this study. In the ITT set, missing values were imputed based on the last observation carried forward method. Continuous variables with normal or approximate normal distribution are described by mean ± standard deviation, whereas continuous variables with skewed distribution are described by median and interquartile range. Paired sample *t*-test and paired sample rank sum test were used for intra-group comparisons. Independent *t*-test and Mann–Whitney test were used for inter-group comparisons, and chi square test for counting data.

In the analysis of gut microbiota, the UPARSE algorithm was utilized for performing operational taxonomic unit (OTU) clustering analysis, while the RDP classifier algorithm was applied for taxonomic analysis. A principal coordinates analysis (PCoA) was conducted using unweighted-UniFrac distances of the OTUs to analyze β diversity. Differential abundance analysis of taxa was executed using linear discriminant analysis effect size (LEfSe). Correlation analysis was conducted using Spearman correlation analysis.

Due to LDL-C being a risk factor for multiple cardiovascular diseases, we conducted subgroup analysis on individuals with baseline LDL-C abnormalities and those without dyslipidemia. (Subgroup1: obese individuals with abnormal LDL-C; subgroup2: obese individuals without dyslipidemia) as the exploratory analysis (30).

$p < 0.05$ indicates a statistically significant difference. SAS 9.4 was used for statistical analysis.

3 Results

3.1 Characteristics of participants

This randomized, double-blind, placebo-controlled study was performed between November 2022 and February 2023. A total of 113 subjects were recruited for screening, out of which 80 subjects were included based on the inclusion criteria (Supplementary Figure S2). The subjects were randomly divided into a synbiotic or placebo group, with 40 subjects in each group. Thirteen subjects discontinued the intervention, leaving 67 subjects finally finishing the trial. At baseline, there were no statistically significant differences ($p > 0.05$) in age, sex, BMI, body fat percentage, waist circumference, hip circumference, soft lean mass between the two groups (Table 1). The final ITT analysis incorporated all 80 individuals who were randomized.

3.2 Effect of synbiotics intervention on body composition and serum indicators of individuals with obesity

As demonstrated in Table 2, the synbiotic group exhibited a significant decrease in BMI ($p = 0.01$), body fat percentage ($p = 0.001$), waist ($p = 0.0001$), and serum LDL-C level ($p = 0.005$) after the intervention, while no significant changes were observed in the placebo group. Moreover, the decrease in body fat percentage (−0.36% vs. −1.26%) and waist (−0.40 cm vs. −2.28 cm) in the synbiotic group was significantly greater than that in the placebo group. Besides, there was a significant inter-group difference regarding the changes of LDL-C (−0.19 mmol/L vs. 0.00 mmol/L, $p = 0.03$). Both groups exhibited remarkable increase in serum PYY ($p < 0.01$) and OXM ($p < 0.001$) levels. However, the synbiotic group showed significantly higher levels of PYY ($p = 0.006$) and OXM ($p = 0.0002$) compared to the placebo group after intervention, with a particularly notable inter-group difference in the change of OXM ($p = 0.02$). Substantial increases in serum CCK ($p = 0.0006$) and ANGPTL4 ($p = 0.04$) was observed in the synbiotic group, but not the placebo group, with a significantly higher serum CCK compared to the placebo group following the synbiotic intervention ($p = 0.03$). As for antioxidant indexes, after intervention, the serum GSH levels of both groups significantly increased ($p < 0.01$), but the GSH levels in the synbiotics group were significantly higher than those in the placebo group after intervention ($p = 0.0001$), and the increase value was significantly greater than that in the placebo group ($p = 0.005$). There was no significant change in T-AOC between the two groups before and after intervention.

Table 3 shows the results of subgroup analysis, respectively, in obese individuals with abnormal LDL-C and those without dyslipidemia. In the obese individuals with abnormal LDL-C, significant reductions in body fat percentage ($p = 0.02$), hip circumference ($p = 0.006$), TG ($p = 0.05$) and LDL-C ($p = 0.05$) levels were observed in the synbiotic

TABLE 1 Subject characteristics at baseline.

	Placebo (n = 40)	Synbiotics (n = 40)	p
Age	34 (25, 38)	29 (22, 37)	0.21
Sex (male: female) (%)	27.50: 72.50	30.00: 70.00	1.00
BMI (kg/m^2)	26.84 (24.85, 30.72)	28.35 (24.25, 31.50)	0.48
Body fat percentage (%)	36.40 ± 4.12	37.12 ± 6.89	0.70
Waist (cm)	88.00 (79.00, 96.00)	89.50 (75.00, 98.50)	0.73
Hip (cm)	102.33 ± 8.43	104.60 ± 8.72	0.32
Soft lean mass (%)	58.74 ± 3.57	59.25 ± 6.57	0.93

BMI, body mass index. p indicates the differences between groups.

TABLE 2 Effect of synbiotics intervention on body composition of individuals with obesity.

	Placebo group				Synbiotic group					
	V0	V1	Change	p_0	V0	V1	Change	p_0	p_1	p_2
BMI (kg/m^2)	26.84 (24.85, 30.72)	26.45 (24.79, 28.81)	−0.11 ± 0.65	0.43	28.35 (24.25, 31.50)	28.05 (23.70, 31.20)	−0.32 ± 0.75	0.01	0.51	0.17
Body fat percentage (%)	36.40 ± 4.12	36.04 ± 4.23	−0.36 ± 1.65	0.21	37.12 ± 6.89	35.86 ± 7.30	−1.26 ± 1.66	0.001	0.89	0.02
Waist (cm)	88.00 (79.00, 96.00)	86.00 (79.00, 93.00)	−0.40 ± 4.44	0.56	89.50 (75.00, 98.50)	87.00 (73.50, 99.00)	−2.28 ± 3.55	0.0001	0.78	0.02
Hip (cm)	102.33 ± 8.43	100.86 ± 9.01	−1.47 ± 3.88	0.03	104.60 ± 8.72	102.23 ± 8.32	−2.38 ± 2.83	0.0001	0.50	0.25
Soft lean mass (%)	58.74 ± 3.57	59.75 ± 4.07	0.89 ± 0.15	0.006	59.25 ± 6.57	60.49 ± 6.95	1.21 ± 1.56	0.0001	0.45	0.76
TG (mmol/L)	1.31 ± 1.04	1.31 ± 0.67	−0.01 ± 0.89	0.96	1.55 ± 1.05	1.59 ± 1.10	0.05 ± 0.79	0.33	0.19	0.75
TC (mmol/L)	4.63 ± 0.88	4.72 ± 1.04	0.05 ± 0.45	0.47	4.80 ± 0.86	4.76 ± 0.86	−0.04 ± 0.50	0.61	0.84	0.39
LDL-C (mmol/L)	3.01 ± 0.72	3.03 ± 0.84	0.00 ± 0.35	0.99	3.12 ± 0.59	2.94 ± 0.57	−0.19 ± 0.39	0.005	0.58	0.03
HDL-C (mmol/L)	1.23 ± 0.25	1.18 ± 0.24	−0.04 ± 0.15	0.09	1.17 ± 0.27	1.12 ± 0.25	−0.06 ± 0.16	0.11	0.32	0.85
PYY (pg/mL)	231.67 ± 23.58	246.65 ± 23.31	15.14 ± 29.59	0.005	239.67 ± 18.71	262.23 ± 21.72	22.57 ± 29.02	0.0001	0.006	0.31
CCK (ng/L)	333.40 ± 26.35	341.08 ± 28.57	8.64 ± 33.96	0.15	332.58 ± 25.49	356.36 ± 26.69	23.78 ± 35.12	0.0006	0.03	0.08
OXM (pg/mL)	2716.78 ± 251.29	2990.24 ± 296.53	288.18 ± 322.17	0.0001	2773.56 ± 209.43	3254.08 ± 249.45	480.53 ± 324.71	0.0001	0.0002	0.02
ANGPTL4 (ng/mL)	39.52 ± 3.38	41.09 ± 3.82	1.61 ± 5.09	0.07	39.88 ± 3.75	41.96 ± 3.69	2.08 ± 5.35	0.04	0.35	0.72
GSH (ng/mL)	61.45 ± 227.30	63.27 ± 5.76	2.06 ± 7.76	0.0002	61.32 ± 5.27	68.67 ± 4.89	7.35 ± 6.82	0.0001	0.0001	0.005
T-AOC (ng/mL)	4.05 ± 0.72	4.06 ± 0.95	−0.01 ± 1.06	0.95	3.88 ± 0.86	4.02 ± 0.84	0.14 ± 1.16	0.50	0.85	0.58

BMI, body mass index; TG, triglyceride; TC, total cholesterol; LDL-C, low density lipoprotein cholesterol; HDL-C, high density lipoprotein cholesterol; PYY, peptide YY; CCK, cholecystokinin; OXM, oxyntomodulin; ANGPTL4, angiopoietin-related 4, GPX, glutathione peroxidase. T-AOC: total antioxidant capacity. p_0 indicates the differences before and after intervention within the group. p_1 indicates the differences between groups after intervention. p_2 indicates the differences between the changes. Individuals in the placebo ($n = 40$) and the synbiotic group ($n = 40$) were administered for BMI, body fat percentage, waist, hip, and soft lean mass. Individuals in the placebo ($n = 35$) and the synbiotic group ($n = 32$) were administered for serum lipids, hormone, and antioxidant indexes.

group while not in the placebo group. Moreover, the synbiotic group showed significantly lower post-intervention-LDL-C levels compared to the placebo group ($p = 0.05$), with a greater reduction in LDL-C ($p = 0.04$). However, in the obese individuals without dyslipidemia, except for reducing waist, the synbiotic intervention did not demonstrate any discernible superior effect compared to the placebo group, as evidenced by similar changes observed in various parameters following the intervention in both groups.

3.3 Safety of synbiotics intervention on individuals with obesity

No adverse events were reported throughout the intervention. Following the intervention, there were no significant changes observed in liver (AST, ALT) and renal (UA, CR, UR) function indexes within both the placebo group and synbiotic group compared to baseline. Additionally, no obvious difference was found between the groups after the intervention, which indicates good safety of the synbiotics MN-Gup-GOS-XOS (Supplementary Table S1).

3.4 Dietary information of individuals with obesity

According to the dietary survey data, there were no significant differences in total energy, carbohydrate, fat, and protein intakes between the placebo and synbiotic group at baseline. After the intervention, dietary intakes did not change in both groups compared

TABLE 3 Effect of synbiotics intervention on body composition of individuals of different subgroups.

	Placebo group		Synbiotic group			
	Change	p_0	Change	p_0	p_1	p_2
Subgroup1	(n = 9)		(n = 12)			
BMI (kg/m^2)	−0.14 ± 0.63	0.34	−0.25 ± 0.82	0.29	0.72	0.48
Body fat percentage (%)	0.19 ± 2.14	0.81	−1.46 ± 1.86	0.02	0.87	0.08
Waist (cm)	0.33 ± 3.24	0.82	−2.69 ± 4.29	0.07	0.87	0.09
Hip (cm)	−1.33 ± 2.69	0.18	−3.69 ± 3.99	0.006	0.76	0.14
Soft lean mass (%)	0.87 ± 0.35	0.01	1.41 ± 1.74	0.01	0.99	0.56
TG (mmol/L)	0.22 ± 0.77	0.39	−0.17 ± 0.28	0.05	0.76	0.15
TC (mmol/L)	0.20 ± 0.60	0.31	−0.30 ± 0.64	0.12	0.16	0.07
LDL-C (mmol/L)	0.04 ± 0.44	0.81	−0.41 ± 0.48	0.01	0.05	0.04
HDL-C (mmol/L)	0.05 ± 0.11	0.24	−0.07 ± 0.14	0.09	0.49	0.09
Subgroup2	(n = 14)		(n = 16)			
BMI (kg/m^2)	−0.09 ± 0.64	0.63	−0.30 ± 0.74	0.18	0.70	0.37
Body fat percentage (%)	−0.68 ± 1.23	0.02	−1.35 ± 1.81	0.004	0.98	0.19
Waist (cm)	−0.14 ± 5.03	0.92	−2.19 ± 3.02	0.01	0.21	0.08
Hip (cm)	−1.5 ± 3.36	0.05	−1.56 ± 1.67	0.002	0.81	0.95
Soft lean mass (%)	0.96 ± 1.34	0.03	1.26 ± 1.68	0.01	0.75	0.62
TG (mmol/L)	0.19 ± 0.37	0.03	0.01 ± 0.33	0.92	0.31	0.13
TC (mmol/L)	−0.03 ± 0.40	0.70	0.07 ± 0.36	0.47	0.27	0.43
LDL-C (mmol/L)	−0.05 ± 0.35	0.57	−0.02 ± 0.29	0.85	0.43	0.82
HDL-C (mmol/L)	−0.11 ± 0.14	0.001	0.002 ± 0.15	0.95	0.32	0.02

BMI, body mass index; TG, triglyceride; TC, total cholesterol; LDL-C, low density lipoprotein cholesterol; HDL-C, high density lipoprotein cholesterol; subgroup1, obese individuals with abnormal LDL-C; subgroup2, obese individuals without dyslipidemia. p_0 indicates the differences before and after intervention within the group. p_1 indicates the differences between groups after intervention. p_2 indicates the differences between the changes.

to baseline, and no significant difference was found between the two groups at post-intervention (Supplementary Table S2).

3.5 Effect of synbiotics intervention on gut microbiota of individuals with obesity

As shown in Supplementary Figures S3A–D, 16S rDNA gene sequencing of feces in subjects were performed to explore the changes in gut microbiota. There was no significant difference in alpha diversity indicated by the Shannon, Simpson, Sobs and ACE index between the placebo and synbiotic groups at baseline and post-intervention. Beta diversity based on PCoA showed that the cluster of placebo group did not clearly separate from the cluster of the synbiotic group at baseline and post-intervention (Supplementary Figures S3E,F). At the level of phylum, the dominant microbes could be classified as four phyla, including *Firmicutes*, *Bacteroidetes*, *Actinobacteriota*, and *Proteobacteria* (Figure 1A). At the level of genus, the dominant bacterial including *Bacteroides*, *Faecalibacterium*, *Blautia*, *Agathobacter*, and so on (Figure 1B). LEfSe analysis revealed that *Eubacterium_nodatum_group* and *Holdemanella* were significantly enriched in the placebo group after intervention, while the synbiotic group enriched *Bifidobacterium*, *Abiotrophia*, *Escherichia-Shigella*, *Romboutsia*, *Solobacterium*, *TM7x*, *Veillonella*, and *Actinomyces* at the level of genus (Figure 1C). KEGG pathway analysis showed that the top three pathways of feces were carbohydrate metabolism, membrane transport, and amino acid metabolism (Supplementary Figure S3G).

3.6 Effect of synbiotics intervention on serum bile acids of individuals with obesity

The regulation of bile acid metabolism by MN-Gup-GOS-XOS is demonstrated in Figure 1D. Notably, the synbiotic group exhibited a significantly higher level of CDCA compared to the placebo group after intervention ($p < 0.05$). Additionally, a significant increase in DCA was observed in the synbiotic group compared to the baseline ($p < 0.05$). There were no significant changes or differences in other bile acid parameters within or between groups.

3.7 Correlation heatmap of bile acids and gut microbiota

The Person's correlation analysis revealed a significant positive association between *Bifidobacterium* and *Romboutsia* with CDCA (Figures 1E,F), whereas *Anaerostipes* exhibited a significant negative correlation with CDCA (Figure 1G). Additionally, *Subdoligranulum*, *Dorea*, and *Eubacterium_hallii_group* demonstrated a significant positive correlation with DCA (Figures 1H–J).

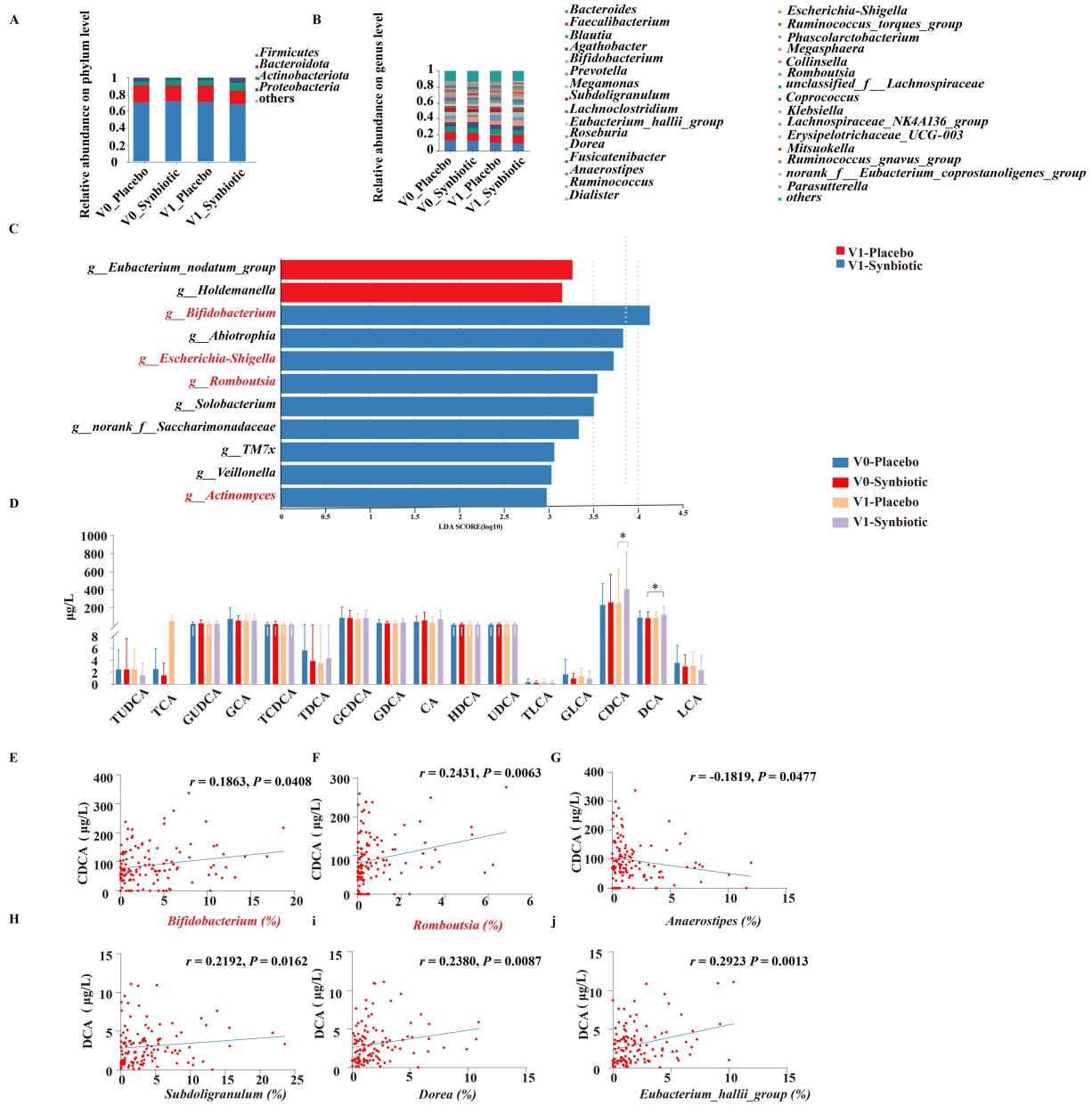

FIGURE 1
Effects of MN-Gup-GOS-XOS on gut microbiota and bile acids of individuals with obesity. V0: baseline, V1: post-intervention. **(A,B)** The average relative abundance of bacteria at the phylum and the genus level. **(C)** LEfSe analysis of gut microbiota at post-intervention. The length of the bar represents the log10 transformed LDA score. The threshold on the logarithmic LDA score for discriminative features was set to 2.0. **(D)** Bile acids in individuals at baseline and post-intervention. TUDCA, tauroursodeoxycholic acid; TCA, taurocholate acid; GUDCA, glycoursodeoxycholic acid; GCA, glycocholic acid; TCDCA, taurochenodeoxycholic acid; TDCA, taurodeoxycholic acid; GCDCA, glycochenodeoxycholic acid; GDCA, glycoursodeoxycholic acid; CA, cholic acid; HDCA, hyodeoxycholic acid; UDCA, ursodeoxycholic acid; TLCA, taurolithocholic acid; GLCA, glycolithocholic acid; CDCA, chenodeoxycholic acid; DCA, deoxycholic acid; LCA, lithocholic acid. **(E–J)** Pearson correlation heatmap of bile acids and gut microbiota.

3.8 Gut microbiota analysis in subgroups stratified by baseline serum lipid levels

The results of gut microbiota analysis in subgroups stratified by baseline serum lipid levels are shown in the Figure 2.

At baseline, among the top 15% of genus abundance, significantly higher levels of *norank_f__norank_o__Clostridia_UCG-014* and *Lachnospiraceae_ND3007_group* were observed in obese individuals with abnormal LDL-C compared to those without dyslipidemia. Conversely, obese individuals without dyslipidemia showed a significant enrichment of *Bifidobacterium*, *Turicibacter*, *Clostridium_innocuum_group*, and *Lachnospiraceae_UCG-008* within their gut microbiota (Figure 2A).

After intervention, individuals with obesity and abnormal LDL-C exhibied significant enrichment of *Bifidobacterium*, *Escherichia-Shigella*, *Streptococcus*, *Veillonella*, *Solobacterium*, *TM7x*, *Clostridium_innocuum_group*, *Actinomyces*, and *Granulicatel* following synbiotics supplementation, while the placebo group enriched in *Paraprevotella*

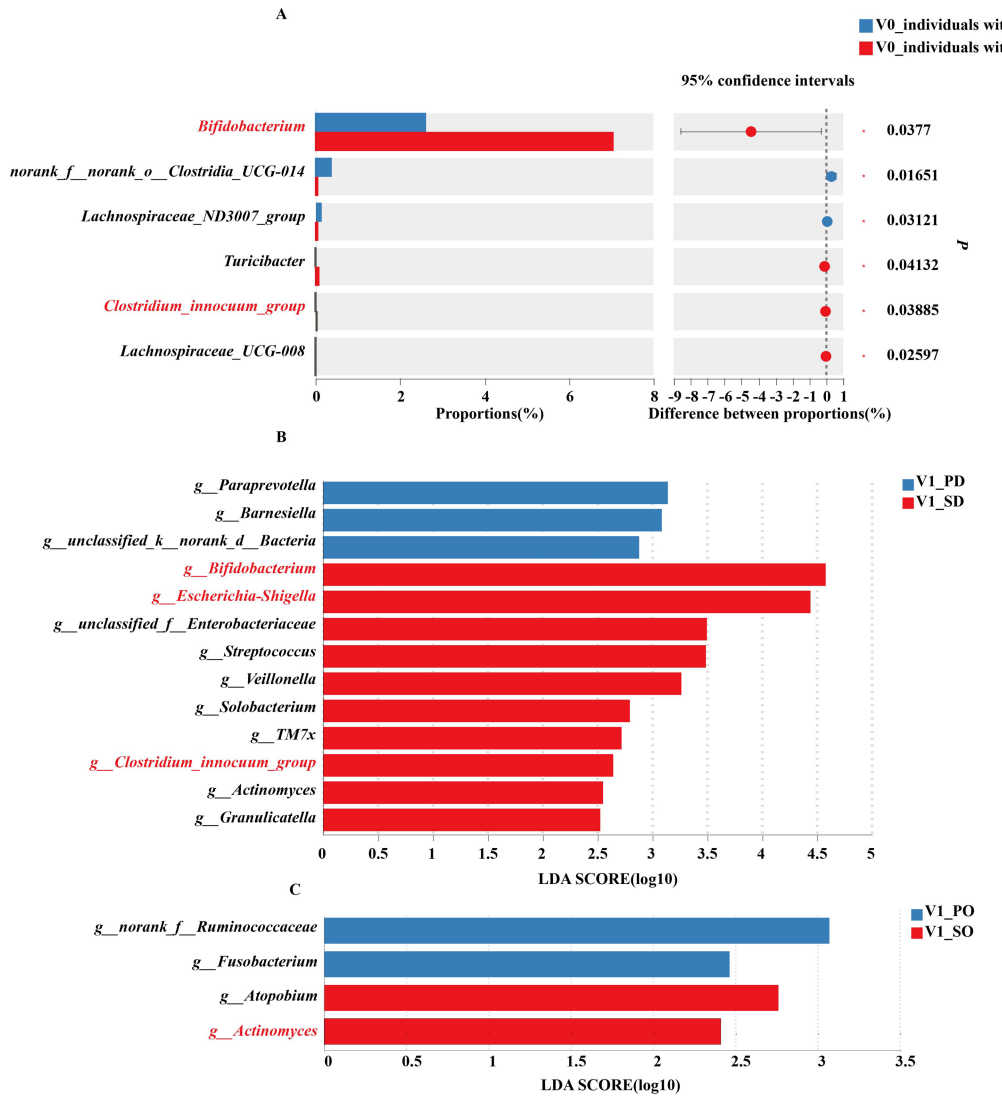

FIGURE 2
Gut microbiota of subgroup analysis. **(A)** Differences in gut microbiota (genus level) between obese individuals with abnormal LDL-C and obese individuals without dyslipidemia at baseline. **(B)** LEfSe analysis of gut microbiota in obese individuals with abnormal LDL-C at post-intervention. **(C)** LEfSe analysis of gut microbiota in obese individuals without dyslipidemia at post-intervention. PD, placebo group in obese individuals with abnormal LDL-C; SD, synbiotic group in obese individuals with abnormal LDL-C; PO, placebo group in obese individuals without dyslipidemia; SO, synbiotic group in obese individuals without dyslipidemia.

and *Barnesiella* (Figure 2B). In obese individuals without dyslipidemia, the placebo group exhibited a significant enrichment of *Fusobacterium*, whereas the synbiotic group demonstrated remarkable enrichment of *Atopobium* and *Actinomyces* (Figure 2C).

4 Discussion

This randomized, double-blind clinical trial showed that daily supplementation of the synbiotics MN-Gup-GOS-XOS for 12 weeks reduced body fat percentage, waist, serum LDL-C, and increased PYY, CCK, OXM, GSH in individuals with obesity. Additionally, the administration of MN-Gup-GOS-XOS resulted in an enhancement of certain gut microbiota and a significant increase in serum CDCA level in obese individuals. Correlation analysis revealed a significant association between certain gut microbiota and CDCA. Subgroup analysis demonstrated that MN-Gup-GOS-XOS had a more pronounced effect on obesity in individuals with abnormal LDL-C. Further analysis indicated that MN-Gup-GOS-XOS primarily improved the gut microbiota of obese individuals with abnormal LDL-C.

Improving obesity entails the crucial objective of reducing body fat and blood lipids. In this study, it was found that MN-Gup-GOS-XOS intervention could significantly reduce body fat percentage and waist, thereby indicating the potential of MN-Gup-GOS-XOS in enhancing body composition. Our study also demonstrated a significant reduction in serum LDL-C levels. Studies have shown that elevated serum LDL-C level is an important risk factor for cardiometabolic diseases in obese people (31). Therefore, it can be seen that MN-Gup-GOS-XOS in this study has the potential to reduce the risk of cardiometabolic disease in obese people. These results are consistent with the findings of other intervention studies, which demonstrated that synbiotic supplementation significantly reduced LDL-C levels in obese children

or adults with overweight or obesity (32, 33). Besides, obesity usually leads to oxidative stress, and GSH helps to reduce the level of oxidative stress in the body (34). Our study indicates that after intervention with synbiotics, the serum GSH content of individuals significantly increased, suggesting that synbiotics can reduce oxidative stress levels in obese patients.

Studies have found that hormones play an important role in the regulation of lipid metabolism. For instance, PYY, CCK, OXM, and ANGPTL4 have been demonstrated to exert inhibitory effects on adipogenesis (15, 35–37). In this study, supplementation of MN-Gup-GOS-XOS increased the levels of PYY, CCK, and OXM in individuals with obesity, which provided a possible explanation for the mechanism of MN-Gup-GOS-XOS reducing LDL-C. Moreover, the metabolites such as bile acids related to the gut microbiota may exert a regulatory role on the aforementioned gastrointestinal hormones (38). Previous researches reported that DCA promotes PYY release in the colon and oral CDCA promoted the increase of OXM in human blood (11, 39). In this study, MN-Gup-GOS-XOS intervention increased the levels of CDCA, which may be the potential promoter of hormone release.

Furthermore, the efficacy of probiotics is inherently intertwined with the regulation of gut microbiota, which serves as the fundamental basis for metabolite production (40, 41). In this study, the relative abundance of *Bifidobacterium* in the synbiotic group was significantly higher compared to the placebo group at post-intervention, indicating that GOS and XOS facilitated the proliferation of *Bifidobacterium*. Furthermore, the synbiotic group exhibited enrichment in several bacteria such as *Escherichia-Shigella*, *Romboutsia*. *Solobacteriumm*, and *Actinomyces*, which have been proven to be beneficial for weight loss in previous animal and human studies (42–46). Additionally, Person's correlation analysis revealed a significant positive association between *Bifidobacterium* and *Romboutsia* with CDCA, suggesting that MN-Gup-GOS-XOS may contribute to bile acid metabolism by promoting the proliferation of *Bifidobacterium* and *Romboutsia*.

Considering the observed beneficial impact of MN-Gup-GOS-XOS on LDL-C levels in individuals, we stratified the population into two subgroups: obese individuals with abnormal LDL-C and obese individuals without dyslipidemia. The intestine contains a large number of microorganisms that interact with the host (47). In this context, we observed that the MN-Gup-GOS-XOS supplement exerted a more favorable effect on serum LDL-C in obese individuals with abnormal LDL-C. In order to gain a more comprehensive understanding of this disparity in effects, we conducted an analysis of differential microbial communities. The relative abundances of *Bifidobacterium*, *Turicibacter*, *Clostridium_innocuum_group*, and *Lachnospiraceae_UCG-008* were significantly higher in obese individuals without dyslipidemia compared to those with abnormal LDL-C at baseline. The abundance of *Bifidobacterium* has been found to have a negative correlation with LDL-C (48). Furthermore, *Turicibacter* was found to increase with weight loss in overweight men (49). Additionally, *Clostridium_innocuum_group* has been identified as a beneficial bacterium associated with lipid metabolism (50). However, gut microbiota of obese individuals with abnormal LDL-C exhibited an enrichment of *Lachnospiraceae_ND3007_group*, which has been previously identified as a biomarker for various diseases in scientific literatures (51, 52). These findings implied, unsurprisingly, that dyslipidemia-free obese individuals harbored a gut microbiota profile indicative of relatively favorable health status. After 12 weeks of synbiotic consumption, the abundance of *Bifidobacterium* and *Clostridium_innocuum_group* in obese individuals with abnormal LDL-C levels exhibited a significantly higher increase compared to the placebo group. These findings suggest that MN-Gup-GOS-XOS can significantly promote the proliferation of beneficial bacteria.

The strengths of this study lie in the inclusion of a novel probiotic strain, MN-Gup, and its synbiotics. Additionally, our findings demonstrate that synbiotics exhibit superior efficacy in ameliorating obesity and lipid metabolism abnormalities among individuals with elevated LDL-C levels. The study also presents certain limitations. Firstly, the direct correlation between gut microbiota and bile acids remains unclarified, while the precise mechanism underlying the impact of MN-Gup-GOS-XOS has not been fully elucidated. Secondly, the examination of beneficial bacteria promotion on CDCA was not conducted, leaving room for future verification through microbiota transplantation. Thirdly, this study only detected bile acids in serum, and future research can further explore the relationship between bile acids and obesity by detecting bile acids in feces. Fourthly, it is important to note that the findings of this study are limited in their applicability to individuals with obesity. Therefore, further recruitment of subjects with different types of obesity is recommended to explore the effects of synbiotics.

In conclusion, a 12-week supplementation of MN-Gup-GOS-XOS demonstrated significant reduction in body fat percentage, waist, and serum LDL-C among obese individuals, accompanied by alterations in gut microbiota (*Bifidobacterium* and *Romboutsia*), bile acid (CDCA), hormones (PYY, CCK, and OXM), and GSH. Furthermore, MN-Gup-GOS-XOS seemed to have a more favorable impact on individuals with abnormal LDL-C levels, which was further supported by the modifications seen in gut microbiota. However, the exact mechanism requires further validation through subsequent studies.

Data availability statement

The datasets presented in this study can be found in online repositories. The names of the repository/repositories and accession number(s) can be found in the article/Supplementary material.

Ethics statement

The studies involving humans were approved by Institutional Review Board of China Agricultural University Ethics Committee. The studies were conducted in accordance with the local legislation and institutional requirements. The participants provided their written informed consent to participate in this study.

Author contributions

XN: Investigation, Software, Writing – original draft. QZ: Investigation, Writing – review & editing. JL: Methodology, Writing – review & editing. YuZ: Methodology, Writing – review & editing. NS: Methodology, Writing – review & editing. SL: Methodology, Writing – review & editing. YinL: Data curation, Writing – review & editing. WX: Data curation, Writing – review & editing. ES: Data curation, Writing – review & editing. YoZ: Formal analysis, Writing – review & editing. HZ: Formal analysis, Writing – review & editing.

YixL: Formal analysis, Writing – review & editing. PW: Formal analysis, Writing – review & editing. BF: Software, Writing – review & editing. LZ: Software, Writing – review & editing. JC: Supervision, Writing – review & editing. FW: Supervision, Writing – review & editing. GP: Supervision, Writing – review & editing. CW: Validation, Writing – review & editing. JH: Conceptualization, Investigation, Writing – review & editing. RW: Conceptualization, Investigation, Writing – review & editing.

Funding

The author(s) declare that financial support was received for the research, authorship, and/or publication of this article. This research was funded by the National Key R&D Program of China (No. 2022YFF1100100) and the 111 Project of the Education Ministry of China (Grant No. B18053).

Conflict of interest

JL, SL, ES, HZ, and CW were employed by Mengniu Hi-Tech Dairy Product Beijing Co., Ltd. FW was employed by Tibet Tianhong Science and Technology Co., Ltd.

The remaining authors declare that the research was conducted in the absence of any commercial or financial relationships that could be construed as a potential conflict of interest.

Generative AI statement

The author(s) declare that no Generative AI was used in the creation of this manuscript.

Publisher's note

Supplementary material

The Supplementary material for this article can be found online at: https://www.frontiersin.org/articles/10.3389/fnut.2024.1510318/full#supplementary-material

References

1. NCD Risk Factor Collaboration (NCD-RisC). Trends in adult body-mass index in 200 countries from 1975 to 2014: a pooled analysis of 1,698 population-based measurement studies with 19.2 million participants. *Lancet*. (2016) 387:1377–96. doi: 10.1016/S0140-6736(16)30054-X

2. Briel M, Ferreira-Gonzalez I, You JJ, Karanicolas PJ, Akl EA, Wu P, et al. Association between change in high density lipoprotein cholesterol and cardiovascular disease morbidity and mortality: systematic review and meta-regression analysis. *BMJ*. (2009) 338:b92. doi: 10.1136/bmj.b92

3. Abenavoli L, Scarpellini E, Colica C, Boccuto L, Salehi B, Sharifi-Rad J, et al. Gut microbiota and obesity: a role for probiotics. *Nutrients*. (2019) 11:2690. doi: 10.3390/nu11112690

4. Luoto R, Kalliomäki M, Laitinen K, Isolauri E. The impact of perinatal probiotic intervention on the development of overweight and obesity: follow-up study from birth to 10 years. *Int J Obes*. (2010) 34:1531–7. doi: 10.1038/ijo.2010.50

5. Nagata S, Chiba Y, Wang C, Yamashiro Y. The effects of the *Lactobacillus casei* strain on obesity in children: a pilot study. *Benef Microbes*. (2017) 8:535–43. doi: 10.3920/BM2016.0170

6. Pedret A, Valls RM, Calderón-Pérez L, Llauradó E, Companys J, Pla-Pagà L, et al. Effects of daily consumption of the probiotic *Bifidobacterium animalis* subsp. *lactis* CECT 8145 on anthropometric adiposity biomarkers in abdominally obese subjects: a randomized controlled trial. *Int J Obes*. (2019) 43:1863–8. doi: 10.1038/s41366-018-0220-0

7. Qiao N, Du G, Zhong X, Sun X. Recombinant lactic acid bacteria as promising vectors for mucosal vaccination. *Exploration*. (2021) 1:20210026. doi: 10.1002/EXP.20210026

8. Zhang C, Fang R, Lu X, Zhang Y, Yang M, Su Y, et al. *Lactobacillus reuteri* J1 prevents obesity by altering the gut microbiota and regulating bile acid metabolism in obese mice. *Food Funct*. (2022) 13:6688–701. doi: 10.1039/D1FO04387K

9. Castellanos-Jankiewicz A, Guzman-Quevedo O, Fenelon VS, Zizzari P, Quarta C, Bellocchio L, et al. Hypothalamic bile acid-TGR5 signaling protects from obesity. *Cell Metab*. (2021) 33:1483–1492.e10. doi: 10.1016/j.cmet.2021.04.009

10. Housset C, Chretien Y, Debray D, Chignard N. Functions of the gallbladder. *Compr Physiol*. (2016) 6:1549–77. doi: 10.1002/cphy.c150050

11. McGlone ER, Malallah K, Cuenco J, Wewer AN, Holst JJ, Vincent RP, et al. Differential effects of bile acids on the postprandial secretion of gut hormones: a randomized crossover study. *Am J Physiol Endocrinol Metab*. (2021) 320:E671–9. doi: 10.1152/ajpendo.00580.2020

12. Xia Y, Xu X, Guo Y, Lin C, Xu X, Zhang F, et al. Mesenchymal stromal cells overexpressing farnesoid × receptor exert cardioprotective effects against acute ischemic heart injury by binding endogenous bile acids. *Adv Sci*. (2022) 9:e2200431. doi: 10.1002/advs.202200431

13. Choudhuri R, Sowers AL, Chandramouli G, Gamson J, Krishna MC, Mitchell JB, et al. The antioxidant tempol transforms gut microbiome to resist obesity in female C3H mice fed a high fat diet. *Free Radic Biol Med*. (2022) 178:380–90. doi: 10.1016/j.freeradbiomed.2021.12.006

14. Valassi E, Scacchi M, Cavagnini F. Neuroendocrine control of food intake. *Nutr Metab Cardiovasc Dis*. (2008) 18:158–68. doi: 10.1016/j.numecd.2007.06.004

15. Wu Y, He H, Cheng Z, Bai Y, Ma X. The role of neuropeptide y and peptide YY in the development of obesity via gut-brain axis. *Curr Protein Pept Sci*. (2019) 20:750–8. doi: 10.2174/1389203720666190125105401

16. Gibson GR, Hutkins R, Sanders ME, Prescott SL, Reimer RA, Salminen SJ, et al. Expert consensus document: the international scientific association for probiotics and prebiotics (ISAPP) consensus statement on the definition and scope of prebiotics. *Gastroenterol Hepatol*. (2017) 14:491–502. doi: 10.1038/nrgastro.2017.75

17. Tian B, Geng Y, Wang P, Cai M, Neng J, Hu J, et al. Ferulic acid improves intestinal barrier function through altering gut microbiota composition in high-fat diet-induced mice. *Eur J Nutr*. (2022) 61:3767–83. doi: 10.1007/s00394-022-02927-7

18. Liu H, Yu Y, Dong A, Elsabahy M, Yang Y, Gao H. Emerging strategies for combating *Fusobacterium nucleatum* in colorectal cancer treatment: systematic review, improvements and future challenges. *Exploration*. (2023) 4:20230092. doi: 10.1002/EXP.20230092

19. Krumbeck JA, Walter J, Hutkins RW. Synbiotics for improved human health: recent developments, challenges, and opportunities. *Annu Rev Food Sci Technol*. (2018) 9:451–79. doi: 10.1146/annurev-food-030117-012757

20. Companys J, Calderón-Pérez L, Pla-Pagà L, Llauradó E, Sandoval-Ramirez BA, Gosalbes MJ, et al. Effects of enriched seafood sticks (heat-inactivated *B. animalis* subsp. *lactis* CECT 8145, inulin, omega-3) on cardiometabolic risk factors and gut microbiota in abdominally obese subjects: randomized controlled trial. *Eur J Nutr*. (2022) 61:3597–611. doi: 10.1007/s00394-022-02904-0

21. Scorletti E, Afolabi PR, Miles EA, Smith DE, Almehmadi A, Alshathry A, et al. Synbiotics alter fecal microbiomes, but not liver fat or fibrosis, in a randomized trial of patients with nonalcoholic fatty liver disease. *Gastroenterology*. (2020) 158:1597–1610.e7. doi: 10.1053/j.gastro.2020.01.031

22. Kukkonen K, Savilahti E, Haahtela T, Juntunen-Backman K, Korpela R, Poussa T, et al. Probiotics and prebiotic galacto-oligosaccharides in the prevention of allergic diseases: a randomized, double-blind, placebo-controlled trial. *J Allergy Clin Immunol*. (2007) 119:192–8. doi: 10.1016/j.jaci.2006.09.009

23. Stenman LK, Lehtinen MJ, Meland N, Christensen JE, Yeung N, Saarinen MT, et al. Probiotic with or without fiber controls body fat mass, associated with serum zonulin, in overweight and obese adults-randomized controlled trial. *EBioMedicine*. (2016) 13:190–200. doi: 10.1016/j.ebiom.2016.10.036

24. Sergeev IN, Aljutaily T, Walton G, Huarte E. Effects of synbiotic supplement on human gut microbiota, body composition and weight loss in obesity. *Nutrients*. (2020) 12:222. doi: 10.3390/nu12010222

25. Crovesy L, El-Bacha T, Rosado EL. Modulation of the gut microbiota by probiotics and symbiotics is associated with changes in serum metabolite profile related to a decrease in inflammation and overall benefits to metabolic health: a double-blind randomized controlled clinical trial in women with obesity. *Food Funct*. (2021) 12:2161–70. doi: 10.1039/d0fo02748k

26. Wang C, Li S, Sun E, Xiao R, Wang R, Ren Y, et al. Effects of fermented milk containing *Bifidobacterium animalis* subsp. *lactis* MN-Gup (MN-Gup) and MN-Gup-based synbiotics on obesity induced by high fat diet in rats. *Nutrients*. (2022) 14:2631. doi: 10.3390/nu14132631

27. Johnstone AM, Kelly J, Ryan S, Romero-Gonzalez R, McKinnon H, Fyfe C, et al. Nondigestible carbohydrates affect metabolic health and gut microbiota in overweight adults after weight loss. *J Nutr*. (2020) 150:1859–70. doi: 10.1093/jn/nxaa124

28. Ghaffarzadegan T, Zanzer YC, Ostman E, Hallenius F, Essen S, Sandahl M, et al. Postprandial responses of serum bile acids in healthy humans after ingestion of turmeric before medium/high-fat breakfasts. *Mol Nutr Food Res*. (2019) 63:e1900672. doi: 10.1002/mnfr.201900672

29. Ji X, Hou C, Gao Y, Xue Y, Yan Y, Guo X. Metagenomic analysis of gut microbiota modulatory effects of jujube (*Ziziphus jujuba* mill.) polysaccharides in a colorectal cancer mouse model. *Food Funct*. (2020) 11:163–73. doi: 10.1039/C9FO02171J

30. Zhu J, Gao R, Zhao S, Lu G, Li D, Li J. Guidelines for the prevention and treatment of dyslipidemia in Chinese adults. *Chin Circu J*. (2016) 31:937–53. doi: 10.3969/j.issn.1000-3614.2016.10.001

31. Ference BA, Ginsberg HN, Graham I, Ray KK, Packard CJ, Bruckert E, et al. Low-density lipoproteins cause atherosclerotic cardiovascular disease. 1. Evidence from genetic, epidemiologic, and clinical studies. A consensus statement from the European atherosclerosis society consensus panel. *Eur Heart J*. (2017) 38:2459–72. doi: 10.1093/eurheartj/ehx144

32. Hadi A, Sepandi M, Marx W, Moradi S, Parastouei K. Clinical and psychological responses to synbiotic supplementation in obese or overweight adults: a randomized clinical trial. *Complement Ther Med*. (2019) 47:102216. doi: 10.1016/j.ctim.2019.102216

33. Ipar N, Aydogdu SD, Yildirim GK, Inal M, Gies I, Vandenplas Y, et al. Effects of synbiotic on anthropometry, lipid profile and oxidative stress in obese children. *Benef Microbes*. (2015) 6:775–82. doi: 10.3920/BM2015.0011

34. Franco C, Sciatti E, Favero G, Bonomini F, Vizzardi E, Rezzani R. Essential hypertension and oxidative stress: novel future perspectives. *Int J Mol Sci*. (2022) 23:14489. doi: 10.3390/ijms232214489

35. Price SL, Bloom SR. Protein PYY and its role in metabolism. *Front Horm Res*. (2014) 42:147–54. doi: 10.1159/000358343

36. Sylvers-Davie KL, Davies B. Regulation of lipoprotein metabolism by ANGPTL3, ANGPTL4, and ANGPTL8. *Am J Physiol Endocrinol Metab*. (2021) 321:E493–508. doi: 10.1152/ajpendo.00195.2021

37. Tan T, Behary P, Tharakan G, Minnion J, Al-Najim W, Albrechtsen N, et al. The effect of a subcutaneous infusion of GLP-1, OXM, and PYY on energy intake and expenditure in obese volunteers. *J Clin Endocrinol Metab*. (2017) 102:2364–72. doi: 10.1210/jc.2017-00469

38. Giovanni S, Alessia P, Ece Y, Gaby EA, Maroun BS, Antimo G, et al. Bile acids signal via TGR5 to activate intestinal stem cells and epithelial regeneration. *Gastroenterology*. (2020) 159:956–968.e8. doi: 10.1053/j.gastro.2020.05.067

39. Ballantyne GH, Longo WE, Savoca PE, Adrian TE, Vukasin AP, Bilchik AJ, et al. Deoxycholate-stimulated release of peptide YY from the isolated perfused rabbit left colon. *Am J Phys*. (1989) 257:G715–24. doi: 10.1152/ajpgi.1989.257.5.G715

40. Green M, Arora K, Prakash S. Microbial medicine: prebiotic and probiotic functional foods to target obesity and metabolic syndrome. *Int J Mol Sci*. (2020) 21:2890. doi: 10.3390/ijms21082890

41. Hijova E. Synbiotic supplements in the prevention of obesity and obesity-related diseases. *Meta*. (2022) 12:313. doi: 10.3390/metabo12040313

42. Fouladi F, Carroll IM, Sharpton TJ, Bulik-Sullivan E, Heinberg L, Steffen KJ, et al. A microbial signature following bariatric surgery is robustly consistent across multiple cohorts. *Gut Microbes*. (2021) 13:1930872. doi: 10.1080/19490976.2021.1930872

43. Li Y, Kang Y, Du Y, Chen M, Guo L, Huang X, et al. Effects of konjaku flour on the gut microbiota of obese patients. *Front Cell Infect Microbiol*. (2022) 12:771748. doi: 10.3389/fcimb.2022.771748

44. Zhang L, Cheng X, Xia L, Liu N, Liu L, Liu S, et al. Analysis of 16S rRNA gene sequencing in feces: the impact of bariatric surgery on the gut microbiota in patients with obesity. *Obes Surg*. (2024) 34:1185–95. doi: 10.1007/s11695-024-07087-7

45. Zhang Q, Fan XY, Cao YJ, Zheng TT, Cheng WJ, Chen LJ, et al. The beneficial effects of *Lactobacillus brevis* FZU0713-fermented *Laminaria japonica* on lipid metabolism and intestinal microbiota in hyperlipidemic rats fed with a high-fat diet. *Food Funct*. (2021) 12:7145–60. doi: 10.1039/D1FO00218J

46. Zhu L, Fu J, Xiao X, Wang F, Jin M, Fang W, et al. Faecal microbiota transplantation-mediated jejunal microbiota changes halt high-fat diet-induced obesity in mice via retarding intestinal fat absorption. *Microb Biotechnol*. (2022) 15:337–52. doi: 10.1111/1751-7915.13951

47. Lu J, Shen X, Li H, Du J. Recent advances in bacteria-based platforms for inflammatory bowel diseases treatment. *Exploration*. (2024) 4:20230142. doi: 10.1002/EXP.20230142

48. Xu D, Feng M, Chu Y, Wang S, Shete V, Tuohy KM, et al. The prebiotic effects of oats on blood lipids, gut microbiota, and short-chain fatty acids in mildly hypercholesterolemic subjects compared with rice: a randomized, controlled trial. *Front Immunol*. (2021) 12:787797. doi: 10.3389/fimmu.2021.787797

49. Lucio H, Anunciacao P, Da SB, Da SA, Queiroz V, De Carvalho C, et al. Consumption of extruded sorghum SC319 improved gut microbiota at genus level and reduced anthropometric markers in men with overweight: a randomized controlled clinical trial. *Nutrients*. (2023) 15:3786. doi: 10.3390/nu15173786

50. Liu J, Hao W, He Z, Kwek E, Zhu H, Ma N, et al. Blueberry and cranberry anthocyanin extracts reduce bodyweight and modulate gut microbiota in C57BL/6J mice fed with a high-fat diet. *Eur J Nutr*. (2021) 60:2735–46. doi: 10.1007/s00394-020-02446-3

51. Lu F, Lei T, Zhou J, Liang H, Cui P, Zuo T, et al. Using gut microbiota as a diagnostic tool for colorectal cancer: machine learning techniques reveal promising results. *J Med Microbiol*. (2023) 72:1699. doi: 10.1099/jmm.0.001699

52. Wu IW, Lin CY, Chang LC, Lee CC, Chiu CY, Hsu HJ, et al. Gut microbiota as diagnostic tools for mirroring disease progression and circulating nephrotoxin levels in chronic kidney disease: discovery and validation study. *Int J Biol Sci*. (2020) 16:420–34. doi: 10.7150/ijbs.37421

frontiers | Frontiers in Nutrition

TYPE Original Research
PUBLISHED 28 January 2025
DOI 10.3389/fnut.2025.1536024

OPEN ACCESS

EDITED BY
Qingyu Wang,
Beijing Hospital, China

REVIEWED BY
Ramkripa Raghavan,
United States Department of Agriculture (USDA), United States
Liyun He,
Sun Yat-sen University Cancer Center (SYSUCC), China
Dae Young Cheon,
Hallym University Dongtan Sacred Heart Hospital, Republic of Korea

*CORRESPONDENCE
Su Zheng
✉ Ying22118365@zuaa.zju.edu.cn

RECEIVED 28 November 2024
ACCEPTED 15 January 2025
PUBLISHED 28 January 2025

CITATION
Ying S, Ding H, Chen Y and Zheng S (2025) Association of oxidative balance score with all-cause and cardiovascular mortality in overweight and obese.
Front. Nutr. 12:1536024.
doi: 10.3389/fnut.2025.1536024

Association of oxidative balance score with all-cause and cardiovascular mortality in overweight and obese

Shuxin Ying, Hongyan Ding, Yanjin Chen and Su Zheng*

Department of Nutrition, Hangzhou Third Hospital Affiliated to Zhejiang Chinese Medical University, Hangzhou, China

Background: The oxidative balance score (OBS) combines diverse dietary components with lifestyle factors to comprehensively evaluate oxidative stress. The investigation focuses on the link between the OBS and mortality outcomes, including cardiovascular and all-cause deaths, in overweight and obese individuals.

Methods: The analysis utilized data from the National Health and Nutrition Examination Survey (NHANES), covering the period from 1999 to 2018. Mortality information, categorized into all-cause and cardiovascular deaths, was gathered from the National Death Index (NDI). Kaplan–Meier survival analysis, along with multivariate Cox regression and restricted cubic spline (RCS) modeling, were utilized to explore the link between OBS and mortality risks. Subgroup analysis and sensitivity analysis were used to assess the robustness of the results and possible effect modifiers. Mediation analysis identifies pathways through which the independent variable affects the dependent variable.

Results: In this study, 26,219 participants with overweight or obesity were enrolled, with an average age of 49.8 $\pm$ 17.4 years. During a median follow-up duration of 115 months, 2,239 participants (8.5%) died, including 837 (3.2%) from cardiovascular disease. According to Kaplan–Meier analysis, mortality was highest among participants in the lowest OBS quartile (Q1) and lowest among those in the highest quartile (Q4). Participants in the fourth OBS quartile experienced a 21.7% decrease in the risk of mortality from all causes and a 29.5% decrease in cardiovascular mortality risk, according to fully adjusted results, compared to those in the first quartile. These results were validated through subgroup analyses. The analysis of RCS revealed a notable inverse association between OBS and mortality outcomes. Mediation analysis indicates that white blood cell count (WBC) and gamma-glutamyl transferase (GGT) serve as significant mediators in the association between OBS and mortality risk.

Conclusion: Elevated levels of OBS were strongly linked to reduced potential for both cardiovascular and all-cause mortality among individuals who are overweight or obese.

KEYWORDS

oxidative balance score, mortality, overweight, obesity, cardiovascular mortality

1 Introduction

The accumulation of excessive or ectopic fat, characteristic of being overweight or obese, greatly raises the likelihood of various metabolic disorders. According to WHO, the percentage of obese adults increased from 7% in 1990 to 16% by 2022. In that year, 43% of adults were categorized as overweight (1, 2). Body Mass Index (BMI) values have also steadily increased, with the average BMI in the United States having reached 27.8 by 2014 (3).

Overweight and obesity are key factors to non-infectious diseases, such as cardiovascular diseases, endocrine diseases, chronic respiratory diseases, and digestive system diseases (4–7). Beyond these health impacts, elevated BMI imposes a significant economic burden. By 2030, global costs associated with overweight and obesity are projected to reach $3 trillion annually, potentially exceeding $18 trillion by 2060 (1). Between 1990 and 2017, high BMI was responsible for a more than twofold rise in deaths and disability-adjusted life years (DALYs) (8).

Oxidative stress, a common pathophysiological condition in obese individuals, is a significant driver of chronic disease development. It arises from a disequilibrium between antioxidant defenses and reactive oxygen species (ROS), where redundant ROS production leads to cellular damage, inflammatory responses, and oxidative injuries, ultimately elevating disease risk (9). The oxidative balance score (OBS) evaluates the balance between the body's oxidative and antioxidative processes, providing a semi-quantitative measure of oxidative stress. Comprising 15 antioxidants and 5 pro-oxidants, this score is derived from 4 lifestyle components and 16 dietary nutrients, with higher scores suggesting greater antioxidant extent and reduced risk of oxidative stress (10–13).

OBS is increasingly utilized in epidemiological research and has been linked to reduced abdominal obesity (14). Furthermore, levels of OBS have shown a negative correlation with depression (15), non-alcoholic fatty liver disease (NAFLD) (10), cardiovascular disease (16), and diabetes mellitus (17).

As far as we know, earlier research has not delved into the relationship between OBS and mortality risk among overweight or obese individuals. Therefore, the objective of this study is to investigate the link between OBS and mortality from all causes and cardiovascular diseases in overweight and obese, based on data sourced from the National Health and Nutrition Examination Survey (NHANES).

2 Methods

2.1 Study design and population

The Centers for Disease Control and Prevention (CDC) oversees NHANES, a long-term, nationwide project. It is designed to comprehensively evaluate the physical health and nutritional profiles of individuals in the U.S. and the associated influencing factors. NHANES utilizes an intricate, multistage probabilistic sampling approach to gather data in biennial cycles, comprising five core components: demographic data, dietary information, physical examination data, laboratory test results, and questionnaire. All participants are required to sign written informed consent forms, following detailed scrutiny and authorization from the NCHS Research Ethics Board.

This study included overweight and obese adult subjects with complete OBS-related information derived from 10 continuous NHANES cycles conducted between 1999 and 2018 (1999–2000, 2001–2002, 2003–2004, 2005–2006, 2007–2008, 2009–2010, 2011–2012, 2013–2014, 2015–2016, and 2017–2018). The specifics of the inclusion and exclusion criteria are illustrated in Figure 1. Initially, 101,316 participants were recruited; however, 42,054 were excluded for being under 18 or over 80 years of age. Additional exclusions include pregnant women (n = 1,722), individuals with incomplete OBS data (n = 19,765), unavailable mortality data (n = 139), and those with a BMI <25 (n = 11,417). Ultimately, 26,219 participants remained for analysis (Figure 1).

2.2 Calculation of OBSs

Due to differences in data across years, dietary data from 1999 to 2002 were based on total nutrient intakes, while dietary data from 2003 to 2018 were derived from the first day's total nutrient intakes. OBS incorporates 16 dietary components, such as niacin, riboflavin, total folate, vitamin E, vitamin B6, vitamin B12, vitamin C, carotenoids, and dietary fiber. It also includes minerals like selenium, calcium, magnesium, zinc, and copper, as well as iron and total fat. In addition to these dietary factors, four lifestyle factors are considered: smoking behavior, alcohol intake, BMI, and physical activity. Out of these, five elements—BMI, total fat, iron, smoking habits, and alcohol consumption—are recognized as pro-oxidants, whereas the other elements are categorized as antioxidants (13). For the antioxidant components, scores are assigned based on tertiles: 0 for the first tertile, 1 for the second, and 2 for the third. On the other hand, for pro-oxidant components, the scoring is reversed, with the first tertile receiving a score of 2 and the third tertile being assigned a score of 0 (18).

The physical activity (PA) levels were determined using the NHANES Physical Activity Questionnaire (PAQ), and the calculation relied on the formula: the metabolic equivalent of task (MET) score * duration * weekly frequency. Due to variations in the PAQ across different cycles, PA calculations were adjusted according to the corresponding survey years. From 1999 to 2006, PA was categorized into walking or bicycling, home or yard tasks, muscle-strengthening activities, and screen time (e.g., watching TV or using a computer). From 2007 to 2018, the classification of PA included two primary categories: work-related activities, which were divided into tasks of moderate and vigorous intensity, and leisure-time activities, which consisted of walking, cycling, as well as vigorous and moderate-intensity recreational activities (19). Cotinine, which is the primary byproduct of nicotine metabolism, was utilized to assess exposure to smoking by measuring cotinine concentrations in plasma samples (20). Alcohol intake was divided into three categories: individuals classified as heavy drinkers (with a daily intake of ≥15 g for women and ≥30 g for men), moderate drinkers (those consuming between 0 and 15 g per day for women and 0–30 g per day for men), and abstainers (<12 drinkers/year), scored as 2, 1, and 0, correspondingly (13). Detailed scoring criteria for each OBS component are provided in Supplementary Table Sl.

2.3 Evaluation of overweight/obesity

Overweight and obesity were assessed based on the BMI, which is calculated as weight (kg)/height (m)^2. The CDC classifies BMI into specific categories: underweight (<18.5 kg/m^2), normal weight

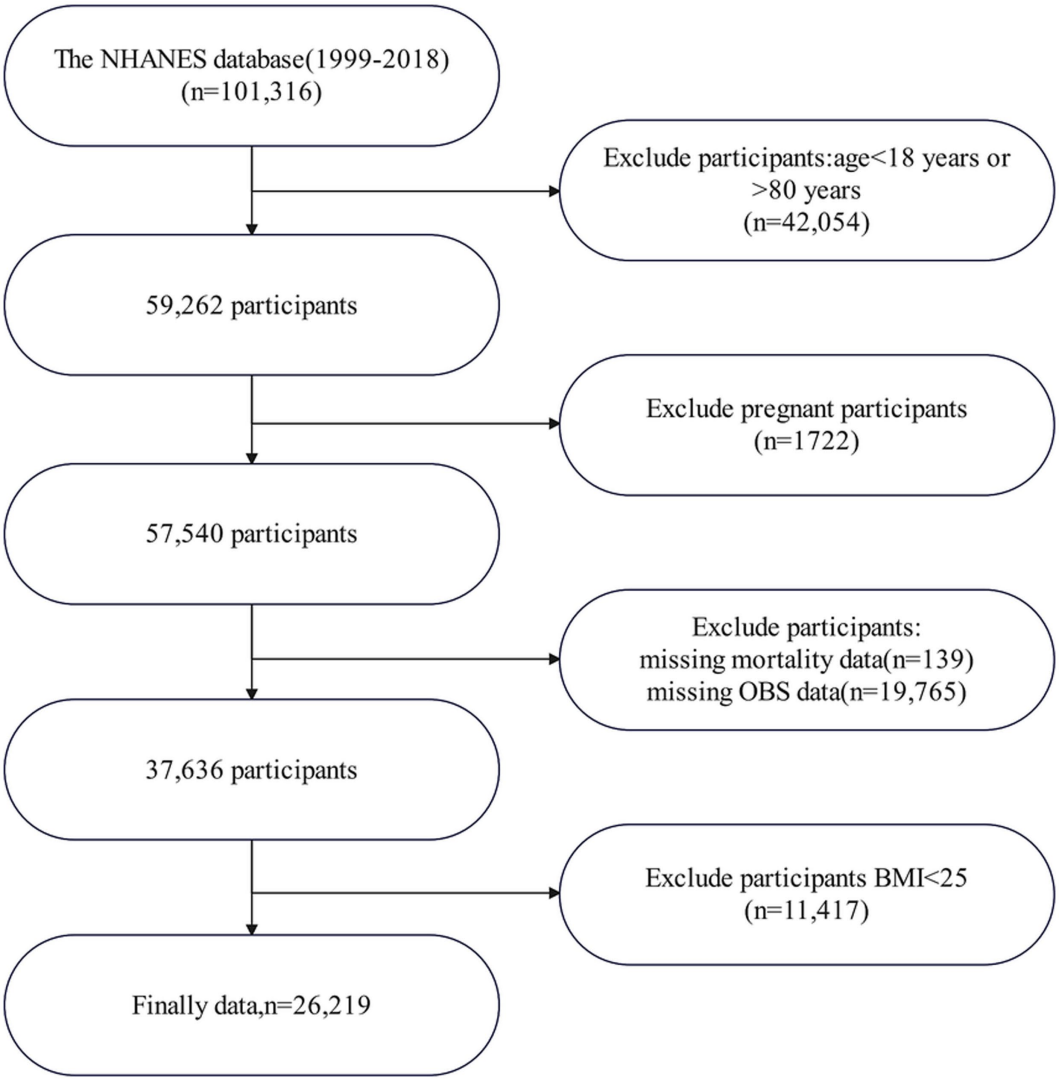

FIGURE 1
Flowchart of patient enrollment. NHANES, National Health and Nutrition Examination Survey; OBS, oxidative balance score; BMI, body mass index.

(18.5–24.9 kg/m^2), overweight (25–29.9 kg/m^2), and obesity (≥30 kg/m^2) (21).

2.4 Covariates

The analysis accounted for various covariates, including demographic and socioeconomic factors such as age, gender, and educational attainment (categorized as Less Than 9th Grade, 9–11th Grade, High School Graduate/GED or equivalent, Some College or Associate's Degree, and College Graduate or higher). Ethnicity/race classifications included Mexican American, Other Hispanic, Non-Hispanic White, Non-Hispanic Black, and others. Marital status was grouped as married, single, or cohabiting. Economic status was assessed using the poverty income ratio, which was classified into low, medium, and high tiers. Smoking history referred to individuals who had smoked 100 cigarettes in their lives at least, while alcohol intake was defined as consuming a minimum of 12 beverages per annum. Medical history included prior diagnoses of hypertension and diabetes. In addition, total energy intake was included as a covariate in the analysis to account for dietary influences.

2.5 Ascertainment of mortality

This research examined two primary outcomes: mortality from all causes and mortality specifically attributed to cardiovascular disease (CVD). Information on mortality was obtained from the National Death Index (NDI) database. Cardiovascular disease (CVD) mortality was determined using diagnostic categories outlined in the 10th Revision of the International Classification of Diseases (ICD-10). The relevant codes include I00–I09, I11, I13, I20–I51, and I60–I69. NHANES baseline data (1999–2018) were matched longitudinally with the NDI database to access mortality information, with follow-up available until December 1, 2019. The NCHS provided the "*2019 Public-Use Linked Mortality Files*."

2.6 Statistical analysis

All data analysis and graphical representation for this research were carried out utilizing R software (V4.4.1), IBM SPSS Statistics (V25), and GraphPad Prism (V9). Baseline characteristics were grouped according to OBS quartiles. The continuous variables were described using the mean and standard deviation (SD), while categorical variables were represented by frequencies and percentages. Differences in continuous variables between groups were examined using one-way analysis of variance (ANOVA), while Pearson's chi-square test was employed for categorical variable analysis. Initially, the survival rates between different groups were compared using Kaplan–Meier (K–M) survival analysis, and the Log-rank test was employed to evaluate statistical significance. Subsequently, to evaluate the influence of various factors on the outcomes, Cox proportional hazard regression models were utilized, calculating hazard ratios (HRs) with 95% confidence intervals (CIs). To control for possible confounding variables, three distinct analytical models were constructed: Model 1 did not include any adjustments, while Model 2 controlled for age, race, and gender. In Model 3, further adjustments were made for age, gender, race, level of education, marital status, poverty-to-income ratio (PIR), alcohol use, smoking habits, as well as past medical history of hypertension and diabetes. To address potential non-linear relationships, Restricted Cubic Splines (RCS) were used to segment continuous variables, enabling a more refined characterization of their relationship with outcomes. Furthermore, subgroup analyses examine if the relationship between variables and outcomes varies across populations with differing characteristics. Subgroup analyses, along with sensitivity analysis, were conducted to verify the stability and generalizability of our results. In addition, we conducted a mediation analysis to investigate whether OBS could influence mortality risk in overweight/obese individuals through white blood cell count (WBC) and gamma-glutamyl transferase (GGT) (22, 23). We computed the average causal mediation effect (ACME), average direct effect (ADE), and proportion mediated through 500 simulations (sim). A p-value less than 0.05 indicates statistical significance.

3 Results

3.1 Baseline characteristics

Stratified by OBS quartiles, Table 1 displays the baseline characteristics. 26,219 overweight or obese participants were incorporated in the study. The participants' average age in this study was 49.83 years, with a standard deviation of ±17.42 years, predominantly comprising non-Hispanic White individuals. Participants in the fourth quartile (Q4) of OBS were more inclined to be male, younger, married, and engage in alcohol consumption, while less likely to smoke or identify as non-Hispanic Black, in contrast to those in the first quartile (Q1). Those in the higher quartiles of OBS were more likely to possess higher educational qualifications, experience greater household earnings, and have a reduced rate of hypertension and diabetes.

3.2 The relationship between OBS and mortality

Figure 2 presents KM curves, illustrating statistical significance in all-cause and cardiovascular mortality across OBS levels ($p < 0.001$). Mortality was highest within the first OBS quartile (Q1) and lowest within the fourth quartile (Q4). With a follow-up duration averaging 115 months, among 26,219 overweight or obese participants, 2,239 (8.5%) deaths occurred, of which 837 (3.2%) were attributable to cardiovascular disease.

Table 2 shows the findings from the Cox regression. In the initial unadjusted model (Model 1), the risk of all-cause mortality reduced as OBS increased (HR 0.977, 95% CI 0.972–0.982, $p < 0.001$). When comparing the highest OBS quartile (Q4) to the lowest quartile (Q1), the former had a 35.0% lower risk of mortality (HR 0.650, 95% CI 0.591–0.714, $p < 0.001$). In Model 2, which controlled for age, sex, and race, individuals in the highest OBS quartile had a 35.4% reduction in mortality risk (HR 0.646, 95% CI 0.585–0.713, $p < 0.001$). In the fully adjusted model (Model 3), the risk of all-cause mortality was 21.7% lower for participants in Q4 compared to Q1 (HR 0.783, 95% CI 0.704–0.870, $p < 0.001$).

The Cox regression analysis of OBS and cardiovascular mortality is shown in Table 2. In the unadjusted model (Model 1), the risk of cardiovascular mortality reduced as OBS increased (HR 0.973, 95% CI 0.966–0.980, $p < 0.001$). Participants in Q4 demonstrated a 43.2% lower cardiovascular mortality risk compared to those in Q1 (HR 0.568, 95% CI 0.486–0.663, $p < 0.001$). In Model 2, individuals in the Q4 group still showed a 43.0% reduction in cardiovascular mortality risk (HR 0.570, 95% CI 0.484–0.670, $p < 0.001$). In the fully adjusted Model 3, an inverse relationship between OBS and cardiovascular mortality persisted (HR 0.983, 95% CI 0.974–0.992, $p < 0.001$). Participants categorized in Q4 exhibited a 29.5% lower risk of cardiovascular mortality compared to those in Q1 (HR 0.705, 95% CI 0.592–0.839, $p < 0.001$).

Based on model 3, we added total energy intake as a covariate for sensitivity analysis (Supplementary Table S2). The results indicate that the association between OBS and both all-cause mortality and cardiovascular mortality remains statistically significant. In Supplementary Table S3, we provide a more detailed breakdown of the differential contributions of OBS categories to mortality outcomes. In the fully adjusted model, both dietary OBS (HR 0.989, 95% CI 0.983–0.994, $p < 0.001$) and lifestyle OBS (HR 0.911, 95% CI 0.887–0.936, $p < 0.001$) were negatively associated with all-cause mortality, and the results were statistically significant. After full adjustment, the risk of cardiovascular mortality decreased with the increase in both dietary OBS (HR 0.983, 95% CI 0.974–0.992, $p < 0.001$) and lifestyle OBS (HR 0.898, 95% CI 0.860–0.938, $p < 0.001$).

We further optimized the RCS analysis based on the completely adjusted model. The findings suggested a linear inverse relationship between OBS and both all-cause and cardiovascular mortality, with non-linearity p-values of 0.1816 and 0.0798, respectively (Figure 3).

3.3 Subgroup analysis

To evaluate the robustness of the relationship between OBS and mortality, the dataset was divided into subcategories according to variables such as age, gender, ethnicity, educational attainment, marital status, income level, smoking and drinking behaviors, as well as histories of hypertension, diabetes, and overweight/obesity (Table 3). The findings demonstrated that the inverse relationship between OBS and mortality remained broadly uniform across various subgroups. Our analysis revealed that the impact of OBS on all-cause mortality was significantly altered by overweight/

TABLE 1 Baseline characteristics according to OBS quartiles in OV/OB patients.

	Q1	Q2	Q3	Q4	*p*-value
N	6,021	6,658	5,908	7,632	
Age, mean ± SD (years)	50.068 ± 18.013	50.934 ± 17.687	50.119 ± 17.233	48.458 ± 16.741	<0.001
Gender (%)					
Male	2014(33.4%)	2,799(42.0%)	3,110(52.6%)	5,112(67.0%)	<0.001
Female	4,007(66.6%)	3,859(58.0%)	2,798(47.4%)	2,520(33.0%)	
Race/ethnicity (%)					
Mexican American	1,065 (17.7%)	1,335 (20.1%)	1,203 (20.4%)	1,590 (20.8%)	<0.001
Other Hispanic	490 (8.1%)	619 (9.3%)	574 (9.7%)	631 (8.3%)	
Non-Hispanic White	2,297 (38.1%)	2,784 (41.8%)	2,679 (45.3%)	3,682 (48.2%)	
Non-Hispanic Black	1862 (30.9%)	1,540 (23.1%)	1,074 (18.2%)	1,165 (15.3%)	
Other Race	307 (5.1%)	380 (5.7%)	378 (6.4%)	564 (7.4%)	
Education (%)					
Less than 9th grade	821 (13.6%)	839 (12.6%)	673 (11.4%)	624 (8.2%)	<0.001
9–11th grade	1,117 (18.6%)	952 (14.3%)	757 (12.8%)	846 (11.1%)	
High school graduate/ GED	1,580 (26.2%)	1,612 (24.2%)	1,305 (22.1%)	1,617 (21.2%)	
Some college or associate degree	1,677 (27.9%)	1994 (29.9%)	1774 (30.0%)	2,239 (29.3%)	
College graduate or above	705 (11.7%)	1,156 (17.4%)	1,320 (22.3%)	2,203 (28.9%)	
Not recorded	121 (2.0%)	105 (1.6%)	79 (1.3%)	103 (1.3%)	
PIR					
Low	2,473 (41.1%)	2076 (31.2%)	1,677 (28.4%)	1882 (24.7%)	<0.001
Middle	1784 (29.6%)	2,206 (33.1%)	1799 (30.5%)	2,229 (29.2%)	
High	1,258 (20.9%)	1830 (27.5%)	1944 (32.9%)	2,966 (38.9%)	
Not recorded	506 (8.4%)	546 (8.2%)	488 (8.3%)	555 (7.3%)	
Marital status					
Married	2,597 (43.1%)	3,473 (52.2%)	3,307 (56.0%)	4,586 (60.1%)	<0.001
Single	2,756 (45.8%)	2,585 (38.8%)	2063 (34.9%)	2,324 (30.5%)	
Living with a partner	477 (7.9%)	421 (6.3%)	417 (7.1%)	564 (7.4%)	
Not recorded	191 (3.2%)	179 (2.7%)	121 (2.0%)	158 (2.1%)	
Smoking					
Yes	2,883 (47.9%)	2,854 (42.9%)	2,556 (43.3%)	3,128 (41.0%)	<0.001
No	3,099 (51.5%)	3,774 (56.7%)	3,330 (56.4%)	4,470 (58.6%)	
Not recorded	39 (0.6%)	30 (0.5%)	22 (0.4%)	34 (0.4%)	
Drinking					
Yes	3,264 (54.2%)	3,737 (56.1%)	3,645 (61.7%)	4,921 (64.5%)	<0.001
No	2,756 (45.8%)	2,920 (43.9%)	2,260 (38.3%)	2,710 (35.5%)	
Not recorded	1 (0.0%)	1 (0.0%)	3 (0.1%)	1 (0.0%)	
Hypertension history					
Yes	2,550 (42.4%)	2,706 (40.6%)	2,298 (38.9%)	2,653 (34.8%)	<0.001
No	3,440 (57.1%)	3,926 (59.0%)	3,601 (61.0%)	4,965 (65.1%)	
Not recorded	31 (0.5%)	26 (0.4%)	9 (0.2%)	14 (0.2%)	
Diabetes status					
Diabetes	884 (14.7%)	972 (14.6%)	788 (13.3%)	856 (11.2%)	<0.001

(Continued)

TABLE 1 (Continued)

	Q1	Q2	Q3	Q4	*p*-value
No	4,975 (82.6%)	5,544 (83.3%)	4,968 (84.0%)	6,593 (86.4%)	
Prediabetes	157 (2.6%)	138 (2.1%)	147 (2.5%)	183 (2.4%)	
Not recorded	5 (0.1%)	4 (0.1%)	5 (0.1%)	0 (0.0%)	
OW/OB					
Overweight	2,489 (41.3%)	3,083 (46.3%)	2,877 (48.7%)	4,255 (55.8%)	<0.001
Obesity	3,532 (58.7%)	3,575 (53.7%)	3,031 (51.3%)	3,377 (44.2%)	

GED, general equivalent diploma; PIR, the ratio of family income to poverty. Continuous variables were presented as mean ± standard error, and categorical variables were reported as numbers (percentages).

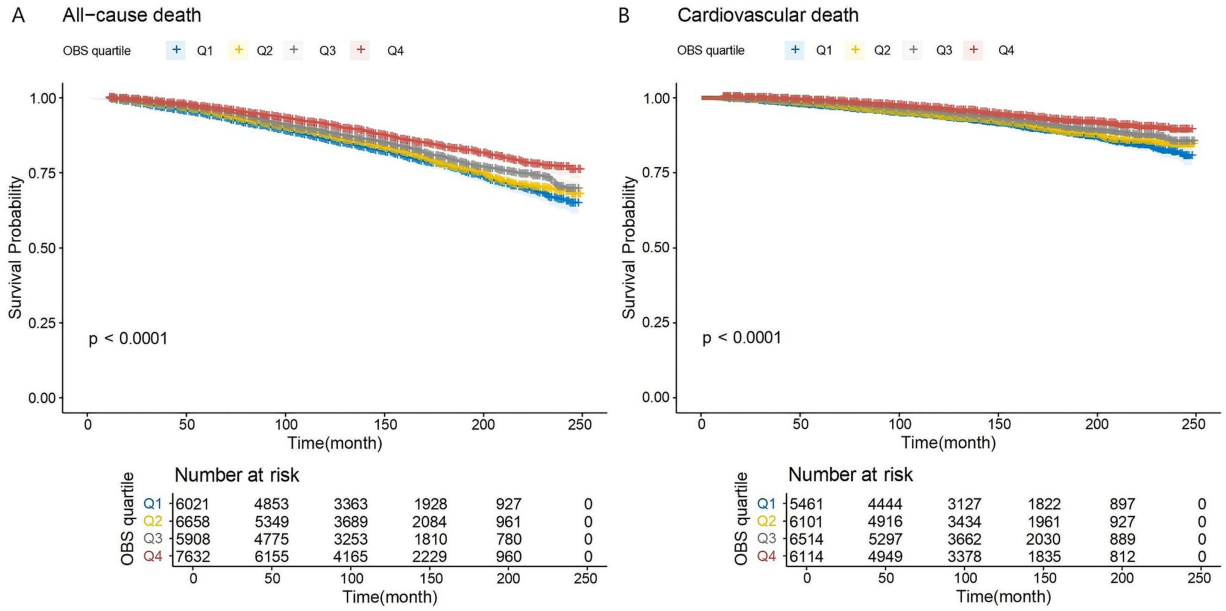

FIGURE 2
(A,B) K–M analyses for mortality among the four groups. Q1–Q4: quartiles 1–4. **(A)** All-cause mortality. **(B)** Cardiovascular mortality.

TABLE 2 Multivariable Cox regression models assessed the association between OBS and mortality in OV/OB.

Exposure	Model1	*P*	Model2	*P*	Model3	*P*
All-cause death						
OBS	0.977(0.972–0.982)	<0.001	0.975(0.970–0.980)	<0.001	0.985(0.980–0.991)	<0.001
OBS quartile						
Q1	Reference		Reference		Reference	
Q2	0.917(0.840–1.002)	0.055	0.824(0.754–0.900)	<0.001	0.916(0.833–1.007)	0.070
Q3	0.817(0.744–0.898)	<0.001	0.761(0.691–0.838)	<0.001	0.856(0.772–0.949)	0.003
Q4	0.650(0.591–0.714)	<0.001	0.646(0.585–0.713)	<0.001	0.783(0.704–0.870)	<0.001
Cardiovascular death						
OBS	0.973(0.966–0.980)	<0.001	0.971(0.963–0.979)	<0.001	0.983(0.974–0.992)	<0.001
OBS quartile						
Q1	Reference		Reference		Reference	
Q2	0.918(0.803–1.050)	0.212	0.816(0.713–0.934)	0.003	0.920(0.796–1.062)	0.255
Q3	0.763(0.665–0.877)	<0.001	0.728(0.632–0.840)	<0.001	0.815(0.700–0.948)	0.008
Q4	0.568(0.486–0.663)	<0.001	0.570(0.484–0.670)	<0.001	0.705(0.592–0.839)	<0.001

Model 1 was unadjusted; Model 2 adjusted for age, race, and sex; and Model 3 further adjusted for age, sex, race, education level, marital status, poverty-to-income ratio, alcohol consumption, smoking status, history of hypertension, and history of diabetes.

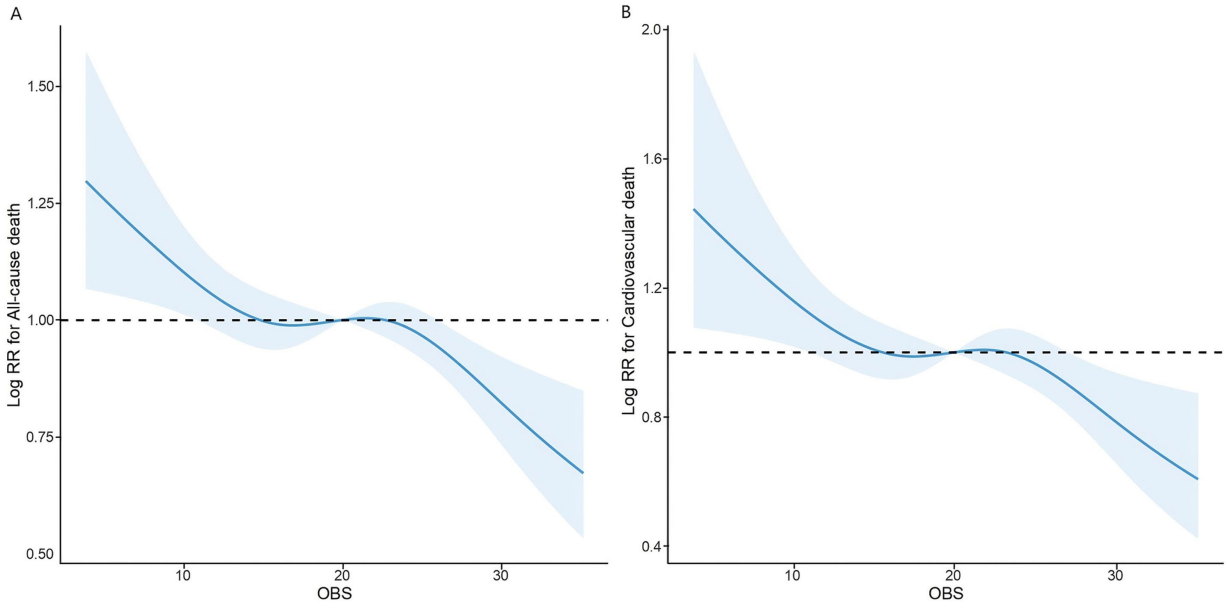

FIGURE 3
The association of OBS with all-cause **(A)** and cardiovascular mortality **(B)** among overweight and obese visualized by restricted cubic spline.

obesity within this population subgroup (p for interaction = 0.002). Age, level of education, and overweight/obesity were recognized as significant modifiers affecting the link between OBS and cardiovascular mortality among overweight or obese individuals (p for interaction = 0.039, 0.014, and 0.017, correspondingly). In addition, although the interaction p-value for the diabetes subgroup analysis was not statistically significant, the observed risk differences suggest a potential trend. Specifically, individuals with diabetes (HR 0.993, 95% CI 0.982–1.004, $p = 0.205$) seem to derive less benefit from higher OBS compared to those with normal glucose metabolism (HR 0.984, 95% CI 0.978–0.990, $p < 0.001$). Therefore, we conducted a subgroup analysis between the impaired glucose metabolism group (pre-diabetes + diabetes group) and the non-diabetic group. The results suggest that impaired glucose metabolism is an important factor influencing the association between OBS and cardiovascular mortality in overweight or obese individuals (p for interaction < 0.001) (Supplementary Table S4).

3.4 Mediation analyses

The WBC and GGT mediated the relationship between OBS and all-cause mortality, with mediation proportions of 1.53 and 1.95% ($p < 0.001$), respectively. Similarly, WBC and GGT also mediated the relationship between OBS and cardiovascular mortality, with mediation proportions of 0.87 and 1.34% ($p < 0.05$), respectively (Figure 4).

4 Discussion

As far as we are aware, this investigation represents the first attempt to explore the relationship between OBS and survival outcomes among overweight and obese individuals, utilizing data derived from the NHANES database. In a cohort of 26,219 overweight or obese individuals throughout 10 NHANES cycles (1999–2018), we found an inverse association between OBS and the risks associated with all-cause as well as cardiovascular mortality, with consistent and stable results across subgroup analyses. These findings suggest that antioxidant-rich diets and lifestyle patterns may confer a protective effect on the survival outcomes of overweight and obese individuals.

Reactive oxygen species are by-products of metabolic pathways in the body, strongly associated with the advancement of overweight, obesity, and related metabolic complications. The generation of ROS predominantly occurs in the mitochondria within cells (24). Overweight and obese increase the mechanical load on the body and myocardial metabolism, thereby leading to increased oxygen consumption. Additionally, inflammatory mediators and bioactive substances, such as TNF-α, interleukins (IL), and angiotensin II, are secreted by adipose tissue and play a pivotal role in stimulating immune cells and activating NADPH oxidase (NOS), which consequently leads to the generation of ROS (25–27). Similarly, ROS production promotes the secretion of inflammatory factors and pro-inflammatory transcription mediators, such as nuclear factor activator protein-1 (AP-1) and kappa B (NF-κB) (28). Furthermore, ROS plays a critical role in adipogenesis by triggering the differentiation of mesenchymal stem/stromal cells into adipocytes and activating adipogenic signaling networks via second messengers (25, 29). Increased ROS in tissues leads to the inactivation of components and enzymes in the respiratory chain, resulting in mitochondrial dysfunction. These processes ultimately contribute to multiple metabolic diseases, such as obesity, type 2 diabetes, aging, and may even increase mortality (30).

Several large-scale cohort studies have shown that the risk of mortality is elevated in overweight and obese populations (31). Our results demonstrate that increased OBS levels are linked to a lower

TABLE 3 Stratified analysis of the relationship between OBS and mortality in overweight and obesity.

	All-cause mortality		Cardiovascular mortality	
	HR (95% CI)	*P*-value	HR (95% CI)	*P*-value
Age				
≤60	0.987(0.977–0.998)	0.022	0.979(0.960–0.998)	0.029
>60	0.986(0.980–0.992)	<0.001	0.984(0.975–0.993)	0.001
P for interaction		0.080		0.039
Gender				
Male	0.988(0.981–0.996)	0.002	0.988(0.977–0.999)	0.031
Female	0.984(0.976–0.993)	<0.001	0.977(0.964–0.990)	0.001
P for interaction		0.550		0.182
Race				
Mexican American	0.991(0.976–1.006)	0.222	0.989(0.966–1.013)	0.359
Other Hispanic	1.002(0.974–1.031)	0.894	1.006(0.962–1.052)	0.787
Non-Hispanic White	0.984(0.977–0.991)	<0.001	0.982(0.971–0.992)	0.001
Non-Hispanic Black	0.986(0.973–0.998)	0.027	0.977(0.958–0.996)	0.016
Other Race	0.989(0.955–1.025)	0.549	1.027(0.965–1.094)	0.401
P for interaction		0.257		0.361
Education				
Less than 9th grade	0.995(0.981–1.008)	0.421	0.992(0.974–1.011)	0.431
9–11th grade	0.986(0.974–0.999)	0.035	0.988(0.970–1.008)	0.238
High school graduate/GED	0.993(0.982–1.003)	0.183	0.997(0.980–1.013)	0.696
Some college or associate degree	0.981(0.970–0.992)	0.001	0.968(0.950–0.985)	<0.001
College graduate or above	0.976(0.962–0.990)	0.001	0.966(0.944–0.988)	0.002
P for interaction		0.055		0.014
Marital status				
Married	0.987(0.979–0.994)	0.001	0.988(0.977–1.000)	0.048
Single	0.986(0.978–0.994)	0.001	0.979(0.966–0.991)	0.001
Living with a partner	0.992(0.961–1.024)	0.629	0.985(0.926–1.047)	0.630
P for interaction		0.967		0.689
Poverty to income ratio				
Low	0.990(0.981–0.998)	0.018	0.983(0.970–0.997)	0.013
Middle	0.986(0.977–0.995)	0.002	0.988(0.975–1.002)	0.083
High	0.982(0.971–0.993)	0.001	0.975(0.957–0.993)	0.007
P for interaction		0.166		0.143
Smoking				
Yes	0.988(0.981–0.995)	0.001	0.986(0.975–0.998)	0.017
No	0.985(0.977–0.994)	0.001	0.981(0.969–0.994)	0.003
P for interaction		0.870		0.301
Drinking				
Yes	0.985(0.978–0.992)	<0.001	0.977(0.966–0.988)	<0.001
No	0.988(0.980–0.997)	0.005	0.992(0.979–1.004)	0.178
P for interaction		0.560		0.135
Hypertension history				
Yes	0.984(0.977–0.991)	<0.001	0.579(0.497–0.675)	<0.001

(Continued)

TABLE 3 (Continued)

	All-cause mortality		Cardiovascular mortality	
	HR (95% CI)	*P*-value	HR (95% CI)	*P*-value
No	0.990(0.982–0.999)	0.030	0.456(0.366–0.568)	<0.001
P for interaction		0.843		0.900
Diabetes status				
Diabetes	0.993(0.982–1.004)	0.205	0.988(0.972–1.005)	0.172
No	0.984(0.978–0.990)	<0.001	0.982(0.972–0.992)	<0.001
Prediabetes	0.990(0.960–1.022)	0.535	0.975(0.929–1.024)	0.308
P for interaction		0.411		0.801
OW/OB				
Overweight	0.981(0.974–0.989)	<0.001	0.535(0.449–0.639)	<0.001
Obesity	0.990(0.982–0.998)	0.014	0.538(0.450–0.644)	<0.001
P for interaction		0.002		0.017

The stratified analysis was performed using the fully adjusted model (Model 3).

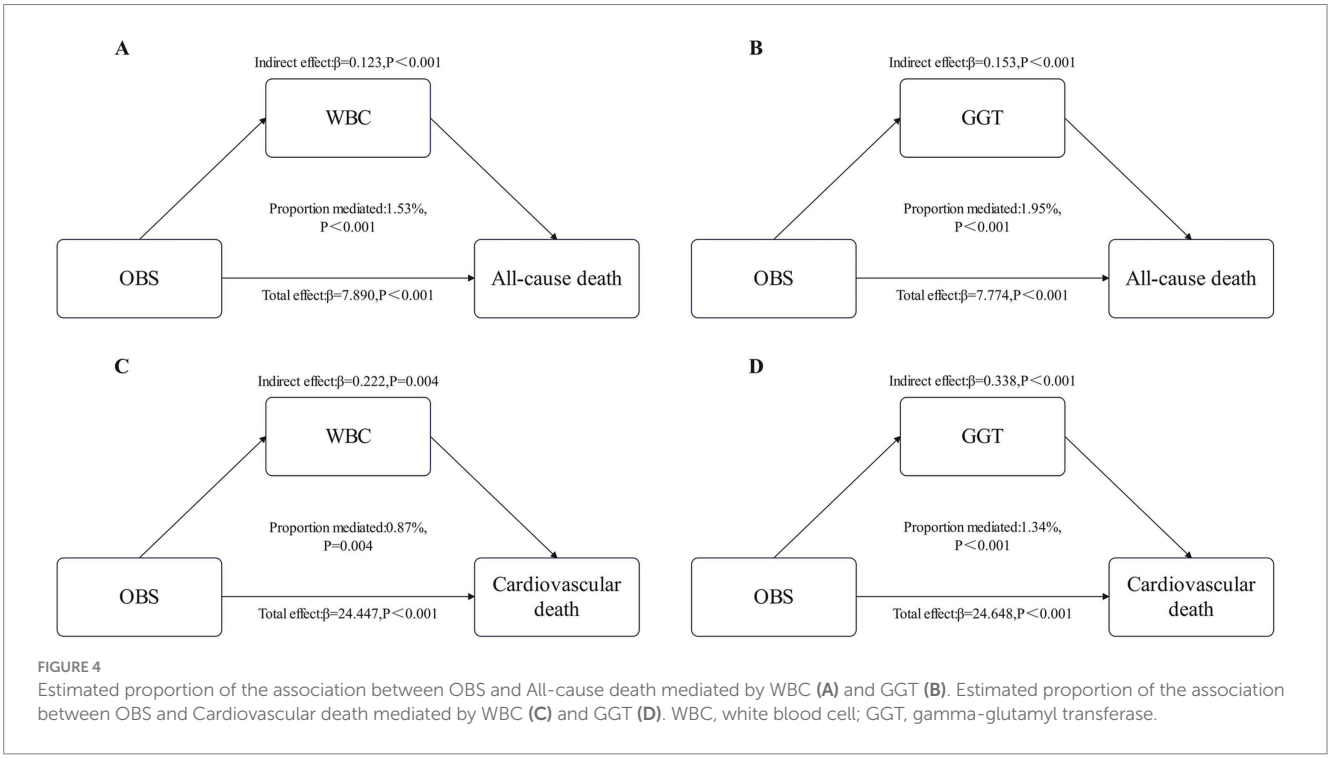

FIGURE 4
Estimated proportion of the association between OBS and All-cause death mediated by WBC **(A)** and GGT **(B)**. Estimated proportion of the association between OBS and Cardiovascular death mediated by WBC **(C)** and GGT **(D)**. WBC, white blood cell; GGT, gamma-glutamyl transferase.

likelihood of both all-cause and cardiovascular mortality in individuals with overweight or obesity, consistent with previous research. Cheng et al. (32) conducted an analysis using seven NHANES cycles and discovered that the link between OBS and the risk of cardiovascular disease was more pronounced among individuals exhibiting greater metabolic abnormalities. Wang et al. (33), utilizing a cross-sectional approach, identified an inverse relationship between OBS and both abdominal adiposity and visceral fat mass. High-quality diets may reduce the risks of cardiovascular and all-cause mortality associated with inflammation, with this effect being particularly pronounced in obese populations (34). High-quality diets are typically distinguished by the intake of abundant fruits, nuts, legumes, and vegetables, which are abundant in antioxidants, unsaturated fatty acids, various vitamins, and dietary fiber (35, 36). Obese individuals with mild to moderate inflammation can significantly reduce their all-cause mortality risk by strictly adhering to a healthy diet, though this effect is not significant in those with severe inflammation. This suggests that early intervention in systemic inflammation in overweight and obese individuals could reduce mortality risk (37). Nevertheless, several studies have reported a lack of a significant association between specific dietary factors and the risk of mortality (38). This discrepancy may stem from interactions between dietary nutrients or the impact of food production and processing stages (39, 40). While there are limited studies specifically examining the effect of OBS on mortality in overweight and obese individuals, various prospective cohort researches have analyzed the association between individual or select OBS components, such as iron, vitamin C, and β-carotene, and mortality. These studies indicate

that elevated levels of antioxidants are linked to a lower incidence of mortality (41, 42). A cohort study including 29,836 obese adults found that moderate to intense exercise effectively reduced the probability of microvascular issues, heart-related diseases, and death from any cause in obese individuals (43). Lai et al. (22), after analyzing 10 cycles of NHANES data, found that WBC and GGT played a potential mediating role between OBS and mortality risk in individuals with cardiometabolic risk factors. OBS provides a comprehensive and objective assessment of antioxidant-rich diets and lifestyles. Previous studies have analyzed the association among OBS and mortality risk, with findings suggesting an inverse association between OBS and mortality rates (17, 38, 44, 45). Romacho et al. (46) carried out a non-randomized controlled study, finding that lifestyle interventions improved systemic inflammation and reduced cardiovascular disease risk in obese patients. Kc et al. (47) discovered that educational level was linked to mortality risk, and we identified a potential interaction between education level and OBS concerning cardiovascular mortality risk in overweight/obese populations.

This study possesses several strengths. First, Multi-stage probability sampling design was utilized in the NHANES data collection to ensure that the sample and data are nationally representative. Second, OBS is a composite index that, compared to individual indicators, provides a more comprehensive analysis of the correlation between oxidative stress and mortality in overweight and obese populations. Thirdly, the data spanning from 1999 to 2018, with a large sample size and extended follow-up period, enhances the credibility as well as the stability of the outcomes. Finally, our study controlled for several potential confounding factors, including demographic characteristics, history of hypertension, smoking, and alcohol consumption.

However, there are several limitations to this study. First, although OBS includes 20 factors, it does not encompass all oxidative stress-related factors, leaving room for further adjustment. Second, dietary data were based solely on the first dietary interview, and may not accurately reflect participants' typical diets, potentially introducing bias into the results. Third, self-reported data from participants may be subject to reporting bias, particularly regarding dietary and lifestyle factors. Fourth, the findings may not be fully applicable to non-U.S. populations or individuals outside the overweight and obese categories. Therefore, caution should be exercised when applying these results to non-U.S. populations or individuals within the normal weight range. Further research in more diverse and broader populations is needed in the future. Fifth, a potential limitation of this study is the reliance on National Death Index (NDI) data to ascertain mortality outcomes. Due to inherent limitations in coding practices and classification systems, misclassification of causes of death may still occur. Finally, while this study utilized large-scale longitudinal data from the NHANES, there is an inherent risk of selection bias due to incomplete data. Some participants were excluded from the analysis because of missing data or other reasons, and as a result, selection bias to some extent is unavoidable.

5 Conclusion

Our study, encompassing 26,219 participants spanning 10 NHANES cycles, demonstrates a negative association between OBS and both all-cause and cardiovascular mortality in overweight and obese populations. A higher OBS score indicates higher exposure to antioxidant factors in diet and lifestyle and correlates with a reduced risk of both all-cause and cardiovascular mortality. The study emphasizes the status of maintaining an antioxidant-enriched diet, along with a healthy lifestyle, as part of management strategies for overweight and obesity.

Data availability statement

The datasets presented in this study can be found in online repositories. The names of the repository/repositories and accession number(s) can be found in the article/Supplementary material.

Ethics statement

Ethical approval was not required for the study involving humans in accordance with the local legislation and institutional requirements. Written informed consent to participate in this study was not required from the participants or the participants' legal guardians/next of kin in accordance with the national legislation and the institutional requirements.

Author contributions

SY: Conceptualization, Data curation, Formal analysis, Investigation, Methodology, Project administration, Resources, Software, Supervision, Validation, Visualization, Writing – original draft, Writing – review & editing. HD: Conceptualization, Investigation, Methodology, Software, Supervision, Validation, Writing – review & editing. YC: Data curation, Investigation, Methodology, Supervision, Validation, Writing – review & editing. SZ: Conceptualization, Data curation, Formal analysis, Investigation, Methodology, Validation, Visualization, Writing – review & editing.

Funding

The author(s) declare that no financial support was received for the research, authorship, and/or publication of this article.

Acknowledgments

We would like to thank the participants for their valuable support and contributions to this study.

Conflict of interest

The authors declare that the research was conducted in the absence of any commercial or financial relationships that could be construed as a potential conflict of interest.

Generative AI statement

The author(s) declare that no Generative AI was used in the creation of this manuscript.

Publisher's note

All claims expressed in this article are solely those of the authors and do not necessarily represent those of their affiliated organizations, or those of the publisher, the editors and the reviewers. Any product that may be evaluated in this article, or claim that may be made by its manufacturer, is not guaranteed or endorsed by the publisher.

Supplementary material

The Supplementary material for this article can be found online at: https://www.frontiersin.org/articles/10.3389/fnut.2025.1536024/full#supplementary-material

References

1. Okunogbe A, Nugent R, Spencer G, Powis J, Ralston J, Wilding J. Economic impacts of overweight and obesity: current and future estimates for 161 countries. *BMJ Glob Health*. (2022) 7:e009773. doi: 10.1136/bmjgh-2022-009773

2. Christopher JLM, Aleksandr YA, Peng Z, Cristiana A, Kaja MA, Mohsen A-K, et al. Global burden of 87 risk factors in 204 countries and territories, 1990–2019: A systematic analysis for the global burden of disease study 2019. *Lancet*. (2020) 396:1223–49. doi: 10.1016/S0140-6736(20)30752-2

3. Caballero B. Humans against obesity: Who will win? *Adv Nutr*. (2019) 10:S4–9. doi: 10.1093/advances/nmy055

4. Blüher M. Obesity: global epidemiology and pathogenesis. *Nat Rev Endocrinol*. (2019) 15:288–98. doi: 10.1038/s41574-019-0176-8

5. Avgerinos KI, Spyrou N, Mantzoros CS, Dalamaga M. Obesity and cancer risk: emerging biological mechanisms and perspectives. *Metab Clin Exp*. (2019) 92:121–35. doi: 10.1016/j.metabol.2018.11.001

6. Piché ME, Tchernof A, Després JP. Obesity phenotypes, diabetes, and cardiovascular diseases. *Circ Res*. (2020) 126:1477–500. doi: 10.1161/CIRCRESAHA.120.316101

7. Maggio CA, Pi-Sunyer FX. Obesity and type 2 diabetes. *Endocrinol Metab Clin N Am*. (2003) 32:805–22. doi: 10.1016/S0889-8529(03)00071-9

8. Dai H, Alsalhe TA, Chalghaf N, Riccò M, Bragazzi NL, Wu J. The global burden of disease attributable to high body mass index in 195 countries and territories, 1990-2017: an analysis of the global burden of disease study. *PLoS Med*. (2020) 17:e1003198. doi: 10.1371/journal.pmed.1003198

9. Roberts CK, Sindhu KK. Oxidative stress and metabolic syndrome. *Life Sci*. (2009) 84:705–12. doi: 10.1016/j.lfs.2009.02.026

10. Li Y, Liu Y. Adherence to an antioxidant diet and lifestyle is associated with reduced risk of cardiovascular disease and mortality among adults with nonalcoholic fatty liver disease: evidence from NHANES 1999-2018. *Front Nutr*. (2024) 11:1361567. doi: 10.3389/fnut.2024.1361567

11. Xu Z, Xue Y, Wen H, Chen C. Association of oxidative balance score and lung health from the National Health and nutrition examination survey 2007-2012. *Front Nutr*. (2022) 9:961950. doi: 10.3389/fnut.2022.961950

12. Liu Y, Chen M. Dietary and lifestyle oxidative balance scores are independently and jointly associated with nonalcoholic fatty liver disease: a 20 years nationally representative cross-sectional study. *Front Nutr*. (2023) 10:1276940. doi: 10.3389/fnut.2023.1276940

13. Zhang W, Peng SF, Chen L, Chen HM, Cheng XE, Tang YH. Association between the oxidative balance score and telomere length from the National Health and nutrition examination survey 1999-2002. *Oxidative Med Cell Longev*. (2022) 2022:1–11. doi: 10.1155/2022/1345071

14. Noruzi Z, Jayedi A, Farazi M, Asgari E, Dehghani Firouzabadi F, Akbarzadeh Z, et al. Association of Oxidative Balance Score with the metabolic syndrome in a sample of Iranian adults. *Oxidative Med Cell Longev*. (2021) 2021:5593919. doi: 10.1155/2021/5593919

15. Liu X, Liu X, Wang Y, Zeng B, Zhu B, Dai F. Association between depression and oxidative balance score: National Health and nutrition examination survey (NHANES) 2005-2018. *J Affect Disord*. (2023) 337:57–65. doi: 10.1016/j.jad.2023.05.071

16. Ilori TO, Wang X, Huang M, Gutierrez OM, Narayan KM, Goodman M, et al. Oxidative balance score and the risk of end-stage renal disease and cardiovascular disease. *Am J Nephrol*. (2017) 45:338–45. doi: 10.1159/000464257

17. Xu Z, Liu D, Zhai Y, Tang Y, Jiang L, Li L, et al. Association between the oxidative balance score and all-cause and cardiovascular mortality in patients with diabetes and prediabetes. *Redox Biol*. (2024) 76:103327. doi: 10.1016/j.redox.2024.103327

18. Zhan F, Lin G, Duan K, Huang B, Chen L, Ni J. Higher oxidative balance score decreases risk of stroke in US adults: evidence from a cross-sectional study. *Front Cardiovasc Med*. (2023) 10:1264923. doi: 10.3389/fcvm.2023.1264923

19. Lei X, Xu Z, Chen W. Association of oxidative balance score with sleep quality: NHANES 2007-2014. *J Affect Disord*. (2023) 339:435–42. doi: 10.1016/j.jad.2023.07.040

20. Brody DJ, Lu Z, Tsai J. Secondhand smoke exposure among nonsmoking youth: United States, 2013-2016. *NCHS Data Brief*. (2019) 348:1–8.

21. Dietz WH. The response of the US Centers for Disease Control and Prevention to the obesity epidemic. *Annu Rev Public Health*. (2015) 36:575–96. doi: 10.1146/annurev-publhealth-031914-122415

22. Lai Q, Ye L, Luo J, Zhang C, Wu Q, Shao Y. The cross-sectional correlation between the oxidative balance score and cardiometabolic risk factors and its potential correlation with longitudinal mortality in patients with cardiometabolic risk factors. *BMC Public Health*. (2024) 24:1452. doi: 10.1186/s12889-024-18967-z

23. Li H, Song L, Cen M, Fu X, Gao X, Zuo Q, et al. Oxidative balance scores and depressive symptoms: mediating effects of oxidative stress and inflammatory factors. *J Affect Disord*. (2023) 334:205–12. doi: 10.1016/j.jad.2023.04.134

24. Pérez-Torres I, Guarner-Lans V, Rubio-Ruiz ME. Reductive stress in inflammation-associated diseases and the pro-oxidant effect of antioxidant agents. *Int J Mol Sci*. (2017) 18:2098. doi: 10.3390/ijms18102098

25. Castro JP, Grune T, Speckmann B. The two faces of reactive oxygen species (ROS) in adipocyte function and dysfunction. *Biol Chem*. (2016) 397:709–24. doi: 10.1515/hsz-2015-0305

26. Martínez-Fernández L, Fernández-Galilea M, Felix-Soriano E, Escoté X, González-Muniesa P, Moreno-Aliaga MJ. Chapter 4 – inflammation and oxidative stress in adipose tissue: nutritional regulation. In: MoralAM del and CM Aguilera García, eds. Obesity. Cambridge (MA): Academic Press (2018) 63–92.

27. Fonseca-Alaniz MH, Takada J, Alonso-Vale MI, Lima FB. Adipose tissue as an endocrine organ: from theory to practice. *J Pediatr*. (2007) 83:S192–203. doi: 10.1590/S0021-75572007000700011

28. Wang B, Trayhurn P. Acute and prolonged effects of TNF-alpha on the expression and secretion of inflammation-related adipokines by human adipocytes differentiated in culture. *Pflugers Arch*. (2006) 452:418–27. doi: 10.1007/s00424-006-0055-8

29. Kono T, Robinson FW, Blevins TL, Ezaki O. Evidence that translocation of the glucose transport activity is the major mechanism of insulin action on glucose transport in fat cells. *J Biol Chem*. (1982) 257:10942–7. doi: 10.1016/S0021-9258(18)33914-0

30. Bhatti JS, Bhatti GK, Reddy PH. Mitochondrial dysfunction and oxidative stress in metabolic disorders – a step towards mitochondria based therapeutic strategies. *Biochim Biophys Acta Mol basis Dis*. (2017) 1863:1066–77. doi: 10.1016/j.bbadis.2016.11.010

31. Wang YB, Page AJ, Gill TK, Melaku YA. The association between diet quality, plant-based diets, systemic inflammation, and mortality risk: findings from NHANES. *Eur J Nutr*. (2023) 62:2723–37. doi: 10.1007/s00394-023-03191-z

32. Cheng S, Han Y, Jiang L, Lan Z, Liao H, Guo J. Associations of oxidative balance score and visceral adiposity index with risk of ischaemic heart disease: a cross-sectional study of NHANES, 2005-2018. *BMJ Open*. (2023) 13:e072334. doi: 10.1136/bmjopen-2023-072334

33. Wang K, Deng M, Wu J, Luo L, Chen R, Liu F, et al. Associations of oxidative balance score with total abdominal fat mass and visceral adipose tissue mass percentages among young and middle-aged adults: findings from NHANES 2011-2018. *Front Nutr*. (2023) 10:1306428. doi: 10.3389/fnut.2023.1306428

34. Brighenti F, Valtueña S, Pellegrini N, Ardigò D, del D, Salvatore S, et al. Total antioxidant capacity of the diet is inversely and independently related to plasma concentration of high-sensitivity C-reactive protein in adult Italian subjects. *Br J Nutr*. (2005) 93:619–25. doi: 10.1079/BJN20051400

35. Furman D, Campisi J, Verdin E, Carrera-Bastos P, Targ S, Franceschi C, et al. Chronic inflammation in the etiology of disease across the life span. *Nat Med*. (2019) 25:1822–32. doi: 10.1038/s41591-019-0675-0

36. Ma Y, Griffith JA, Chasan-Taber L, Olendzki BC, Jackson E, Stanek EJ 3rd, et al. Association between dietary fiber and serum C-reactive protein. *Am J Clin Nutr*. (2006) 83:760–6. doi: 10.1093/ajcn/83.4.760

37. Talavera-Rodriguez I, Fernandez-Lazaro CI, Hernández-Ruiz Á, Hershey MS, Galarregui C, Sotos-Prieto M, et al. Association between an oxidative balance score and mortality: a prospective analysis in the SUN cohort. *Eur J Nutr*. (2023) 62:1667–80. doi: 10.1007/s00394-023-03099-8

38. Hu FB. Dietary pattern analysis: a new direction in nutritional epidemiology. *Curr Opin Lipidol*. (2002) 13:3–9. doi: 10.1097/00041433-200202000-00002

39. Kong SY, Goodman M, Judd S, Bostick RM, Flanders WD, McClellan W. Oxidative balance score as predictor of all-cause, cancer, and non-cancer mortality in a biracial US cohort. *Ann Epidemiol*. (2015) 25:256–62.e1. doi: 10.1016/j.annepidem.2015.01.004

40. Cilla A, Bosch L, Barberá R, Alegría A. Effect of processing on the bioaccessibility of bioactive compounds – a review focusing on carotenoids, minerals, ascorbic acid, tocopherols and polyphenols. *J Food Compos Anal*. (2018) 68:3–15. doi: 10.1016/j.jfca.2017.01.009

41. Abulmeaty MMA, Ghneim HK, Alkhathaami A, Alnumair K, Al Zaben M, Razak S, et al. Inflammatory cytokines, redox status, and cardiovascular diseases risk after weight loss via bariatric surgery and lifestyle intervention. *Medicina*. (2023) 59:751. doi: 10.3390/medicina59040751

42. Aune D, Keum N, Giovannucci E, Fadnes LT, Boffetta P, Greenwood DC, et al. Dietary intake and blood concentrations of antioxidants and the risk of cardiovascular disease, total cancer, and all-cause mortality: a systematic review and dose-response meta-analysis of prospective studies. *Am J Clin Nutr*. (2018) 108:1069–91. doi: 10.1093/ajcn/nqy097

43. Sabag A, Ahmadi MN, Francois ME, Postnova S, Cistulli PA, Fontana L, et al. Timing of moderate to vigorous physical activity, mortality, cardiovascular disease, and microvascular disease in adults with obesity. *Diabetes Care*. (2024) 47:890–7. doi: 10.2337/dc23-2448

44. Van Hoydonck PG, Temme EH, Schouten EG. A dietary oxidative balance score of vitamin C, beta-carotene and iron intakes and mortality risk in male smoking Belgians. *J Nutr*. (2002) 132:756–61. doi: 10.1093/jn/132.4.756

45. Mao Z, Prizment AE, Lazovich D, Bostick RM. Associations of dietary and lifestyle oxidative balance scores with mortality risk among older women: the Iowa Women's health study. *Eur J Nutr*. (2021) 60:3873–86. doi: 10.1007/s00394-021-02557-5

46. Romacho T, Glosse P, Richter I, Elsen M, Schoemaker MH, van Tol EA, et al. Nutritional ingredients modulate adipokine secretion and inflammation in human primary adipocytes. *Nutrients*. (2015) 7:865–86. doi: 10.3390/nu7020865

47. Kc S. The effect of education on adult mortality and disability: a global perspective. *Vienna Yearbook Populat Res*. (2010) 8:201–36. doi: 10.1553/populationyearbook2010s201

frontiers | Frontiers in Nutrition

TYPE Hypothesis and Theory
PUBLISHED 29 April 2025
DOI 10.3389/fnut.2025.1532961

OPEN ACCESS

EDITED BY
Qingyu Wang,
Beijing Hospital, China

REVIEWED BY
Carmen Rubio,
Manuel Velasco Suárez National Institute of Neurology and Neurosurgery, Mexico
Wasim Khan,
University of Illinois Chicago, United States

*CORRESPONDENCE
Catherine Shanahan
✉ Info@DrCate.com

RECEIVED 22 November 2024
ACCEPTED 31 March 2025
PUBLISHED 29 April 2025

CITATION
Shanahan C (2025) The energy model of insulin resistance: A unifying theory linking seed oils to metabolic disease and cancer. *Front. Nutr.* 12:1532961. doi: 10.3389/fnut.2025.1532961

The energy model of insulin resistance: A unifying theory linking seed oils to metabolic disease and cancer

Catherine Shanahan*

Rebel Well, LLC, Orlando, FL, United States

The problem of insulin resistance has exploded in recent decades, from practically nonexistent in 1950, to nearly ubiquitous today. Despite this, the dietary origins of insulin resistance remain elusive. Many have identified the Western Diet, focusing on saturated fat. However, population-scale consumption data shows that our consumption of saturated fat has remained unchanged, while our consumption of polyunsaturated fats has increased by more than 300%. This paper discusses the primary source of those polyunsaturated fatty acids (PUFA), a collection of eight chemically similar refined, bleached, and deodorized (RBD) seed oils, i.e., soy and canola, that now, together, represent the number one source of calories in the United States today, or approximately 30 percent of the average person's daily intake. The Energy Model of Insulin Resistance hypothesizes that RBD seed oil consumption can promote cellular oxidative stress, forcing cells to change their fueling strategy to reduce oxidative stress. This is accomplished by increasing aerobic glycolysis to minimize fat oxidation. Observed in both cancerous and insulin resistance cells, aerobic glycolysis is also known as the Warburg Effect. While beneficial to individual cells, at the whole-organism level, it disrupts intravascular glucose homeostasis, ultimately elevating insulin and counter-regulatory hormones (CRH) simultaneously. CRH oppose the insulin signal, leading to the phenotype of insulin resistance. In summary, the Energy Model of Insulin Resistance provides a framework for understanding that the primary metabolic deficit in people with insulin resistance may not be abnormal insulin signaling, but rather an abnormally increased metabolic demand for sugar. If correct, this would elucidate the mitochondrial origins of the Warburg Effect and suggest that avoiding RBD oils represents an important and understudied dietary strategy for addressing insulin resistance and cancer.

KEYWORDS

mitochondria, seed oil, PUFA, oxidative stress, cancer, insulin resistance, Warburg effect, obesity

Introduction: the unexplained rise of insulin resistance

Metabolic health is at an all-time low, hovering just under 7% of US Adults (1). According to the latest NHANES dataset, fewer than 25% of adolescents have an ideal HOMA-IR score of 1 or less (2). IR often progresses to type 2 diabetes. But it is also associated with many disabling and fatal conditions even before this progression has occurred. In spite of its prevalence and devastating consequences, the dietary root cause and cellular mechanism of insulin resistance remain unclear.

Various models have been proposed, each with it is own shortcomings from failing to be fully supported by epidemiological or mechanistic considerations. I will highlight the most important models here.

Perhaps the most enduring model of insulin resistance proposes that obesity itself drives insulin resistance. But this fails to explain the increasing prevalence of insulin resistance in normal weight individuals (3). Lack of exercise has also been put forth as a driver of insulin resistance, but this does not explain how athletes become insulin resistant (4). It is notable that both obesity and lack of exercise are thought to cause insulin resistance by some combination of inflammation and oxidative stress (5).

The Western Diet has also been identified as a causative agent, again linked to oxidative stress (6, 7). In terms of macronutrients (as opposed to minor constituents such as pesticide residue and artificial coloring agents), the focus is generally on fat and sugar. However more attention is generally paid to fat, especially saturated fat, than sugar, and this is reflected in the dietary guidelines for Americans, which place caps on total fat and saturated fat intakes that must be adhered to in order for any institution to qualify for federal funding. No similar sugar intake cap exists (8). Additionally, articles on the Western diet such as those cited in the above two review articles more frequently discuss animal experiments where insulin resistance was induced by high fat feeding than by high sugar feeding.

In contrast to those focusing on fat as the driver of the oxidative stress inducing insulin resistance, proponents of the newer carbohydrate model of insulin resistance focus on carbohydrate-driven oxidative stress. They hypothesize that refined sugar and carbohydrates may elevate insulin too often, such that they "wear out" the body's ability to respond to insulin (9). In this case, oxidative stress is provoked by elevated serum glucose (10). However, by definition blood glucose levels do not exceed 200 mg/dL for any significant period of time until insulin resistance has *already* progressed to type 2 diabetes, calling this mechanism to question.

RBD seed oils: an overlooked component of the western diet

The controversy over carbohydrate versus fat as a causative agent may exist in part because the characterization of the Western Diet is fundamentally flawed. Clemente-Suárez et al., write in 2023 that the Western Diet is "…a modern dietary pattern that is characterized by high intakes of processed and refined foods, red and processed meats, added sugars, and *saturated and trans* fats [emphasis mine]…." (6) Other authors make similar inaccurate remarks about saturated fat and trans fat (7, 11). While trans-fats had increased in the US diet during the 20th century, since 2000 they have declined as a result of the trans-fat ban, and by 2018 were largely eliminated (12). Secondly, and more pertinent, our saturated fat consumption is not increased compared to what it was before the incidence of metabolic disease began its precipitous rise in the middle of the 20th century. According to Figure 20, of the USDA publication Nutrient Content of the US Food Supply, 1909–2000 (13), our saturated fat consumption has remained remarkably stable in that time period, hovering between 50 and 58gm per day per person. However the same figure shows that our consumption of polyunsaturated fats increased nearly 300% between 1909 and 2000. The primary source of these polyunsaturated fats is the collection of eight refined, bleached, deodorized (RBD) seed oils that are the focus of this article and that remain critically under examined as a source of the oxidative stress (and inflammation) that many authors agree drives insulin resistance.

Oxidative stress: the crucial common theme?

From a mechanistic standpoint, many existing models of insulin resistance share the common theme of oxidative stress, as I briefly outlined above. These authors typically invoke inflammation as well as oxidation, as if the two processes are unrelated and must be examined independently. Others have made the same kinds of statements, and it seems to be a prevailing assumption that the two processes are independent (14–16). However this is not quite accurate.

It is important to recognize that inflammation generally begins with oxidative insults to the cell, particularly cell membrane phospholipids, whose oxidation initiates the activation of eicosanoids that drive the inflammatory cascade (17–19). If inflammation is only a secondary response to a primary insult, as appears may be the case in many if not all scenarios, then it may be unnecessary to invoke inflammation as a separate root cause driver of insulin resistance, and more logical to focus on oxidative process.

Indeed, Denham Harmon identified free radicals and their resultant oxidative insults as the root cause of cellular damage and aging in 1954 (20). The theory has been modified over the years, but the general thrust is the same: oxidative damage drives disease, inflammation, and aging (21). Thus, it is highly relevant that RBD seed oils are uniquely susceptible to free radical damage.

RBD seed oil, a novel food for humans

What is RBD seed oil?

The majority of edible oils in our food supply undergo refining, bleaching, and deodorizing after extraction. The edible oil industry refers to these as RBD oils. The term seed oil does not have an industry definition. For the purposes of this article, the term "RBD seed oil" will refer to the collection of eight vegetable seed oils with the highest concentrations of easily oxidized polyunsaturated fatty acids: corn, canola, cottonseed, soy, sunflower, safflower, rice bran, and grapeseed. Palm, coconut, peanut, olive and avocado can also be RBD but are lower in PUFAs and thus less of a concern.

These eight oils collectively comprise up to 80 percent of the average American's fat calories and nearly one-third of their total caloric intake (22). Any food constituting such a large portion of the daily caloric intake demands scrutiny, particularly a novel food that has no precedent of safe use by human prior to it is widespread introduction into the food supply during the 20th century.

Notably, over the last century we can appreciate a striking similarity between the rise of RBD oil consumption and the rise of metabolic disease, as illustrated in Figure 1. The similarity is greater than that of sugar, which has more often been implicated as a root cause of metabolic disease.

Recommendations to consume RBD oils

During the 20th century, the prevailing public health advice was to reduce saturated fatty acid and increase polyunsaturated fatty acids (PUFA). This emerged from the assumption that, because saturated fat consumption elevates cholesterol, that necessarily means it also causes heart attacks. Notably, the American Heart Association recommended these oils starting in 1961, but preliminary data from the first human trial to test this idea was not even collected until 1963, and not published until 1966 (23, 24). This is remarkable, and worthy of more attention that it has received, given the AHA's claims that it is an evidence based organization.

Since the AHA first made its recommendation, multiple reviews have found no evidence of increased cardiac mortality from saturated fat (25–29) and the same holds for elevated cholesterol (30–32). Although this evidence significantly undermines the saturated-fat-cholesterol theory, the Dietary Guidelines (DGA) are based on low quality evidence and expert opinion (33, 34). Although calls have been made for the DGA to use higher quality evidence, the experts involved assert that there is enough evidence that saturated fat does increase cardiac mortality (35). As a result, the Dietary Guidelines for Americans continue to make the same recommendation to consume more polyunsaturated oils, as they have since first published in 1980. And without a cap on their consumption, our dietary intakes of RBD seed oils have trended upwards for decades (see Figure 1). Today, the average American gets the majority—approximately 80 percent—of their fat calories from these eight RBD seed oils.

It is also remarkable that these oils were initially manufactured for purposes other than human consumption and never tested on any scale before being released into the food supply (36). Given their widespread consumption and the lack of long term safety data, it is critically important to understand that their chemical makeup is unique among food ingredients in several key aspects that must be considered together to understand their impact on human metabolic health.

RBD seed oil's novel chemistry

RBD seed oils are chemically distinct from fats and oils humanity has typically consumed in several aspects that pertain to their potential health effects. Unfortunately, dietitians and other nutrition experts often lump all "plant based" oils together, sending the strong message that if a consumer cannot afford more expensive extra virgin olive oil, they can simply purchase an RBD seed oil and get equivalent nutrition and expect the same health outcomes. This is erroneous. Four differentiators that pertain to their potential to promote significant redox imbalance will be highlighted here, and summarized in Figure 2.

Higher PUFA content

When compared to traditional fats, these new oils have less saturated fat and more easily oxidizable polyunsaturated fat, primarily linoleic acid. This reflects the fatty acid profile of the seeds from which they are derived. The eight seed oils mentioned above contain from 25 to 75 percent PUFA fatty acids. The predominant PUFA is the 18 carbon omega-6 linoleic acid, although canola also contains approximately 10 percent omega-3 linolenic. Soy oil is the dominant RBD seed oil in the US food supply representing 80 to 90 percent of all RBD seed oils consumed (37). It contains approximately 55 percent polyunsaturated fatty acids. Butter, tallow, lard, chicken fat, coconut, and olive were previously the dominant fats in the American food supply. Their PUFA content ranges from a low of 4 percent for tallow, and a high of 20 percent for chicken fat.

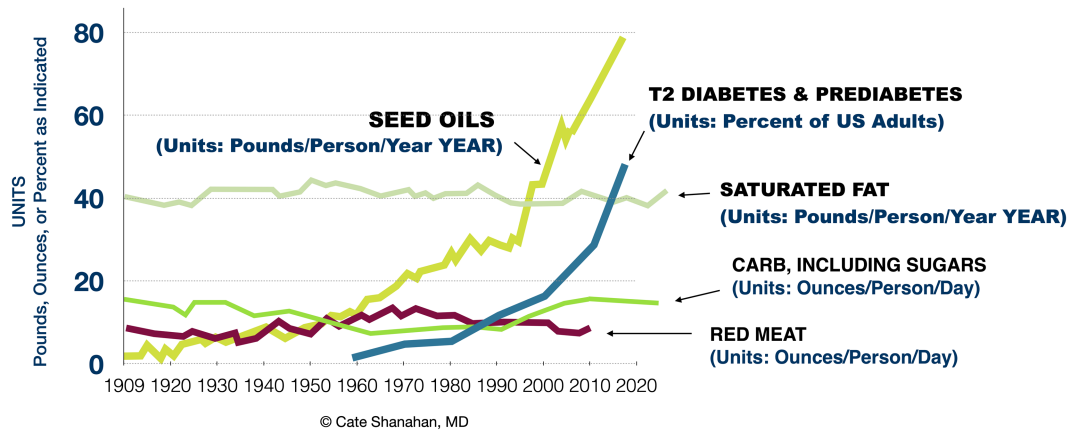

FIGURE 1
Associations between major dietary components and rates of advanced insulin resistance in the US population from 1909 to 2020.

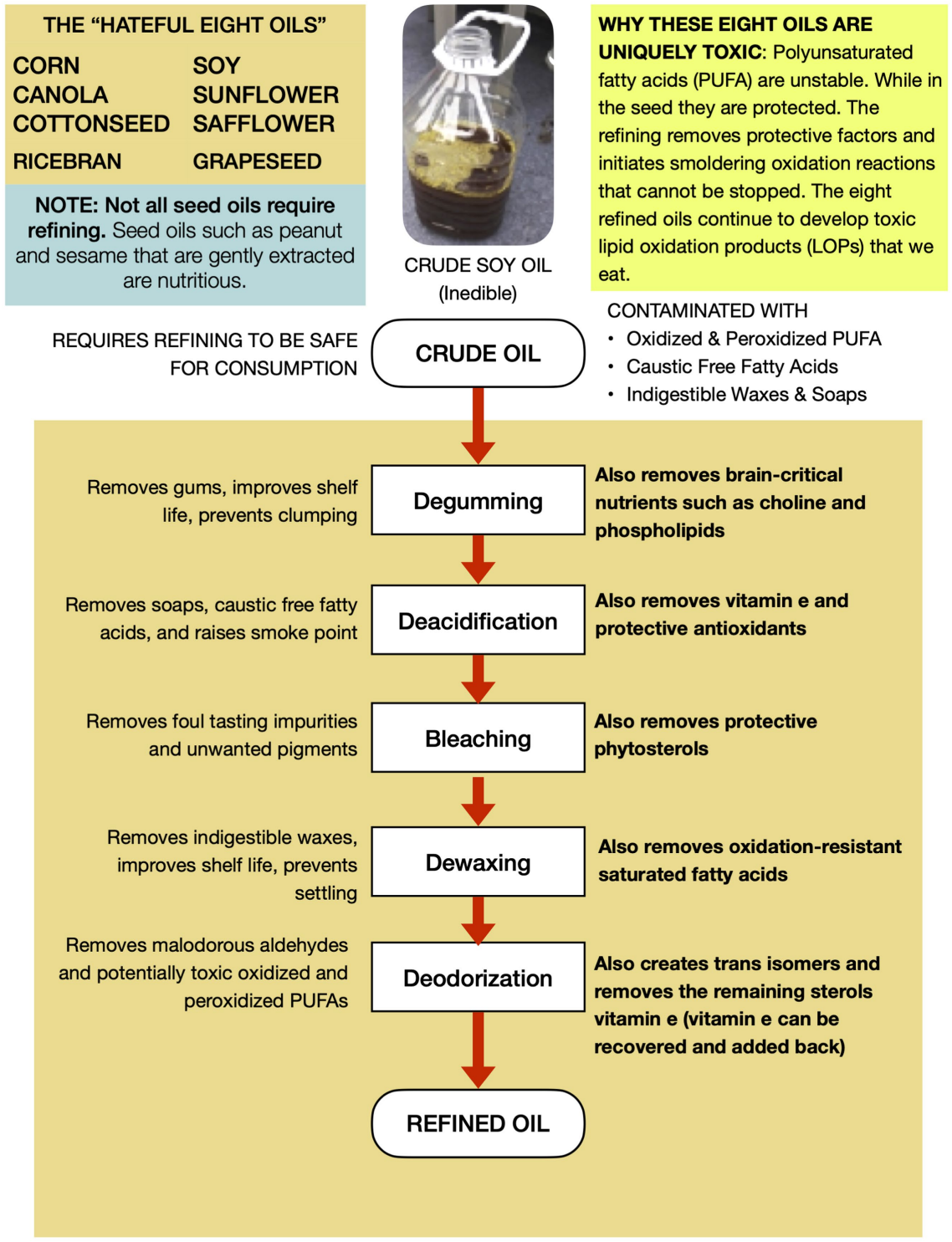

FIGURE 2
RBD seed oils are uniquely non-nutritive and easily oxidize into aldehydes and other toxins.

Inedible when first extracted

In contrast to the first press of other culinary oils like olive, sesame, and coconut, the crude oil that is extracted during the industrial processing of the eight aforementioned oilseeds is initially unsuitable for human consumption due to "process contaminants" such as free fatty acids, waxes, soaps, and oxidized lipids. Thus crude seed oils must be refined to remove those unwanted elements (38). Unfortunately, refining also removes important nutrients that impact human health significantly.

Lower antioxidant and vitamin content

The second differentiator is an unintended but unavoidable byproduct of the processing that the vast majority of RBD seed oils consumed undergo, which reduces their nutrient content significantly.

Unlike other oils, which reflect the nutritional profile of the seeds from which they are derived, RBD seed oils do not. Nutrients lost to oil refining vary by type but include a 25–35% reduction in soybean oil tocopherols (39, 40), a 60% reduction in Canola oil polyphenols (41), 99.8 percent loss of soybean oil phospholipids (39, 40). 90.7 percent loss of iron (39), and significant losses of copper, iron, magnesium, and calcium (40). Some of these nutrients function to protect the oil from oxidation, and their removal during refining makes the PUFA more susceptible to oxidation, with important consequences to their toxicity, discussed next.

Lipid oxidation products

PUFA oxidize more readily than saturated and monounsaturated fatty acids, and the resultant products are broadly called "lipid oxidation products." As a result, bottles leaving the factory contain a variety of partly oxidized PUFA that often have toxic properties (42). The concentration of toxins increases over time due to the removal of stabilizing factors, the small amount of oxygen and the fact that many lipid oxidation products (LOPs) are themselves more susceptible to oxidation than the native linoleic and linolenic molecules (43, 44).

Lipid oxidation products can be quite toxic. Two of the most well studied LOPs are 4HHE and 4HNE. 4HHE is derived from oxidation of the omega-3 alpha-linolenic acid, and 4HNE is derived from oxidation of the omega-6 linoleic acid (45, 46). Alpha-beta unsaturated aldehydes represent another important class of LOPs present in RBD seed oils. Martin Grootveld and his associates measured the concentration of alpha-beta unsaturated aldehydes that form during shallow pan frying for 30 min as well as in fast food deep fryers subject to continuous heating for several days and found levels of both exposures to be similarly high. They detected crotonaldehyde at levels of 1.8–5.7 mg, and n-hexanal at levels of 2.5–9.5 mg. To help readers conceptualize the potential health hazard, he explained that these levels are "not dissimilar" to the alpha-beta unsaturated aldehyde exposure from "smoking of a (daily) allocation of 25 tobacco cigarettes" (47, 48).

With these considerations in mind, let us now return to the hypothesis.

The energy model of insulin resistance

The Energy Model of Insulin Resistance is a multi-disciplinary hypothesis that draws connections between the recent changes to our food supply that have produced alterations in human adipose fat, and their likely impacts upon cellular redox homeostasis that could lead to altered whole-body glucose homeostasis and ultimately insulin resistance (see Figure 3 for a visual guide through the process.). The model posits that RBD seed oil consumption contributes to significantly altered adipose composition such that cells metabolizing body fat are likely to experience more oxidative stress than cells metabolizing historically normed adipose fat. Oxidative stress, in turn, induces aerobic glycolysis, also known as The Warburg Effect. Increased glucose utilization at the cell level potentially disrupts whole body glucose homeostasis and culminates in insulin resistance, as will be discussed. Cellular oxidative stress can simultaneously promote inflammatory disease, developmental disease, infertility, and cancer, and represent a unifying mechanism we can invoke to explain the observed links between metabolic disease and the other chronic diseases that are increasing in prevalence in tandem with the obesity epidemic.

Glucose oxidation in the presence of oxygen is called aerobic glycolysis, and is also known as The Warburg Effect. This metabolic state has long been associated with cancer but more recently recognized in insulin resistance. The Energy Model hypothesizes that, when many cells simultaneously transport more glucose into the cell than normal, this can lead to episodes of subclinical hypoglycemia, discussed in Figure 1B.

The energy model of insulin resistance: a four component hypothesis

This section outlines the four-components of the hypothesis that a shift in our food supply, from traditional fat to novel seed oils, is the primary driver of a shift in our metabolic health from that of normoglycemia to insulin resistance. The four components, described herein, have long been observed and discussed. However, they have not yet been considered together as components of an important story—the story of the rise of metabolic disease during the past 120 years.

The four components are:

I. Replacing animal fats with RBD seed oil promotes cellular oxidative stress.
II. High seed oil diets produce high PUFA body fat and harm mitochondria.
III. Mitochondrial adaptation to increased oxidative stress may involve increased aerobic glycolysis.
IV. Increased aerobic glycolysis profoundly disrupts glucose homeostasis, leading to insulin resistance.

The four components are inter-related and partly sequential. Components I and II likely represent the initial insults that lead to the development of Components III and IV, the latter representing physiologic adaptations to the initial insults.

Components I and II initiate the cascading sequence of events that lead to insulin resistance by depleting antioxidant capacity, according to the evidence presented below in the sections covering these components. Depleted antioxidant capacity likely has numerous consequences and the one this paper discusses is the possibility that mitochondria become more susceptible to oxidative stress. In the section covering Component III, I will discuss the evidence that oxidative stress leads to increases in aerobic glycolysis, also known as The Warburg Effect. The final component, Component IV, discusses the consequences of supra-normal cellular glucose consumption. Drawing higher than typical levels of glucose from circulation could lead to repeated episodes of subclinical hypoglycemia. This has consequences to multiple tissues that must be considered together in order to comprehend their true impact.

The Energy Model provides a framework for understanding that the important initial defect in insulin resistance is an increased metabolic demand for sugar rather than a decreased sensitivity to insulin. This increased metabolic demand for sugar does not abate as insulin resistance progresses to prediabetes and type 2 diabetes; indeed it appears to accelerate.

Some aspects of the theory are more well supported by direct experimental data than others, and those aspects that have only indirect support will be discussed in additional detail in the next section. Additionally, since saturated fat is more often highlighted as

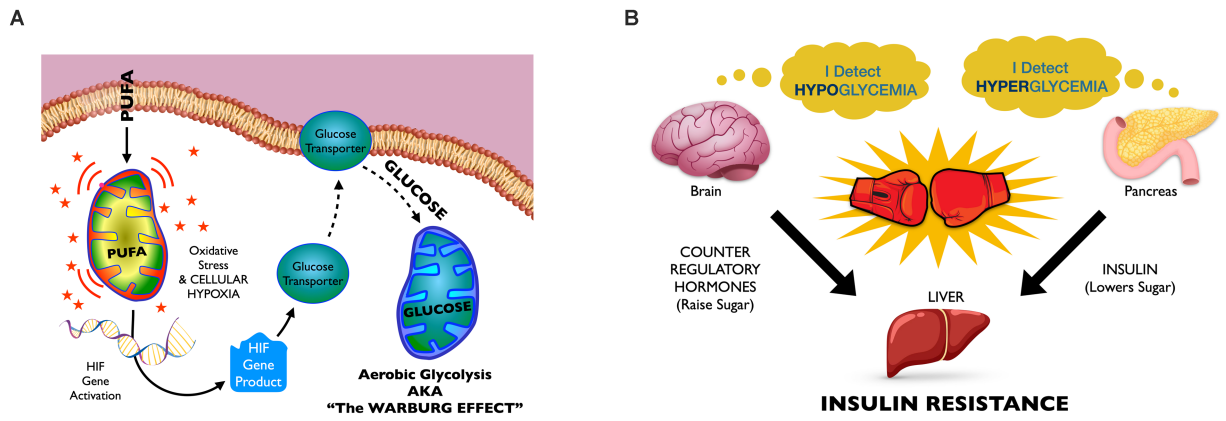

FIGURE 3
The energy model of insulin resistance: **(A) The intracellular level. Mitochondrial PUFA oxidation harms cell structures, causing a shift to glucose oxidation as a protective measure**. High-PUFA oils build high-PUFA body fat, and their mobilization between meals likely increases intracellular PUFA concentrations above historical norms. Mitochondrial PUFA oxidation promotes more oxidative stress than does oxidation of more saturated fatty acids. Oxidative stress, in turn, can promote periods of hypoxia that, among other effects, activate hypoxia inducible factor (HIF) genes. HIF genes increase GLUT-1 production, increasing mitochondrial glucose oxidation. **(B) The tissue level. Due to the excessive glucose utilization by cells throughout the body, blood glucose levels start to decline, causing subclinical hypoglycemia**. Hypoglycemia triggers counter regulatory "stress" hormone release and glucose elevations that can stimulate pancreatic insulin release. However, the presence of stress hormones blunts insulin's ability to tell the liver to stop elevating glucose, thus the liver "resists" insulin signal. As insulin resistance progresses, the brain "defends" higher levels of glucose, and hyperglycemia predominates.

the driver of metabolic disease than is polyunsaturated fat, this topic will also be discussed.

Component I: Replacing animal fats with RBD seed oils promotes cellular oxidative stress

It is a fundamental principle of chemistry that double bonds are more susceptible to oxidation than single bonds, and that the 1, 4 diene structure of polyunsaturated fatty acids' double bonds renders them particularly susceptible to oxidative attack compared to monounsaturated and saturated fatty acids (49). To protect those fragile fatty acids from oxygen attacks, biological systems embed membranes with vitamin E. Those membrane structures with higher PUFA concentrations require greater vitamin E concentrations to protect them (50). However, Buettner, G. R., makes it clear in his 1993 publication "The Pecking Order of Free Radicals and Antioxidants" that to protect cell membrane PUFA, antioxidants must work in teams. Vitamin E passes off its radical to vitamin C, which passes off its radical to Glultathione, which must be "recharged" by the enzyme glutathione reductase (51). If any one of the nutrients involved is in short supply, the membrane protection system fails.

Animal experiments support the related idea that as you increase the PUFA content of an animal's diet without also increasing antioxidants, the tissue levels of antioxidants are likely to decline or become depleted, with increases in oxidative stress. Raederstorff et al. cite experiments showing that as dietary linoleic acid content increases, vitamin E levels in tissues such as liver or plasma drop unless intake is adjusted upward (50). Bazinet and Layne note that in brain tissue, GSH levels often drop acutely under high PUFA conditions due to this oxidative burden (52). These authors also note that chronic PUFA exposure might upregulate GSH synthesis as an adaptation—via pathways like Nrf2 activation—*if* precursors (e.g., cysteine) are not limiting. Chronic PUFA exposure might ramp up GSH production if the system adapts, but if not—like in nutrient deficiency or disease—depletion of just one of the many nutrients involved in any given enzyme system could lead to failure of the entire system. The implication is that a high PUFA diet demands a specific set of nutrients to sustain without which the organisms will suffer harms related to oxidative stress.

A variety of investigators have shown experimentally that high linoleic acid diets induce oxidative stress in humans and experimental animals (53–55). Additionally, human observational studies have linked linoleic acid consumption to inflammatory disorders, obesity, immune disorders, infertility, ALS, psychological disorders (56–58). These authors propose the effects are mediated by oxidative stress.

In 2001, Kanner and Lapidot performed a series of experiments that considered an additional variable of stomach acid. They fed animals soy oil (55–58% PUFA) with meats and found the iron catalyzed Fenton reactions, leading to rapid lipid peroxidation with resultant hydroperoxide and reactive aldehyde production (59). This suggests that not only are fried foods going to increase our exposure to harmful LOPs like hydroperoxides and reactive aldehydes, certain food combinations will do so, too (53, 54, 60).

Having established that seed oils can, at least under certain circumstances, deplete antioxidant capacity in ways that would disrupt redox homeostasis, let us next discuss another consequence of seed oil consumption.

Component II: High seed oil diets produce high PUFA body fat and harm mitochondria

Changes to human adipose PUFA content during the past half century

Numerous animal studies have shown that dietary PUFA concentrates in adipose tissue in proportion to dietary consumption. Scant human studies have been done, but those that have have shown similar results. Guyenet (61) compiled data from studies published

between 1955 and 2006 that evaluated the linoleic acid content of human adipose. (Linoleic acid is the predominant PUFA in RBD seed oil.) The data shows that in 1955 year the average linoleic content in adipose tissue ranged from 5 to10%, and by 2008 it rose to over 20%. Hodson et al. found that omega-3 fatty acids, alpha-linolenic, EPA, and DHA represent 0.7–1.0% of total fatty acids, and arachidonic acid accounts for another 0.5–1.0% (62). Current per capita RBD seed oil consumption is likely significantly greater than it was in 2006, due to the replacement of hydrogenated oils by liquid seed oils, thus our adipose total PUFA concentration is likely significantly higher than 20%.

Lipolysis of this adipose between meals releases PUFA into the circulation as free fatty acids to be taken up by cells where it may be utilized as substrates for mitochondrial beta-oxidation, with potentially detrimental effects to mitochondrial function.

Evidence that mitochondrial PUFA oxidation induces mitochondrial oxidative stress, apoptosis and ferroptosis

In 2002, researchers from the Institute for Neurosciences in Padua, Italy, demonstrated that just a few minutes of exposure to omega-6 linoleic acid depleted mitochondrial antioxidant capacity, after which time mitochondrial energy production plummeted to less than 50 percent of normal, and apoptosis ensued (63). The effects were more pronounced with omega-3 alpha-linolenic acid. In 2010, Shamato-Nagai et al. similarly demonstrated that PUFAs induce oxidative stress and cell death (64).

In 2012, Dixon SJ et al. identified a form of cell death called ferroptosis. They identified the peroxidation of polyunsaturated fatty acids as a key driver of the oxidative damage to cellular membranes leading to cell death. In 2019, Gao et al. demonstrated that mitochondria play a pivotal role in a subtype of ferroptosis induced by cysteine-deprivation (65). 2018, Picou et al. showed that omega-3 fish oils induced mitochondrial damage and ferroptosis in human derived leukemia cells (66). In 2023, Watts et al. showed that omega-6 and omega-3 fatty acids increase ferroptosis sensitivity in C elegans (67). In 2023, Petan et al. observed that when fat droplets that normally aggregate in cells release polyunsaturated fatty acids too rapidly, that process initiates ferroptosis and, subsequently, results in cell death (68). Also in 2023 Mortensen et al. compiled a review of multiple articles showing that, relative to PUFA, dietary monounsaturated fatty acids reduced susceptibility to ferroptosis (69).

When mitochondrial antioxidant capacity is overwhelmed, oxidative damage accumulates, leading to dysfunction that impacts the entire cell (70, 71). Thus it is incumbent upon the cell to support mitochondrial health, and this may involve changing fueling strategies. This will be discussed next.

Component III: Aerobic glycolysis and the Warburg effect

In the 1930s, Otto Warburg had observed tumors taking up enormous amounts of glucose compared to the surrounding cells, and suspected it was related to dysfunctional mitochondria. In subsequent decades other investigators noted that cancer cells tended to up regulate glycolysis in aerobic conditions rather than solely in anaerobic conditions. Eventually, the term The Warburg Effect because synonymous with aerobic glycolysis.

In 1977, Sidney Weinhouse, speculated that "The Warburg Effect might protect cells from oxidative damage by limiting mitochondrial respiration under conditions of high metabolic demand." Although his perspective was that glycolysis was an attempt by the cell to *minimize* oxidative stress, not a result of it. Later investigators, with better instrumentation, were able to flip the script, showing that reactive oxygen species did indeed drive the Warburg Effect (72). Thus, oxidative stress can provoke aerobic glycolysis and if PUFA induce oxidative stress, they can likely induce aerobic glycolysis.

Meanwhile, others were linking PUFA to cancer. Efraim Racker, PhD, a pioneer in mitochondrial research, made an early link between dysfunctional mitochondria and polyunsaturated fatty acids, specifically having observed that polyunsaturates were mitochondrial uncouplers. In a 1963 editorial, he expressed concern that their long term use would likely "give rise to toxic reactions" and potentially cause cancer (73). He was gravely concerned that American Heart Association's recommendation to swap out saturated fats for high-PUFA oils might prove unsound. In the same editorial, he cautioned that "More extensive studies on the toxicity of unsaturated fatty acids may be in order before their indiscriminate use in foods or drugs is condoned."

Is glycolysis a survival strategy for cells chronically exposed to oxidative stress?

While a thorough investigation of this possibility is beyond the scope of this article, I want to raise the point because, as discussed, RBD oils are changing the chemistry of human body fat and potentially inducing a chronic state of increased oxidative stress. Reverting to glycolysis may be an atavistic survival strategy that many cells adopt in order to limit their exposure to damaging oxidative stress (69, 74). It benefits the individual cell, but ultimately harms the body.

Several lines of evidence have since converged around the notion that PUFAs induce not only oxidative stress but also glycolysis. Cellular oxidative stress induces a response that shifts fuel substrate from fatty acid to glucose. This is mediated by hypoxia-inducible factor (HIF)-1α nuclear accumulation, which activates glycolysis, while suppressing mitochondrial oxidative phosphorylation and fat oxidation (75–80). We have fairly ample evidence that oxidative stress can induce hypoxia inducible factor (HIF) gene expression (81–83). What is more, while the Warburg Effect has long been linked to cancer, newer evidence also links the Warburg effect to insulin resistance (84–86). And finally, patients with type 2 diabetes have increased activity of glycolysis and lactate production (87, 88). All of this taken together should serve to bolster the notion that seed oil consumption can shift cellular fueling strategy in ways that lead to increased blood glucose consumption.

The downstream effects of this will be discussed next.

Component IV: Increased cellular glucose consumption disrupts glucose homeostasis, leading to insulin resistance

It is self-evident that increased glucose consumption occurring between meals and overnight could potentially promote at least a mild form of hypoglycemia. In the postabsorptive (aka fasted) state, the supply of blood sugar is limited to a teaspoon's worth of glucose at any

given time, roughly16 calories. The circulatory system is simply not capable of distributing these scant calories over thousands of miles of capillaries with perfect efficiency. Ordinarily, mobilized free fatty acids provide cells with energy between meals, preventing blood glucose from dropping below the body's normal set points. But, the shift from fat oxidation to glycolysis will increase body-wide glucose utilization, potentially causing blood sugar to dip.

The key to understanding the full impact of repeated episodes of subclinical hypoglycemia involves examining how the body's various organs response to it. The brain vigorously defends against hypoglycemia by releasing counter regulatory hormones (CRH), frequently referred to as "stress hormones," and the net effect is often slightly elevated glucose (89), leading to the subsequent pancreatic release of insulin. Thus, we have insulin and counter regulatory hormones present simultaneously. CRH, by definition, resist insulin's signaling—thus leading to the phenotype of insulin resistance: high blood sugar and high insulin occurring simultaneously, and continuously.

Counter regulatory hormones (CRH) fiercely defend blood glucose. Mild drops in blood glucose, to 65–70 mg/dL, can trigger CRH release well before symptoms of more severe hypoglycemia (<50 mg/dL) appear (90, 91). Thus, if enough cells shift to aerobic glycolysis, it could lower glucose enough to stimulate release of CRH, although evidence for this is indirect (see below). Elevated levels of CHR, in turn, can induce mild *hyper*glycemia even in the presence of insulin. Simultaneously elevated insulin and CRH actions at the level of the hepatocyte produce the early stage phenotype of insulin resistance.

Indeed, chronic emotional stress is thought to induce insulin resistance by way of cortisol and catecholamines. In 1993, Surwit et al. (92) proposed that "The effects of stress on glucose metabolism are mediated by a variety of 'counter-regulatory' hormones that are released in response to stress and that result in elevated blood glucose levels and decreased insulin action." Similarly in 2022, Sharma et al. (93) hypothesized that "The release of catecholamines and a rise in serum glucocorticoid concentrations caused by psychological stress enhance the requirement for insulin and insulin resistance."

Interestingly, hypoglycemia can cause hunger and concentration problems. Over the past few decades, the number of people snacking between meals has increased, and one of the most commonly cited reasons for snacking between meals is inability to concentrate. According to an industry report published by Mintel called "Snacking Motivations and Attitudes U.S. 2015," 39 percent of millennials report snacking to "stay focused" throughout the day (94). Thus, along with the epidemic of insulin resistance, we may also be in the midst of an unrecognized epidemic of subclinical hypoglycemia.

Human experiments showing dietary PUFA promotes hypoglycemia

A number of investigations suggest that PUFA increases the body's reliance on blood glucose for energy between meals. In 1988, Jones et al. (95) placed participants on either a high- or low-PUFA diet for 1 week. They then measured the participants' glucose versus fat utilization after an overnight fast. Individuals on a high-PUFA diet burned 23% more glucose and 25% less fat compared to those on a low-PUFA diet. In 2004, Manco et al. (96) wrote that PUFAs lower glucose by increasing GLUT4 transport. In 2013, Gadgil et al. (97) found that increasing PUFA from 8 to 10% of calories for 1 week reduced fasting glucoses.

Although these studies both support the notion that dietary PUFA can increase cellular glucose dependence, this effect was interpreted as a benefit. Thus, both studies have been used incorrectly (in this author's view) as evidence that PUFA *improves* insulin resistance.

To resolve this apparent discrepancy, it is important to consider the following shortcomings of their perspective. First, it overlooks the broader metabolic consequences of relying on glucose, rather than fat, for energy, especially between meals when blood glucose is limited. Secondly, neither author discussed the possibility that increasing cellular glucose utilization may disrupt whole body glucose homeostasis leading to excessive counter regulatory hormone release. Third, neither author pointed out that their short term studies are incapable of determining longer term impacts. These failings are a predictable outgrowth of the ideology that PUFA are universally beneficial, which has, for many decades, prevented authors from interpreting their results objectively and has prevented others from determining the root cause of metabolic disease.

Additional evidence linking RBD seed oils to insulin resistance

Animal studies linking seed oils to insulin resistance

Prolonged elevations of free fatty acids (FFA) have long been observed to impair glucose-stimulated insulin secretion (GSIS), but until 2002, no one had investigated the different effects of differing types of fatty acids. In 2002, Dobbins et al. studied rats fed a diet high in saturated and monounsaturated fats (lard) versus high in PUFA (soy oil). After 4 weeks on the different diets, they tested GSIS and found the insulin sensitivity of "rats consuming Lard diets consistently exceeded that of the soy oil group," indicating that soy oil in the animals' diets promoted insulin resistance more powerfully than lard (98).

In 2012, Masi et al. evaluated the effects of two types of high fat diets on C57BL/6 mice, which develop obesity, insulin resistance (IR), diabetes mellitus, advanced fatty liver, and fatty pancreatic diseases when submitted to a high-fat diet. Both groups got a standard high fat diet mainly enriched with saturated fatty acids, but one group was subjected to oral savage with sunflower oil at 2gm/kg twice a week for the duration of the 12 week study. Mice were sacrificed after 12 weeks, and their soleus muscles were subjected to a variety of insulin sensitivity tests. The sunflower oil group had significantly less response to infused insulin, in spite of the fact that the mice subjected to the gavage gained less weight (99).

In 2015, Frances Sladek at the University of California, Riverside, provided important experimental evidence linking dietary soy oil to insulin resistance. Her work in this area began with the observation that soybean oil consumption in the U.S. has dramatically increased over the past century, and that saturated fat intake had not increased significantly, as is commonly stated. She subsequently designed a study that would directly test whether dietary saturated fat or polyunsaturated fat (from RBD soybean oil) promoted more insulin resistance. In a 2015 study, her team demonstrated that mice fed a diet similar in its total PUFA content to that of the average US consumer exhibited greater insulin resistance, weight gain, adiposity, and fatty liver compared to those fed a diet high in saturated fats from coconut

oil. This provides direct experimental evidence that the unsaturated fats in soybean oil might be driving insulin resistance (100). Sladek highlighted the role of oxidative stress in driving the liver and mitochondrial damage associated with insulin resistance.

In 2017 Sladek designed a similar study this time with a genetically modified (GM) soybean oil (Plenish®), engineered to have lower linoleic acid levels, resembling olive oil's fatty acid profile. While this GM oil caused less obesity and insulin resistance than conventional soybean oil, it still induced diabetes and fatty liver to a similar degree, indicating that reducing linoleic acid alone does not fully mitigate the oil's negative effects, suggesting that some of the harms from consuming RBD seed oils emerge from removing nutrients (101).

Adiposopathy

Adiposopathy, colloquially known as "sick fat" or "inflammatory fat," is a condition that occurs when adipose cells fail to develop or function normally. Affected fat cells are typically larger than healthy fat cells due to impaired adipogenesis, produce less leptin, fewer adipokines, and "spill" fatty acids into the bloodstream inappropriately (102–104). The link between "sick fat" and excess visceral fat is so strong that some consider the presence of excess visceral fat a surrogate maker for gauging adiposopathy. People with "sick fat" also have more ectopic fat, visceral fat, higher rates of insulin resistance, and greater risk of cardiovascular diseases, cancer, dementia, and complex or fatal infections, including covid-19 (105). Obesity medicine experts have pointed out that adiposopathy is effectively "pathological adipose tissue dysfunction," suggesting it might warrant reframing as a form of organ failure (106, 107).

A variety of human and animal studies suggest a link between greater RBD seed oil consumption and a variety of hallmarks of adiposopathy. Sladek et al. showed that an RBD oil diet promotes more visceral and ectopic fat formation than coconut oil, which is virtually PUFA-free (100). Human studies detect higher levels of partially oxidized PUFAs in individuals with adiposopathy than in those without (108–110). These compounds also trigger cytokine release, attracting white blood cells to fat tissue and contributing to the hyper coagulable state (111).

Additional considerations: the elevated glucose "set point"

The role of the brain in the metabolic tug-of-war

When other cells consume more glucose than usual, the brain may experience relative hypoglycemia, triggering CRH activation even while peripheral blood glucose levels are well are within the normal range. Indeed, people with obesity or type 2 diabetes have otherwise inexplicably lower brain glucose blood levels than peripheral, and this is not the case in lean individuals (112–115). These observations are consistent with a model in which whole body utilization of glucose exceeds the ability of the bloodstream to deliver adequate glucose to the brain under conditions of normoglycemia, and, in response, the brain raises the defended blood glucose level "set point."

As insulin resistance worsens, blood sugar continues to rise. Initially, blood glucose may only rise slightly, but over time, it increases to the point where physicians diagnose prediabetes. As blood sugar rises, the lows do not dip as sharply, but individuals continue to feel symptoms of low blood sugar during these dips. Eventually, individuals feel hypoglycemic while their glucose levels are technically normal.

The progression to type 2 diabetes

The final stage involves gradual adjustment of the blood sugar "set point" to progressively higher fasting levels. There is little examination of the concept of blood sugar set point in the literature. This model hypothesizes that downstream consequences of persistent oxidative stress and chronic hepatic gluconeogenesis certainly play important roles. Suffice it to say this last step of the process is complex and poorly understood.

Thus, paradoxically, insulin resistant individuals may feel hypoglycemic even when their blood sugar is high enough to trigger insulin release. This phenomenon is not discussed in the literature, however it is commonly observed among people with type 2 diabetes, as any practicing clinician can attest to. In professional but non-peer review articles, authors invoke a notion of altered set point (116).

Unchecked insulin resistance pushes blood glucose into the range characteristic of full-blown type 2 diabetes. In advanced cases, individuals only feel "normal" when their blood sugar is high, as their baseline glucose rises progressively. As diabetes progresses, both peak and baseline blood sugar levels rise higher and higher. In severe cases, some individuals may go years without achieving normoglycemia even for short time periods.

Discussion

The Energy First Model has many implications. It directly conflicts with the large majority of literature suggesting saturated fat is the cause of oxidative stress and metabolic diseases. One possible explanation for this apparent shortcoming is that the ideology of saturated fat being a cause of heart disease is actually incorrect. Indeed, several authors have pointed out that the idea was ensconced in government guidelines and taught at universities in spite of the fact that the evidentiary quality is poor (33, 34, 117, 118). Furthermore, evidence from the largest and most well controlled randomized human clinical trial showed that RBD seed oil increased cancer and overall mortality (119). Yet Harvard's Walter Willet claimed this finding was "an interesting historical footnote that has no relevance to current dietary recommendations" (120). As a result, the unsupported dietary guidelines continue to influence nutrition education and research. If correct, The Energy First Model paints a clear path toward dietary reversal of insulin resistance and other oxidative stress-related diseases.

The energy model explains a variety of otherwise unexplained phenomena

The framework provided is that insulin resistance stems from oxidative stress that increases the metabolic demand for sugar and gradually shifts the "set point" upward. This framework helps to

explain a number of otherwise unexplained or incompletely explained observations. This section will briefly illustrate how several such enigmas fit into the framework.

Hypercortisolism

Higher cortisol levels correlate with the severity of insulin resistance as well as its complications (121, 122). This phenomenon is not well explained by current theories of insulin resistance. Component Three of The Energy Model explains how this occurs.

The low carb flu

During the first few days to weeks of carbohydrate restriction, many people experience symptoms of fatigue, brain fog, extreme hunger, weakness, and more. These symptoms have been dubbed "the low carb flu" or "keto flu." Since they often go away, few people have bothered to investigate their origins. It is striking that all these symptoms are also consistent with hypoglycemia and the resultant stress hormone response. When symptoms do go away, it is likely due to a chronic up regulation of gluconeogenesis that may result from the stress hormones thus released. This adaptation would be expected to come at the expense of increased muscle catabolism. Interestingly, Hall et al. noted increased muscle loss during a highly controlled low carb experiment (123).

Reduced fat oxidation in type 2 diabetes

Investigators coined the term "metabolic flexibility" to describe the loss of ability to change fuel substrate from carbohydrate to fat. This is a common finding in people with insulin resistance and type two diabetes, as measured by respiratory quotient (124, 125). This finding has been attributed to elevated insulin, which reduces the release of free fatty acids into the circulation (126). But this overlooks the fact people with diabetes and insulin resistance have chronically elevated free fatty acid levels (127). The energy model proposes that increasing glycolysis and reducing fat oxidation are simultaneous adaptive responses the occur frequently in the setting of the modern, oxidative stress inducing diet.

The assumption that obese people already have high serum free fatty acids before they develop insulin resistance

People with obesity who do not have type 2 diabetes often have elevated free fatty acid levels (128). This consistent finding has led many authors to assume free fatty acids play a causal role in promoting insulin resistance (127). However this hinges on how insulin resistance is defined. While this article proposes a threshold of greater than 1.0, most authors use values significantly higher than 1.0, which could confuse the understanding of whether insulin resistance develops before or after elevated free fatty acid levels. Furthermore, reduced fat oxidation would be expected to contribute to free fatty acid elevations in the serum.

Conclusion

The energy model of insulin resistance offers a new framework to understand metabolic disease. Insulin resistance is both nearly ubiquitous in the population and linked to innumerable disease states, thus likely sharing a root cause. The model capitalizes on the large body of evidence identifying oxidative stress as a player in insulin resistance, cancer, and virtually all chronic diseases, and springboards from the assumption that oxidative stress is not incidental but rather a driver of these conditions. By identifying RBD oils as an underappreciated source of excessive dietary PUFA, the model also provides mechanistic rationale that explains the observed near perfect parallel between RBD oil intake and rates of prediabetes and diabetes in the United States. Future researchers should take into account the fact that today's PUFA intake is out of step with our genetics, and likely to increase our cellular oxidative stress. Because past research has likely suffered from confirmation bias due to the widely accepted notion that RBD oils are "heart healthy," future researchers should consider setting such notions aside and examining the existing global data at face value.

Data availability statement

The datasets presented in this study can be found in online repositories. The names of the repository/repositories and accession number(s) can be found in the article/Supplementary material.

Author contributions

CS: Conceptualization, Funding acquisition, Writing – original draft, Investigation, Writing – review & editing.

Funding

The author(s) declare that no financial support was received for the research and/or publication of this article.

Conflict of interest

CS is the owner of the online educational and support company, Rebel Well LLC.

Generative AI statement

The author(s) declare that no Gen AI was used in the creation of this manuscript.

Publisher's note

Supplementary material

The Supplementary material for this article can be found online at: https://www.frontiersin.org/articles/10.3389/fnut.2025.1532961/full#supplementary-material

References

1. O'Hearn M, Lauren MB, Wong JB, Kim DD, Mozaffarian D. Trends and disparities in Cardiometabolic health among U.S. adults, 1999-2018. *J Am Coll Cardiol*. (2022) 80:138–51. doi: 10.1016/j.jacc.2022.04.046

2. Parcha V, Heindl B, Kalra R, Li P, Gower B, Arora G, et al. Insulin resistance and Cardiometabolic risk profile among non-diabetic American young adults: insights from NHANES 2007-2018. *J Clin Endocrinol Metab*. (2022) 107:e25–37. doi: 10.1210/clinem/dgab645

3. McLaughlin T. Prevalence of insulin resistance and associated cardiovascular disease risk factors among normal weight, overweight, and obese individuals. *Metabolism*. (2004) 53:495–9. doi: 10.1016/j.metabol.2003.10.032

4. Almuraikhy S, Doudin A, Domling A, Althani AAJF, Elrayess MA. Molecular regulators of exercise-mediated insulin sensitivity in non-obese individuals. *J Cell Mol Med*. (2024) 28:e18015. doi: 10.1111/jcmm.18015

5. Huang CJ, McAllister MJ, Slusher AL. Obesity-related oxidative stress: the impact of physical activity and diet manipulation. *Sports Med - Open*. (2015) 1:32. doi: 10.1186/s40798-015-0031-y

6. Clemente-Suárez VJ, Beltrán-Velasco AI, Redondo-Flórez L, Martín-Rodríguez A, Tornero-Aguilera JF. Global impacts of Western diet and its effects on metabolism and health: A narrative review. *Nutrients*. (2023) 15:2749. doi: 10.3390/nu15122749

7. Biobaku F, Ghanim H, Batra M, Dandona P. Macronutrient-mediated inflammation and oxidative stress: relevance to insulin resistance, obesity, and Atherogenesis. *J Clin Endocrinol Metab*. (2019) 104:6118–28. doi: 10.1210/jc.2018-01833

8. Congressional Research Service. USDA's latest update to nutrition standards for school meals. (2024). Available online at: https://crsreports.congress.gov (Accessed March 21, 2025)

9. Ludwig DS, Ebbeling CB. The carbohydrate-insulin model of obesity: beyond 'calories in, calories out'. *JAMA Intern Med*. (2018) 178:1098–103. doi: 10.1001/jamainternmed.2018.2933

10. Walke PB, Bansode SB, More NP, Chaurasiya AH, Joshi RS, Kulkarni MJ. Molecular investigation of glycated insulin-induced insulin resistance *via* insulin signaling and AGE-RAGE axis. *Biochim Biophys Acta Mol basis Dis*. (2021) 1867:166029. doi: 10.1016/j.bbadis.2020.166029

11. Tan BL, Norhaizan ME. Effect of high-fat diets on oxidative stress, cellular inflammatory response and cognitive function. *Nutrients*. (2019) 11:2579. doi: 10.3390/nu11112579

12. Duke University Sanford, World Food Policy Center. E223: food policy lessons from removing trans fats from our diet. (2023). Available online at: https://wfpc.sanford.duke.edu/podcasts/food-policy-lessons-from-removing-trans-fats-from-our-diet [Accessed March 21, 2025]

13. United States Department of Agriculture. Nutrient Content of the U.S. Food supply, 1909–2000, home economics research report number 56. US: Center for Nutrition Policy and Promotion (2004).

14. de Luca C, Olefsky JM. Inflammation and insulin resistance. *FEBS Lett*. (2008) 582:97–105. doi: 10.1016/j.febslet.2007.11.057

15. Shoelson SE, Lee J, Goldfine AB. Inflammation and insulin resistance. *J Clin Invest*. (2006) 116:1793–801. doi: 10.1172/JCI29069

16. Rehman K, Akash MSH. Mechanisms of inflammatory responses and development of insulin resistance: how are they interlinked? *J Biomed Sci*. (2016) 23:87. doi: 10.1186/s12929-016-0303-y

17. Feng L, Xia Y, Garcia GE, Hwang D, Wilson CB. Involvement of reactive oxygen intermediates in cyclooxygenase-2 expression induced by interleukin-1, tumor necrosis factor-α, and lipopolysaccharide. *J Clin Invest*. (1995) 95:1669–75. doi: 10.1172/JCI117842

18. Barbieri SS, Eligini S, Brambilla M, Tremoli E, Colli S. Reactive oxygen species mediate cyclooxygenase-2 induction during monocyte to macrophage differentiation: critical role of NADPH oxidase. *J Biol Chem*. (2003) 60:187–97. doi: 10.1016/S0008-6363(03)00365-1

19. Dennis EA, Norris PC. Eicosanoid storm in infection and inflammation. *Nat Rev Immune*. (2015) 15:511–23. doi: 10.1038/nri3859

20. Harman D. Origin and evolution of the free radical theory of aging: a brief personal history, 1954–2009. *Biogerontology*. (2009) 10:773–81. doi: 10.1007/s10522-009-9234-2

21. Gladyshev VN. The free radical theory of aging is dead. Long live the damage theory! *Antioxid Redox Signal*. (2014) 20:727031:727–31. doi: 10.1089/ars.2013.5228

22. Lee JH, Duster M, Roberts T, Devinsky O. United States dietary trends since 1800: lack of association between saturated fatty acid consumption and non-communicable diseases. *Front Nutr*. (2022) 8:748847. doi: 10.3389/fnut.2021.748847

23. Rinzler SH. Primary prevention of coronary heart disease by diet. *Bull N Y Acad Med*. (1968) 44:8.

24. Christakis G, Rinzler SH, Archer M, Winslow G, Jampel S, Stephenson J, et al. The anti-coronary club. A dietary approach to the prevention of coronary heart disease--a seven-year report. *Am J Public Health Nations Health*. (1966) 56:299–314. doi: 10.2105/AJPH.56.2.299

25. Nettleton JA, Brouwer IA, Geleijnse JM. Gerard Hornstra; saturated fat consumption and risk of coronary heart disease and ischemic stroke: A science update. *Ann Nutr Metab*. (2017) 70:26–33. doi: 10.1159/000455681

26. Steur M, Johnson L, Sharp SJ, Imamura F, Sluijs I, Key TJ, et al. Dietary fatty acids, macronutrient substitutions, food sources and incidence of coronary heart disease: findings from the EPIC-CVD case-cohort study across nine European countries. *J Am Heart Assoc*. (2021) 10:e019814. doi: 10.1161/JAHA.120.019814

27. Trieu K, Bhat S, Dai Z, Leander K, Gigante B, Qian F. Biomarkers of dairy fat intake, incident cardiovascular disease, and all-cause mortality: A cohort study, systematic review, and meta-analysis. *PLoS Med*. (2021) 18:e1003763. doi: 10.1371/journal.pmed.1003763

28. Gaeini Z, Mirmiran P, Bahadoran Z, Aghayan M, Azizi F. The association between dietary fats and the incidence risk of cardiovascular outcomes: Tehran lipid and glucose study. *Nutr Metab (Lond)*. (2021) 18:96. doi: 10.1186/s12986-021-00624-6

29. Gribbin S, Enticott J, Hodge AM. Association of carbohydrate and saturated fat intake with cardiovascular disease and mortality in Australian women. *Heart*. (2022) 108:932–9. doi: 10.1136/heartjnl-2021-319654

30. Nago N, Ishikawa S, Goto T, Kayaba K. Low cholesterol is associated with mortality from stroke, heart disease, and cancer: the Jichi medical school cohort study. *J Epidemiol*. (2011) 21:67–74. doi: 10.2188/jea.JE20100065

31. Anderson KM, Castelli WP, Levy D. Cholesterol and mortality: 30 years of follow-up from the Framingham study. *JAMA*. (1987) 257:2176–80. doi: 10.1001/jama.1987.03390160062027

32. Bae JM, Yang YJ, Li ZM, Ahn YO. Low cholesterol is associated with mortality from cardiovascular diseases: a dynamic cohort study in Korean adults. *J Korean Med Sci*. (2012) 27:58–63. doi: 10.3346/jkms.2012.27.1.58

33. Teicholz N. The scientific report guiding the US dietary guidelines: is it scientific? *BMJ*. (2015) 351:h4962. doi: 10.1136/bmj.h4962

34. Achterberg C, Astrup A, Bier DM, King JC, Krauss RM, Teicholz N. An analysis of the recent US dietary guidelines process in light of its federal mandate and a National Academies report. *PNAS Nexus*. (2022) 1:pgac107. doi: 10.1093/pnasnexus/pgac107

35. de Jesus JM, Stoody EE, DeSilva DM, Quam JB, Obbagy JE, Anderson-Villaluz D. Addressing misinformation about the dietary guidelines for Americans. *Am J Clin Nutr*. (2024) 119:1101–10. doi: 10.1016/j.ajcnut.2024.02.034

36. Shanahan C. Dark calories: How vegetable oil stole our health and how we Can get it Back. New York: Hachette Go! (2024). 416 p.

37. Blasbalg TL, Hibbeln JR, Ramsden CE, Majchrzak SF, Rawlings RR. Changes in consumption of omega-3 and omega-6 fatty acids in the United States during the 20th century. *Am J Clin Nutr*. (2011) 93:950–62. doi: 10.3945/ajcn.110.006643

38. Refining GS, Oils V. Chemical and physical Refining. *ScientificWorldJournal*. (2022) 2022:6627013. doi: 10.1155/2022/6627013

39. Min DB, Li TL, Lee HO. Effects of processing steps on the contents of minor compounds and oxidation of soybean oil. Process-induced chemical changes in food. Advances in experimental medicine and biology, vol *434*. Springer, Boston, MA. (1998) 161–180.

40. Xie D, Zhou H, Jiang X. Effect of chemical refining on the levels of bioactive components and hazardous substances in soybean oil. *Food Measurement Characterization*. (2019) 13:1423–30. doi: 10.1007/s11694-019-00058-y

41. Farhoosh R, Einafshar S, Sharayei P. The effect of commercial refining steps on the rancidity measures of soybean and canola oils. *Food Chem*. (2009) 115:933–8. doi: 10.1016/j.foodchem.2009.01.035

42. Martin-Rubio AS, Sopelana P, Guillén MD. Assessment of soybean oil oxidative stability from rapid analysis of its minor component profile. *Molecules*. (2020) 25:4860. doi: 10.3390/molecules25204860

43. Grootveld M, Percival BC, Moumtaz S, Gibson M, Woodason K. Akhtar, A commentary: iconoclastic reflections on the 'safety' of polyunsaturated fatty acid-rich culinary frying Oils: some cautions regarding the laboratory analysis and dietary ingestion of lipid oxidation product toxins. *Appl Sci*. (2021) 11:2351. doi: 10.3390/app11052351

44. Södergren E. (2000). Lipid peroxidation in vivo. Evaluation and application of methods for measurement. Acta Universitatis Upsaliensis. Comprehensive summaries of Uppsala dissertations from the Faculty of Medicine (dissertation) Uppsala.

45. Manar A, Soulage CO, Meynier A, Lagarde M, Genot C. Dietary oxidized n-3 PUFA induce oxidative stress and inflammation: role of intestinal absorption of 4-HHE and reactivity in intestinal cells. *J Lipid Res*. (2012) 53:2069–80. doi: 10.1194/jlr.M026179

46. Schuster S, Johnson CD, Hennebelle M, Holtmann T, Taha AY, Kirpich IA. Oxidized linoleic acid metabolites induce liver mitochondrial dysfunction, apoptosis, and NLRP3 activation in mice. *J Lipid Res*. (2018) 59:1597–609. doi: 10.1194/jlr.M083741

47. Grootveld M, Ruiz-Rodado V, Silwood CJL. Detection, monitoring and deleterious health effects of lipid oxidation products generated in culinary oils during thermal stressing episodes. *AOCS/Inform*. (2014) 25:614–24.

48. Grootveld M, Percival BC, Grootveld KL. Chronic non-communicable disease risks presented by lipid oxidation products in fried foods. *Hepatobiliary Surg Nutr*. (2018) 7:305–12. doi: 10.21037/hbsn.2018.04.01

49. Murray J. Organic chemistry. *9th* ed. Boston: Cenage Learning (2016). 1512 p.

50. Raederstorff D, Wyss A, Calder PC, Weber P, Eggersdorfer M. Vitamin E function and requirements in relation to PUFA. *Br J Nutr*. (2015) 114:1113–22. doi: 10.1017/S000711451500272X

51. Buettner GR. The pecking order of free radicals and antioxidants: lipid peroxidation, α-tocopherol, and ascorbate. *Arch Biochem Biophys*. (1993) 300:535–43. doi: 10.1006/abbi.1993.1074

52. Bazinet R, Layé S. Polyunsaturated fatty acids and their metabolites in brain function and disease. *Nat Rev Neurosci*. (2014) 15:771–85. doi: 10.1038/nrn3820

53. Yuan T, Fan WB, Cong Y, Xu HD, Li CJ, Meng J, et al. Linoleic acid induces red blood cells and hemoglobin damage via oxidative mechanism. *Int J Clin Exp Pathol*. (2015) 8:5044–52.

54. Can X, Guo H, Day Y, Jiang G, Lui W, Li X. Excessive linoleic acid induces muscle oxidative stress through 5-lipoxygenase-dependent peroxidation. *Redox Biol*. (2024) 71:103096. doi: 10.1016/j.redox.2024.103096

55. Turpeinen A, Basu S, Mutanen M. A high linoleic acid diet increases oxidative stress in vivo and affects nitric oxide metabolism in humans. *Prostaglandins Leukot Essent Fat Acids*. (1998) 59:229–33.

56. Innis SM, Jacobson K. Dietary lipids in early development and intestinal inflammatory disease. *Nutr Rev*. (2007) 65:S188–93. doi: 10.1111/j.1753-4887.2007.tb00361.x

57. Mohammadi S, Keshteli AH, Saneei AH, Esmailzadeh A, Abidi P. The relationship between linoleic acid intake and psychological disorders in adults. *Front Nutr*. (2022) 9:841282. doi: 10.3389/fnut.2022.841282

58. Xiv K, Wang Y, Zhang L, Tang L, Zhang G, Huang T. Dietary-derived essential nutrients and amyotrophic lateral sclerosis: A two-sample Mendelian randomization study. *Nutrients*. (2022) 14:920. doi: 10.3390/nu14050920

59. Kanner J, Lapidot T. The stomach as a bioreactor: dietary lipid peroxidation in the gastric fluid and the effects of plant-derived antioxidants. *Free Radic Biol Med*. (2001) 31:1388–95. doi: 10.1016/S0891-5849(01)00718-3

60. Basiricò L, Morera P, Dipasquale D, Tröscher A. Comparison between conjugated linoleic acid and essential fatty acids in preventing oxidative stress in bovine mammary epithelial cells. *J Dairy Sci*. (2017) 100:2299–309. doi: 10.3168/jds.2016-11729

61. Guyenet SJ, Carlson SE. Increase in adipose tissue linoleic acid of US adults in the last half century. *Adv Nutr*. (2015) 6:660–4.

62. Hodson L, Skeaff CM, Fielding BA. Fatty acid composition of adipose tissue and blood in humans and its use as a biomarker of dietary intake. *Prog Lipid Res*. (2008) 47:348–80. doi: 10.1016/j.plipres.2008.03.003

63. Penzo D, Tagliapietra C, Colonna R, Petronilli V, Bernardi P. Effects of fatty acids on mitochondria: implications for cell death. *Biochim Biophys Acta*. (2002) 1555:160–5. doi: 10.1016/S0005-2728(02)00272-4

64. Shamoto-Nagai M, Kurokawa-NoseMakoto Y, Maruyama N. Polyunsaturated fatty acids induce oxidative stress and cell death in dopaminergic SH-SY5Y cells. *Neurosci Res*. (2010) 68:e306. doi: 10.1016/j.neures.2010.07.1359

65. Gao M, Yi J, Zhu J, Minikes AM, Monian P, Thompson CB, et al. Role of mitochondria in Ferroptosis. *Mol Cell*. (2019) 73:354–363.e3. doi: 10.1016/j.molcel.2018.10.042

66. Picou F, Debeissat C, Bourgeais J, Gallay N, Ferrié E, Foucault A. N-3 polyunsaturated fatty acids induce acute myeloid leukemia cell death associated with mitochondrial glycolytic switch and Nrf2 pathway activation. *Pharmacol Res*. (2018) 136:45–55. doi: 10.1016/j.phrs.2018.08.015

67. Perez MA, Clostitio AJ, Houston IR, Jimena R, Magtanong L, Dixon SJ. Ether lipid deficiency disrupts lipid homeostasis leading to ferroptosis sensitivity. *PLoS Genet*. (2022) 18:e1010436. doi: 10.1371/journal.pgen.1010436

68. Danielli M, Perne L, Jarc Jovičić E, Petan T. Lipid droplets and polyunsaturated fatty acid trafficking: balancing life and death. *Front Cell Dev Biol*. (2023) 11:1104725. doi: 10.3389/fcell.2023.1104725

69. Liberti MV, Locasale JW. The Warburg effect: how does it benefit Cancer cells? *Trends Biochem Sci*. (2016) 41:211–8. doi: 10.1016/j.tibs.2015.12.001

70. Harman D. The biologic clock: the mitochondria? *J Am Geriatr Soc*. (1972) 20:145–7. doi: 10.1111/j.1532-5415.1972.tb00787.x

71. Finkel T, Holbrook NJ. Oxidants, oxidative stress and the biology of ageing. *Nature*. (2000) 408:239–47. doi: 10.1038/35041687

72. Shi D, Xie F, Zhai C, Stern JS, Liu Y, Liu SL. The role of cellular oxidative stress in regulating glycolysis energy metabolism in hepatoma cells. *Mol Cancer*. (2009) 8:32. doi: 10.1186/1476-4598-8-32

73. Racker E. Calories don't count if you don't use them. *Am J Med*. (1963) 35:143–4.

74. Cassim S, Vučetić M, Ždralević M, Pouyssegur J. Warburg and beyond: the power of mitochondrial metabolism to collaborate or replace fermentative glycolysis in Cancer. *Cancers (Basel)*. (2020) 12:1119. doi: 10.3390/cancers12051119

75. Zhu X, Dingkao R, Sun N, Han L, Yu Q. Hypoxia-inducible factor-1α nuclear accumulation via a MAPK/ERK-dependent manner partially explains the accelerated glycogen metabolism in yak longissimus dorsi postmortem under oxidative stress. *LWT*. (2022) 168:113951. doi: 10.1016/j.lwt.2022.113951

76. Semenza GL. HIF-1: upstream and downstream of cancer metabolism. *Curr Opin Genet Dev*. (2010) 20:51–6. doi: 10.1016/j.gde.2009.10.009

77. Semenza GL. Hypoxia-inducible factors in physiology and medicine. *Cell*. (2012) 148:399–408. doi: 10.1016/j.cell.2012.01.021

78. Kim JW, Tchernyshyov I, Semenza GL, Dang CV. HIF-1-mediated expression of pyruvate dehydrogenase kinase: a metabolic switch required for cellular adaptation to hypoxia. *Cell Metab*. (2006) 3:177–85. doi: 10.1016/j.cmet.2006.02.002

79. Warburg O. On the origin of cancer cells. *Science*. (1956) 123:309–14.

80. Taylor CT, Scholz CC. The effect of HIF on metabolism and immunity. *Nat Rev Nephrol*. (2022) 18:573–87. doi: 10.1038/s41581-022-00587-8

81. Movafagh S, Crook S, Vo K. Regulation of hypoxia-inducible factor-1a by reactive oxygen species: new developments in an old debate. *J Cell Biochem*. (2015) 116:696–703. doi: 10.1002/jcb.25074

82. Honda T, Hirakawa Y, Nangaku M. The role of oxidative stress and hypoxia in renal disease. *Kidney Res Clin Pract*. (2019) 38:414–26. doi: 10.23876/j.krcp.19.063

83. Bonello S, Zahringer C, BelAiba RS, Djordjevic T, He's J, Michiels C. Reactive oxygen species activate the HIF-1α promoter via a functional NFκB site. *Arterioscler Thromb Vasc Biol*. (2007) 27:755–61. doi: 10.1161/01.ATV.0000258979.92828.bc

84. Trayhurn P. Hypoxia and adipose tissue function and dysfunction in obesity. *Physiol Rev*. (2013) 93:1–21. doi: 10.1152/physrev.00017.2012

85. Regazzetti C, Peraldi P, Grémeaux T, Najem-Lendom R, Ben-Sahra I, Cormont M. Hypoxia decreases insulin signaling pathways in adipocytes. *Diabetes*. (2009) 58:95–103. doi: 10.2337/db08-0457

86. Trayhurn P, Wang B, Wood S. Hypoxia in adipose tissue: a basis for the dysregulation of tissue function in obesity? *Br J Nutr*. (2008) 100:227–35. doi: 10.1017/S0007114508971282

87. Del Prato S, Bonadonnna RC, Bonora E, Gulli G, Solini A, Shank M. Characterization of cellular defects of insulin action in type 2 (non-insulin-dependent) diabetes mellitus. *J Clin Invest*. (1993) 91:484–94. doi: 10.1172/JCI116226

88. Simoneau J, Colberg SR, That FL, Kelley DE. Skeletal muscle glycolytic and oxidative enzyme capacities are determinants of insulin sensitivity and muscle composition in obese women. *FASEB J*. (1995) 9:273–8. doi: 10.1096/fasebj.9.2.7781930

89. Hirschberg PR, Sarkar P, Teegala SB, Routh VH. Ventromedial hypothalamus glucose-inhibited neurones: A role in glucose and energy homeostasis? *J Neuroendocrinol*. (2020) 32:1e12773. doi: 10.1111/jne.12773

90. Schwartz NS, Clutter WE, Shah SD, Cryer PE. Glycemic thresholds for activation of glucose counterregulatory systems are higher than the threshold for symptoms. *J Clin Invest*. (1987) 79:777–81. doi: 10.1172/JCI112884

91. Cryer PE. Glucose counterregulation in man. *Diabetes*. (1981) 30:261–4. doi: 10.2337/diab.30.3.261

92. Surwit RS, Schneider MS. Role of stress in the etiology and treatment of diabetes mellitus. *Psychosom Med*. (1993) 55:380–93. doi: 10.1097/00006842-199307000-00005

93. Sharma K, Akre S, Chakole S, Wanjari MB. Stress-induced diabetes: A review. *Cureus*. (2022) 14:e29142. doi: 10.7759/cureus.29142

94. Supply Side Supplement Journal. 94% of Americans Snack Daily; 60% Want Healthier Options. (2015). Available online at: https://www.supplysidesj.com/branding-marketing/94-of-americans-snack-daily-60-want-healthier-options (Accessed March 24, 2025).

95. Jones PJ, Schoeller DA. Polyunsaturated:saturated ratio of diet fat influences energy substrate utilization in the human. *Metabolism*. (1988) 37:145–51. doi: 10.1016/S0026-0495(98)90009-9

96. Manco M, Calvani M, Mingrone G. Effects of dietary fatty acids on insulin sensitivity and secretion. *Diabetes Obes Metab*. (2004) 6:402–13. doi: 10.1111/j.1462-8902.2004.00356.x

97. Gadgil MD, Appel LJ, Yeung E, Anderson CAM, Sacks FM, Miller ER. The effects of carbohydrate, unsaturated fat, and protein intake on measures of insulin sensitivity: results from the OmniHeart Tria. *Diabetes Care*. (2013) 36:1132–7. doi: 10.2337/dc12-0869

98. Dobbins RL, Szczepaniak LS, Myhill J, Tamura Y, Uchino H, Giacca A. The composition of dietary fat directly influences glucose-stimulated insulin secretion in rats. *Diabetes*. (2002) 51:1825–33. doi: 10.2337/diabetes.51.6.1825

99. Masi LN, Martins AR, Neto J, Amaral C, Crisma AR, Vinolo MA. Sunflower oil supplementation has Proinflammatory effects and does not reverse insulin resistance in obesity induced by high-fat diet in C57BL/6 mice. *J Biomed Biotechnol*. (2012) 2012:945131:1–9. doi: 10.1155/2012/945131

100. Diol P, Evans JR, Dhahbi J, Chellappa K, Han DS, Spindler S. Soybean oil is More obesogenic and Diabetogenic than coconut oil and fructose in mouse: potential role for the liver. *PLoS One*. (2015) 10:e0132672. doi: 10.1371/journal

101. Deol P, Fahrmann J, Evans YJ. Omega-6 and omega-3 oxylipins are implicated in soybean oil-induced obesity in mice. *Sci Rep*. (2017) 7:12488. doi: 10.1038/s41598-017-12624-9

102. Christofides EA, Gonzalez-Campoy JM. Adiposopathy In: J Gonzalez-Campoy, D Hurley and W Garvey, editors. Bariatric endocrinology. Springer: Cham (2018). 99–120.

103. Bays HE, González-Campoy JM, Bray GA, Kitabchi AE, Bergman DA, Schorr AB. Pathogenic potential of adipose tissue and metabolic consequences of adipocyte hypertrophy and increased visceral adiposity. *Expert Rev Cardiovasc Ther*. (2008) 6:343–68. doi: 10.1586/14779072.6.3.343

104. Bays H. Central obesity as a clinical marker of adiposopathy; increased visceral adiposity as a surrogate marker for global fat dysfunction. *Curr Opin Endocrinol Diabetes Obes*. (2014) 21:345–51. doi: 10.1097/MED.0000000000000093

105. Bays H, Gonzalez-Campoy JM, Henry RR, Bergman DA, Kitabchi AE, Schoor AB. Is adiposopathy (sick fat) an endocrine disease? *Int J Clin Pract*. (2008) 62:1474–83. doi: 10.1111/j.1742-1241.2008.01848.x

106. Bays H, Blonde L, Rosenson R. Adiposopathy: how do diet, exercise and weight loss drug therapies improve metabolic disease in overweight patients? *Expert Rev Cardiovasc Ther*. (2006) 4:871–95. doi: 10.3945/an.115.009944

107. Fitch AK, Bays HE. Obesity definition, diagnosis, bias, standard operating procedures (SOPs), and telehealth: an obesity medicine association (OMA) clinical practice statement (CPS). *Obesity Pillars*. (2022) 1:100004. doi: 10.1016/j.obpill.2021.100004

108. Murdolo G, Piroddi M, Luchetti F, Tortoioli C, Canonico B, Zerbinati C. Oxidative stress and lipid peroxidation by-products at the crossroad between adipose organ dysregulation and obesity-linked insulin resistance. *Biochimie*. (2013) 95:585–94. doi: 10.1016/j.biochi.2012.12.014

109. Cohen G, Riahi Y, Sasson S. Lipid peroxidation of poly-unsaturated fatty acids in normal and obese adipose tissues. *Arch Physiol Biochem*. (2011) 117:131–9. doi: 10.3109/13813455.2011.557387

110. Murdolo G, Bartolini D, Tortoioli C, Piroddi M, Iuliano L, Gali F. Lipokines and oxysterols: novel adipose-derived lipid hormones linking adipose dysfunction and insulin resistance. *Free Radic Biol Med*. (2013) 65:811–20. doi: 10.1016/j.freeradbiomed.2013.08.007

111. Warner DR, Liu H, Miller ME, Ramsden CE, Gao B, Feldstein AE. Dietary linoleic acid and its oxidized metabolites exacerbate liver injury caused by ethanol via induction of hepatic Proinflammatory response in mice. *Am J Pathol*. (2017) 187:2232–45. doi: 10.1016/j.ajpath.2017.06.008

112. Hwang JJ, Jiang L, Hamza M, Sanchez Rangel E, Dai F, Belfort-DeAguiar R. Blunted rise in brain glucose levels during hyperglycemia in adults with obesity and T2DM. *JCI Insight*. (2017) 2:e95913. doi: 10.1172/jci.insight

113. Eskian M, Alavi A, Khorasanizadeh M, Vitilanti BL, Jacobson H, Barwick TD. Effect of blood glucose level on standardized uptake value (SUV) in 18 F- FDG PET-scan: a systematic review and meta-analysis of 20,807 individual SUV measurements. *Eur J Nucl Med Mol Imaging*. (2019) 46:224–37. doi: 10.1007/s00259-018-4194-x

114. Sprinz C, Altmayer S, Zanon M, Watte G, Irion K, Marchiori E. Effects of blood glucose level on 18F-FDG uptake for PET/CT in normal organs: A systematic review. *PLoS One*. (2018) 13:e0193140. doi: 10.1371/journal.pone.0193140

115. Li W, Risacher SL, Huang E, Saykin AJ. Type 2 diabetes mellitus is associated with brain atrophy and hypometabolism in the ADNI cohort. *Neurology*. (2016) 87:595–600. doi: 10.1212/WNL.0000000000002950

116. Cleveland Clinic. Hypoglycemia (Low Blood Sugar). (2023). Available online at: https://my.clevelandclinic.org/health/diseases/11647-hypoglycemia-low-blood-sugar [Accessed March 25, 2025]

117. Astrup A, Teicholz N, Magkos F, Bier DM, Brenna JT, King JC. Dietary saturated fats and health: are the U.S. guidelines evidence-based? *Nutrients*. (2021) 13:3305. doi: 10.3390/nu13103305

118. Harcombe Z, Baker JS, Davies B. Evidence from prospective cohort studies did not support the introduction of dietary fat guidelines in 1977 and 1983: a systematic review. *Br J Sports Med*. (2017) 51:1737–42. doi: 10.1136/bjsports-2016-096409

119. Ramsden CE, Zamora D, Majchrzak-Hong S, Raurot KR, Broste SK, Franz RP. Re-evaluation of the traditional diet-heart hypothesis: analysis of recovered data from Minnesota coronary experiment (1968-73). *BMJ*. (2016) 353:i1246. doi: 10.1136/bmj.i1246

120. Harvard TH. Chan School of Public Health. Research Review: Old data on dietary fats in context with current recommendations. (2016). Available online at: https://nutritionsource.hsph.harvard.edu/2016/04/13/diet-heart-ramsden-mce-bmj-comments/ [Accessed March 25, 2025]

121. Salehi M, Mesgarani A, Karimipour S, Pasha SZ, Kashi Z, Abedian S. Comparison of salivary cortisol level in type 2 diabetic patients and pre-diabetics with healthy people. *Open Access Maced J Med Sci*. (2019) 7:2321–7. doi: 10.3889/oamjms.2019.340

122. Chiodini I, Adda G, Scillitani A, Coletti F, Morelli V, Di Lembo S. Cortisol secretion in patients with type 2 diabetes: relationship with chronic complications. *Diabetes Care*. (2007) 30:83–8. doi: 10.2337/dc06-1267

123. Hall KD, Chen KY, Guo J, Lam YY, Leibel RL, Mayer LE. Energy expenditure and body composition changes after an isocaloric ketogenic diet in overweight and obese men. *Am J Clin Nutr*. (2016) 104:324–33. doi: 10.1371/journal.pone.0222971

124. Pujia A, Mazza E, Ferro Y, Gazzaruso C, Coppola A, Doldo P. Lipid oxidation assessed by indirect calorimetry predicts metabolic syndrome and type 2 diabetes. *Front Endocrinol*. (2019) 9:806. doi: 10.3389/fendo.2018.00806

125. Galgani JE, Moro C, Ravussin E. Metabolic flexibility and insulin resistance. *Am J Physiol Endocrinol Metab*. (2008) 295:E1009–17. doi: 10.1152/ajpendo.90558.2008

126. Nakaya Y, Ohnaka M, Sakamoto S, Niwa Y, Okada K, Nomura M. Respiratory quotient in patients with non-insulin-dependent diabetes mellitus treated with insulin and oral hypoglycemic agents. *Ann Nutr Metab*. (1998) 42:333–40. doi: 10.1159/000012753

127. Lobczak AIS, Blindauer CA, Stewart AJ. Changes in plasma free fatty acids associated with Type-2 diabetes. *Nutrients*. (2019) 11:2022. doi: 10.3390/nu11092022

128. Boden G. Obesity and free fatty acids. *Endocrinol Metab Clin N Am*. (2008) 37:635–46. doi: 10.1016/j.ecl.2008.06.007

frontiers | Frontiers in Nutrition

TYPE Original Research
PUBLISHED 21 May 2025
DOI 10.3389/fnut.2025.1572610

OPEN ACCESS

EDITED BY
Qingyu Wang,
Beijing Hospital, China

REVIEWED BY
Sourish Bhattacharya,
Central Salt & Marine Chemicals Research Institute (CSIR), India
Munkhtuya Tumurkhuu,
Wake Forest Baptist Medical Center, United States

*CORRESPONDENCE
Gang Wang
✉ gang_wang@xjtu.edu.cn

†These authors have contributed equally to this work

RECEIVED 07 February 2025
ACCEPTED 02 May 2025
PUBLISHED 21 May 2025

CITATION
Hou Y, Qin L, Jin X, Ren J, Li J, Zhang X, Zhang J, Li R, Gao Y, Wang X and Wang G (2025) Systematic analysis of the burden of chronic kidney disease due to type 2 diabetes attributable to dietary risks based on the global burden of disease study 2021. *Front. Nutr.* 12:1572610. doi: 10.3389/fnut.2025.1572610

Systematic analysis of the burden of chronic kidney disease due to type 2 diabetes attributable to dietary risks based on the global burden of disease study 2021

Yanli Hou[1†], Lingzhi Qin[1†], Xuting Jin[1], Jiajia Ren[1], Jiamei Li[1], Xiaoling Zhang[1], Jingjing Zhang[1], Ruohan Li[1], Ya Gao[1], Xiaochuang Wang[1] and Gang Wang[1,2]*

[1]Department of Critical Care Medicine, The Second Affiliated Hospital of Xi'an Jiaotong University, Xi'an, Shaanxi, China, [2]Key Laboratory of Surgical Critical Care and Life Support (Xi'an Jiaotong University), Ministry of Education, Xi'an, Shaanxi, China

Background: Dietary factors play a crucial role in the development of chronic kidney disease due to diabetes mellitus type 2 (T2D-related CKD). However, comprehensive data on the global burden of T2D-related CKD attributable to dietary risks remain limited.

Methods: This study conducted a secondary analysis of the Global Burden of Diseases, Injuries, and Risk Factors Study 2021. Mortality and disability-adjusted life years (DALYs) of T2D-related CKD attributable to dietary risks, stratified by sex, age and sociodemographic index (SDI) quantiles, were analyzed in global, 21 regions, and 204 countries and territories from 1990 to 2021.

Results: In 2021, 79,990 (95% confidence interval [*CI*]: 32,730–128,880) death and 1,999,210 (95% *CI*: 856,190–3,167,220) DALYs of T2D-related CKD were attributable to dietary risk factors, approximately 2.5 times as many as those in 1990. The age-standardized mortality rate (ASMR) and age-standardized DALY rate (ASDR) grew with an estimated annual percentage change (EAPC) of 0.76% (95%*CI*: 0.69–0.83%) and 0.47% (95%*CI*: 0.41–0.53%). The low SDI regions experienced the highest burden of T2D-related CKD attributable to dietary risks, with ASMR of 1.16 (95% *CI*: 0.44–2.02) per 100,000 persons and the ASDR of 27.41 (95% *CI*: 11.32–46.78) per 100,000 persons. Males and the elderly over 70 years demonstrated a higher burden of T2D-related CKD influenced by dietary risks. Diet low in fruits, whole grains, and vegetables, as well as diet high in red and processed meat serve as the main dietary risks contributed to the burden of T2D-related CKD.

Conclusion: Dietary factors play a significant role in the development of T2D-related CKD. Further strategies should focus on men, the elderly, low-SDI regions and specific dietary components to mitigate dietary risks associated with T2D-related CKD.

KEYWORDS

global burden of disease, chronic kidney disease due to type 2 diabetes, dietary risks, mortality, disability-adjusted life years

1 Introduction

In recent decades, Type 2 diabetes mellitus (T2DM) has emerged as the tenth leading cause of death globally, with a significant enhance in disability burden since 1990 (1). The disease burden in individuals with T2DM predominantly stems from diabetes-induced organ dysfunction and failure, including kidneys, eyes, and nerves (2), and within the spectrum of complications, chronic kidney disease due to type 2 diabetes (T2D-related CKD) is identified as the primary driver of elevated death rates and disability-adjusted life years (DALYs) among T2DM patients with diabetic comorbidities (3, 4). From 1990 to 2021, there was a significantly increase on T2D-related CKD cases, moving from the 49th to the 25th leading cause of death and from the 103rd to the 55th leading cause of DALYs (5). The burden of T2D-related CKD approximately doubled by 2021 compared to 1990, accounting for 477,000 deaths and 11.3 million DALYs (6). Although the overall burden of T2D-related CKD continued to rise, the trend across different countries and regions exhibited notable variations, which have suggested gaps in the current status of CKD prevention and management capabilities over the world (7). Therefore, accurately assessing global trends and risk factors in T2D-related CKD is crucially essential. This will facilitate evidence-based resource allocation for effective prevention and intervention measures worldwide (8, 9).

Monitoring and managing modifiable risk factors, such as unhealthy lifestyle habits, can be a cost-effective approach for the prevention and intervention of T2D-related CKD (10). Dietary risks, defined as the consumption of food and nutrient, are recognized as potential risk factors for T2D-related CKD and offer opportunities for targeted intervention (3). Previous researches indicated that high sodium intake remained an important dietary risk factor for the global CKD burden, particularly in males, the elderly, and the population in the middle sociodemographic index (SDI) regions (11–13), which have contributed to the ongoing global increase in the burden of CKD. Targeting dietary factors in prevention and intervention efforts could effectively reduce the burden of CKD (14). Furthermore, substantial evidence exists regarding the impact of high red and processed meat consumption and inadequate whole grain, fruit, and vegetable intake on T2D-related CKD progression (15–20). However, it lacks comprehensive researches to definitively establish the relationship between dietary risks and T2D-related CKD. Moreover, focusing solely on specific dietary risks does not adequately capture the global spatiotemporal patterns of dietary influences on the T2D-related CKD burden (21–23). Further investigation is necessary to completely evaluate the impact of dietary risk factors on the T2D-related CKD burden.

In this context, we conducted a comprehensive analysis of the impact of dietary risks on T2D-related CKD by considering seven dietary risk factors across 21 Global Burden of Disease (GBD) regions, 5 SDI regions, and 204 countries and territories. The objective was aimed to present a detailed report of the global landscape of T2D-related CKD attributable to seven dietary risk factors, enhancing a deeper understanding of the role of dietary risks in terms of mortality and disability.

2 Methods

2.1 Data source and measures of burden

Data on the burden of T2D-related CKD attributable to dietary risks utilized in this study were obtained from the Global Burden of Diseases, Injuries, and Risk Factors Study 2021 (GBD 2021) (24). The GBD 2021 study provides a comprehensive and up-to-date estimation of the epidemiology of diseases, injuries and risk factors across different sexes and age groups. It covers 204 countries and territories, including 371 diseases and injuries across 21 regions, and leverages 328,938 data sources from 1990 to 2021. Details about the study design and methods of GBD studies have been extensively described in existing GBD literature (1, 11). Data from the GBD studies are publicly accessible and can be analyzed using the Global Health Data Exchange query tool.

2.2 T2D-related CKD

According to the GBD Study 2021 guidelines, diabetes is defined as a fasting blood glucose concentration of ≥126 mg/dL (7 mmol/L) or diabetes treatment reported (25). T2D-related CKD is defined as chronic kidney disease resulting from T2DM, characterized by a progressive decline in kidney function over a period of 3 months or more. It is primarily identified by an urinary albumin-to-creatinine ratio of ≥30 mg/g and/or an estimated glomerular filtration rate (eGFR) of <60 mL/min per 1.73 m^2 (26).

2.3 Dietary risk factors

In GBD 2021, risk factors were categorized as behavioral, environmental and occupational, and metabolic. Dietary risks belong to behavioral risks. For the burden of T2D-related CKD, data on seven specific dietary risk factors were gathered: a diet low in fruits, vegetables, whole grains, and high in red meat, processed meat, sodium, and sugar-sweetened beverages. To address specific biases in data sources for estimating nutrient intake, GBD 2021 employed a network meta-regression (MR-BRT) approach to adjust data from various methods, aligning them with those from gold standard methods (27). Data for dietary risk factors were obtained from a 24-h dietary recall survey, which reported food and nutrient consumption in grams per individual per day (14). The exposure estimates for each dietary risk, representing the average intake in grams per person per day for each nutrient, were modeled by age, sex, year, and location using a spatiotemporal Gaussian process regression (ST-GPR) frame work (28, 29). Detailed methodological specifications regarding MR-BRT and ST-GPR are provided in Supplementary material 1.

2.4 Socio-demographic index

SDI is regarded as a composite indicator of background social and economic conditions that influence health outcomes in each location, and a higher SDI indicates a better socioeconomic condition, which was calculated from the indices of total fertility rate for women under 25 years, average years of schooling for individuals aged 15 and older, and lag-distributed income per capita. The 204 countries and regions were categorized into five super-regions (high, high-middle, middle, low-middle, and low levels) (30, 31) based on the SDI. Furthermore, the world was further categorized into 21 geographic regions.

2.5 Statistical analyses

To evaluate the burden of T2D-related CKD associated with dietary risk factors, we utilized variables such as the number of deaths, DALYs, and their age-standardized rates (ASRs) to analyze among different groups by sex, age, year, location. Temporal changes in age-standardized mortality and DALY rates of T2D-related CKD attributable to dietary factors from 1990 to 2021 were analyzed using estimated annual percentage changes (EAPC). It was assumed that the natural logarithm of ASR follows a linear trend over time. Therefore, the EAPC was calculated using the formula: $ASR = \alpha + \beta \times year + \varepsilon$. The EAPC and its 95% confidence interval (CI) were derived from the formula: $100 \times (\exp(\beta) - 1)$. A linear regression analysis was conducted to explore the relationship between ASR, EAPC in ASR and SDI values, which were evaluated using Spearman's rank correlation tests and visualized with Locally Weighted Scatterplot Smoothing (LOWESS) curves. All statistical analyses were performed using R software (version 4.0.3). A *p* value of less than 0.05 was regarded as statistically significant.

3 Results

3.1 Global trend in T2D-related CKD burden attributable to dietary risk factors

From 1990 to 2021, ASMR and ASDR of T2D-related CKD attributable to dietary risk factors in global have increased by more than 2.5 times, exhibiting fluctuations but showing an overall upward trend (Figures 1A,B). In 2021, the global number of death and DALYs in T2D-related CKD attributable to dietary risks were estimated at 79,990 (95% *CI*: 32,730–128,880) and 1,999,210 (95% *CI*: 856,190–3,167,220) (Tables 1, 2). Global ASMR attributed to dietary risk factors in T2D-related CKD increased from 0.78 (95% *CI*: 0.31–1.23) per 100,000 persons in 1990 to 0.96 (95% *CI*: 0.40–1.54) per 100,000 persons in 2021 (Table 1), while the ASDR rose from 20.55 (95% *CI*: 8.42–32.26) per 100,000 persons in 1990 to 23.21 (95% *CI*: 9.95–36.61) per 100,000 persons in 2021 (Table 2). Furthermore, the overall burden of T2D-related CKD was on the rise. From 1990 to 2021, the EAPC of global ASMR and ASDR in T2D-related CKD attributed to dietary risk factors showed a gradual increase, with EAPCs of 0.76% (95% *CI*: 0.69–0.83%) and 0.47% (95% *CI*: 0.41–0.53%) for ASMR and ASDR, respectively (Tables 1, 2). Similar trends were observed across genders.

3.2 The burden of T2D-related CKD attributable to dietary risk factors by SDI levels

At different SDI regional levels, high-middle SDI regions exhibited the lowest ASMR and ASDR for T2D-related CKD attributable to dietary risks, whereas low SDI regions had the highest ASMR and ASDR from 1990 to 2021. In 2021, the ASMR in high-middle SDI regions was 0.59 (95% *CI*: 0.24–0.97) per 100,000 persons, compared to 1.16 (95% *CI*: 0.44–2.02) per 100,000 persons in low SDI regions (Figure 2A; Table 1). The ASDR was 14.70 (95% *CI*: 5.96–23.77) per 100,000 persons in the high-middle SDI regions and 27.41 (95% *CI*: 11.32–46.78) per 100,000 persons in the low SDI regions (Figure 2B; Table 2). From 1990 to 2021, the ASMR of T2D-related CKD attributable to dietary risks generally showed an increasing trend across different SDI regions, with a highest EAPC in high SDI regions of 1.45% (95% *CI*: 1.36–1.54%) (Figure 2B; Table 1). Notably, the high SDI regions also experienced maximal increase in the ASDR, with an EAPC of 1.05% (95% *CI*: 0.97–1.13%), while the trend of high-middle and low SDI regions decreased (Figures 2A,B; Tables 1, 2). Detailed data on ASMR, ASDR and the EAPCs for T2D-related CKD attributable to dietary risks in various regions in 1990 and 2021, are presented in Figure 2 and Tables 1, 2.

3.3 Location burden in T2D-related CKD attributable to dietary risks

At the regional and national levels, the burden of T2D-related CKD attributable to dietary factors exhibited substantial

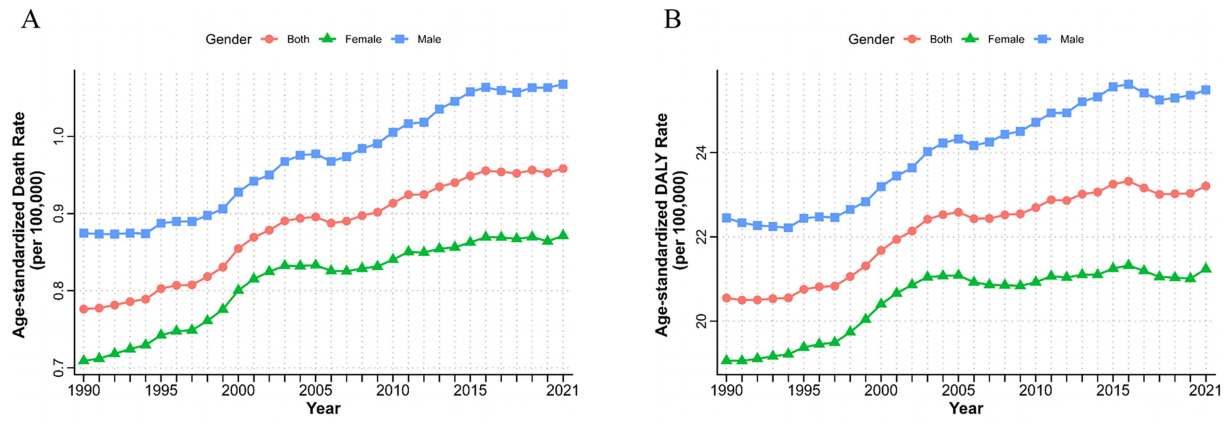

FIGURE 1
Burden of chronic kidney disease due to type 2 diabetes attributable to dietary risks by sex from 1990 to 2021. Age-standardized deaths **(A)** and DALYs **(B)** rate of chronic kidney disease due to type 2 diabetes attributable to dietary risks. DALYs, disability-adjusted life years.

TABLE 1 Deaths and ASMR of T2D-related CKD burden attributable to dietary risk factors in 1990 and 2021 and the temporal trends from 1990 to 2021.

Characteristics	Death cases, No. ×10^3 (95% *CI*)		ASMR per 100,000 people (95% *CI*)		EAPC of ASMR, % (95% *CI*)
	1990	2021	1990	2021	1990–2021
Global	27.23 (11.10–42.89)	79.99 (32.73–128.88)	0.78 (0.31–1.23)	0.96 (0.40–1.54)	0.76 (0.69–0.83)
Sex					
Male	13.11 (5.27–21.57)	39.19 (16.13–64.11)	0.87 (0.35–1.42)	1.07 (0.44–1.75)	0.77 (0.72–0.82)
Female	14.12 (5.83–22.25)	40.80 (16.96–65.21)	0.71 (0.29–1.14)	0.87 (0.36–1.39)	0.70 (0.60–0.79)
SDI groups					
High SDI	7.83 (3.58–11.80)	24.87 (10.72–38.33)	0.70 (0.32–1.07)	1.06 (0.45–1.61)	1.45 (1.36–1.54)
High-middle SDI	4.89 (1.86–8.06)	11.43 (4.58–18.95)	0.57 (0.22–0.93)	0.59 (0.24–0.97)	0.11 (0.04–0.18)
Middle SDI	7.92 (2.95–13.16)	25.47 (9.85–42.81)	0.94 (0.35–1.59)	1.03 (0.40–1.73)	0.42 (0.36–0.47)
Low-middle SDI	4.35 (1.72–7.19)	13.26 (5.43–22.59)	0.84 (0.32–1.40)	1.01 (0.41–1.72)	0.68 (0.65–0.72)
Low SDI	2.20 (0.89–3.66)	4.89 (1.97–8.49)	1.15 (0.46–1.92)	1.16 (0.44–2.02)	0.00 (−0.05 to 0.05)
GBD region					
East Asia	6.16 (1.84–10.78)	16.12 (5.18–28.75)	0.95 (0.30–1.67)	0.82 (0.26–1.43)	−0.57 (−0.70 to −0.44)
Southeast Asia	1.68 (0.52–3.13)	5.23 (1.55–10.12)	0.79 (0.25–1.48)	0.90 (0.27–1.74)	0.53 (0.48–0.58)
Oceania	0.03 (0.01–0.05)	0.08 (0.03–0.15)	1.13 (0.32–2.10)	1.38 (0.43–2.50)	0.56 (0.47–0.66)
Central Asia	0.10 (0.05–0.16)	0.31 (0.15–0.48)	0.22 (0.11–0.35)	0.41 (0.20–0.64)	1.34 (0.86–1.82)
Central Europe	0.49 (0.23–0.77)	0.68 (0.31–1.12)	0.35 (0.16–0.54)	0.29 (0.13–0.47)	−0.55 (−0.80 to −0.30)
Eastern Europe	0.48 (0.20–0.73)	0.90 (0.43–1.41)	0.17 (0.07–0.26)	0.25 (0.12–0.39)	0.81 (0.37–1.26)
High-income Asia Pacific	2.41 (1.22–3.57)	5.56 (2.41–8.76)	1.34 (0.68–1.99)	0.86 (0.37–1.31)	−1.54 (−1.65 to −1.43)
Australasia	0.04 (0.02–0.06)	0.14 (0.06–0.25)	0.18 (0.08–0.29)	0.24 (0.10–0.41)	1.68 (1.22–2.14)
Western Europe	2.79 (1.26–4.41)	5.75 (2.55–9.58)	0.46 (0.20–0.75)	0.46 (0.20–0.75)	0.46 (0.22–0.69)
Southern Latin America	0.63 (0.23–1.09)	1.00 (0.4–1.66)	1.44 (0.52–2.47)	1.11 (0.44–1.84)	−0.47 (−0.85 to −0.09)
High-income North America	2.67 (1.11–4.16)	12.93 (4.94–19.98)	0.74 (0.31–1.15)	1.90 (0.71–2.91)	3.18 (2.91–3.46)
Caribbean	0.32 (0.13–0.53)	0.92 (0.40–1.60)	1.32 (0.52–2.20)	1.70 (0.74–2.95)	1.37 (1.17–1.57)
Andean Latin America	0.29 (0.10–0.51)	1.15 (0.42–2.08)	1.55 (0.51–2.77)	2.01 (0.73–3.63)	0.95 (0.76–1.14)
Central Latin America	0.84 (0.36–1.41)	4.39 (1.89–7.26)	1.17 (0.49–1.99)	1.79 (0.76–2.97)	2.03 (1.51–2.55)
Tropical Latin America	1.09 (0.46–1.76)	3.94 (1.67–6.32)	1.38 (0.57–2.25)	1.57 (0.66–2.52)	0.40 (0.17–0.63)
North Africa and Middle East	1.23 (0.46–2.19)	3.01 (1.15–5.15)	0.86 (0.32–1.54)	0.73 (0.28–1.24)	−0.53 (−0.67 to −0.39)
South Asia	3.89 (1.62–6.62)	13.04 (5.23–23.15)	0.79 (0.32–1.34)	0.96 (0.37–1.68)	0.62 (0.53–0.71)
Central Sub-Saharan Africa	0.29 (0.10–0.50)	0.59 (0.21–1.07)	1.59 (0.55–2.76)	1.37 (0.45–2.54)	−0.76 (−0.87 to −0.66)
Eastern Sub-Saharan Africa	1.12 (0.45–1.96)	2.63 (1.11–4.47)	1.81 (0.70–3.15)	1.99 (0.81–3.37)	0.18 (0.13–0.23)
Southern Sub-Saharan Africa	0.12 (0.05–0.22)	0.34 (0.14–0.59)	0.52 (0.19–0.93)	0.67 (0.26–1.19)	1.27 (0.95–1.59)
Western Sub-Saharan Africa	0.58 (0.19–1.02)	1.24 (0.44–2.15)	0.80 (0.26–1.41)	0.77 (0.27–1.33)	−0.21 (−0.30 to −0.13)

ASMR, age-standardized mortality rate; T2D-related CKD, chronic kidney disease due to diabetes mellitus type 2; EAPC, estimated annual percentage change; CI, uncertainty interval; CI, confidence interval; SDI, socio-demographic index; GBD, Global Burden of Disease.

heterogeneity. In 2021, the East Asia region reported the highest burden of T2D-related CKD, with deaths of 16,120 (95% *CI*: 5,180–28,750) per 100,000 persons and DALYs of 396,710 (95%*CI*: 123,410–701,900) (Tables 1, 2). The top three regions with the highest ASMR in 2021 were Andean Latin America (2.01, 95%*CI*: 0.73–3.63 per 100,000 persons), Eastern Sub-Saharan Africa (1.99, 95%*CI*: 0.81–3.37 per 100,000 persons), and High-income North America (1.90, 95% *CI*: 0.71–2.91 per 100,000 persons) (Figure 3A; Table 1). And the regions with the highest ASDR in 2021 were High-income North America (47.82, 95% *CI*: 17.94–73.13 per 100,000 persons), Central Latin America (44.94, 95% *CI*: 20.14–71.41 per 100,000 persons), and Andean Latin America (43.69, 95% *CI*: 16.77–76.52 per 100,000 persons) (Figure 3B; Table 2). Among all countries, American Samoa bear the heaviest burden of T2D-related CKD attributable to dietary factors (Supplementary Figure 1). In 2021, the ASMR and ASDR were 6.66 (95% *CI*: 2.00–12.21) per 100,000 persons and 140.02 (95% *CI*: 43.91–257.50) per 100,000 persons, respectively (Supplementary Tables 1, 2).

From 1990 to 2021, the region with the most pronounced increase in the burden of T2D-related CKD attributable to dietary risks was High-income North America, with an EAPCs of 3.18% (95% *CI*:

TABLE 2 DALYs and ASDR of T2D-related CKD burden attributable to dietary risk factors in 1990 and 2021 and the temporal trends from 1990 to 2021.

Characteristics	DALY cases, No. x10^3 (95% *CI*)		ASDR per 100,000 people (95% *CI*)		EAPC of ASDR, % (95% *CI*)
	1990	2021	1990	2021	1990–2021
Global	798.26 (322.75–1,247.38)	1,999.21 (856.19–3,167.22)	20.55 (8.42–32.26)	23.21 (9.95–36.61)	0.47 (0.41–0.53)
Sex					
Male	397.11 (162.06–642.07)	1,018.88 (430.05–1,628.74)	22.45 (9.26–36.27)	25.49 (10.72–40.90)	0.53 (0.48–0.58)
Female	401.15 (162.17–633.67)	980.33 (421.04–1,545.52)	19.06 (7.76–30.00)	21.24 (9.13–33.47)	0.37 (0.30–0.45)
SDI groups					
High SDI	219.66 (102.02–333.64)	541.20 (234.39–830.25)	19.92 (9.21–30.27)	26.48 (11.50–40.29)	1.05 (0.97–1.13)
High-middle SDI	155.75 (62.29–245.39)	289.16 (117.29–466.91)	16.11 (6.39–25.55)	14.70 (5.96–23.77)	−0.30 (−0.36 to −0.24)
Middle SDI	229.50 (84.92–377.62)	656.54 (265.08–1,054.87)	22.81 (8.40–37.40)	24.46 (9.87–39.17)	0.34 (0.27–0.40)
Low-middle SDI	129.91 (51.28–208.95)	374.36 (156.64–628.27)	21.66 (8.39–35.07)	25.88 (10.81–43.48)	0.66 (0.62–0.70)
Low SDI	62.65 (24.92–103.25)	136.37 (56.00–233.05)	28.19 (11.42–46.20)	27.41 (11.32–46.78)	−0.13 (−0.16 to −0.10)
GBD region					
East Asia	175.25 (50.36–311.38)	396.71 (123.41–701.90)	21.51 (6.33–37.83)	18.46 (5.75–32.68)	−0.45 (−0.59 to −0.31)
Southeast Asia	47.64 (14.38–84.81)	140.94 (44.68–259.24)	19.28 (6.13–34.36)	21.51 (6.85–39.70)	0.47 (0.41–0.52)
Oceania	0.86 (0.22–1.57)	2.40 (0.77–4.38)	28.15 (7.59–51.39)	31.79 (9.99–57.16)	0.33 (0.25–0.41)
Central Asia	7.36 (3.71–11.22)	14.22 (7.16–21.36)	15.57 (7.85–23.69)	16.80 (8.37–25.05)	−0.09 (−0.34 to 0.17)
Central Europe	17.85 (9.01–26.58)	21.05 (10.85–33.16)	11.99 (6.10–18.00)	9.62 (4.95–15.10)	−0.58 (−0.70 to −0.45)
Eastern Europe	30.71 (14.09–45.58)	31.97 (15.91–48.33)	10.99 (5.08–16.43)	9.00 (4.48–13.60)	−1.11 (−1.28 to −0.94)
High-income Asia Pacific	57.08 (29.92–84.08)	96.93 (43.80–145.72)	29.20 (15.28–43.02)	18.93 (8.98–28.32)	−1.37 (−1.51 to −1.23)
Australasia	1.73 (0.80–2.64)	4.36 (1.94–6.89)	7.47 (3.44–11.52)	8.37 (3.70–13.03)	0.60 (0.35–0.84)
Western Europe	81.56 (37.21–126.68)	117.70 (52.84–183.08)	14.04 (6.41–21.64)	11.89 (5.35–18.39)	−0.37 (−0.47 to −0.26)
Southern Latin America	14.94 (5.54–24.53)	21.15 (8.61–33.75)	32.57 (12.21–53.52)	24.26 (9.93–39.12)	−0.61 (−0.92 to −0.30)
High-income North America	79.22 (31.92–122.66)	298.15 (114.21–458.53)	23.00 (9.35–35.74)	47.82 (17.94–73.13)	2.53 (2.30–2.77)
Caribbean	8.11 (3.35–13.08)	21.57 (9.69–36.12)	31.48 (12.93–50.63)	39.96 (18.02–66.79)	1.28 (1.11–1.45)
Andean Latin America	6.71 (2.27–11.72)	25.76 (9.99–45.11)	33.58 (11.37–58.71)	43.69 (16.77–76.52)	0.95 (0.76–1.15)
Central Latin America	23.58 (10.20–37.51)	114.05 (51.69–183.13)	28.83 (12.59–46.01)	44.94 (20.14–71.41)	1.97 (1.48–2.45)
Tropical Latin America	31.21 (13.63–49.49)	95.99 (41.54–153.25)	34.39 (14.81–54.83)	37.19 (16.04–59.24)	0.15 (−0.09 to 0.38)
North Africa and Middle East	34.32 (13.05–59.04)	84.42 (31.87–141.58)	20.37 (7.78–35.35)	17.65 (6.78–29.90)	−0.48 (−0.55 to −0.41)
South Asia	121.19 (49.98–198.22)	377.97 (158.41–645.46)	21.25 (8.66–34.94)	25.33 (10.52–43.10)	0.61 (0.53–0.68)
Central Sub-Saharan Africa	8.48 (3.19–14.39)	17.81 (6.61–31.90)	38.50 (14.00–65.95)	32.62 (11.15–58.23)	−0.80 (−0.89 to −0.70)
Eastern Sub-Saharan Africa	28.03 (11.33–48.86)	63.95 (27.42–109.06)	39.33 (15.91–69.14)	40.98 (17.42–69.45)	0.00 (−0.05 to 0.05)
Southern Sub-Saharan Africa	4.62 (1.80–7.91)	11.66 (4.88–19.76)	16.67 (6.45–29.41)	19.57 (8.21–33.40)	0.78 (0.54–1.02)
Western Sub-Saharan Africa	17.81 (5.88–31.26)	40.44 (15.57–67.10)	20.69 (6.80–35.96)	20.18 (7.41–33.81)	−0.10 (−0.16 to −0.04)

T2D-related CKD, chronic kidney disease due to diabetes mellitus type 2; ASDR, Age-standardized DALY rate; DALY, disability-adjusted life year; CI, confidence interval; EAPC, estimated annual percentage change; SDI, socio-demographic index; GBD, Global Burden of Disease.

2.91–3.46%) and 2.53% (95% *CI*: 2.30–2.77%) in ASMR and ASDR, respectively. In contrast, the region with the largest decrease was High-income Asia Pacific, with EAPCs of −1.54% (95% *CI*: −1.65% to −1.43%) and −1.37% (95% *CI*: −1.51% to −1.23%) in ASMR and ASDR, respectively (Figures 3A,B; Tables 1, 2). Among individual countries, Ukraine exhibited the highest increase in ASMR, with an EAPC of 12.82% (95% *CI*: 10.80–14.87%) (Figure 3C; Supplementary Table 1), while American Samoa had the highest growth trend in the ASDR, with an EAPC of 3.46% (95% *CI*: 3.20–3.73%) (Figure 3D; Supplementary Table 2). Detailed data on EAPCs for ASMR and ASDR are presented in Figure 3 and Tables 1, 2.

We analyzed the correlation between the burdens of T2D-related CKD attributable to dietary risks and SDI levels. In 2021, ASMR and ASDR were negatively correlated with SDI, with coefficients of $R = -0.34$ ($p < 0.05$) and $R = -0.36$ ($p < 0.05$), respectively (Figures 3A,B). From 1990 to 2021, the EAPC of ASMR across countries and regions was positively correlated with SDI, yielding a coefficient of 0.18 ($p = 0.009$). Whereas the EAPC of ASDR did not

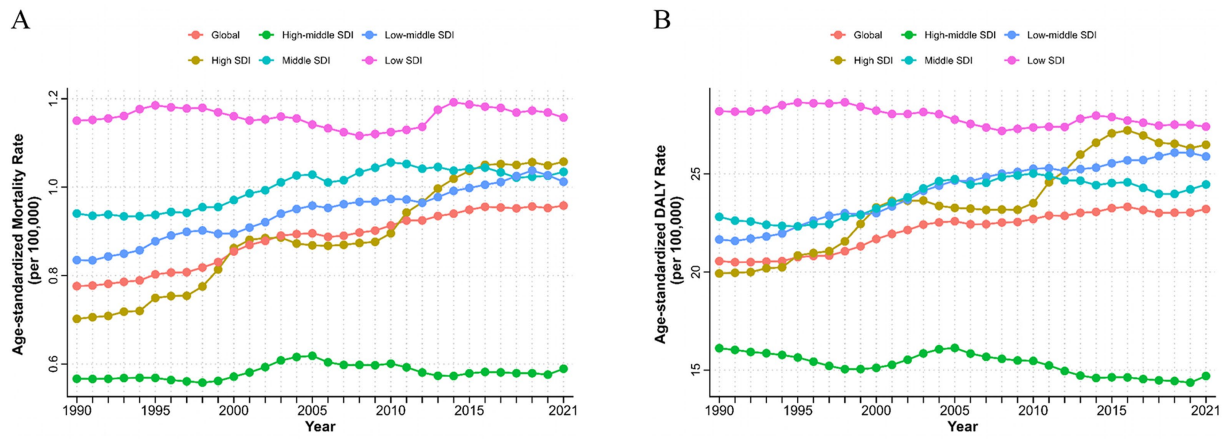

FIGURE 2
Burden of chronic kidney disease due to type 2 diabetes attributable to dietary risks with different SDI levels from 1990 to 2021. AMSR **(A)** and age-standardized DALYs rate **(B)** of T2D-related CKD attributable to dietary risks. SDI, Socio-demographic Index; ASMR, age-standardized mortality rate; DALYs, disability-adjusted life years; T2D-related CKD, chronic kidney disease due to type 2 diabetes.

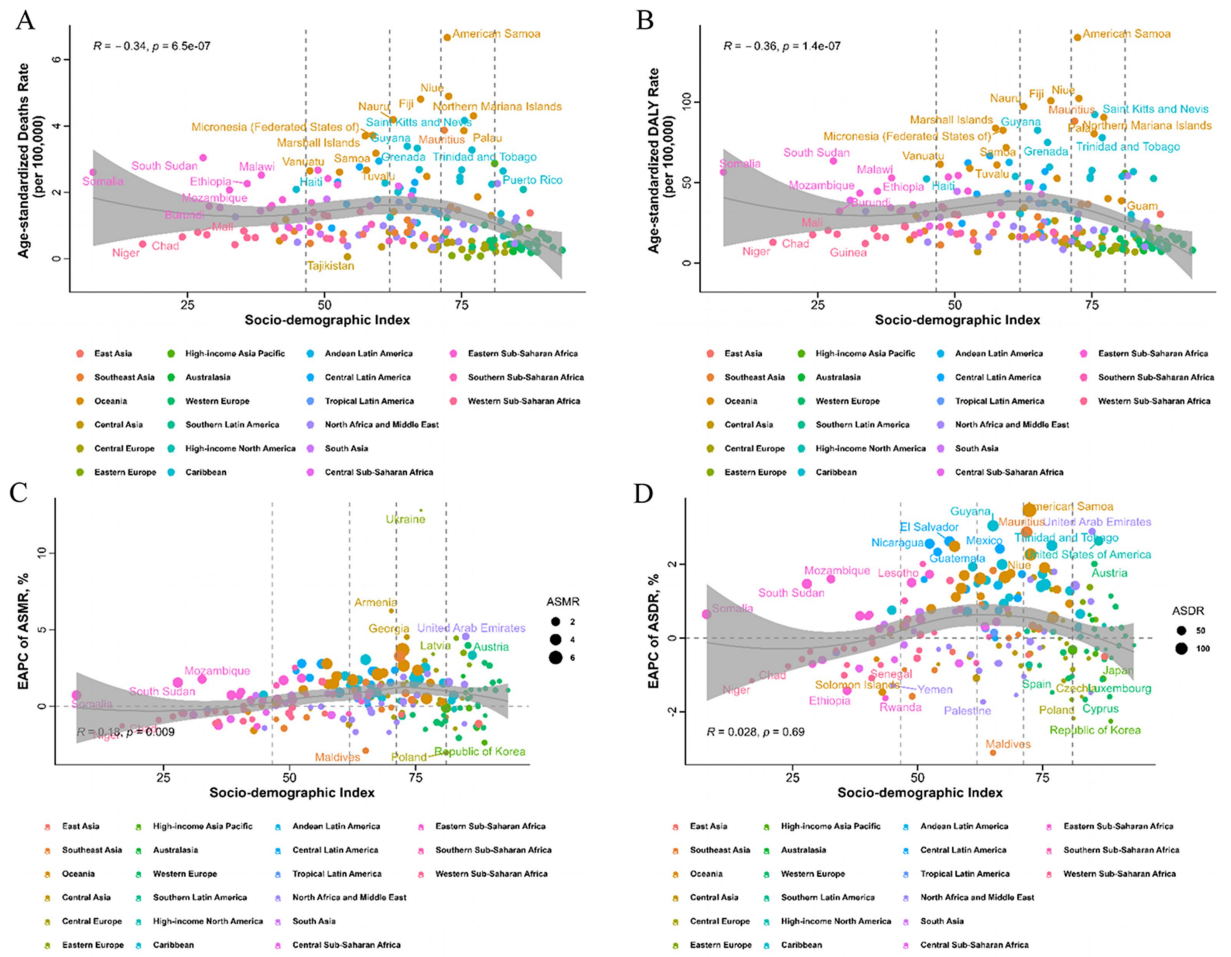

FIGURE 3
Location burden of chronic kidney disease due to type 2 diabetes attributable to dietary risks with different SDI levels. Correlation between ASMR **(A)** or ASDR **(B)** and countries of T2D-related CKD attributable to dietary risks in 2021. Correlation between EAPC of ASMR **(C)** or ASDR **(D)** and countries of T2D-related CKD attributable to dietary risks from 1990 to 2021. Every dot represented a country or territory and its color implied the region that the country or territory located. SDI, Socio-demographic Index; ASMR, age-standardized mortality rate; ASDR, age-standardized DALYs rate; DALYs, disability-adjusted life years; T2D-related CKD, chronic kidney disease due to type 2 diabetes; EAPC, estimated annual percentage change; ASDR, age-standardized disability-adjusted life years rate.

show significant correlation with SDI level ($R = 0.028$, $p = 0.69$) (Figure 3D).

3.4 Burden of T2D-related CKD attributable to dietary risk in different sexes and age groups

From 1990 to 2021, both sexes exhibited upward trends consistent with the overall population. However, the burden of T2D-related CKD remained consistently higher in males compared to females. ASMR for males increased from 0.87 (95% *CI*: 0.35–1.42) per 100,000 persons in 1990 to 1.07 (95% *CI*: 0.44–1.75) per 100,000 persons in 2021, and for females, it rose from 0.71 (95% *CI*: 0.29–1.14) per 100,000 persons to 0.87 (95% *CI*: 0.36–1.39) per 100,000 persons over the same period (Table 1; Figure 1A). ASDR for males increased from 22.45 (95% *CI*: 9.26–36.27) to 25.49 (95% *CI*: 10.72–40.90) per 100,000 persons, and for females, from 19.06 (95% *CI*: 7.76–30.00) in 1990 to 21.24 (95% *CI*: 9.13–33.47) per 100,000 persons in 2021, respectively, resulting in a male-to-female ratio of approximately 1.2 (Figure 1B; Table 2). The EAPC for ASMR was 0.77% (95% *CI*: 0.72–0.82%) for males and 0.70% (95% *CI*: 0.60–0.79%) for females, and the EAPC for DALY was 0.53% (95% *CI*: 0.48–0.58%) and 0.37% (95% *CI*: 0.30–0.45%), respectively (Tables 1, 2). Male mortality and DALY rates in T2D-related CKD attributable to dietary risks were consistently higher across all age groups compared to females (Supplementary Figure 3). In 2021, the mortality and DALY rates in T2D-related CKD attributable to dietary risks peaked among males and females aged >80 years (Figures 4A,B), particularly concentrated in the age group >70 years, showing a sharp upward trend.

3.5 Detailed dietary risk factors contributed to the burden of T2D-related CKD

Globally, the top four dietary risk factors contributed to ASMR and ASDR related to T2D-related CKD were as follows: diet low in whole fruits, diet low in whole grains, diet high in processed meat, and diet high in red meat (Figures 4A,B; Table 3). Thereinto, diet low in fruits demonstrated the highest contribution, with an ASMR of 0.26 (95% *CI*: 0.09–0.48) per 100,000 persons and an ASDR of 6.54 (95% *CI*: 2.42–11.73) per 100,000 persons in 2021. From 1990 to 2021, the burden of all detailed dietary factors exhibited a significant upward trend and diet high in sugar-sweetened beverages had the highest growth rate, with an EAPC of 3.78% (95% *CI*: 3.66–3.89%) for ASMR and 3.25% (95% *CI*: 3.15–3.35%) for the ASDR (Table 3). The ASMR and ASDR of diet-induced T2D-related CKD attributable to these four dietary factors collectively exceed 80% (Supplementary Figure 2). Regardless of the specific detailed dietary factors, ASMR and ASDR were consistently higher in males than females (Figures 4A,B). At the SDI level, the attribution of ASMR and ASDR to detailed dietary factors showed a general similarity, yet high SDI regions exhibited a greater attribution to diet high in processed meat (Figure 5). Conversely, in low-middle and low SDI regions, the leading specific dietary risk factors that contributed to T2D-related CKD ranked as follows: diet low in whole fruits, diet low in vegetables, diet low in whole grains, and diet high in processed meat and red meat, emphasizing insufficient intake of healthy foods as a primary dietary risk (Figure 5). Globally, from 1990 to 2021, there was a consistent slow upward trend observed in both ASMR and ASDR. Diet low in whole fruits, diet low in whole grains, and diet high in processed meat and red meat consistently remained the predominant specific dietary risk factors contributing to T2D-related CKD (Supplementary Figure 2).

4 Discussion

Our analysis, for the first time, has provided a comprehensive overview of the global burden of T2D-related CKD attributable to detailed dietary risks in different sex, age and location groups from 1990 to 2021. Based on GBD 2021, this study revealed a consistent increase in the burden of T2D-related CKD over the past 30 years, with a notable contribution from dietary risk factors such as low fruit and whole grains intake, and high consumption of red and processed meats, particularly in males, the elderly, and the population in the low

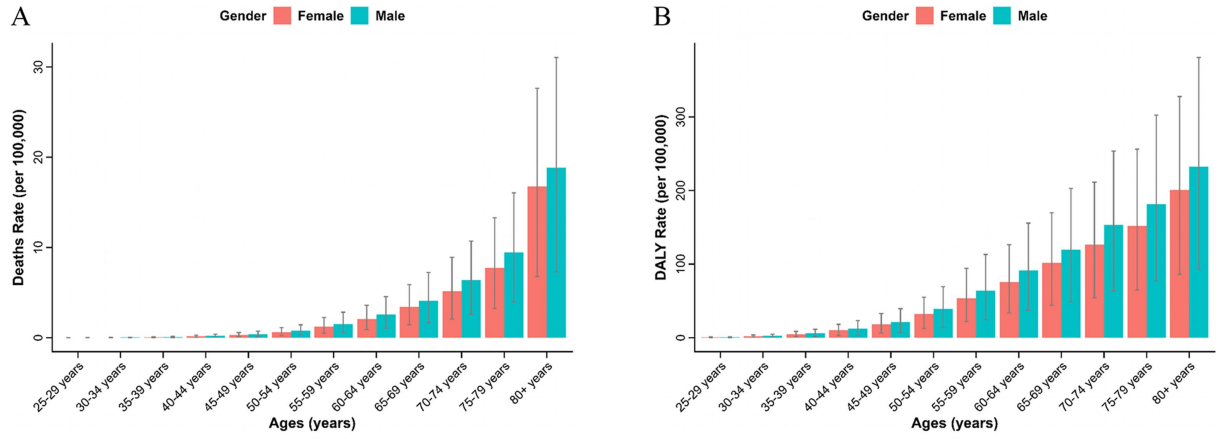

FIGURE 4
Chronic kidney disease due to type 2 diabetes attributable to dietary risk in different age groups in 2021. Mortality **(A)** and DALY **(B)** rates of chronic kidney disease due to diabetes mellitus. DALY, disability-adjusted life year.

TABLE 3 Detailed dietary factors burden of T2D-related CKD attributable to dietary risks in 1990 and 2021, and the estimated annual percentage changes of death and DALY from 1990 to 2021.

Dietary risk	Age-standardized death and DALY rate per 100,000 people (95% *CI*)		EAPC of dietary risk, % (95% *CI*)
	1990	2021	1990–2021
Death			
Diet low in whole grains	0.12 (0.03–0.21)	0.21 (0.06–0.38)	1.88 (1.84–1.92)
Diet high in sodium	0.04 (0.00–0.14)	0.08 (0.00–0.32)	2.08 (1.98–2.18)
Diet low in fruits	0.15 (0.05–0.27)	0.26 (0.09–0.48)	1.74 (1.70–1.79)
Diet low in vegetables	0.08 (0.02–0.17)	0.14 (0.04–0.32)	2.07 (1.99–2.14)
Diet high in processed meat	0.08 (0.02–0.15)	0.18 (0.05–0.31)	2.75 (2.64–2.86)
Diet high in sugar-sweetened beverages	0.02 (0.01–0.03)	0.06 (0.03–0.09)	3.78 (3.66–3.89)
Diet high in red meat	0.08 (0.00–0.18)	0.18 (0.00–0.39)	2.83 (2.76–2.91)
DALY			
Diet low in whole grains	3.49 (0.92–6.29)	5.30 (1.37–9.59)	1.41 (1.37–1.46)
Diet high in sodium	1.07 (0.07–3.89)	1.87 (0.04–7.59)	1.71 (1.61–1.82)
Diet low in fruits	4.40 (1.64–7.74)	6.54 (2.42–11.73)	1.27 (1.23–1.31)
Diet low in vegetables	2.15 (0.53–4.41)	3.43 (0.91–7.51)	1.59 (1.50–1.69)
Diet high in processed meat	2.81 (0.72–5.00)	4.77 (1.21–8.29)	1.91 (1.81–2.01)
Diet high in sugar-sweetened beverages	0.67 (0.34–1.04)	1.69 (0.87–2.57)	3.25 (3.15–3.35)
Diet high in red meat	2.44 (0.00–5.16)	4.56 (0.00–9.80)	2.24 (2.16–2.32)

T2D-related CKD, chronic kidney disease due to diabetes mellitus type 2; DALY, disability-adjusted life year; CI, confidence interval; EAPC, estimated annual percentage change.

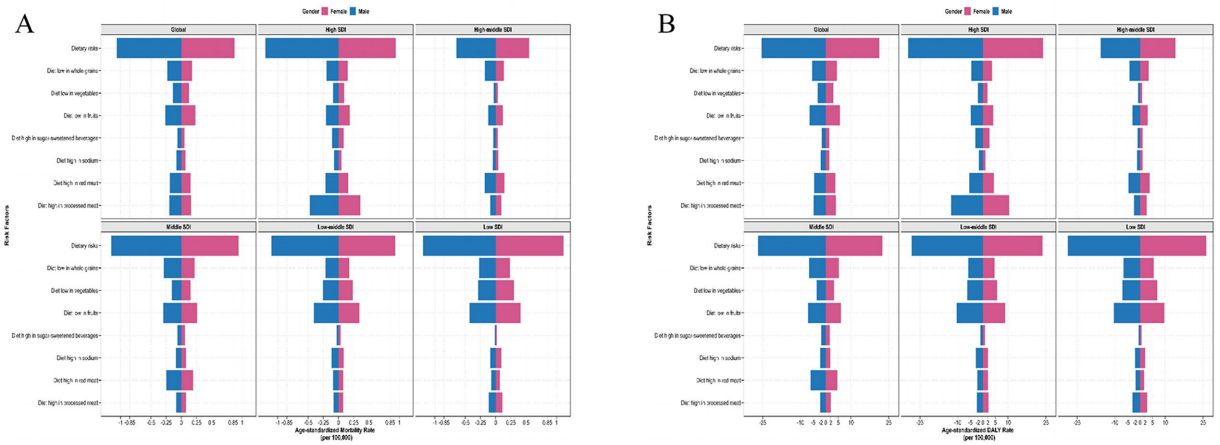

FIGURE 5
The detailed dietary risks burden for chronic kidney disease due to type 2 diabetes by sex with different SDI levels in 2021. ASMR **(A)** and ASDR **(B)** of detailed dietary risks factor of T2D-related CKD. SDI, Socio-demographic Index; ASMR, age-standardized mortality rate; DALY, disability-adjusted life years; T2D-related CKD, chronic kidney disease due to type 2 diabetes; ASDR, age-standardized disability-adjusted life years rate.

SDI regions. Our systematic analysis of T2D-related CKD attributable to dietary risks revealed a significant lack of awareness regarding the potential dangers of unhealthy dietary components in most countries. These findings provide valuable insights for the development of future food policies and programs that are flexible, integrated, and tailored to specific genders, age and geographic regions.

Over the past three decades, mortality and DALYs associated with T2D-related CKD attributable to dietary risks have increased significantly. Among these dietary risks, high sugar-sweetened beverage (SSBs) has the steepest increase in attributable burden globally from 1990 to 2021, which have been implicated in stimulating reward signals and contributing to 'food addiction', due to their rapid absorption and delivery of simple carbohydrates to the central nervous system (32). This rapid growth likely stems from widespread urbanization and economic development, which has increased the availability of SSBs, ultimately driving a global rise in sugar-sweetened beverage consumption (33). In addition, diet low in fruits, vegetables, and whole grains, alongside diet high in red and processed meats were

also increased in attributable T2D-related CKD burden globally from 1990 to 2021. Despite the proposal of various dietary intervention measures, including mass media campaigns, food and menu labeling, food pricing strategies (subsidies and taxes), school procurement policies, and workplace wellness programs (34, 35), the efficacy of most of these interventions falls to achieve the levels required for optimal global diets (36–38). It is important that inexpensive, unhealthy ultra-processed foods face little taxation, while even when nutrition labels are understood, individuals have little incentive to opt for healthier alternatives (39, 40). Hence, our findings substantively align with the urgent imperatives outlined in Sustainable Development Goal 2 (41), emphasizing dietary risks are indeed crucial considerations in the management of future disease burden. Notably, American Samoa in Oceania shows the highest ASMR and age-standardized DALY rates attributable to dietary risks. This could be attributed to the higher prevalence of type 2 diabetes and kidney damage associated with filariasis in this region (42, 43). However, it does not directly indicate a correlation between diet and the high burden of T2D-related CKD in the region, and further research is needed to clarify this association in the aspect of cultural dietary norms, health access, or genetic susceptibility.

Different SDI regions exhibit divergent epidemiological patterns in dietary contributors to T2D-related CKD, with the most significantly increase observed in high SDI regions from 1990 to 2021. With sound medical systems, adequate medical resources and aging populations, T2D-related CKD patients are more likely to be reported in high SDI regions. Meanwhile, this can be explained by high excessive consumption of red and processed meat, leading to significant renal damage due to high concentrations of preservatives and other additives (44). Additionally, processed meat served as a primary source of dietary sodium (45), which has been proven to be significantly detrimental to T2D-related CKD, along with associations with the elevated blood pressure, proteinuria, obesity, insulin resistance, and metabolic syndrome (36). Our study has also revealed that low SDI regions consistently experience the highest disease burden due to dietary risks, as evidenced by the highest ASMR and ASDR from 1990 to 2021. In these regions, diets low in whole grains, vegetables, and fruits are identified as top three dietary risk factors, but high sugar-sweetened beverage has the lowest impact for T2D-related CKD. Other contributing factors included food security, unavailability of affordable whole grains, and insufficient public awareness on healthy dietary. The accessibility of cheap, ultra-processed foods, and unhealthy fats, coupled with the high cost of fresh fruits and vegetables, jointly contribute to the diet-related disease burden in low-SDI regions (46–49). Future intervention measures for reducing T2D-related CKD need to take into account the differences in dietary structure among regions.

Our study also found that from 1990 to 2021, the burden of T2D-related CKD attributable to dietary risks remained consistently higher in males compared to females across all age groups. Previous evidence indicated that hyperpalatable foods characterized by high salt content exhibited stronger addictive properties in male consumers, whereas females demonstrate greater dietary adherence to fruits and vegetables (50, 51). Our results also observed high greater red meat or sodium intake and lower fruits or grains among men globally. In addition, diagnostic criteria may also contribute to the imbalance of T2D-related CKD burden in between sexes. Clinical practice often employs a fixed body surface area (BSA) for GFR estimation, assuming equal kidney size between males and females (52). However, male kidneys tend to have larger volumes than female kidneys in reality (53). Even formulas like the CKD-EPI equation that incorporate gender as a variable tend to underestimated, GFR in males tends to be overestimated (54). This discrepancy suggests that the true burden of T2D-related CKD may be more severe in males compared to females.

From 1990 to 2021, the burden of T2D-related CKD was predominantly concentrated in individuals aged 70 and above. We observed an increasing trend in the burden of T2D-related CKD attributable to dietary risks with advancing age, especially in females. Given the longer life expectancy of females, consideration should be given to the natural decline in renal function among elderly women (55), which may have implications for their health outcomes. Moreover, it is believed that the protective effects of endogenous estrogen on renal function and structure contribute to the differences in T2D-related CKD prevalence between pre-menopausal and post-menopausal age groups (56). However, the average age of menopause is considered to be around 50 years (57), which does not align with the burden of T2D-related CKD being predominantly concentrated in individuals aged 70 and above in this study. This discrepancy may be explained by the slow progression of CKD (58).

This study still has certain limitations. The research data is derived from the GBD database, where the epidemiological evidence of causal relationships between dietary risks and disease endpoints largely comes from observational studies, which typically have weaker evidence strength compared to randomized controlled trials. Furthermore, data on various dietary risk factors originate from different sources and may not necessarily adhere to uniform assessment standards, which contribute to statistical uncertainties in our estimates of dietary risk exposure. Additionally, when estimating the dietary burden of T2D-related CKD, dietary factors are assumed to be independently distributed across each analytic unit. However, processed meat consumption often correlates with low fruit intake, which may oversimplify real-world dietary patterns. Finally, CKD staging significantly impacts the analysis of T2D-related CKD burden attributable to dietary risk factors, but there is a paucity of such data in the GBD database. These will require us to conduct newer, region-specific cohort studies or dietary assessments with sensitivity analysis or co-linearity in the future to verify current findings.

In conclusion, our study found an increasing global burden of T2D-related CKD attributable to dietary risks underscores the urgent need for targeted public health interventions focused on enhancing dietary quality. Our analysis offers a comprehensive, multidimensional assessment of the impact of dietary risks on T2D-related CKD. Researches and policy initiatives addressing specific dietary components, as well as focusing on men, the elderly, and low-SDI regions, could be highly effective to reduce the burden. For the aim of SDGs, collaborative efforts across sectors and stakeholders, including ministries of heath, agriculture, education and commerce will be essential to addressing the complex challenges posed by T2D-related CKD.

Data availability statement

Publicly available datasets were analyzed in this study. This data can be found at: https://vizhub.healthdata.org/gbd-results/.

Ethics statement

Ethical approval was not required for the study involving humans in accordance with the local legislation and institutional requirements. Written informed consent to participate in this study was not required from the participants or the participants' legal guardians/next of kin in accordance with the national legislation and the institutional requirements.

Author contributions

YH: Conceptualization, Data curation, Formal analysis, Investigation, Methodology, Project administration, Software, Supervision, Writing – review & editing, Writing – original draft. LQ: Conceptualization, Data curation, Formal analysis, Investigation, Methodology, Project administration, Software, Supervision, Writing – original draft, Writing – review & editing. XJ: Data curation, Methodology, Software, Writing – original draft. JR: Data curation, Methodology, Writing – original draft, Formal analysis. JL: Formal analysis, Supervision, Writing – review & editing. XZ: Formal analysis, Supervision, Writing – original draft. JZ: Formal analysis, Supervision, Investigation, Methodology, Writing – review & editing. RL: Investigation, Methodology, Writing – review & editing, Data curation. YG: Investigation, Conceptualization, Project administration, Writing – original draft. XW: Conceptualization, Investigation, Supervision, Writing – review & editing. GW: Conceptualization, Investigation, Supervision, Writing – review & editing, Data curation, Formal analysis, Funding acquisition, Methodology, Project administration, Software.

Funding

The author(s) declare that financial support was received for the research and/or publication of this article. This study was supported by National Natural Science Foundation of China [81770057], and the Top Young Talents Project of the "Special Support Program for High-Level Talents" in Shaanxi, China.

Conflict of interest

The authors declare that the research was conducted in the absence of any commercial or financial relationships that could be construed as a potential conflict of interest.

Generative AI statement

The authors declare that no Gen AI was used in the creation of this manuscript.

Publisher's note

All claims expressed in this article are solely those of the authors and do not necessarily represent those of their affiliated organizations, or those of the publisher, the editors and the reviewers. Any product that may be evaluated in this article, or claim that may be made by its manufacturer, is not guaranteed or endorsed by the publisher.

Supplementary material

The Supplementary material for this article can be found online at: https://www.frontiersin.org/articles/10.3389/fnut.2025.1572610/full#supplementary-material

References

1. Liu W, Zhang D, Wang R, Chen J, Zhang J, Tao D, et al. Global trends in the burden of chronic kidney disease attributable to type 2 diabetes: an age-period-cohort analysis. *Diabetes Obes Metab*. (2024) 26:602–10. doi: 10.1111/dom.15349

2. Goodall R, Alazawi A, Hughes W, Bravis V, Salciccioli JD, Marshall DC, et al. Trends in type 2 diabetes mellitus disease burden in European Union countries between 1990 and 2019. *Sci Rep*. (2021) 11:15356. doi: 10.1038/s41598-021-94807-z

3. Deng Y, Li N, Wu Y, Wang M, Yang S, Zheng Y, et al. Global, regional, and national burden of diabetes-related chronic kidney disease from 1990 to 2019. *Front Endocrinol*. (2021) 12:672350. doi: 10.3389/fendo.2021.672350

4. Cheng AYY, Gomes MB, Kalra S, Kengne AP, Mathieu C, Shaw JE. Applying the WHO global targets for diabetes mellitus. *Nat Rev Endocrinol*. (2023) 19:194–200. doi: 10.1038/s41574-022-00793-1

5. GBD 2021 Diabetes Collaborators. Global, regional, and national burden of diabetes from 1990 to 2021, with projections of prevalence to 2050: a systematic analysis for the global burden of disease study 2021. *Lancet (London, England)*. (2023) 402:203–34. doi: 10.1016/s0140-6736(23)01301-6

6. Cundiff DK, Wu C. The EAT-lancet commission's planetary health diet compared with the institute for health metrics and evaluation global burden of disease ecological data analysis. *Cureus*. (2023) 15:e40061. doi: 10.7759/cureus.40061

7. Bowe B, Xie Y, Li T, Mokdad AH, Xian H, Yan Y, et al. Changes in the US burden of chronic kidney disease from 2002 to 2016: an analysis of the global burden of disease study. *JAMA Netw Open*. (2018) 1:e184412. doi: 10.1001/jamanetworkopen.2018.4412

8. Fraser SDS, Roderick PJ. Kidney disease in the global burden of disease study 2017. *Nat Rev Nephrol*. (2019) 15:193–4. doi: 10.1038/s41581-019-0120-0

9. Xie D, Ma T, Cui H, Li J, Zhang A, Sheng Z, et al. Global burden and influencing factors of chronic kidney disease due to type 2 diabetes in adults aged 20-59 years, 1990-2019. *Sci Rep*. (2023) 13:20234. doi: 10.1038/s41598-023-47091-y

10. Ueki K, Sasako T, Okazaki Y, Miyake K, Nangaku M, Ohashi Y, et al. Multifactorial intervention has a significant effect on diabetic kidney disease in patients with type 2 diabetes. *Kidney Int*. (2021) 99:256–66. doi: 10.1016/j.kint.2020.08.012

11. Liu W, Zhou L, Yin W, Wang J, Zuo X. Global, regional, and national burden of chronic kidney disease attributable to high sodium intake from 1990 to 2019. *Front Nutr*. (2023) 10:1078371. doi: 10.3389/fnut.2023.1078371

12. McMahon EJ, Campbell KL, Bauer JD, Mudge DW, Kelly JT. Altered dietary salt intake for people with chronic kidney disease. *Cochrane Database Syst Rev*. (2021) 2021:CD010070. doi: 10.1002/14651858.CD010070.pub3

13. Stuart KV, Biradar MI, Luben RN, Dhaun N, Wagner SK, Warwick AN, et al. The association of urinary sodium excretion with glaucoma and related traits in a large United Kingdom population. *Ophthalmol Glaucoma*. (2024) 7:499–511. doi: 10.1016/j.ogla.2024.04.010

14. GBD Chronic Kidney Disease Collaboration. Global, regional, and national burden of chronic kidney disease, 1990-2017: a systematic analysis for the global burden of disease study 2017. *Lancet (London, England)*. (2020) 395:709–33. doi: 10.1016/s0140-6736(20)30045-3

15. Cao L, Yu P, Zhang L, Yao Q, Zhou F, Li X, et al. Association between dietary patterns and chronic kidney disease in elderly patients with type 2 diabetes: a community-based cross-sectional study. *Nutr J*. (2025) 24:1. doi: 10.1186/s12937-024-01070-9

16. Saglimbene VM, Wong G, Ruospo M, Palmer SC, Garcia-Larsen V, Natale P, et al. Fruit and vegetable intake and mortality in adults undergoing maintenance hemodialysis. *Clin J Am Soc Nephrol*. (2019) 14:250–60. doi: 10.2215/cjn.08580718

17. Schwarz A, Hernandez L, Arefin S, Sartirana E, Witasp A, Wernerson A, et al. Sweet, bloody consumption - what we eat and how it affects vascular ageing, the BBB and kidney health in CKD. *Gut Microbes*. (2024) 16:2341449. doi: 10.1080/19490976.2024.2341449

18. Kelly JT, Palmer SC, Wai SN, Ruospo M, Carrero JJ, Campbell KL, et al. Healthy dietary patterns and risk of mortality and ESRD in CKD: a meta-analysis of cohort studies. *Clin J Am Soc Nephrol*. (2017) 12:272–9. doi: 10.2215/cjn.06190616

19. Winkelman D, Smith-Gagen J, Rebholz CM, Gutierrez OM, St-Jules DE. Association of intake of whole grains with health outcomes in the chronic renal insufficiency cohort study. *Clin J Am Soc Nephrol*. (2024) 19:1435–43. doi: 10.2215/cjn.0000000000000538

20. Luo W, Gong L, Chen X, Gao R, Peng B, Wang Y, et al. Lifestyle and chronic kidney disease: a machine learning modeling study. *Front Nutr*. (2022) 9:918576. doi: 10.3389/fnut.2022.918576

21. Rossing P, Caramori ML, Chan JCN, Heerspink HJL, Hurst C, Khunti K, et al. Executive summary of the KDIGO 2022 clinical practice guideline for diabetes management in chronic kidney disease: an update based on rapidly emerging new evidence. *Kidney Int*. (2022) 102:990–9. doi: 10.1016/j.kint.2022.06.013

22. Zannad F. Heart failure and kidney disease in type 2 diabetes: 2 sides of the same coin. *J Am Coll Cardiol*. (2022) 80:1732–4. doi: 10.1016/j.jacc.2022.08.773

23. Guo J, Wei M, Zhang W, Jiang Y, Li A, Wang C, et al. Clinical efficacy and safety of sodium-glucose cotransporter protein-2 (SGLT-2) inhibitor, glucagon-like peptide-1 (GLP-1) receptor agonist, and Finerenone in type 2 diabetes mellitus with non-dialysis chronic kidney disease: a network meta-analysis of randomized clinical trials. *Front Pharmacol*. (2025) 16:1517272. doi: 10.3389/fphar.2025.1517272

24. Dai H, Alsalhe TA, Chalghaf N, Riccò M, Bragazzi NL, Wu J. The global burden of disease attributable to high body mass index in 195 countries and territories, 1990-2017: an analysis of the global burden of disease study. *PLoS Med*. (2020) 17:e1003198. doi: 10.1371/journal.pmed.1003198

25. Xie J, Wang M, Long Z, Ning H, Li J, Cao Y, et al. Global burden of type 2 diabetes in adolescents and young adults, 1990-2019: systematic analysis of the global burden of disease study 2019. *BMJ (Clin Res Ed)*. (2022) 379:e072385. doi: 10.1136/bmj-2022-072385

26. Mottl AK, Nicholas SB. KDOQI commentary on the KDIGO 2022 update to the clinical practice guideline for diabetes management in CKD. *Am J Kidney Dis*. (2024) 83:277–87. doi: 10.1053/j.ajkd.2023.09.003

27. GBD 2019 Risk Factors Collaborators. Global burden of 87 risk factors in 204 countries and territories, 1990-2019: a systematic analysis for the global burden of disease study 2019. *Lancet (London, England)*. (2020) 396:1223–49. doi: 10.1016/s0140-6736(20)30752-2

28. Liu Y, Ying X, Li Y, Zhu X, Jing W, Wang X, et al. Age at first sexual intercourse, age at menarche, and age at menopause: a Mendelian randomization study on lung cancer risk. *Transl Lung Cancer Res*. (2024) 13:1718–26. doi: 10.21037/tlcr-24-480

29. Tannor EK, Sarfo FS, Mobula LM, Sarfo-Kantanka O, Adu-Gyamfi R, Plange-Rhule J. Prevalence and predictors of chronic kidney disease among Ghanaian patients with hypertension and diabetes mellitus: a multicenter cross-sectional study. *J Clin Hypertens (Greenwich)*. (2019) 21:1542–50. doi: 10.1111/jch.13672

30. Ilic I, Ilic M. The burden of type 2 diabetes mellitus in Latin America, 1990-2019: findings from the global burden of disease study. *Public Health*. (2024) 233:74–82. doi: 10.1016/j.puhe.2024.05.009

31. Yi M, Li A, Zhou L, Chu Q, Song Y, Wu K. The global burden and attributable risk factor analysis of acute myeloid leukemia in 195 countries and territories from 1990 to 2017: estimates based on the global burden of disease study 2017. *J Hematol Oncol*. (2020) 13:72. doi: 10.1186/s13045-020-00908-z

32. Malik VS, Hu FB. The role of sugar-sweetened beverages in the global epidemics of obesity and chronic diseases. *Nat Rev Endocrinol*. (2022) 18:205–18. doi: 10.1038/s41574-021-00627-6

33. Malik VS, Willett WC, Hu FB. Global obesity: trends, risk factors and policy implications. *Nat Rev Endocrinol*. (2013) 9:13–27. doi: 10.1038/nrendo.2012.199

34. Afshin A, Penalvo J, del Gobbo L, Kashaf M, Micha R, Morrish K, et al. CVD prevention through policy: a review of mass media, food/menu labeling, taxation/subsidies, built environment, school procurement, worksite wellness, and marketing standards to improve diet. *Curr Cardiol Rep*. (2015) 17:98. doi: 10.1007/s11886-015-0658-9

35. Mozaffarian D, Afshin A, Benowitz NL, Bittner V, Daniels SR, Franch HA, et al. Population approaches to improve diet, physical activity, and smoking habits: a scientific statement from the American Heart Association. *Circulation*. (2012) 126:1514–63. doi: 10.1161/CIR.0b013e318260a20b

36. Lu TY, Zhang WS, Zhu T, Jiang CQ, Zhu F, Jin YL, et al. Associations of meat, fish and seafood consumption with kidney function in middle-aged to older Chinese: a cross-sectional study based on the Guangzhou biobank cohort study. *BMJ Open*. (2023) 13:e073738. doi: 10.1136/bmjopen-2023-073738

37. Mafra D, Borges NA, LFMF C, Anjos JS, Black AP, Moraes C, et al. Red meat intake in chronic kidney disease patients: two sides of the coin. *Nutrition (Burbank, Los Angeles County, Calif)*. (2018) 46:26–32. doi: 10.1016/j.nut.2017.08.015

38. Xu ZH, Qiu CS, Qi J, Tang XL, Li HM, Zhang LW, et al. Association between whole grain intake and chronic kidney disease. *J Nutr*. (2024) 154:1262–70. doi: 10.1016/j.tjnut.2024.02.013

39. Piccoli GB, Moio MR, Fois A, Sofronie A, Gendrot L, Cabiddu G, et al. The diet and haemodialysis dyad: three eras, four open questions and four paradoxes. A narrative review, towards a personalized, patient-centered approach. *Nutrients*. (2017) 9:372. doi: 10.3390/nu9040372

40. Clase CM, Carrero JJ, Ellison DH, Grams ME, Hemmelgarn BR, Jardine MJ, et al. Potassium homeostasis and management of dyskalemia in kidney diseases: conclusions from a kidney disease: improving global outcomes (KDIGO) controversies conference. *Kidney Int*. (2020) 97:42–61. doi: 10.1016/j.kint.2019.09.018

41. Gil JDB, Reidsma P, Giller K, Todman L, Whitmore A, van Ittersum M. Sustainable development goal 2: improved targets and indicators for agriculture and food security. *Ambio*. (2019) 48:685–98. doi: 10.1007/s13280-018-1101-4

42. McLure A, Graves PM, Lau C, Shaw C, Glass K. Modelling lymphatic filariasis elimination in American Samoa: GEOFIL predicts need for new targets and six rounds of mass drug administration. *Epidemics*. (2022) 40:100591. doi: 10.1016/j.epidem.2022.100591

43. Xiang J, Morgenstern H, Li Y, Steffick D, Bragg-Gresham J, Panapasa S, et al. Incidence of ESKD among native Hawaiians and Pacific islanders living in the 50 US states and Pacific Island territories. *Am J Kidney Dis*. (2020) 76:340–349.e1. doi: 10.1053/j.ajkd.2020.01.008

44. Micha R, Michas G, Mozaffarian D. Unprocessed red and processed meats and risk of coronary artery disease and type 2 diabetes--an updated review of the evidence. *Curr Atheroscler Rep*. (2012) 14:515–24. doi: 10.1007/s11883-012-0282-8

45. Delgado J, Ansorena D, van Hecke T, Astiasarán I, de Smet S, Estévez M. Meat lipids, NaCl and carnitine: do they unveil the conundrum of the association between red and processed meat intake and cardiovascular diseases?_Invited review. *Meat Sci*. (2021) 171:108278. doi: 10.1016/j.meatsci.2020.108278

46. Parajára MC, Colombet Z, Machado ÍE, Menezes MC, Verly-Jr E, O'Flaherty M, et al. Mortality attributable to diets low in fruits, vegetables, and whole grains in Brazil in 2019: evidencing regional health inequalities. *Public Health*. (2023) 224:123–30. doi: 10.1016/j.puhe.2023.08.028

47. GBD 2021 Adult BMI Collaborators. Global, regional, and national prevalence of adult overweight and obesity, 1990-2021, with forecasts to 2050: a forecasting study for the global burden of disease study 2021. *Lancet (London, England)*. (2025) 405:813–38. doi: 10.1016/s0140-6736(25)00355-1

48. Abraham S, Breeze P, Sutton A, Lambie-Mumford H. Household food insecurity and child health outcomes: a rapid review of mechanisms and associations. *Lancet (London, England)*. (2023) 402:S16. doi: 10.1016/s0140-6736(23)02139-6

49. Chokshi DA. Income, poverty, and health inequality. *JAMA*. (2018) 319:1312–3. doi: 10.1001/jama.2018.2521

50. Barrea L, Verde L, Suárez R, Frias-Toral E, Vásquez CA, Colao A, et al. Sex-differences in Mediterranean diet: a key piece to explain sex-related cardiovascular risk in obesity? A cross-sectional study. *J Transl Med*. (2024) 22:44. doi: 10.1186/s12967-023-04814-z

51. Gearhardt AN, Grilo CM, DiLeone RJ, Brownell KD, Potenza MN. Can food be addictive? Public health and policy implications. *Addiction*. (2011) 106:1208–12. doi: 10.1111/j.1360-0443.2010.03301.x

52. Neugarten J, Kasiske B, Silbiger SR, Nyengaard JR. Effects of sex on renal structure. *Nephron*. (2002) 90:139–44. doi: 10.1159/000049033

53. Inker LA, Shafi T, Okparavero A, Tighiouart H, Eckfeldt JH, Katz R, et al. Effects of race and sex on measured GFR: the multi-ethnic study of atherosclerosis. *Am J Kidney Dis*. (2016) 68:743–51. doi: 10.1053/j.ajkd.2016.06.021

54. Inker LA, Levey AS, Tighiouart H, Shafi T, Eckfeldt JH, Johnson C, et al. Performance of glomerular filtration rate estimating equations in a community-based sample of blacks and whites: the multiethnic study of atherosclerosis. *Nephrol Dial Transpl*. (2018) 33:417–25. doi: 10.1093/ndt/gfx042

55. Partridge L, Deelen J, Slagboom PE. Facing up to the global challenges of ageing. *Nature*. (2018) 561:45–56. doi: 10.1038/s41586-018-0457-8

56. Lapi F, Azoulay L, Niazi MT, Yin H, Benayoun S, Suissa S. Androgen deprivation therapy and risk of acute kidney injury in patients with prostate cancer. *JAMA*. (2013) 310:289–96. doi: 10.1001/jama.2013.8638

57. Liu G, Li CM, Xie F, Li QL, Liao LY, Jiang WJ, et al. Colorectal cancer's burden attributable to a diet high in processed meat in the belt and road initiative countries. *World J Gastrointest Oncol*. (2024) 16:182–96. doi: 10.4251/wjgo.v16.i1.182

58. Carriazo S, Ortiz A. European east-west divide in kidney disease: the need to understand the drivers of chronic kidney disease outcomes. *Clin Kidney J*. (2021) 14:1–4. doi: 10.1093/ckj/sfaa217

frontiers | Frontiers in Nutrition

TYPE Original Research
PUBLISHED 30 June 2025
DOI 10.3389/fnut.2025.1435429

OPEN ACCESS

EDITED BY
Dongxian Guan,
Boston Children's Hospital and Harvard Medical School, United States

REVIEWED BY
Zhen Feng,
Wenzhou Medical University, China
Anna Paradowska-Stolarz,
Wroclaw Medical University, Poland
Jingjing He,
China Agricultural University, China

*CORRESPONDENCE
Mingwei Zhu
✉ zhumw2013@163.com

†These authors have contributed equally to this work

RECEIVED 20 May 2024
ACCEPTED 06 June 2025
PUBLISHED 30 June 2025

CITATION
Liu C, Chen L, Liu P, Li L, Cheng B, Xu J, Cui H and Zhu M (2025) Frailty and GLIM-defined malnutrition contribute to poor clinical outcomes in older adult inpatients in the general surgery department.
Front. Nutr. 12:1435429.
doi: 10.3389/fnut.2025.1435429

Frailty and GLIM-defined malnutrition contribute to poor clinical outcomes in older adult inpatients in the general surgery department

Chengyu Liu[1†], Liru Chen[2†], Peng Liu[1], Lei Li[1], Bo Cheng[2], Jingyong Xu[1], Hongyuan Cui[1] and Mingwei Zhu[1*]

[1]Department of General Surgery, Department of Hepato-bilio-pancreatic Surgery, Beijing Hospital, National Center of Gerontology, Institute of Geriatric Medicine, Chinese Academy of Medical Sciences, Beijing, China, [2]Department of Nutrition, Beijing Hospital, National Center of Gerontology, Institute of Geriatric Medicine, Chinese Academy of Medical Sciences, Beijing, China

Background and aims: Frailty and malnutrition are prevalent among older adult inpatients. Our study aimed to analyze the correlation between frailty and malnutrition and determine their effects on the clinical outcomes in older adult surgical inpatients.

Methods: This cross-sectional observational study included older adult inpatients (≥ 65 years old) undergoing scheduled surgery. Anthropometric measurements and hematological examination results were collected at the time of admission. Frailty and malnutrition were assessed using the frailty phenotype and the Global Leadership Initiative on Malnutrition (GLIM) criteria. Nutritional support during hospitalization and clinical outcomes, such as the occurrence of postoperative complications, in-hospital death, length of hospital stays, and hospital costs, were recorded. The chi-squared and rank-sum tests were used for comparison. Univariate and multivariate logistic regression analyses were used to calculate the odds ratios (OR) and 95% confidence intervals (CI) for frailty, malnutrition, and postoperative complications.

Results: In 394 patients, the frailty prevalence was 17.3% (68/394), and 146 inpatients (37.1%) were malnourished. The overlapping prevalence rate of frailty and malnutrition was 12.2% (48/394). Frailty and malnutrition were correlated ($r = 0.464$, $p < 0.001$). Multivariate analysis revealed that frailty significantly increased the risk of postoperative complications (OR: 2.937, 95% CI: 1.475–5.850, $p = 0.002$). There were significant differences in the length of hospital stays and hospital costs among the four groups of patients with frailty and malnutrition, frailty and no malnutrition, malnutrition and no frailty, and no frailty and malnutrition ($p < 0.001$; $p < 0.001$).

Conclusion: A significant positive correlation was observed between frailty and malnutrition. Frailty and malnutrition are significantly associated with adverse clinical outcomes. Therefore, it is necessary to manage frailty and malnutrition to improve the prognosis.

KEYWORDS

frailty, malnutrition, aged, general surgery, clinical outcome

1 Background

Frailty is an age-related clinical syndrome characterized by a decline in the physiological capabilities of multiple organ systems, resulting in increased vulnerability to stressful events (1). Malnutrition is a state of altered body composition (loss of fat mass) and decreased body cell mass due to insufficient intake or absorption of nutrients, leading to decreased physical and mental function and impaired clinical outcomes of disease (2). Malnutrition is caused by diseases, hunger, improper diet, poor physical function, poor appetite, and psychological problems (3, 4). The Global Leadership Initiative on Malnutrition (GLIM) proposed a global consensus on the diagnosis of malnutrition in adults in clinical settings in 2019 (3). The first step involves identifying "at risk" individuals to use validated screening tools, and the second step involves assessing the diagnosis and severity of malnutrition, with one phenotypic and one etiologic criterion to diagnose malnutrition (3). Frailty and malnutrition are widespread among older hospitalized patients and are common problems in geriatric surgical patients (5, 6). With the rapid increase in population aging, the prevalence of frailty in older adult patients has increased, which puts greater pressure on global healthcare systems (1).

These recent cross-sectional studies reveal that frailty and malnutrition are closely related (7, 8). A meta-analysis that pooled 10 studies (2,427 patients) shows that there is considerable overlap (49.7%) between physical (pre-)frailty and (risk of) malnutrition in hospitalized older adults (5). Evidence-based studies have demonstrated that frailty and malnutrition, even independently, can sufficiently contribute to adverse clinical outcomes. Frailty is associated with a higher risk of death, functional dependence, longer length of hospital stays (LOS), and impaired quality of life (9–11). In addition, malnutrition is associated with poor clinical outcomes, including increased incidence of complications, mortality, longer LOS, and higher hospital costs (12, 13). There is a lack of analysis combining the Global Leadership Initiative on Malnutrition (GLIM) criteria with other acceptable diagnostic methods of frailty in older adult surgical patients to analyze their impact on clinical outcomes (14).

The purpose of our study was to investigate the prevalence of frailty and malnutrition among older adult inpatients in the Department of General Surgery, analyze the correlation between frailty and malnutrition, and determine their impact on clinical outcomes, including the incidence of postoperative complications.

2 Methods

2.1 Study design and subjects

This is a single-center cross-sectional observational study conducted from 1 January 2021 to 1 July 2022. Older adult inpatients undergoing scheduled surgery were recruited from the Department of General Surgery of Beijing Hospital. Three investigators conducted the study and received centralized training on research methods before the study began. A case report form was filled out at the time of admission. Baseline surveys, frailty assessments, and nutritional assessments were conducted, and outcome information was collected after discharge. All collected data were then entered into an Excel spreadsheet.

Prior to the investigation, the study was approved by the Ethics Committee of Beijing Hospital (approval number: 2020BJYYEC-265-01) and registered in the Chinese Clinical Trial Registry (registration number: ChiCTR2000040512) on 1 December 2020. Informed consent was obtained from all patients.

The inclusion criteria for the participants were as follows: (1) age 65 years or older; (2) undergoing general surgical treatment; (3) being conscious; and (4) being willing to accept assessment and provide signed informed consent. The exclusion criteria for the participants were as follows: (1) inability to cooperate with the evaluation procedure (such as severe cognitive impairment, communication difficulties, and critical illness); (2) refusal to sign the informed consent form; (3) withdrawal of informed consent; and (4) refusal to undergo evaluation.

2.2 Data collection

Demographic information such as gender, age, and marital status was recorded. Anthropometric measurements were taken after admission to record the height, weight, right upper arm circumference, right calf circumference, and right handgrip strength. Hematological examination, including lymphocyte count, serum albumin, and serum total protein, was conducted after admission. Serum albumin levels can serve as a supportive proxy measure of inflammation, and a concentration of < 35 g/L was defined as hypoalbuminemia (15, 16). Diagnoses of malignant tumors, biliary calculi, and other diseases were collected from the home pages of inpatients and discharge medical records. Comorbidities such as diabetes mellitus, hypertension, coronary heart disease, and a history of cerebral infarction were recorded. Nutritional support was defined as follows: parenteral nutrition (PN) was defined as the infusion of intravenous macronutrients to provide energy of 10 kcal/kg/day for at least 3 days; enteral nutrition (EN) was defined as the continuous use of oral nutritional supplements (> 500 kcal/day) or gavage (> 10 kcal/kg/day) for at least 3 days; and PN + EN was defined as the use of both parenteral and enteral nutrition, with an energy supply of not less than 80% of the target intake. Otherwise, the patients were considered as not receiving any nutritional support (17).

The primary outcome was postoperative complications, defined according to the Clavien–Dindo classification system grades II-V (18). Secondary outcomes included all-cause in-hospital death, LOS, and total hospital costs. The length of stay (LOS) was defined as the cumulative number of days from admission to discharge. Hospital costs refer to the medical expenses incurred by hospitalization due to illness, which are determined according to the collection vouchers of medical expenses and hospitalization expenses issued by medical institutions, combined with medical records, diagnosis reports, and other relevant evidence.

2.3 Fried frailty phenotype

The frailty phenotype method is recommended for frailty assessment according to the Frailty Guidelines of the International Conference of Frailty and Sarcopenia Research (19).

The frailty phenotype identifies five characteristics of frailty, namely, weight loss, slow walking speed, decreased handgrip strength,

low physical activity, and fatigue. Those with three or more indicators were diagnosed as frail, those with one or two indicators as pre-frail, and those without the above five indicators as robust (20). Pre-frail and robust patients were collectively referred to as non-frail patients.

2.4 Nutritional screening and assessment

The prevalence of nutritional risk and malnutrition was prospectively defined using the Nutritional Risk Screening 2002 (NRS-2002) and the GLIM criteria. The NRS-2002 included three aspects: impaired nutritional status, disease severity, and age ≥ 70 years. A total score of 3 or higher indicates that a patient is at nutritional risk (21). Patients identified as being at nutritional risk were further assessed for malnutrition diagnosis and severity using the GLIM criteria. The GLIM criteria include three phenotypic components (non-volitional weight loss, low BMI, and reduced muscle mass) and two etiologic components (reduced food intake or assimilation, and disease burden or inflammation). A diagnosis of malnutrition requires the presence of at least one phenotypic criterion and one etiological criterion (3).

In the phenotypic criteria, weight loss > 5% within the past 6 months or >10% beyond 6 months was considered to be non-volitional weight loss; we evaluated low BMI using Asian BMI data (18.5 kg/m^2 and 20 kg/m^2 for patients aged < 70 years and ≥ 70 years, respectively). Appendicular skeletal muscle was measured using direct segmental multi-frequency bioelectrical impedance analysis with InBody 720 device. Reduced muscle mass was defined by the appendicular skeletal muscle index (ASMI), with cutoff values of < 7 kg/m^2 for men or < 5 kg/m^2 for women. For the etiologic criteria, reduced food intake or assimilation was defined as energy intake of less than 50% of the required amount over a period of 1 week, or any decrease in energy intake sustained over 2 weeks. Disease burden or inflammation was considered present in patients with either an acute illness or injury (e.g., a serious infection) or a chronic disease (e.g., a malignant disease). Severe malnutrition was diagnosed when either of the following conditions was met: (i) weight loss > 10% within the past 6 months or > 20% beyond 6 months; (ii) BMI < 17.0 kg/m^2 for individuals < 70 years or < 17.8 kg/m^2 for those aged 70 years or older. Moderate malnutrition was defined as the diagnosis of malnutrition without meeting severe malnutrition conditions.

2.5 Sample size

This study used a cross-sectional observational design. The exposure group was the frail group, and the control group was the non-frail group. The incidence of postoperative complications was the observed outcome indicator. According to a previous meta-analysis (22), the incidence of frailty was expected to be 20%, so the sample size ratio between the exposed and control groups was prespecified as 1:4. The incidence of complications was predicted to be 24% in the experimental group and 5% in the control group (22). With a two-sided $\alpha = 0.05$ and a power of 80%, PASS 15 software was used to calculate the sample size of the exposure group. The minimum sample size of the exposure group was 50 and that of the control group was 200. Accounting for an estimated 10% of participants potentially lost to follow-up or refusing follow-up, a total sample size of more than 278 participants was determined for inclusion.

2.6 Statistical analysis

SPSS software (Version 25.0. Armonk, NY: IBM Corp.) was used for data analysis. The Shapiro–Wilk test was used to determine the distribution type of the quantitative variables, and the homogeneity of variance was evaluated using the *F*-test. Normally distributed variables were expressed as means (standard deviation), non-normally distributed variables were expressed as medians (interquartile range), and categorical variables were expressed as numbers (percentages). The chi-squared test was used for differences in the distribution of categorical variables between the groups. For continuous variables, analysis of variance (ANOVA), the Mann–Whitney rank-sum test, or the Kruskal–Wallis rank-sum test were used for comparison between different groups. Spearman's correlation was used to analyze the correlation between frailty and malnutrition, and the chi-squared test was used to analyze the correlation between five indicators of the frailty phenotype diagnosis and malnutrition. Logistic regression analysis was conducted to explore independent risk factors for postoperative complications. A univariate logistic regression (input) analysis was conducted to examine the correlation between risk factors and postoperative complications, and for categorical variables that are statistically significant in the univariate logistic regression analysis, along with identified confounding factors such as age and gender, a multivariate logistic regression analysis using the forward: likelihood ratio was conducted. An interaction analysis between frailty and malnutrition was performed using an ANOVA test for LOS and hospital costs. A two-tailed *p*-value of <0.05 was considered as statistically significant.

3 Results

3.1 Patient characteristics

Among the 394 older adult inpatients enrolled, with a median age of 71 (interquartile range of 8) years, 134 (34.0%) had biliary calculi, 74 (18.8%) had colorectal cancer, 28 (7.1%) had gastric cancer, 60 (15.2%) had other gastrointestinal malignancies, and 98 (24.9%) had other diseases. There were 199 (50.5%) men and 195 (49.5%) women. The baseline characteristics of the enrolled inpatients are shown in Table 1.

3.2 Correlation analysis between frailty and malnutrition

In total, 68 inpatients (17.3%) were frail, 201 (51.0%) were pre-frail, and 125 (31.7%) were robust.

The incidence of nutritional risk was 48.2% (190/394). A total of 146 inpatients (37.1%) had malnutrition, including 88 (22.3%) with moderate malnutrition and 58 (14.7%) with severe malnutrition.

The overlap between frailty and malnutrition was 12.2% (48/394), and the overlap between pre-frailty and malnutrition was 21.8% (86/394). A total of 20 patients (5.1%) had frailty but no malnutrition,

TABLE 1 Demographic and clinical characteristics of older adult inpatients with frailty and malnutrition in the Department of General Surgery.

Characteristics	Frailty			Nutritional status		
	Frailty (n = 68)	Without frailty (n = 326)	p-value	Malnutrition (n = 146)	Without malnutrition (n = 248)	p-value
Age (years)	74.5 (13.0)	70.0 (7.0)	<0.001	72.0 (10.0)	70.0 (7.0)	<0.001
Sex, female (%)	32 (47.1%)	163 (50.0%)	0.659	68 (46.6%)	127 (51.2%)	0.374
Height (cm)	163.4 (12.7)	163.3 (12.4)	0.773	163.3 (13.1)	163.3 (11.5)	0. 768
Weight (kg)	62.0 (12.9)	65.0 (12.7)	0.026	61.0 (12.4)	66.1 (13.4)	<0.001
BMI (kg/m^2)	22.9 (4.4)	24.2 (3.9)	0.010	22.8 (3.7)	24.6 (4.4)	<0.001
CC (cm)	33.5 (4.4)	34.3 (4.5)	0.026	33.5 (4.5)	34.5 (4.5)	0.003
Upper arm circumference (cm)	26.1 (4.2)	26.8 (4.0)	0.215	26.0 (3.7)	27.0 (3.5)	< 0.001
Handgrip strength (kg)	19.35 (10.3)	25.15 (11.7)	<0.001	22.1 (10.7)	25.4 (12.3)	0.001
TLC (10^9/ L)	1.77 (0.95)	1.80 (0.92)	0.956	1.79 (1.10)	1.79 (0.90)	0.572
Serum albumin (g/dL)	3.65 (0.70)	3.90 (0.40)	<0.001	3.70 (0.60)	3.90 (0.30)	0.015
Serum total protein (g/dL)	6.45 (0.60)	6.50 (0.70)	0.036	6.40 (0.80)	6.50 (0.60)	0.073
Appendicular skeletal muscle (kg)	16.76 (4.39)	16.56 (4.85)	0.720	16.55 (4.78)	16.82 (6.49)	0.216
Skeletal muscle (kg)	22.65 (4.70)	22.65 (5.20)	0.258	22.65 (5.03)	22.90 (5.10)	0.160
Body fat (kg)	17.70 (10.73)	19.7 (9.45)	0.142	18.35 (10.17)	19.90 (9.27)	0.017
Fat-free mass (kg)	42.60 (8.48)	42.35 (9.68)	0.482	42.10 (9.20)	42.95 (10.45)	0.497

All values are expressed as median (IQR) or n (%). CC, calf circumference; TLC, total lymphocyte count; IQR, interquartile range.

TABLE 2 Overlapping prevalence of frailty and malnutrition [n (%)].

Frailty phenotype	GLIM criteria		
	Without malnutrition	Moderate malnutrition	Severe malnutrition
Robust	113 (28.7%)	11 (2.8%)	1 (0.3%)
Pre-frailty	115 (29.2%)	58 (14.7%)	28 (7.1%)
Frailty	20 (5.1%)	19 (4.8%)	29 (7.4%)

98 (24.9%) had malnutrition but no frailty, and 228 patients (57.9%) had neither frailty nor malnutrition.

Frailty was positively correlated with malnutrition, and the Spearman correlation coefficient r for frailty and malnutrition was 0.464 (p < 0. 001) (Table 2). All five diagnostic indicators of the frailty phenotype were significantly associated with the occurrence of malnutrition (all p < 0.05) (Table 3).

3.3 Univariate and multivariate analyses of postoperative complications

The overall postoperative complication rate was 13.5% (53/394). Frailty (p = 0.001), nutritional risk (p < 0.001), malnutrition (p < 0.001), age (p = 0.018), hypoalbuminemia (p = 0.022), coronary heart disease (p = 0.001), malignant tumor (p < 0.001), PN (p < 0.001), and PN + EN (p = 0.003) were significantly associated with the incidence of postoperative complications. However, sex (p = 0.068), marital status (p = 0.379), medical expenses type (p = 0.270), education level (p = 0.406), BMI (p = 0.054), diabetes mellitus (p = 0.538), hypertension (p = 0.703), a history of cerebral infarction (p = 0.659), and EN (p = 0.069) were not significantly associated with the incidence of postoperative complications (Table 4).

After excluding the confounding factors such as gender, age, hypoalbuminemia, coronary heart disease, and malignant tumor, frailty was an independent risk factor for postoperative complications [odds ratio (OR): 2.937, 95% confidence intervals (CI): 1.475–5.850, p = 0.002]. In addition, there was no multiplicative interaction between frailty and malnutrition (p = 0.709) (Table 4).

3.4 Effects of frailty and malnutrition on LOS and hospital costs

Significant differences in the LOS were observed among the four groups of patients with frailty and malnutrition, frailty and no malnutrition, malnutrition and no frailty, and no frailty and malnutrition, with mean (SD) values of 15 (12), 9 (12), 15 (15), 9 (10) days, respectively (p < 0.001). The interaction of frailty and malnutrition between the two factors had no significant effect on the LOS (F = 0.279, p = 0.757).

Significant differences in hospital costs were observed among the four groups, with mean (SD) values of 8.08 (12.54), 2.69 (3.39), 10.79 (11.63), 2.65 (7.56) thousand US dollars, respectively (p < 0.001). However, the interaction between the two factors did not have a significant effect on hospital costs (F = 0.655, p = 0.520).

TABLE 3 Correlation between diagnostic indicators of the frailty phenotype and malnutrition in older adult inpatients in the Department of General Surgery [n (%)].

Frailty phenotype indicators	With malnutrition (n = 146)	Without malnutrition (n = 248)	χ^2	p-value
Weight loss			172.984	< 0.001
Yes	105 (71.9%)	20 (8.1%)		
No	41 (28.1%)	228 (91.9%)		
Slow gait speed Slowness			20.032	< 0.001
Yes	46 (31.5%)	32 (12.9%)		
No	100 (68.5%)	216 (87.1%)		
Weakness			17.452	< 0.001
Yes	77 (52.7%)	78 (31.5%)		
No	69 (47.3%)	170 (68.5%)		
Low physical activity			6.120	0.013
Yes	51 (34.9%)	58 (23.4%)		
No	95 (65.1%)	190 (76.6%)		
Exhaustion			4.303	0.038
Yes	26 (17.8%)	26 (10.5%)		
No	120 (82.2%)	222 (89.5%)		

3.5 Nutritional support during hospitalization

The total proportion of inpatients who received nutritional support was 33.5% (132/394), including 8.9% (35/394) receiving PN, 10.9% (43/394) receiving EN, and 13.7% (54/394) receiving PN + EN.

Among inpatients with malnutrition, 50% (73/146) received nutritional support, while 23.8% (59/248) of inpatients without malnutrition received nutritional support. There was a significant difference in nutritional support between the two groups ($\chi^2 = 28.337$, $p < 0.001$).

4 Discussion

This study found a significant positive correlation between frailty and malnutrition. Frailty is an independent risk factor for postoperative complications, and patients with both frailty and malnutrition tend to have poor clinical outcomes. The association between frailty and malnutrition is reflected by the fact that they share common pathophysiological pathways, including body tissue loss and chronic inflammation. Symptoms such as weight loss, slow gait speed, decreased handgrip strength, and fatigue are characteristic of both malnutrition and frailty (23–26). Additionally, frailty and malnutrition are associated with decreased intrinsic capacity and share common sociodemographic, physical, and cognitive risk factors (27). Low intake of energy, protein, and vitamin D is associated with the onset and progression of frailty and malnutrition. Patients with frailty often have insufficient food intake, making it difficult to meet their nutritional requirements, including energy and protein. Patients in the pre-frailty stage or frailty stage typically exhibit poor nutritional status (28). Malnutrition and frailty are intricately connected in their pathogenesis, influencing each other in a complex and synergistic manner (29).

Screening assessment tools for frailty and malnutrition also have overlapping factors such as weight loss and impaired physical function (3, 6, 20). One factor of the frailty phenotype is decreased handgrip strength, which is a manifestation of reduced muscle mass in the diagnosis of malnutrition, and low physical activity is consistent with mobility in the subjective global assessment for malnutrition (3, 30). This is supported by our finding that all five of the frailty phenotypes were associated with the diagnosis of malnutrition. A prospective study by Khajoueinejad et al. (31) found that, in combination with preoperative nutritional indicators, the frailty assessment tool risk analysis index can be used to identify patients with abdominal malignancies who may benefit from additional preoperative risk stratification and increased postoperative evaluation. Emerging approaches that combine nutritional assessment and frailty diagnosis can objectively identify patients at risk during the perioperative period and guide perioperative treatment (6).

Active aging and regular physical activity can significantly improve older adults' physical function, cognitive ability, and mental health, thereby delaying the progression of frailty and enhancing quality of life (32, 33). However, age-related physiological changes may exacerbate frailty risk, while sedentary behavior and insufficient physical activity can further accelerate this process (34). Cocnurrently, malnutrition is a key contributing factor to frailty, with relevant mechanisms including insufficient nutrient intake, increased metabolic demands, and reduced nutrient bioavailability (35, 36). These findings underscore the need for comprehensive interventions targeting both physical activity and nutritional status to mitigate frailty and its adverse outcomes.

In our study, the multivariate analysis revealed that frailty was an independent risk factor for the occurrence of postoperative complications, whereas malnutrition had no significant effect, and there was no multiplicative interaction between them. Possible reasons include the following: the frailty assessment already encompasses

TABLE 4 Univariate and multivariate regression analyses of postoperative complications.

Characteristics	Category	OR	Univariate regression analysis		OR	Multivariate regression analysis	
			95% CI	*p*-value		95% CI	*p*-value
Sex	Female	0.575	0.317–1.042	0.068			0.203
	Male	Reference					
Age[a]		1.058	1.010–1.109	0.018			0. 443
Marital status	Married	1.342	0.697–2.584	0.379			
	Widowed or other	Reference					
Medical expenses type	Other	1.583	0.809–3.100	0.180			
	Medical insurance	Reference					
Education level	College or above	0.768	0.399–1.477	0.428			
	Middle school	1.667	0.754–3.682	0.207			
	Primary school and below	Reference					
BMI[a]		0.922	0.848-1.001	0.054			
Hypoalbuminemia	Yes	2.275	1.125–4.601	0.022			0.250
	No	Reference					
Diabetes mellitus	Yes	1.231	0.635–2.384	0.538			
	No	Reference					
Hypertension	Yes	0.893	0.500–1.597	0.703			
	No	Reference					
Coronary heart disease	Yes	3.148	1.585–6.252	0.001	2.615	1.255–5.449	0.010
	No	Reference					
Malignant tumor	Yes	4.804	2.392–9.649	<0.001	4.713	2.307–5.850	<0.001
	No	Reference					
History of cerebral infarction	Yes	1.317	0.481–3.604	0.592			
	No	Reference					
Frailty	Yes	2.993	1.574–5.692	0.001	2.937	1.475–5.850	0.002
	No	Reference					
Nutritional risk	Yes	4.403	2.235–8.672	<0.001			
	No	Reference					
Malnutrition	Yes	3.034	1.674–5.499	<0.001			0.093
	No	Reference					
Frailty × Malnutrition	Yes	2.841	1.387–5.819	0.004			0.709
	No	Reference					
Nutritional support	PN	0.038	0.016–0.090	<0.001			
	EN	0.431	0.174–1.067	0. 069			
	PN + EN	0.246	0.097–0.627	0.003			
	No	Reference					

BMI, body mass index; OR, odds ratio; CI, confidence interval; PN, parenteral nutrition; EN, enteral nutrition.
[a]Indicated as quantitative variables.

comprehensive risks such as nutritional deficiencies, thereby diminishing the independent contribution of malnutrition; the regression analysis included only 53 complication cases, potentially resulting in insufficient statistical power; and the mechanisms of postoperative complications are complex—while malnutrition may exert indirect effects (e.g., delaying recovery), frailty has a more direct and significant impact on physiological reserve. However, large-scale studies support the association between frailty, malnutrition, and adverse clinical outcomes, suggesting that they may have additive rather than synergistic effects. Tjeertes et al. (37) included 56 studies with a total of 1, 106, 653 patients in a meta-analysis and found that frailty significantly increased the risk of 30-day mortality in older adult patients undergoing non-cardiac surgery. Specifically, frailty was associated with a higher risk of 30-day mortality (31 studies, 673,387

patients; relative risk: 3.71, 95% CI: 2.89–4.77) and 30-day complications (37 studies, 627,991 patients; relative risk: 2.39, 95% CI: 2.02–2.83), and the risk of 1-year mortality was increased by a factor of 3 (6 studies, 341,769 patients; relative risk: 3.40, 95% CI: 2.42–4.77). A recent meta-analysis by Matsui et al. (38) found that malnutrition may worsen overall survival (hazard ratio: 1.56; 95% CI: 1.38–1.75) and increase the risk of postoperative complications (relative risk: 1.82; 95% CI: 1.28–2.60). Chew et al. (39) found that, the more severe the frailty, the more likely the patients were to expereince geriatric syndromes such as cognitive impairment, falls, and malnutrition. Frail patients with geriatric syndromes also had longer LOS and increased 30-day readmission rates. Stretton et al. (40) conducted a large multicenter cohort study involving 21,976 surgical patients, which showed that, after controlling for confounding factors, malnutrition, and socioeconomic status, the average LOS for patients at high risk of frailty was 3.46 times longer (mean ratio: 3.46; 95% CI: 3.20–3.73). In addition, poor nutritional status was significantly associated with worse clinical outcomes (40).

Frailty clinical practice guidelines strongly recommend multicomponent exercise programs, including resistance training, for the management of frailty. Protein and calorie supplementation is also recommended when weight loss or malnutrition occurs (19). Recent trials support that nutritional supplementation combined with exercise training may be more effective in frailty interventions (41). A systematic review found that frailty is associated with a low intake of micronutrients and protein, while a high dietary antioxidant capacity is associated with a lower risk of developing frailty (28). A longitudinal study by Rabassa et al. (42) found that habitual antioxidant diet in older adults was associated with a lower risk of frailty syndrome, suggesting that antioxidant dietary interventions could help manage frailty.

Frailty and malnutrition are significantly associated with adverse clinical outcomes. The principles of individualized medicine should guide in the management of malnutrition and frailty in older adult surgical patients, and the benefits of interventions should not outweigh the potential harm to patients (19). Malnourished or frail older adult surgical patients are more likely to undergo unnecessary tests and treatments, which may expose them to unnecessary burdens and risks. These findings support the use of GLIM criteria and frailty phenotypes to assess malnutrition and frailty in older adult general surgical inpatients for the intervention and improvement of clinical outcomes and may help general surgeons select appropriate preoperative risk stratification assessment tools to help determine the best treatment strategy. Future clinical studies could explore the benefits of personalized interventions in frail and malnourished older adult patients undergoing surgery.

Our study has two strengths. The frailty phenotype and GLIM criteria, which are globally recognized as standard diagnostic methods, were used to investigate the prevalence of frailty and malnutrition among older adult general surgery inpatients. In addition, we comprehensively analyzed the impact of frailty and malnutrition on clinical outcomes, such as postoperative complications, in-hospital death, LOS, and hospital costs.

Our study has some limitations. First, it was a single-center, small-sample, cross-sectional observational study; future studies should involve several research institutions and a large sample size. Second, surgery-related risk factors, such as preoperative American Society of Anesthesiologists classification, operation time, and intraoperative blood loss, were not examined, and subgroup analyses based on surgical methods were not performed owing to the small sample size and the insufficient effective sample size for regression analysis. Third, frailty and nutritional status are dynamic and may vary significantly depending on the frailty and nutritional status of patients with different disease states and treatment stages. Future studies should dynamically investigate frailty and malnutrition during admission and discharge.

In conclusion, there was a significant positive correlation between frailty and malnutrition among older adult inpatients in the General Surgery department. Frailty and malnutrition are significantly associated with adverse clinical outcomes.

Data availability statement

The raw data supporting the conclusions of this article will be made available by the authors, without undue reservation.

Ethics statement

The studies involving humans were approved by Ethics Committee of Beijing Hospital. The studies were conducted in accordance with the local legislation and institutional requirements. The participants provided their written informed consent to participate in this study.

Author contributions

CL: Data curation, Formal analysis, Writing – original draft, Writing – review & editing. LC: Data curation, Writing – original draft. PL: Data curation, Investigation, Writing – review & editing. LL: Investigation, Writing – review & editing. BC: Investigation, Resources, Writing – review & editing. JX: Investigation, Resources, Writing – review & editing. HC: Data curation, Investigation, Writing – review & editing. MZ: Funding acquisition, Supervision, Writing – review & editing.

Funding

The author(s) declare that financial support was received for the research and/or publication of this article. This study received funding from the Food Science Foundation of Chinese Institute of Food Science and Technology (2020-14), the Chinese Academy of Medical Sciences Clinical Research Fund (2021-I2M-C&T-B-094), and the Jinqiao Project of Beijing Association for Science and Technology (ZZ22058).

Conflict of interest

The authors declare that the research was conducted in the absence of any commercial or financial relationships that could be construed as a potential conflict of interest.

Publisher's note

References

1. Hoogendijk EO, Afilalo J, Ensrud KE, Kowal P, Onder G, Fried LP. Frailty: implications for clinical practice and public health. *Lancet*. (2019) 394:1365–75. doi: 10.1016/S0140-6736(19)31786-6

2. Cederholm T, Barazzoni R, Austin P, Ballmer P, Biolo G, Bischoff SC, et al. ESPEN guidelines on definitions and terminology of clinical nutrition. *Clin Nutr*. (2017) 36:49–64. doi: 10.1016/j.clnu.2016.09.004

3. Cederholm T, Jensen GL, Correia MITD, Gonzalez MC, Fukushima R, Higashiguchi T, et al. GLIM criteria for the diagnosis of malnutrition - a consensus report from the global clinical nutrition community. *Clin Nutr*. (2019) 38:1–9. doi: 10.1016/j.clnu.2018.08.002

4. O'Keeffe M, Kelly M, O'Herlihy E, O'Toole PW, Kearney PM, Timmons S, et al. Potentially modifiable determinants of malnutrition in older adults: a systematic review. *Clin Nutr*. (2019) 38:2477–98. doi: 10.1016/j.clnu.2018.12.007

5. Ligthart-Melis GC, Luiking YC, Kakourou A, Cederholm T, Maier AB, de M. Frailty, sarcopenia, and malnutrition frequently (co-)occur in hospitalized older adults: a systematic review and meta-analysis. *J Am Med Dir Assoc*. (2020) 21:1216–28. doi: 10.1016/j.jamda.2020.03.006

6. Prado CM, Ford KL, Gonzalez MC, Murnane LC, Gillis C, Wischmeyer PE, et al. Nascent to novel methods to evaluate malnutrition and frailty in the surgical patient. *JPEN J Parenter Enteral Nutr*. (2023) 47:S54–s68. doi: 10.1002/jpen.2420

7. Wang L, Li P, Hu Y, Cheng B, Ding L, Li L, et al. Relationship between preoperative malnutrition, frailty, sarcopenia, body composition, and anthropometry in elderly patients undergoing major pancreatic and biliary surgery. *Front Nutr*. (2023) 10:1135854. doi: 10.3389/fnut.2023.1135854

8. Kocyigit SE, Ates Bulut E, Aydin AE, Dost FS, Kaya D, Isik AT. The relationship between cognitive frailty, physical frailty and malnutrition in Turkish older adults. *Nutrition*. (2024) 126:112504. doi: 10.1016/j.nut.2024.112504

9. Liu Y, Huang L, Hu F, Zhang X. Frailty, polypharmacy, malnutrition, chronic conditions, and quality of life in the elderly: large population-based study. *JMIR Public Health Surveill*. (2024) 10:e50617. doi: 10.2196/50617

10. da Costa Pereira JP, Diniz ADS, de Lemos MCC, Pinho Ramiro CPS, Cabral PC. Frailty but not low muscle quality nor sarcopenia is independently associated with mortality among previously hospitalized older adults: a prospective study. *Geriatr Gerontol Int*. (2023) 23:736–43. doi: 10.1111/ggi.14660

11. Cunha AIL, Veronese N, de Melo Borges S, Ricci NA. Frailty as a predictor of adverse outcomes in hospitalized older adults: a systematic review and meta-analysis. *Ageing Res Rev*. (2019) 56:100960. doi: 10.1016/j.arr.2019.100960

12. Le B, Flier S, Madill J, Joyes C, Dawson E, Wellington C, et al. Malnutrition risk, outcomes, and costs among older adults undergoing elective surgical procedures: a retrospective cohort study. *Nutr Clin Pract*. (2023) 38:1045–62. doi: 10.1002/ncp.11043

13. Chiavarini M, Ricciotti GM, Genga A, Faggi MI, Rinaldi A, Toscano OD, et al. Malnutrition-related health outcomes in older adults with hip fractures: a systematic review and meta-analysis. *Nutrients*. (2024) 16:1069. doi: 10.3390/nu16071069

14. Jensen GL, Cederholm T. Exploring the intersections of frailty, sarcopenia, and cachexia with malnutrition. *Nutr Clin Pract*. (2024) 39:1286–91. doi: 10.1002/ncp.11180

15. Weaving G, Batstone G, Jones R. Age and sex variation in serum albumin concentration: an observational study. *Ann Clin Biochem*. (2016) 53:106–11. doi: 10.1177/0004563215593561

16. Gatta A, Verardo A, Bolognesi M. Hypoalbuminemia. *Intern Emerg Med*. (2012) 7:S193-9. doi: 10.1007/s11739-012-0802-0

17. Zhu M, Wei J, Chen W, Yang X, Cui H, Zhu S. Nutritional risk and nutritional status at admission and discharge among Chinese hospitalized patients: a prospective, nationwide, multicenter study. *J Am Coll Nutr*. (2017) 36:357–63. doi: 10.1080/07315724.2017.1304293

18. Dindo D, Demartines N, Clavien PA. Classification of surgical complications: a new proposal with evaluation in a cohort of 6336 patients and results of a survey. *Ann Surg*. (2004) 240:205–13. doi: 10.1097/01.sla.0000133083.54934.ae

19. Dent E, Morley JE, Cruz-Jentoft AJ, Woodhouse L, Rodríguez-Mañas L, Fried LP, et al. Physical frailty: ICFSR international clinical practice guidelines for identification and management. *J Nutr Health Aging*. (2019) 23:771–87. doi: 10.1007/s12603-019-1273-z

20. Fried L, Tangen C, Walston J, Newman A, Hirsch C, Gottdiener J, et al. Frailty in older adults: evidence for a phenotype. *J Gerontol A Biol Sci Med Sci*. (2001) 56:M146–56. doi: 10.1093/gerona/56.3.m146

21. Kondrup J, Rasmussen H, Hamberg O, Stanga Z. Nutritional risk screening (NRS 2002): a new method based on an analysis of controlled clinical trials. *Clin Nutr*. (2003) 22:321–36. doi: 10.1016/s0261-5614(02)00214-5

22. Hewitt J, Long S, Carter B, Bach S, McCarthy K, Clegg A. The prevalence of frailty and its association with clinical outcomes in general surgery: a systematic review and meta-analysis. *Age Ageing*. (2018) 47:793–800. doi: 10.1093/ageing/afy110

23. Jeejeebhoy K. Malnutrition, fatigue, frailty, vulnerability, sarcopenia and cachexia: overlap of clinical features. *Curr Opin Clin Nutr Metab Care*. (2012) 15:213–9. doi: 10.1097/MCO.0b013e328352694f

24. Muñoz-Redondo E, Morgado-Pérez A, Pérez-Sáez MJ, Pascual J, Tejero-Sánchez M, Curbelo YG, et al. New perspectives on frailty in light of the global leadership initiative on malnutrition, the global leadership initiative on sarcopenia, and the WHO'S concept of intrinsic capacity: a narrative review. *Maturitas*. (2023) 177:107799. doi: 10.1016/j.maturitas.2023.107799

25. Wei K, Nyunt MSZ, Gao Q, Wee SL, Ng TP. Frailty and malnutrition: related and distinct syndrome prevalence and association among community-dwelling older adults: Singapore longitudinal ageing studies. *J Am Med Dir Assoc*. (2017) 18:1019–28. doi: 10.1016/j.jamda.2017.06.017

26. Laur CV, McNicholl T, Valaitis R, Keller HH. Malnutrition or frailty? Overlap and evidence gaps in the diagnosis and treatment of frailty and malnutrition. *Appl Physiol Nutr Metab*. (2017) 42:449–58. doi: 10.1139/apnm-2016-0652

27. Boulos C, Salameh P, Barberger-Gateau P. Malnutrition and frailty in community dwelling older adults living in a rural setting. *Clin Nutr*. (2016) 35:138–43. doi: 10.1016/j.clnu.2015.01.008

28. Lorenzo-López L, Maseda A, de Labra C, Regueiro-Folgueira L, Rodríguez-Villamil J, Millán-Calenti J. Nutritional determinants of frailty in older adults: a systematic review. *BMC Geriatr*. (2017) 17:108. doi: 10.1186/s12877-017-0496-2

29. Roberts S, Collins P, Rattray M. Identifying and managing malnutrition, frailty and sarcopenia in the community: a narrative review. *Nutrients*. (2021) 13:2316. doi: 10.3390/nu13072316

30. Detsky A, McLaughlin J, Baker J, Johnston N, Whittaker S, Mendelson R, et al. What is subjective global assessment of nutritional status? *JPEN J Parenter Enteral Nutr*. (1987) 11:8–13. doi: 10.1177/014860718701100108

31. Khajoueinejad N, Sarfaty E, Yu AT, Buseck A, Troob S, Imtiaz S, et al. Preoperative frailty and malnutrition in surgical oncology patients predicts higher postoperative adverse events and worse survival: results of a blinded, prospective trial. *Ann Surg Oncol*. (2023) 31:2668–78. doi: 10.1245/s10434-023-14693-9

32. Dogra S, Dunstan DW, Sugiyama T, Stathi A, Gardiner PA, Owen N. Active aging and public health: evidence, implications, and opportunities. *Annu Rev Public Health*. (2022) 43:439–59. doi: 10.1146/annurev-publhealth-052620-091107

33. Cunningham C, R OS, Caserotti P, Tully MA. Consequences of physical inactivity in older adults: a systematic review of reviews and meta-analyses. *Scand J Med Sci Sports*. (2020) 30:816–27. doi: 10.1111/sms.13616

34. Hemmeter UM, Ngamsri T. Physical activity and mental health in the elderly. *Praxis (Bern 1994)*. (2022) 110:193–8. doi: 10.1024/1661-8157/a003853

35. Dent E, Wright ORL, Woo J, Hoogendijk EO. Malnutrition in older adults. *Lancet*. (2023) 401:951–66. doi: 10.1016/s0140-6736(22)02612-5

36. Volkert D, Kiesswetter E, Cederholm T, Donini LM, Eglseer D, Norman K, et al. Development of a model on determinants of malnutrition in aged persons: a MaNuEL project. *Gerontol Geriatr Med*. (2019) 5:2333721419858438. doi: 10.1177/2333721419858438

37. Tjeertes E, Fessem VJ, Mattace-Raso F, Hoofwijk A, Stolker R, Hoeks S. Influence of frailty on outcome in older patients undergoing non-cardiac surgery - a systematic review and meta-analysis. *Aging Dis*. (2020) 11:1276–90. doi: 10.14336/ad.2019.1024

38. Matsui R, Rifu K, Watanabe J, Inaki N, Fukunaga T. Impact of malnutrition as defined by the GLIM criteria on treatment outcomes in patients with cancer: a systematic review and meta-analysis. *Clin Nutr*. (2023) 42:615–24. doi: 10.1016/j.clnu.2023.02.019

39. Chew J, Chia JQ, Kyaw KK, Fu KJ, Lim C, Chua S, et al. Frailty screening and detection of geriatric syndromes in acute inpatient care: impact on hospital length of stay and 30-day readmissions. *Ann Geriatr Med Res*. (2023) 27:315–23. doi: 10.4235/agmr.23.0124

40. Stretton B, Booth AEC, Kovoor J, Gupta A, Edwards S, Hugh T, et al. Impact of frailty, malnutrition and socioeconomic status on perioperative outcomes. *Age Ageing*. (2024) 53:53. doi: 10.1093/ageing/afae263

41. Ni Lochlainn M, Cox NJ, Wilson T, Hayhoe RPG, Ramsay SE, Granic A, et al. Nutrition and frailty: opportunities for prevention and treatment. *Nutrients*. (2021) 13:13. doi: 10.3390/nu13072349

42. Rabassa M, Zamora-Ros R, Urpi-Sarda M, Bandinelli S, Ferrucci L, Andres-Lacueva C, et al. Association of habitual dietary resveratrol exposure with the development of frailty in older age: the Invecchiare in chianti study. *Am J Clin Nutr*. (2015) 102:1534–42. doi: 10.3945/ajcn.115.118976

frontiers | Frontiers in Nutrition

TYPE Original Research
PUBLISHED 22 August 2025
DOI 10.3389/fnut.2025.1607162

OPEN ACCESS

EDITED BY
Qingyu Wang,
Capital Medical University, China

REVIEWED BY
Muniyappan Madesh,
Yangzhou University, China
Keith Martin,
University of Memphis, United States

*CORRESPONDENCE
Wen Fan
✉ 2023721094@yangtzeu.edu.cn

RECEIVED 07 April 2025
ACCEPTED 05 August 2025
PUBLISHED 22 August 2025

CITATION
Han Y, Li L, Wang Y and Fan W (2025) Association of dietary inflammatory index and oxidative balance score with all-cause and cardiovascular mortality in US non-diabetic adults.
Front. Nutr. 12:1607162.
doi: 10.3389/fnut.2025.1607162

Association of dietary inflammatory index and oxidative balance score with all-cause and cardiovascular mortality in US non-diabetic adults

YuNan Han[1], Lin Li[1], YongXiang Wang[2] and Wen Fan[1]*

[1]Department of Endocrinology, The First Affiliated Hospital of Yangtze University, Jingzhou, Hubei, China, [2]Department of Medicine, Yangtze University, Jingzhou, Hubei, China

Background: Inflammation and oxidative stress (OS) are critical factors in the pathogenesis of chronic diseases (CDs), with dietary factors being a central modifiable determinant. This study aimed to assess the association of the Dietary Inflammation Index (DII) and Dietary Oxidative Balance Score (DOBS) with all-cause and cardiovascular (CV) mortality in non-diabetic adults.
Methods: Data on non-diabetic adults were extracted from the National Health and Nutrition Examination Survey (NHANES) (2009–2018). Dietary information was collected via 24-h recalls, and DII and DOBS were calculated. Multivariate weighted Cox proportional hazards models, Kaplan–Meier (KM) survival analysis, and restricted cubic spline (RCS) analyses were conducted to assess mortality associations. Subgroup analyses were performed based on gender, age, BMI, smoking status, hypertension, and hyperlipidemia.
Results: After applying multivariable–weighted Cox proportional hazards regression, participants with the highest DII quartile exhibited elevated risks of all-cause mortality [Q4: HR = 1.554 (1.258, 1.934)] and CV mortality [Q4: HR = 2.100 (1.307, 3.375)]. In contrast, the highest DOBS quartile was linked to reduced all-cause mortality [Q4: HR = 0.724 (0.553, 0.946)], with no significant association observed for CV mortality. RCS analyses confirmed a positive dose–response between DII and both mortality outcomes, as well as an inverse relationship for DOBS. Subgroup analyses revealed that high DOBS (Q4) scores were negatively associated with all-cause and CV mortality in women, individuals aged ≥60 years, current smokers, hypertensive individuals, and those without dyslipidemia. High DII (Q4) scores were positively associated with all-cause mortality across all sexes, individuals aged ≥60 years, smokers, and those with hypertension or dyslipidemia. Additionally, high DII scores were associated with CV mortality among women, both smokers and non-smokers, and individuals without hypertension or dyslipidemia.
Conclusion: Higher DOBS levels are associated with lower all-cause mortality, while higher DII levels are linked to increased all-cause and CV mortality. Dietary interventions targeting inflammation may reduce mortality risks, thereby informing public health strategies.

KEYWORDS

dietary inflammatory index, dietary oxidative balance score, all-cause death, cardiovascular mortality, non-diabetic patients, NHANES

1 Introduction

Inflammation and oxidative stress (OS) are identified as physiological responses to external stimuli and endogenous damage. Moreover, they play essential roles in maintaining immune homeostasis and the repair process (1). However, chronic inflammation and OS at elevated levels not only disrupt organismal homeostasis but are also considered primary drivers of various chronic diseases, including cardiovascular diseases (CVDs), cancer, and neurodegenerative disorders (2, 3). Numerous studies have shown that biological markers of inflammation and OS (such as C-reactive protein [CRP] and redox imbalance) are closely associated with disease progression and risk of death (4, 5). Therefore, to prevent chronic diseases, it is now crucial to identify the key factors regulating inflammation and OS levels.

The dietary inflammatory index (DII) and the dietary oxidative balance score (DOBS) are two key indicators to quantify the effects of diets on inflammation and OS, respectively. These two indicators are used to evaluate the pro-inflammatory/anti-inflammatory potential and the pro-oxidative/antioxidant capacity of diets (6, 7). DOBS and DII have been shown to be associated with the mortality and incidence of CVDs in patients with diabetes and prediabetes. Each unit increase in DOBS was associated with a 1.8% reduction in all-cause mortality and a 4% reduction in cardiovascular mortality among patients with diabetes and prediabetes (8). DOBS is also inversely associated with the incidence of chronic kidney disease (9), hypertension (10), depression (11), and other conditions. Meanwhile, in patients with diabetes and prediabetes, a high DII is more strongly associated with the risk of CVDs (12). Additionally, a prospective cohort study revealed that DOBS and DII were significantly associated with all-cause, CVDs, and cancer mortality (13). Thus, it is evident that existing research primarily focuses on individuals with diabetes or metabolic disorders, as well as the general population. However, patients with diabetes often exhibit metabolic disturbances such as insulin resistance, hyperglycemia, and dyslipidemia. These factors, by promoting chronic inflammation and OS, complicate the mechanistic pathways through which dietary factors exert their effects (14). Notably, although natural antioxidants (e.g., polyphenols) can effectively scavenge reactive oxygen species (ROS), the chronic inflammatory milieu in diabetes persistently suppresses the activity of antioxidant enzymes (such as superoxide dismutase [SOD] and glutathione peroxidase [GPx]), thereby significantly diminishing the efficacy of exogenous antioxidants. For example, quercetin exerts potent effects in healthy models but typically requires higher doses to achieve comparable efficacy in diabetic models. This inflammatory microenvironment suppresses the Nrf2 pathway, diminishes endogenous antioxidant defenses, and elevates the threshold at which dietary antioxidants can exert their protective effects [39674630]. Moreover, these metabolic abnormalities not only drive diabetes progression but may also interfere with nutrient metabolism and utilization (15), thereby modulating the independent effects of dietary factors on disease progression and mortality risk. In other words, among individuals with metabolic dysfunction, it is difficult to discern whether the observed increase in mortality risk is attributable to intrinsic metabolic derangements or dietary intake patterns. Conversely, the specific metabolic disorders mentioned above were not observed in non-diabetic patients. Within this group, the levels of inflammation and OS are more likely to be directly influenced by dietary variables and less likely to be confused by metabolic disorders associated with diabetes. To better elucidate the causal relationship between diet and health outcomes, the independent associations of DII and DOBS with the risk of death should be assessed in a non-diabetic population.

However, the association of DOBS and DII with the risk of death in non-diabetic patients has not been previously examined. To address this research gap, the present study utilized data from the National Health and Nutrition Examination Survey (NHANES) to investigate the association of DOBS and DII with both all-cause mortality and cardiovascular mortality in non-diabetic patients. We hypothesized that, in non-diabetic individuals, a higher DII is associated with increased all-cause and cardiovascular mortality, whereas a higher DOBS is associated with decreased all-cause and cardiovascular mortality.

2 Data and methods

2.1 Study participants

The NHANES is an ongoing survey performed in the United States by the CDC using a stratified, multi-stage sampling design. When linked with follow-up mortality data, it functions as a widely utilized, nationally representative prospective cohort study (16). Data from 2009 to 2018 were used in this research, involving individuals aged 18 years or older. Diabetes was defined as a self-reported physician diagnosis of fasting blood glucose (FBG) $\geq$ 7 mmol/L, glycosylated hemoglobin (HbA1c) $\geq$ 6.5%, or current use of hypoglycemic medications (17). We excluded participants who met the definition of diabetes (N = 3,123), those with missing covariate data (hyperlipidemia: N = 1,952, hypertension: N = 13, poverty: N = 1,480, educational level: N = 591, ethnicity: N = 2,079, smoking history: N = 7, annual family income: N = 18, body mass index (BMI): N = 107), and those with missing death data (N = 45). After excluding the aforementioned individuals, a total of 13,408 patients were included in the final research (Figure 1).

The NHANES obtained approval from the National Center for Health Statistics Research Ethics Review Board and was performed in accordance with the ethical standards as laid down in the 1964 Declaration of Helsinki and its later amendments or comparable ethical standards. Each participant gave a written informed consent agreement when they were enrolled in the NHANES, and the National Center for Health Statistics' ethics review board approved the study.

2.2 Dietary data

The assessment of daily dietary intake was performed through 24-h dietary recall interviews conducted on 2 consecutive days. Each dietary nutrient and the overall dietary energy were computed following the guidelines outlined in the USDA's Food and Nutrient Database for Dietary Studies (FNDDS) (18). Information on dietary supplement use was collected through specialized questionnaires. In addition, the nutrient assessment did not include dietary components derived from dietary supplements.

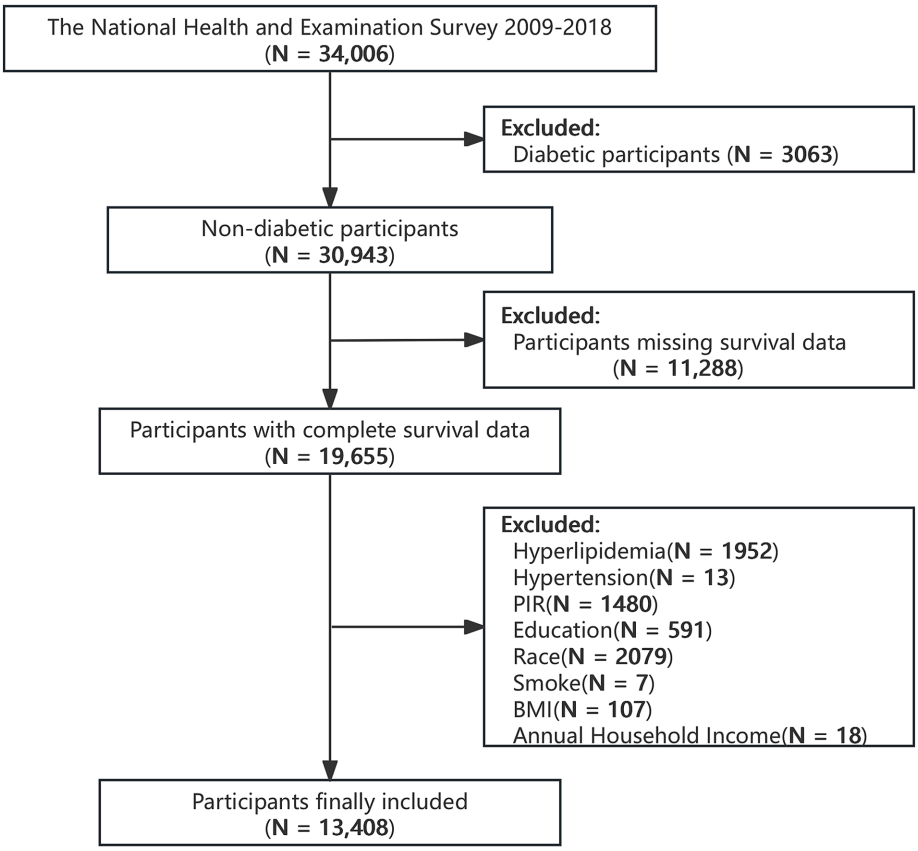

FIGURE 1
Flowchart of the selection strategy.

2.3 Assessment of DOBS

The DOBS was calculated by scoring the combination of pro-oxidant and antioxidant nutrients in the diet (7). Drawing on previous insights regarding the connection between certain nutrients and DOBS, 16 nutrients were comprehensively evaluated, including 2 pro-oxidants and 14 antioxidants (19). The nutritional data were collected from two 24-h dietary reviews. The continuous dietary components were categorized into tertiles, with antioxidant scores ranging from 1 to 3 and pro-oxidant scores assigned in the opposite manner. Each participant's dietary intake level was determined by summing the scores assigned to all dietary components. The detailed composition of DOBS components is provided in Supplementary Table 1.

2.4 Assessment of DII

The dietary inflammatory index (DII) is a dietary tool designed to assess the overall pro- and anti-inflammatory properties of an individual's diet. It incorporates 45 dietary components identified from the scientific literature and selected based on their effects on inflammatory indicators, including CRP, interleukin-6 (IL-6), and tumor necrosis factor alpha (TNF-α). The scoring scale for each component ranges from −1 (anti-inflammatory) to +1 (pro-inflammatory) (20). The Food Frequency Questionnaire (FFQ) or 24-h dietary recall was applied to assess participants' dietary intake. Considering the differences in energy intake, the intake was standardized per 1,000 kcal. Subsequently, the intake was adjusted using the formula [(daily intake - global average daily intake) divided by the standard deviation of the global average daily intake]. The modified intake values were then multiplied by the cumulative inflammatory response score of each dietary component (21). The total DII scores for each participant were calculated, with a higher score indicating a greater consumption of pro-inflammatory foods. Information on DII dietary components is detailed in Supplementary Table 2.

2.5 Determination of mortality

Within our research, the main outcome parameters encompassed all-cause mortality and cardiovascular (CV) mortality, as ascertained through the ICD-10 classification system [International Classification of Diseases (ICD), 10th edition]. The classification codes for CV deaths were I00–I09, I11, I13, and I20–I51. More detailed information is available at https://www.cdc.gov/nchs/linked-data/mortality-files/?CDC_AAref_Val=https://www.cdc.gov/nchs/data-linkage/mortality.htm.

2.6 Covariate assessment

The covariates included in this study were gender, age, ethnicity, smoking status, BMI, hypertension, hyperlipidemia, educational level,

and poverty–income ratio (PIR). Among these covariates, demographic data were collected through family interviews. Smoking was defined as having smoked at least 100 cigarettes in one's lifetime. BMI was calculated as weight divided by height squared (kg/m^2). Hypertension was defined as a systolic blood pressure greater than or equal to 130 mmHg and a diastolic blood pressure greater than or equal to 80 mmHg. Hyperlipidemia was defined as LDL-C levels ≥ 4.9 mmol/L (22). Educational attainment was categorized as high school or lower, high school graduates, some college, or college or higher. PIR was applied as an indicator of poverty status, calculated as the total household income divided by the poverty threshold. According to the guidelines, PIR was classified into three groups: ≤1.3, 1.3–3.5, and >3.5 (23).

2.7 Statistical analysis

All analyses in this study adhered to NHANES analysis guidelines. We applied the multi-stage sampling design by incorporating the main sampling units, pseudo variances, and masked variances in sampling weights to ensure nationally representative estimates. Given the intricate sampling structure of NHANES, a 2-day dietary sample was chosen following appropriate weighting procedures (1/5 * WTDR2D). Median values were used to represent continuous variables (P25, P75), whereas categorical variables were depicted using numbers (percentages). In this study, the comparison of categorical variables between groups was conducted using Pearson's chi-square test. Since the continuous variables in this research did not follow a normal distribution according to the Kolmogorov–Smirnov test, non-parametric tests were used to assess group differences.

DII and DOBS were categorized into quartiles for statistical analysis purposes (taking the lowest quartile Q1 as the reference group). A multivariable weighted Cox regression model with restricted cubic spline (RCS) analysis was utilized to estimate hazard ratios (HRs) and 95% confidence intervals (CIs), assessing the correlation of DII and DOBS with all-cause and CV death in non-diabetic patients. Adjustments were made based on gender, age, BMI, ethnicity, smoking status, hypertension, hyperlipidemia, and educational level. Log-rank tests and Kaplan–Meier (KM) survival analyses were performed to examine the differences in survival rates according to DOBS and DII in the non-diabetic population. Subsequently, subgroup analyses were performed to explore the potential modifying impacts of key demographic and clinical variables on the associations between DII, DOBS, and mortality outcomes. All covariates (excluding those used for stratification) were adjusted in the model. These analyses were stratified based on gender (male/female), smoking status (yes/no), presence of hypertension (yes/no), and hyperlipidemia (yes/no). The interaction of DII and DOBS with these variables was assessed by incorporating interaction terms into the Cox proportional hazards regression model. Specifically, multiplicative interaction terms (DII × covariate and DOBS × covariate) were included to assess whether the association between dietary scores and mortality differed across subgroups. Analysis of variance was performed to assess the significance of interactions. The propensity score matching (PSM) was utilized to mitigate potential selection bias and confounding variables. A logistic regression model incorporating relevant covariates (gender, age, ethnicity/nationality, educational level, BMI, smoking status, hypertension, and hyperlipidemia) was applied to estimate propensity scores. Based on these propensity scores, a 1:2 nearest-neighbor matching algorithm was adopted to pair participants. The balance after matching was assessed by comparing standardized mean differences (SMDs) of covariates between matched groups, with SMD < 0.1 indicating an acceptable balance. Subsequently, a weighted Cox proportional hazards regression model was used in the matched cohort to evaluate the associations of DII and DOBS with mortality outcomes, aiming to minimize potential bias and ensure the reliability of the study results. Finally, participants with prediabetes and those receiving insulin therapy were excluded, and the primary analyses were re-conducted to assess the robustness of the findings. Statistical analyses were carried out using R 4.3.0 (R Foundation for Statistical Computing, Vienna, Austria), with statistical significance defined as a p-value of < 0.05.

3 Results

3.1 Baseline characteristics

A total of 13,408 non-diabetic patients aged over 18 years were enrolled. Table 1 displays the baseline characteristics of participants stratified by all-cause mortality and survival status. The median age of the cohort was 46 years, with 53% of participants being female (N = 7,207) and 74% identifying as non-Hispanic White (N = 6,843). This study examined differences in variables including gender, age, ethnicity, educational level, family income, PIR, smoking status, hypertension, hyperlipidemia, and BMI between deceased and surviving participants ($p < 0.05$).

3.2 Associations of DOBS and DII with all-cause and cardiovascular mortality

Tables 2, 3 present the correlation of DOBS and DII with all-cause mortality and CV mortality. It could be concluded from Table 2 that in both the rough and adjusted models, DOBS showed a negative association with all-cause mortality ($p < 0.05$), whereas DII showed a positive association with all-cause mortality ($p < 0.01$). Specifically, after adjusting for all covariates, individuals in the highest quartile (Q4) of DOBS exhibited a 27.6% lower risk of all-cause mortality in comparison to those in the lowest quartile (Q1) [HR = 0.724 (95%CI: 0.553, 0.946)], whereas individuals in the highest quartile (Q4) of DII showed a 55.4% higher risk of all-cause mortality [HR = 1.554 (95%CI: 1.248, 1.934)]. It could be observed from Table 3 that DII had a positive association with CV mortality in both the rough and adjusted models, while DOBS was not significantly associated with CV mortality in participants ($p > 0.05$). Individuals in the highest quartile (Q4) of DII showed a 110% higher risk of CV death [HR = 2.100 (95%CI: 1.307, 3.375)] in comparison to those in the lowest quartile (Q1). Participants in the highest quartile (Q4) of DOBS exhibited the lowest risk of all-cause and cardiovascular mortality, whereas those in the lowest quartile (Q1) showed the highest risk (log-rank $p < 0.0001$; log-rank $p = 0.011$, respectively) (Figures 2A,B). In contrast, participants in the highest quartile (Q4) of DII experienced the highest risk of all-cause and cardiovascular mortality, while those in the lowest quartile (Q1) had the lowest risk (log-rank $p = 0.008$; log-rank $p = 0.015$, respectively) (Figures 2C,D).

TABLE 1 Baseline information from the death and survival groups.

Characteristic	Overall, N = 13,408[1]	Death, N = 12,511[1]	Survival, N = 897[1]	p-value[2]
Gender				<0.001
Male (%)	6,201 (47%)	5,691 (47%)	510 (56%)	
Female (%)	7,207 (53%)	6,820 (53%)	387 (44%)	
Age, years	46 (33, 59)	45 (32, 58)	70 (57, 80)	<0.001
Ethnicity				<0.001
Mexican American (%)	1,892 (8.6%)	1,834 (8.9%)	58 (3.4%)	
Other Hispanic (%)	1,468 (6.0%)	1,430 (6.2%)	38 (2.0%)	
Non-Hispanic White (%)	6,843 (74%)	6,208 (74%)	635 (86%)	
Non-Hispanic Black (%)	3,205 (11%)	3,039 (11%)	166 (8.9%)	
Education level				<0.001
Below high school	2,590 (12%)	2,349 (12%)	241 (19%)	
High school	3,151 (23%)	2,905 (22%)	246 (28%)	
Some college	4,384 (32%)	4,139 (33%)	245 (29%)	
College graduate or above	3,283 (33%)	3,118 (33%)	165 (24%)	
Annual household income	9.0 (6.0,15.0)	9.0 (6.0,15.0)	7.0 (5.0,10.0)	<0.001
Poverty income ratio	3.15 (1.53,5.00)	3.23 (1.57,5.00)	2.23 (1.22,4.25)	<0.001
Smoking status	5,879 (42%)	5,330 (42%)	549 (60%)	<0.001
BMI, kg/m^2	28 (24, 33)	28 (24, 33)	27 (24, 32)	0.3
Hypertension (%)	4,518 (29%)	3,940 (27%)	578 (60%)	<0.001
Hyperlipidemia (%)	4,404 (32%)	3,979 (31%)	425 (47%)	<0.001

Continuous variables were represented by weighted mean (SE). Categorical variables were expressed in the form of counts (weighted percentages).
[1]Median (25, 75%); n (unweighted) (%); [2]Wilcoxon rank-sum test for complex survey samples; chi-square test with Rao–Scott's second-order correction.

TABLE 2 Correlation of DOBS and DII with all-cause mortality.

All-cause mortality	Model 1		Model 2	
	HR (95%CI)	p	HR (95%CI)	p
DOBS				
Q1	—	—	—	—
Q2	0.750 (0.591, 0.953)	0.018	0.837 (0.662, 1.057)	0.135
Q3	0.722 (0.564, 0.925)	0.01	0.793 (0.608, 1.035)	0.088
Q4	0.642 (0.486, 0.850)	0.002	0.724 (0.553, 0.946)	0.018
DII				
Q1	—	—	—	—
Q2	1.345 (1.020, 1.772)	0.035	1.372 (1.052, 1.790)	0.02
Q3	1.158 (0.886, 1.520)	0.286	1.254 (0.975, 1.613)	0.078
Q4	1.510 (1.189, 1.918)	<0.001	1.554 (1.248, 1.934)	<0.001

The data were represented by weighted HR estimates and 95%CIs. Model 1 was a rough model, and the adjustment factors in Model 2 included gender, age, ethnicity, BMI, educational level, smoking status, hypertension, and hyperlipidemia.
Model 1: No covariates were adjusted.
Model 2: Gender, age, ethnicity, education, PIR, smoking status, BMI, hypertension, and hyperlipidemia were adjusted.

3.3 Analysis of restricted cubic spline regression

Multivariate-adjusted RCS plots revealed a non-linear association of DOBS and DII with all-cause and CV deaths in non-diabetic participants. As shown in Figure 3, DOBS showed a linearly negative correlation with all-cause mortality (p-non-linear: 0.157) and CV mortality (p-non-linear: 0.0797) in non-diabetic patients. Furthermore, DII showed a linearly positive correlation with all-cause mortality (p-non-linear: 0.2985) and CV mortality (p-non-linear: 0.1638) in non-diabetic patients.

3.4 Subgroup analysis

To assess whether the associations of DOBS and DII with mortality differ across subgroups, subgroup analyses were

TABLE 3 Correlation of DOBS and DII with CV mortality.

Cardiovascular mortality	Model 1		Model 2	
	HR (95%CI)	*p*	HR (95%CI)	*p*
DOBS				
Q1	—	—	—	—
Q2	1.239 (0.827, 1.858)	0.299	1.397 (0.919, 2.124)	0.118
Q3	0.953 (0.636, 1.428)	0.816	1.073 (0.705, 1.633)	0.742
Q4	0.707 (0.398, 1.257)	0.238	0.837 (0.458, 1.532)	0.565
DII				
Q1	—	—	—	—
Q2	2.228 (1.332, 3.729)	0.002	2.206 (1.288, 3.779)	0.004
Q3	1.494 (0.897, 2.488)	0.123	1.599 (0.944, 2.709)	0.081
Q4	2.046 (1.334, 3.139)	0.001	2.100 (1.307, 3.375)	0.002

The data were represented by weighted HR estimates and 95%CIs. Model 1 was a rough model, and the adjustment factors in Model 2 included gender, age, ethnicity, BMI, educational level, smoking status, hypertension, and hyperlipidemia.
Model 1: No covariates were adjusted.
Model 2: Gender, age, ethnicity, education, PIR, smoking status, BMI, hypertension, and hyperlipidemia were adjusted.

performed. Participants were initially classified based on gender, age, BMI, smoking status, hypertension, and hyperlipidemia. Subsequently, further regression model analysis was conducted on these subgroups. All covariates were adjusted in the model, except for those used for stratification. As shown in Figure 4A, high levels of DOBS (Q4) were significantly negatively associated with all-cause mortality in females (HR = 0.539, 95%CI: 0.341–0.851), individuals aged ≥60 (HR = 0.647, 95%CI: 0.485–0.862), smokers (HR = 0.649, 95%CI: 0.459–0.919), and individuals with hypertension (HR = 0.662, 95%CI: 0.447–0.980). In addition, as shown in Figure 4B, high levels of DOBS (Q4) were significantly negatively associated with CV mortality in females (HR = 0.248, 95%CI: 0.072–0.849) and individuals without hyperlipidemia (HR = 0.469, 95%CI: 0.227–0.968). As shown in Figure 5A, high levels of DII (Q4) showed an obviously positive association with all-cause mortality in males (HR = 1.432, 95%CI: 1.045–1.963), females (HR = 1.705, 95%CI: 1.185–2.454), those aged ≥60 (HR = 1.489, 95%CI: 1.164–1.904), individuals with BMI ≥ 25 (HR = 1.850, 95%CI: 1.395–2.454), smokers (HR = 1.599, 95%CI: 1.143–2.238), individuals with high blood pressure (HR = 2.006, 95%CI: 1.425–2.825), and individuals with hyperlipidemia (HR = 1.712, 95%CI: 1.185–2.473) ($p < 0.05$). Figure 5B illustrates a notable positive correlation between elevated levels of DII (Q4) and CV mortality specifically among females (HR = 2.944, 95%CI: 1.351–6.415), smokers (HR = 2.205, 95%CI: 1.101–4.416), non-smokers (HR = 1.991, 95%CI: 1.024–3.871), and individuals without hypertension (HR = 2.613, 95%CI: 1.083–6.304) or hyperlipidemia (HR = 3.067, 95%CI: 1.664–5.654) ($p < 0.05$). There was no significant interaction between the stratified variables of DOBS and DII subgroups in relation to all-cause and CV death, as indicated by a non-significant *p*-value for interaction ($p > 0.05$).

3.5 Sensitivity analysis

To mitigate the influence of confounding variables, we performed a PSM analysis, applied a multivariate Cox risk regression model, and adjusted for various potential confounders in the original (unmatched) cohort. The results were similar to the main estimates reported. The matched results showed that, as shown in Supplementary Table 3, individuals in the highest quartile (Q4) of OBS showed a 28.3% lower risk of all-cause mortality [HR = 0.717 (95%CI: 0.537, 0.956)] in comparison to those in the lowest quartile (Q1). Individuals in the highest quartile (Q4) of DII showed a 55.4% higher risk of all-cause mortality [HR = 1.554 (95%CI: 1.253, 1.928)]. Supplementary Table 4 illustrates no marked association between OBS and CV mortality among participants ($p > 0.05$). Individuals in the highest quartile (Q4) of DII showed a 110% lower risk of CV mortality [HR = 2.100 (95%CI: 1.307, 3.375)] in comparison to those in the lowest quartile (Q1). Furthermore, the potential influence of prediabetes and insulin therapy on the study outcomes was evaluated. To ensure robustness, participants with prediabetes or receiving insulin therapy ($N = 1{,}127$) were excluded, and the primary analyses were repeated. The effect estimates remained consistent with the main findings (Supplementary Table 5).

4 Discussion

By incorporating 45 dietary components associated with inflammation and 16 specific pro-inflammatory and antioxidant nutrients, 2 scoring systems were developed to investigate dietary inflammatory potential and antioxidant nutrient levels in individuals. The research findings suggested that a higher level of DOBS was significantly correlated with a lower risk of all-cause mortality, whereas a higher level of DII was significantly correlated with a higher risk of all-cause and CV mortality. Moreover, DOBS showed a linearly negative correlation with all-cause and CV mortality, while DII showed a linearly positive correlation with all-cause and CV mortality.

Previous studies have demonstrated that elevated DII scores are closely associated with increased risks of obesity, type 2 diabetes mellitus, and cardiovascular disease (24, 25). This relationship is hypothesized to arise because higher DII scores reflect greater consumption of proinflammatory dietary components—such as saturated fats, trans fats, and refined sugars—which have been shown to activate nuclear factor κB

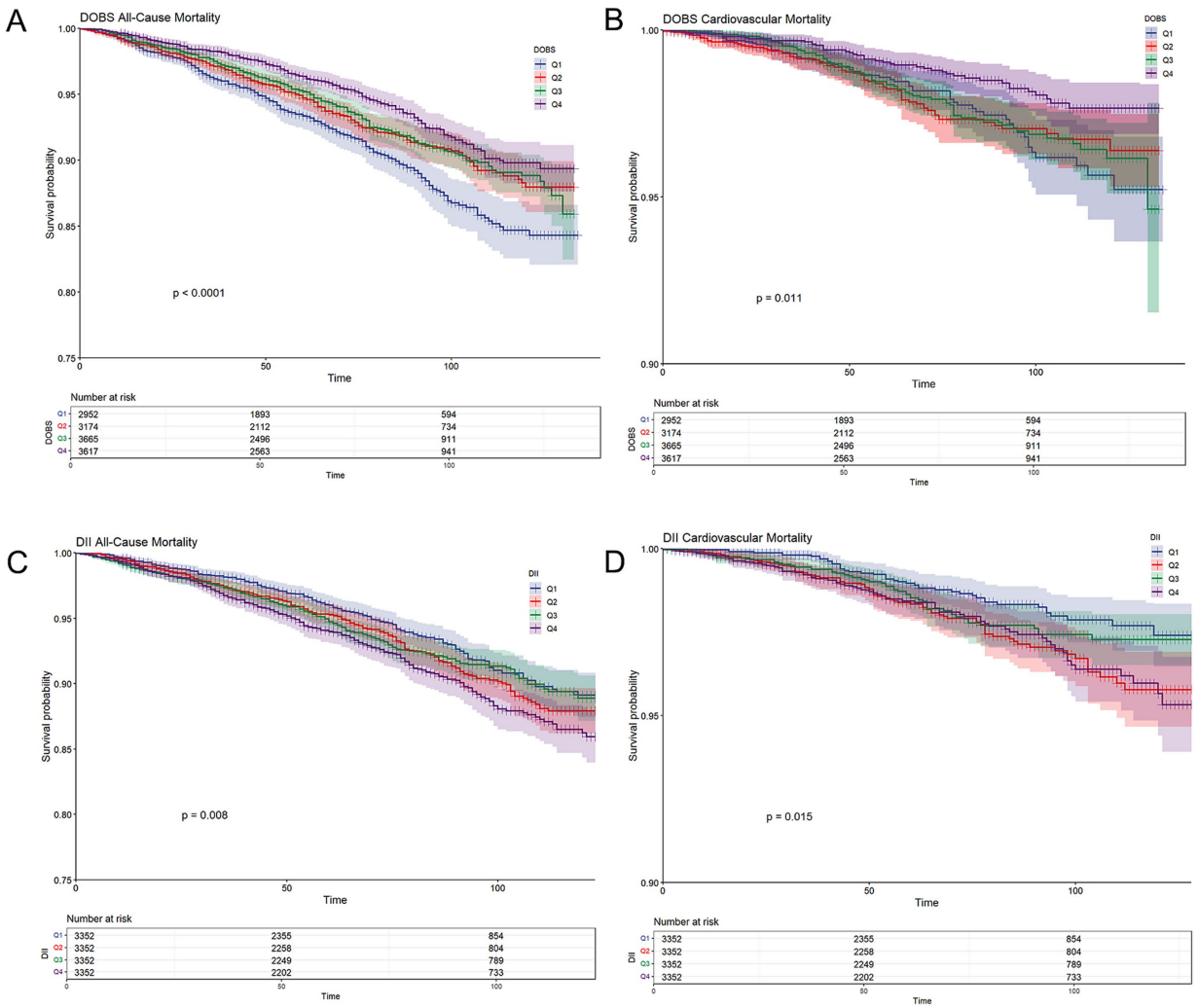

FIGURE 2
(A) Kaplan–Meier survival curves for all-cause mortality stratified by dietary oxidative balance score (DOBS) quartiles; **(B)** Kaplan–Meier survival curves for cardiovascular mortality stratified by DOBS quartile; **(C)** Kaplan–Meier survival curves for all-cause mortality stratified by dietary inflammatory index (DII) quartiles; and **(D)** Kaplan–Meier survival curves for cardiovascular mortality stratified by DII quartile. Non-diabetic participants were grouped into quartiles based on cohort-specific distributions of DOBS and DII. Survival probabilities (solid lines) and 95% confidence intervals (shaded bands) were estimated using the Kaplan–Meier method, and between-group differences were assessed using the log-rank test.

(NF-κB) and other inflammatory signaling pathways, thereby promoting systemic inflammation (26, 27). Moreover, increased consumption of these components has been linked to elevated levels of inflammatory biomarkers, including C-reactive protein (CRP) and interleukin-6 (IL-6) (28, 29). These mediators are thought to promote endothelial activation and monocyte adhesion, thereby contributing to arterial injury, atherosclerosis progression, and a heightened risk of cardiovascular events. While prior investigations focused predominantly on diabetic or metabolic syndrome populations, the present study is the first to extend the evaluation of DII in a non-diabetic cohort, revealing similar proinflammatory effects. This finding carries important clinical implications, suggesting that even individuals with relatively healthy metabolic profiles may experience subclinical inflammation induced by a persistently proinflammatory diet, thereby adversely affecting long-term cardiovascular health and increasing all-cause mortality risk.

For instance, in metabolically healthy cohorts, adherence to anti-inflammatory dietary patterns has been associated with reduced oxidative stress and lower levels of inflammatory markers, whereas proinflammatory diets have been correlated with increased inflammation and an elevated risk of metabolic abnormalities (30). Even in non-diabetic individuals with normal glycemic metabolism, chronic exposure to a high-DII diet may induce a subclinical low-grade inflammatory state that eludes routine clinical detection but nonetheless progressively impairs endothelial function and accelerates atherogenesis (31). This chronic inflammation may influence cardiovascular health through multiple pathways, such as affecting insulin signaling or exacerbating oxidative stress. Even if it is insufficient to cause diabetes, it is still capable of inflicting cumulative damage on the vascular system (32).

In addition, a study on the Food Inflammation Index (FII) indicated that the FII performs excellently in predicting individual inflammation levels (such as high-sensitivity C-reactive protein) and is highly correlated with the DII model. It further revealed significant pro- or anti-inflammatory heterogeneity within different food groups, and this

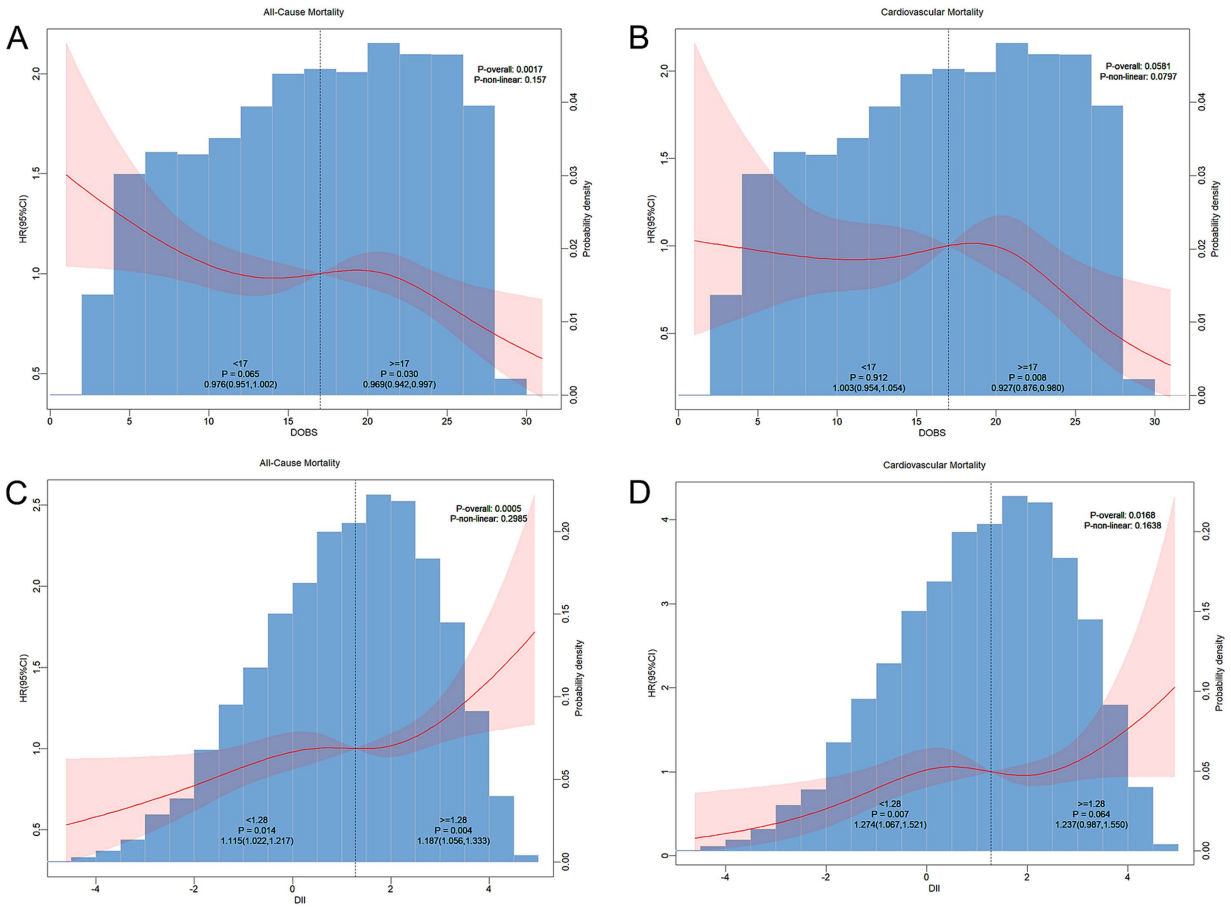

FIGURE 3
(A) RCS curve depicting the association of dietary oxidative balance score (DOBS) with all-cause mortality in non-diabetic participants; **(B)** DOBS with cardiovascular mortality; **(C)** dietary inflammatory index (DII) with all-cause mortality; and **(D)** DII with cardiovascular mortality. Adjustments were made based on gender, age, ethnicity, BMI, educational level, smoking status, hypertension, and hyperlipidemia. The central estimate was represented by a red solid line, and the red shaded area indicated the 95%CI.

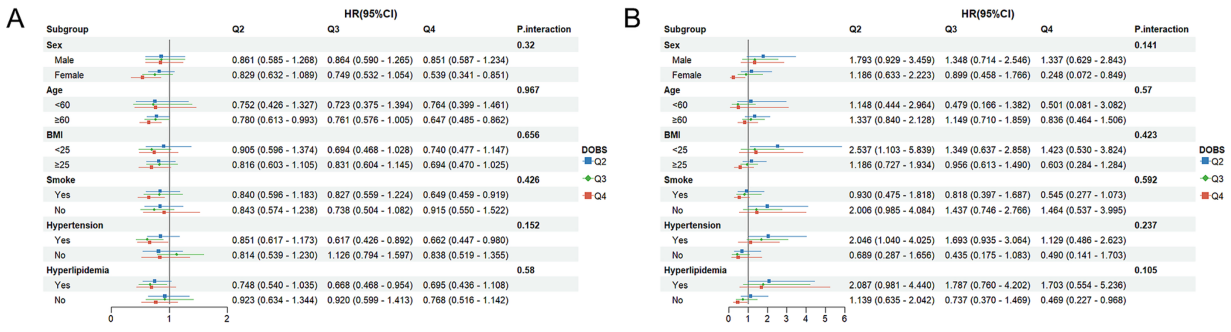

FIGURE 4
(A) Subgroup analysis of OBS and all-cause mortality; **(B)** Subgroup analysis of OBS and CV mortality. The adjustment factors included gender, age, ethnicity, BMI, educational level, smoking status, hypertension, and hyperlipidemia.

heterogeneity may affect the applicability of inflammation indices to specific dietary patterns or populations. For example, mackerel and cod exhibited markedly different anti-inflammatory effects due to differences in their DHA and EPA content (33). This phenomenon suggests that, among populations with different metabolic states or dietary compositions, the effects of the DII may vary. In the current study, the pro-inflammatory effect of a high DII in a non-diabetic cohort may be partly attributed to variations in dietary components. The heterogeneity revealed by the FII within food groups implies that future research may enhance the predictive power of DII in specific populations by incorporating more detailed food classifications, thereby enabling a more accurate elucidation of its mechanisms.

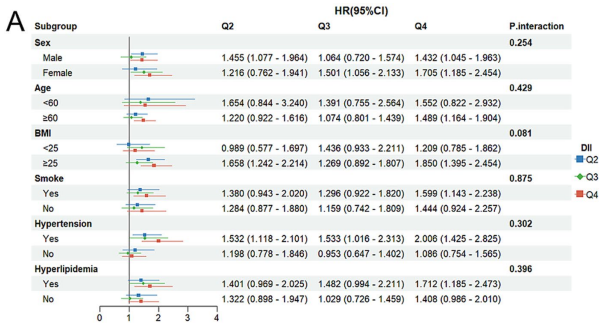

FIGURE 5
(A) Subgroup analysis of DII and all-cause mortality; **(B)** Subgroup analysis of DII and CV mortality. The adjustment factors included gender, age, ethnicity, BMI, educational level, smoking status, hypertension, and hyperlipidemia.

On this basis, another important finding of the present study was that higher Dietary Oxidative Balance Scores (DOBS) were significantly associated with lower all-cause mortality in the non-diabetic population. This finding highlighted the critical role of dietary antioxidant capacity in maintaining health within this specific cohort. In a prospective cohort of 24,527 U.S. participants, Wang et al. (13) reported a significant inverse association between DOBS and all-cause mortality in the general population, but no significant relationship with cardiovascular diseases (CVDs) or cancer mortality was observed. Since the general population includes a substantial proportion of non-diabetic individuals whose metabolic and inflammatory profiles may align more closely with those of our study cohort, Wang's findings partially support our results. Conversely, the Seguimiento Universidad de Navarra (SUN) cohort study (34) found a strong inverse association between DOBS and cardiovascular mortality (35). This discrepancy may stem from differences in study population characteristics. The SUN cohort consisted of highly educated, middle-aged Spanish adults who adhered to a Mediterranean dietary pattern, potentially enhancing the protective effects of DOBS through their diet and lifestyle. Furthermore, a German cohort of 2,125 diabetic patients demonstrated that elevated oxidative stress biomarkers were significantly associated with both major cardiovascular events and all-cause mortality (36), suggesting that redox imbalance may be a key driver of mortality in diabetic populations. Thus, in contrast to the German study's diabetic subjects, our focus on non-diabetic individuals may explain why the observed inverse relationship between DOBS and all-cause mortality reflects a lower degree of redox imbalance and fewer metabolic disturbances.

The study has the following advantages. First, our findings are more broadly applicable and generalizable, as they are based on data from a nationally representative, high-quality sample. Second, higher statistical power was embodied in larger sample sizes, longer follow-up periods, as well as stable and reliable outcomes. Third, a more comprehensive understanding of the possible association between diet-related variables and mortality in non-diabetic individuals can be gained by assessing OS and inflammatory responses using two composite indicators, DOBS and DII, rather than a single measure. However, certain limitations are inevitable in this study. First, our study design was observational, precluding causal inferences. Future research could consider Mendelian randomization to explore causality. Second, our dietary data were based on participants' self-reports, which may be subject to recall and reporting biases. Third, although multiple covariates were adjusted, residual confounding may still exist. Finally, our study included only non-diabetic individuals and did not exclude those with prediabetes, which may limit the generalizability of the findings to fully metabolically healthy populations and hinder the precise assessment of dietary effects across differing health statuses.

5 Conclusion

Our research findings indicate that higher DOBS scores are significantly associated with lower all-cause mortality, whereas higher DII scores are significantly associated with higher all-cause mortality. For CV mortality, higher DII scores are significantly correlated with lower mortality rates, while no significant association was observed between DOBS and CV mortality. These findings suggest that improving dietary quality—particularly by reducing the consumption of pro-inflammatory dietary components and increasing the intake of antioxidant-rich foods—may effectively lower inflammation and oxidative stress levels, thereby reducing mortality risk.

Data availability statement

The datasets presented in this study can be found in online repositories. The names of the repository/repositories and accession number(s) can be found in the article/Supplementary material.

Ethics statement

The studies involving humans were approved by National Centre for Health Statistics Research Ethics Review Board. The studies were conducted in accordance with the local legislation and institutional requirements. The participants provided their written informed consent to participate in this study.

Author contributions

YH: Writing – review & editing, Writing – original draft. LL: Supervision, Writing – review & editing. YW: Writing – review &

editing, Resources. WF: Funding acquisition, Writing – original draft, Writing – review & editing, Conceptualization.

Funding

The author(s) declare that no financial support was received for the research and/or publication of this article.

Conflict of interest

The authors declare that the research was conducted in the absence of any commercial or financial relationships that could be construed as a potential conflict of interest.

Generative AI statement

The authors declare that no Gen AI was used in the creation of this manuscript.

Any alternative text (alt text) provided alongside figures in this article has been generated by Frontiers with the support of artificial intelligence and reasonable efforts have been made to ensure accuracy, including review by the authors wherever possible. If you identify any issues, please contact us.

Publisher's note

Supplementary material

The Supplementary material for this article can be found online at: https://www.frontiersin.org/articles/10.3389/fnut.2025.1607162/full#supplementary-material

References

1. Reuter S, Gupta SC, Chaturvedi MM, Aggarwal BB. Oxidative stress, inflammation, and cancer: how are they linked? *Free Radic Biol Med*. (2010) 49:1603–16. doi: 10.1016/j.freeradbiomed.2010.09.006

2. Fang J, Seki T, Maeda H. Therapeutic strategies by modulating oxygen stress in cancer and inflammation. *Adv Drug Deliv Rev*. (2009) 61:290–302. doi: 10.1016/j.addr.2009.02.005

3. Grivennikov SI, Greten FR, Karin M. Immunity, inflammation, and cancer. *Cell*. (2010) 140:883–99. doi: 10.1016/j.cell.2010.01.025

4. Watson JD. Type 2 diabetes as a redox disease. *Lancet*. (2014) 383:841–3. doi: 10.1016/S0140-6736(13)62365-X

5. Steven S, Frenis K, Oelze M, Kalinovic S, Kuntic M, Bayo Jimenez MT, et al. Vascular inflammation and oxidative stress: major triggers for cardiovascular disease. *Oxidative Med Cell Longev*. (2019) 2019:1–26. doi: 10.1155/2019/7092151

6. Li L, Yang X. The essential element manganese, oxidative stress, and metabolic diseases: links and interactions. *Oxidative Med Cell Longev*. (2018) 2018:7580707. doi: 10.1155/2018/7580707

7. Goodman M, Bostick RM, Dash C, Flanders WD, Mandel JS. Hypothesis: oxidative stress score as a combined measure of pro-oxidant and antioxidant exposures. *Ann Epidemiol*. (2007) 17:394–9. doi: 10.1016/j.annepidem.2007.01.034

8. Xu Z, Liu D, Zhai Y, Tang Y, Jiang L, Li L, et al. Association between the oxidative balance score and all-cause and cardiovascular mortality in patients with diabetes and prediabetes. *Redox Biol*. (2024) 76:103327. doi: 10.1016/j.redox.2024.103327

9. Wen H, Li X, Chen J, Li Y, Yang N, Tan N. Association of oxidative balance score with chronic kidney disease: NHANES 1999–2018. *Front Endocrinol (Lausanne)*. (2024) 15:1396465. doi: 10.3389/fendo.2024.1396465

10. Lee JH, Son DH, Kwon YJ. Association between oxidative balance score and new-onset hypertension in adults: a community-based prospective cohort study. *Front Nutr*. (2022) 9:1066159. doi: 10.3389/fnut.2022.1066159

11. Liu X, Liu X, Wang Y, Zeng B, Zhu B, Dai F. Association between depression and oxidative balance score: national health and nutrition examination survey (NHANES) 2005-2018. *J Affect Disord*. (2023) 337:57–65. doi: 10.1016/j.jad.2023.05.071

12. Liu Z, Wang X, Liu H, Zhang Z, Poh WC, Luo F, et al. Dietary inflammation influences the prevalence of cardiovascular diseases in prediabetes and diabetes patients: findings from the national health and nutrition examination survey (NHANES 2001-2018). *J Health Popul Nutr*. (2024) 43:114. doi: 10.1186/s41043-024-00609-0

13. Wang X, Hu J, Liu L, Zhang Y, Dang K, Cheng L, et al. Association of dietary inflammatory index and dietary oxidative balance score with all-cause and disease-specific mortality: findings of 2003-2014 national health and nutrition examination survey. *Nutrients*. (2023) 15:3148. doi: 10.3390/nu15143148

14. Zhang P, Li T, Wu X, Nice EC, Huang C, Zhang Y. Oxidative stress and diabetes: antioxidative strategies. *Front Med*. (2020) 14:583–600. doi: 10.1007/s11684-019-0729-1

15. Tamura Y, Omura T, Toyoshima K, Araki A. Nutrition management in older adults with diabetes: a review on the importance of shifting prevention strategies from metabolic syndrome to frailty. *Nutrients*. (2020) 12:3367. doi: 10.3390/nu12113367

16. Chen F, Du M, Blumberg JB, Ho Chui KK, Ruan M, Rogers G, et al. Association among dietary supplement use, nutrient intake, and mortality among U.S. adults: a cohort study. *Ann Intern Med*. (2019) 170:604–13. doi: 10.7326/M18-2478

17. Kramer H, Boucher RE, Leehey D, Fried L, Wei G, Greene T, et al. Increasing mortality in adults with diabetes and low estimated glomerular filtration rate in the absence of albuminuria. *Diabetes Care*. (2018) 41:775–81. doi: 10.2337/dc17-1954

18. Montville JB, Ahuja JKC, Martin CL, Heendeniya KY, Omolewa-Tomobi G, Steinfeldt LC, et al. USDA food and nutrient database for dietary studies (FNDDS), 5.0. *Procedia Food Sci*. (2013) 2:99–112. doi: 10.1016/j.profoo.2013.04.016

19. Wang J, Xing F, Sheng N, Xiang Z. Associations of dietary oxidative balance score with femur osteoporosis in postmenopausal women: data from the national health and nutrition examination survey. *Osteoporos Int*. (2023) 34:2087–100. doi: 10.1007/s00198-023-06896-3

20. Shivappa N, Steck SE, Hurley TG, Hussey JR, Hébert JR. Designing and developing a literature-derived, population-based dietary inflammatory index. *Public Health Nutr*. (2014) 17:1689–96. doi: 10.1017/S1368980013002115

21. Liu P, Wang X, Liu H, Wang SX, Xu QG, Wang L, et al. Sirolimus improves the prognosis of liver recipients with hepatocellular carcinoma: a single-center experience. *Hepatobiliary Pancreat Dis Int*. (2023) 22:34–40. doi: 10.1016/j.hbpd.2022.11.010

22. Kittleson MM, Breathett K, Ziaeian B, Aguilar D, Blumer V, Bozkurt B, et al. 2024 update to the 2020 ACC/AHA clinical performance and quality measures for adults with heart failure: a report of the American Heart Association/American College of Cardiology Joint Committee on performance measures. *Circ Cardiovasc Qual Outcomes*. (2024) 17:e000132. doi: 10.1161/HCQ.0000000000000132

23. Johnson CL, Paulose-Ram R, Ogden CL, Carroll MD, Kruszon-Moran D, Dohrmann SM, et al. National health and nutrition examination survey: analytic guidelines, 1999-2010. *Vital Health Stat*. (2013) 161:1–24.

24. Hariharan R, Odjidja EN, Scott D, Shivappa N, Hébert JR, Hodge A, et al. The dietary inflammatory index, obesity, type 2 diabetes, and cardiovascular risk factors and diseases. *Obes Rev*. (2022) 23:e13349. doi: 10.1111/obr.13349

25. Namazi N, Anjom-Shoae J, Najafi F, Ayati MH, Darbandi M, Pasdar Y. Pro-inflammatory diet, cardio-metabolic risk factors and risk of type 2 diabetes: a cross-sectional analysis using data from RaNCD cohort study. *BMC Cardiovasc Disord*. (2023) 23:5. doi: 10.1186/s12872-022-03023-8

26. Lawrence T. The nuclear factor NF-kappaB pathway in inflammation. *Cold Spring Harb Perspect Biol*. (2009) 1:a001651. doi: 10.1101/cshperspect.a001651

27. de Souza RJ, Mente A, Maroleanu A, Cozma AI, Ha V, Kishibe T, et al. Intake of saturated and trans unsaturated fatty acids and risk of all cause mortality, cardiovascular disease, and type 2 diabetes: systematic review and meta-analysis of observational studies. *BMJ*. (2015) 351:h3978. doi: 10.1136/bmj.h3978

28. Cavicchia PP, Steck SE, Hurley TG, Hussey JR, Ma Y, Ockene IS, et al. A new dietary inflammatory index predicts interval changes in serum high-sensitivity C-reactive protein. *J Nutr*. (2009) 139:2365–72. doi: 10.3945/jn.109.114025

29. Ruiz-Canela M, Bes-Rastrollo M, Martínez-González MA. The role of dietary inflammatory index in cardiovascular disease, metabolic syndrome and mortality. *Int J Mol Sci*. (2016) 17:1265. doi: 10.3390/ijms17081265

30. Abdurahman AA, Azadbakhat L, Rasouli M, Chamari M, Qorbani M, Dorosty AR. Association of dietary inflammatory index with metabolic profile in metabolically healthy and unhealthy obese people. *Nutr Diet*. (2019) 76:192–8. doi: 10.1111/1747-0080.12482

31. Steyers CM 3rd, Miller FJ Jr. Endothelial dysfunction in chronic inflammatory diseases. *Int J Mol Sci*. (2014) 15:11324–49. doi: 10.3390/ijms150711324

32. Hadid KA, Alassaf FA, M A. Mechanisms and linkage of insulin signaling, resistance, and inflammation. Iraq University of Mosul (2023).

33. Wang Z, Yuan C, Zhang Y, Abdelaty NS, Chen C, Shen J, et al. Food inflammation index reveals the key inflammatory components in foods and heterogeneity within food groups: how do we choose food? *J Adv Res*. (2024) 74:87–98. doi: 10.1016/j.jare.2024.10.010

34. Hernández-Ruiz Á, García-Villanova B, Guerra-Hernández EJ, Carrión-García CJ, Amiano P, Sánchez MJ, et al. Oxidative balance scores (OBSs) integrating nutrient, food and lifestyle dimensions: development of the NutrientL-OBS and FoodL-OBS. *Antioxidants (Basel)*. (2022) 11:300. doi: 10.3390/antiox11020300

35. Talavera-Rodriguez I, Fernandez-Lazaro CI, Hernández-Ruiz Á, Hershey MS, Galarregui C, Sotos-Prieto M, et al. Association between an oxidative balance score and mortality: a prospective analysis in the SUN cohort. *Eur J Nutr*. (2023) 62:1667–80. doi: 10.1007/s00394-023-03099-8

36. Xuan Y, Gào X, Anusruti A, Holleczek B, Jansen E, Muhlack DC, et al. Association of serum markers of oxidative stress with incident major cardiovascular events, cancer incidence, and all-cause mortality in type 2 diabetes patients: pooled results from two cohort studies. *Diabetes Care*. (2019) 42:1436–45. doi: 10.2337/dc19-0292

frontiers | Frontiers in Nutrition

TYPE Original Research
PUBLISHED 12 September 2025
DOI 10.3389/fnut.2025.1563220

OPEN ACCESS

EDITED BY
Dongxian Guan,
Harvard Medical School, United States

REVIEWED BY
Jiang Zhu,
Sichuan University, China
Zhengyuan Zhai,
China Agricultural University, China

*CORRESPONDENCE
Jian-Ping Cai
✉ caijp61@vip.sina.com

RECEIVED 19 January 2025
ACCEPTED 29 August 2025
PUBLISHED 12 September 2025

CITATION
Ma Y-Q, Dang Y-M, Zeng L-T, Gao X, Li S-J, Zhang L-Q, Li J, Zhou X-Y, Ren S-S, Liu H-L, Qi R-M, Pang J, Cui J, Zhang T-M and Cai J-P (2025) Utilizing nutrition-related biomarkers to develop a nutrition-related aging clock for the chinese demographic. *Front. Nutr.* 12:1563220. doi: 10.3389/fnut.2025.1563220

Utilizing nutrition-related biomarkers to develop a nutrition-related aging clock for the chinese demographic

Ya-Qing Ma[1,2], Ya-Min Dang[2], Lv-Tao Zeng[1,2], Xin Gao[2], Si-Jia Li[2], Li-Qun Zhang[2], Jin Li[2], Xiao-Yang Zhou[2], Shan-Shan Ren[3], Hong-Lei Liu[4], Ruo-Mei Qi[2], Jing Pang[2], Ju Cui[2], Tie-Mei Zhang[2] and Jian-Ping Cai[1,2]*

[1]Fifth School of Clinical Medicine, Peking University, Beijing, China, [2]The Key Laboratory of Geriatrics, Beijing Hospital, National Center of Gerontology of National Health Commission, Beijing Institute of Geriatrics, Institute of Geriatric Medicine, Chinese Academy of Medical Sciences, Beijing, China, [3]Department of Clinical Nutrition, Beijing Hospital, National Center of Gerontology, Institute of Geriatric Medicine, Chinese Academy of Medical Sciences, Beijing, China, [4]Beijing Advanced Innovation Center for Big Data-based Precision Medicine, Capital Medical University, Beijing, China

Introduction: This study aims to investigate the relationship between nutrition-related biomarkers, body composition, and oxidative stress indicators in the human aging process, so as to provide new insights for understanding individual aging differences and developing targeted intervention strategies.

Methods: A total of 100 healthy participants aged 26–85 years were enrolled. Plasma concentrations of 9 amino acids and 13 vitamins were quantitatively analyzed, along with urinary oxidative stress markers 8-oxoGuo and 8-oxodGuo. Body composition was assessed using bioelectrical impedance analysis (BIA). A nutrition-based aging clock model was constructed using the Light Gradient Boosting Machine algorithm, with model performance evaluated by mean absolute error (MAE) and coefficient of determination (R^2).

Results: The younger group showed significantly lower levels of oxidative stress markers compared to the older group. Multiple amino acids and vitamins exhibited age-dependent changes in plasma concentrations. The developed aging clock model demonstrated high predictive accuracy, with an MAE of 2.5877 and R^2 of 0.8807. Correlation analyses further indicated associations between model-predicted biological age and physiological changes reflected in biochemical and physical examination indicators.

Discussion: This study establishes a significant link between nutrition-related biomarkers, oxidative stress, body composition, and aging. The proposed model serves as a reliable tool for predicting biological age and offers a scientific basis for future research on aging mechanisms and personalized interventions.

KEYWORDS

the nutrition-related aging clock, bioelectrical impedance analysis, aging biomarkers, oxidative stress markers, interindividual aging variation

1 Introduction

In response to the challenges posed by an aging population, researchers have focused on developing aging biomarkers for health identification and assessment (1). In recent years, aging clocks constructed based on various biological markers have emerged, aiming to predict an individual's biological age and monitor the rate of aging (2). Among the existing aging clocks, those based on DNA methylation (3) and plasma proteome (4) are particularly notable.

Nutrition refers to the process by which the body meets its physiological needs through the intake and metabolism of food. This includes both essential macronutrients (such as proteins, fats, and carbohydrates) and micronutrients (such as vitamins and minerals) (5). Nutrition involves not only caloric intake but also the balance of many biomolecules essential for maintaining physiological function, enhancing health, and preventing diseases (6). Nutritional assessment is a comprehensive process that analyzes nutrition-related health issues by collecting data on food intake and metabolism, alongside biochemical indicators, physical examination results, and other relevant information (7–9). Nutritional science plays a crucial role in promoting healthy aging. Healthy aging not only refers to extending lifespan but also, more importantly, to increasing the number of years of healthy life expectancy (10). The adequacy of nutrition directly influences the health condition and quality of life of the elderly (11). Poor nutritional status in the elderly increases the risk of aging-related chronic diseases. Deficiencies in vitamin B6, B12, and folic acid, for instance, are associated with cognitive decline and Alzheimer's disease (5, 7, 12). Therefore, nutritional status significantly impacts the aging process, and developing a nutrition-related aging assessment clock is essential for a deeper understanding of aging.

Plasma levels of amino acids and vitamins are closely related to an individual's nutritional and health status. Tappia et al.'s research indicates that specific vitamins, such as vitamin C and vitamin B6, may help prevent cardiovascular diseases in high-risk individuals (13). Bioelectrical impedance analysis (BIA), a non-invasive technology, can help identify age-related nutritional and metabolic changes, including key indicators such as basal metabolic rate (BMR), muscle mass, total body water, and extracellular water (14, 15). Whether these indicators could contribute to the aging clock establishment remain unknown.

Oxidative stress is closely linked to nutritional status. The free radical theory of aging is one of the most widely known aging theories, with oxidative stress being a key factor in cellular damage and aging (16, 17). Recent research indicates that 8-oxoguanosine (8-oxoGuo) and 8-oxodeoxyguanosine (8-oxo-dGuo) are significant indicators of oxidative stress and aging (18–23). Canfield et al.'s research suggests that reducing oxidative stress may contribute to the positive correlation between free amino acid levels and lifespan (24). Good nutritional status helps neutralize oxidative stress, supports neuroplasticity, and positively impacts recovery outcomes after a stroke. Conversely, malnutrition or poor nutritional status can exacerbate oxidative stress, leading to inflammatory responses and damaging health (25). Therefore, we included the oxidative stress markers 8-oxoGuo and 8-oxo-dGuo in urine as part of the aging clock related to nutritional status.

This study aims to develop an aging clock based on nutrition-related biomarkers, including amino acids and vitamin levels in plasma, body composition, and oxidative stress markers in urine, to assess biological age in individuals. This model has the potential to reveal variations in aging rates between individuals. The construction of this model has significant implications for designing tailored aging intervention strategies and offers new perspectives on the biological basis of aging.

2 Materials and methods

2.1 Study design and study participants

The Ethics Committee of Beijing Hospital approved the protocol for this study (Approval No. 2019BJYYEC-054-02), and the study was conducted in accordance with the Declaration of Helsinki. Each participant provided a signed informed consent form after receiving comprehensive information about the study's objectives, methods, and potential risks. The PENG ZU cohort is a health aging cohort study covering populations from seven major regions of China (26). We randomly selected 100 healthy volunteers, aged 26–85 years, for this study. The participants were from various age groups. Individuals with serious chronic illnesses or other health issues that could affect the research results were excluded. To ensure that the sample accurately represented a broad range of age demographics and genders, we employed random sampling techniques. The study outline is shown in **Figure 1**.

2.2 Biomarker assessment

2.2.1 Plasma sample analysis

The quantitative analysis of 9 amino acids and 13 vitamins was performed using liquid chromatography-tandem mass spectrometry (LC-MS/MS). The measured amino acids include ethanolamine, L-serine, L-proline, L-cystine, taurine, L-aspartic acid, L-arginine, L-histidine, and 1-methyl-L-histidine. The vitamins include vitamin B1, B2, B3, B5, B6, B7, 5-methyltetrahydrofolate, vitamin A, D2, D3, E, K1, and MK4.

2.2.2 Urine sample analysis

The levels of 8-oxodGuo and 8-oxoGuo in the urine were measured using liquid chromatography-tandem mass spectrometry (LC-MS/MS). The urine creatinine concentration was determined using the Jaffe reaction method with a 7,600 series automatic biochemical analyzer (Hitachi, Japan), following the manufacturer's instructions. To determine the levels of oxidative stress, we used the 8-oxodGuo/Cre and 8-oxoGuo/Cre ratios. Urine samples were promptly preserved at −80 °C after being collected midstream in the morning. Prior to analysis, the samples were thawed, warmed in a 37 °C water bath for 5 min, centrifuged at 7,500 g for 5 min, and the supernatant was collected (27). To each 200 μL of supernatant, 200 μL of working solution (70% methanol, 30% water, 0.1% formic acid, 5 mmol/L ammonium acetate) was added, along with 10 μL of internal standard 8-oxo-[$^{15}N_5$]dGuo and 10 μL of internal standard 8-oxo-[$^{15}N_2{}^{13}C_1$]Guo (both at a concentration of 240 pg/μL). The mixture was incubated at 37 °C for 10 min and

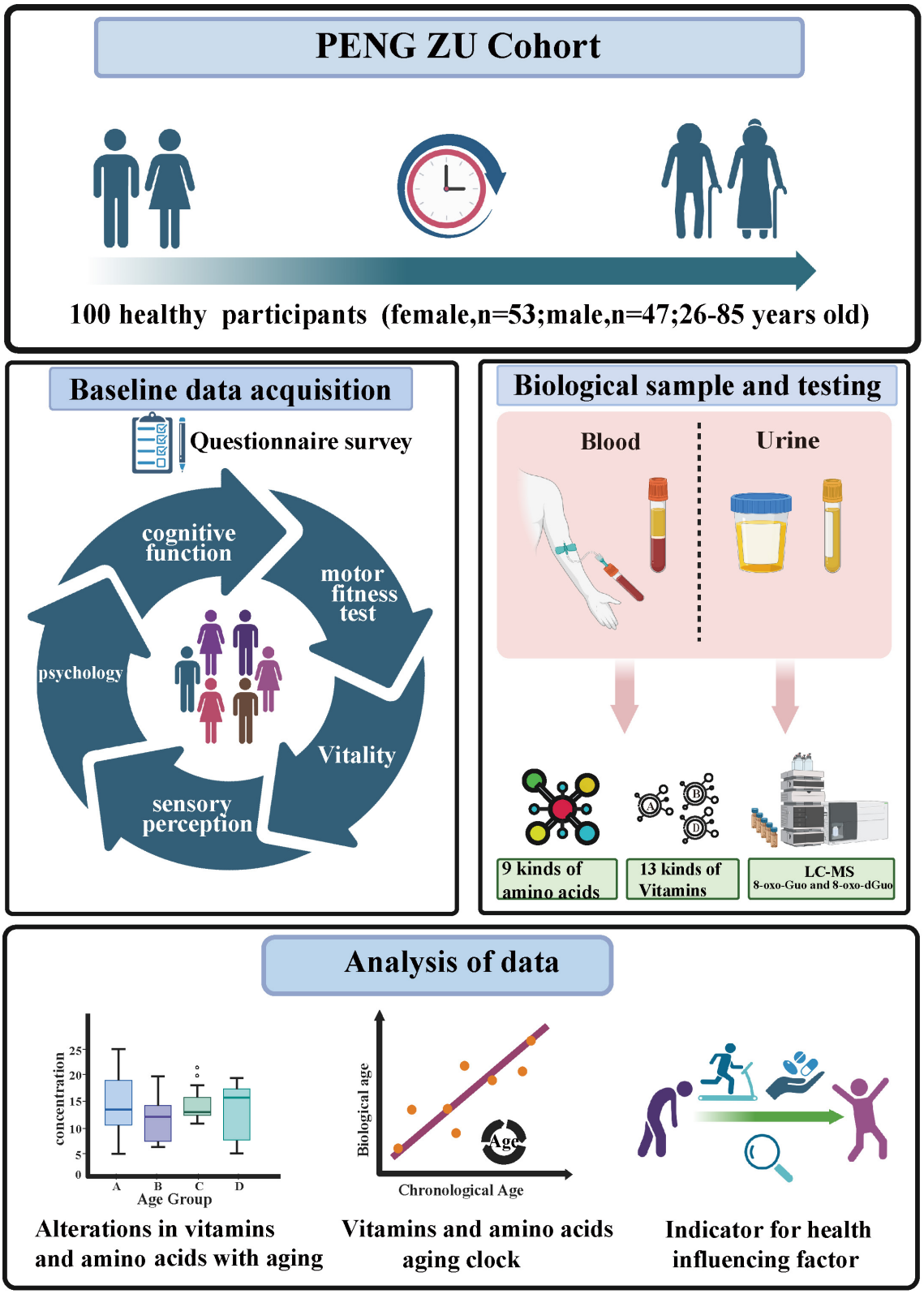

FIGURE 1
The study outline (Figure created with BioRender.com).

then centrifuged at 12,000 g for 15 min. The samples were separated using an Agilent 1290 UPLC connected to an Agilent 6490 triple quadrupole mass spectrometer (MS/MS) for detection.

2.2.3 Biochemical parameters

In addition to the aforementioned biomarker analyses, we conducted routine biochemical parameter tests on plasma and

urine samples, quantitatively analyzing a range of metabolites to comprehensively assess participants' health status.

2.3 BIA

Body composition was assessed using the BCA-2A bioelectrical impedance analyzer (BIA; Tsinghua Tongfang Co., Ltd., Beijing, China). The device operates at frequencies of 5, 50, 100, 250, and 500 kHz, collecting comprehensive bioimpedance data. A set of eight-point contact electrodes was used for six-channel whole-body testing, ensuring measurement accuracy and uniformity. The primary criteria measured included basal metabolic rate, muscle mass, total body water, extracellular water, intracellular water, fat mass, and visceral fat. Participants were instructed to stand barefoot on the electrode plate of the equipment, with their arms abducted at approximately 30 degrees in a standard posture. Intense exercise was prohibited before the assessment. Qualified personnel conducted all measurements following established procedures to ensure consistency and reliability.

2.4 Developing an aging clock model using machine learning approaches

This study employed a systematic approach to construct a nutrition-related aging clock model for predicting biological age. The dataset was randomly divided into a training set (70%) and a test set (30%) to evaluate the model's generalization ability. Five machine learning algorithms were selected for model construction: gradient boosting, LASSO, Light Gradient Boosting Machine (LightGBM), random forest, and XGBoost. All models were implemented using machine learning packages such as caret and XGBoost in R software (version 4.4.1).

To enhance the interpretability and predictive accuracy of the models, we performed feature selection to identify features that significantly contribute to predictions. Additionally, we optimized the models by adjusting parameters such as the number of trees, depth, and learning rate. Using cross- validation and grid search, we determined the optimal parameters to achieve the lowest root mean square error. The optimized models were then used to predict the training set, test set, and entire dataset using the predict function. Model performance was evaluated using the coefficient of determination (R^2) and mean absolute error (MAE), where R^2 measures explanatory power and MAE reflects predictive accuracy.

In this study, we defined the age difference (AgeDiff) as the difference between predicted age and actual age. The locally weighted scatterplot smoothing (LOESS) method was applied to regress AgeDiff against age, resulting in the corrected age difference (cAgeDiff): cAgeDiff = AgeDiff–LOESS (AgeDiff∼Age) (28, 29). This method quantifies the predictive bias of the model and categorizes the study subjects into subgroups with different aging rates based on the quartiles of cAgeDiff, providing a new perspective for understanding interindividual differences in aging. Study participants were categorized into subgroups with different aging rates based on the quartiles of cAgeDiff. Those with cAgeDiff values in the bottom quartile (< Q1) were classified as the "decelerated aging" group; those in the middle two quartiles (Q1 ≤ cAgeDiff ≤ Q3) as the "normal aging" group; and those in the top quartile (> Q3) as the "accelerated aging" group.

2.5 Statistical analysis

The statistical analysis for this study, including the establishment of the nutrition-related aging clock, was carried out as described in section "2.4 Developing an aging clock model using machine learning approaches." Data were processed using SPSS 23.0 (SPSS Inc., Chicago, IL, United States) and GraphPad Prism 8 (GraphPad Inc., San Diego, CA, United States). First, the normality of the data was assessed using the Shapiro-Wilk test. If the data did not meet normality, the Kruskal-Wallis H test and Dunn's *post hoc* comparison were employed. Homogeneity of variance was tested using Levene's test to satisfy the assumptions of ANOVA; if not met, Welch's ANOVA was used. After identifying significant differences between groups, multiple comparisons were conducted using the least significant difference or Tamhane's T2 method. Additionally, the correlation between variables was analyzed using Pearson and Spearman rank correlation coefficients. The level of statistical significance was set at $P < 0.05$.

3 Results

3.1 Characteristics of the studied cohort

This study included a healthy population across different age groups to construct a nutrition-related aging clock (**Table 1** and **Supplementary Table 1**). We stratified the participants into four age groups based on the median (range): the young group [31 years (26–33)], the young and middle-aged group [45 years (42–48)], the middle-aged group [59 years (56–63)], and the senior group [77.5 years (73–85)]. The sex ratio in each group was relatively equitable, with men constituting between 43.75% and 50.00%. No notable variations in body mass index (BMI) were found across the groups ($P = 0.551$). Differences in drinking and smoking behaviors among age groups were not statistically significant ($P = 0.588$ and $P = 0.555$). However, significant disparities in educational attainment and marital status were observed ($P < 0.01$ and $P < 0.001$), reflecting sociodemographic differences across age cohorts. Psychological stress was more common in the young and middle-aged cohorts ($P < 0.001$), although drinking habits showed no significant variation across the groups ($P = 0.206$). Vegetable eating habits and exercise habits showed a statistically significant difference across age groups ($P < 0.001$). Anthropometric measures and functional assessments revealed physiological changes associated with aging, including significant differences in grip strength ($P < 0.01$) and the light response test ($P < 0.001$). Participants also underwent BIA, which measured key parameters such as total body water, muscle mass, extracellular water, intracellular water, fat mass, and visceral fat, among 35 others (**Supplementary Table 2** and **Supplementary Figure 1**), which provided valuable information for assessing body composition and nutritional status.

TABLE 1 Characteristics of study participants.

Baseline characteristics	Young group	Young and middle-aged group	Middle-aged group	Senior group	*P*-value
Number of cases	28	30	26	16	NA
Age (year)	31 (26–33)	45 (42–48)	59 (56–63)	77.50 (73–85)	NA
Sex: male, *n* (%)	13 (46.43%)	15 (50.00%)	12 (46.15%)	7 (43.75%)	NA
Weight	65.85 (42.2–92.3)	70.20 (53.70–104.30)	66.10 (49.60–86.20)	57.85 (46.00–79.10)	0.064
Height	1.686 ± 0.067	1.687 ± 0.077	1.653 ± 0.067	1.595 ± 0.086	< 0.01
BMI (kg/m^2)	23.32 (16.08–30.49)	23.89 (19.49–32.09)	24.56 (19.81–30.20)	22.67 (17.53–27.58)	0.551
Highest education, *n* (%)					< 0.01
Primary or below	0 (0.00)	0 (0.00)	1 (4.00)	1 (6.25)	NA
Middle school or high school	0 (0.00)	0 (0.00)	5 (20.00)	5 (31.25)	NA
College degree or above	28 (100)	30 (100)	19 (76.00)	10 (62.50)	NA
Marital status, *n* (%)					< 0.001
Spinsterhood	10 (35.71)	1 (3.33)	1 (4.00)	0 (0.0)	NA
Married	18 (64.29)	29 (96.67)	24 (96.00)	16 (100.0)	NA
Psychological stress: yes, *n* (%)	19 (67.86)	21 (70.00)	8 (30.77)	2 (12.50)	< 0.001
Vegetable eating habits, *n* (%)					< 0.001
Occasionally	4 (14.29)	0 (0.0)	3 (11.54)	0 (0.0)	NA
Often	9 (32.14)	15 (50.00)	7 (26.92)	2 (12.50)	NA
Every day	15 (53.57)	15 (50.00)	16 (61.54)	14 (87.50)	NA
Physical exercise habits: yes, *n* (%)	10 (35.71)	18 (62.07)	23 (88.46)	14 (87.50)	< 0.001
Left hand grip strength	29.45 (18.70–57.30)	32.80 (20.70–58.90)	30.83 (21.70–47.60)	23.72 (12.30–39.10)	< 0.01
Right hand grip strength	33.90 (21.60–62.10)	36.45 (23.20–64.20)	30.60 (22.50–50.60)	22.05 (15.70–41.30)	< 0.01
Light reaction test (hand)	0.23 (0.19–0.37)	0.26 (0.20–0.49)	0.29 (0.20–0.82)	0.41 (0.21–1.02)	< 0.001
Light reaction test (foot)	0.30 (0.21–0.44)	0.29 (0.22–0.49)	0.32 (0.21–0.60)	0.47 (0.28–0.95)	< 0.001

Data are expressed as mean ± standard deviation for variables with normal distribution, as the median (minimum–maximum) for variables with non-normal distribution, and as *n* (%) for categorical variables. BMI, body mass index.

3.2 Differential analysis of plasma amino acids and vitamins in four age groups, as well as biomarkers in urine samples

In this study, we compared the levels of 9 amino acids and 13 vitamins in plasma across four age groups, as well as the levels of oxidative stress markers 8-oxoGuo and 8-oxo-dGuo in the urine, to explore the physiological differences among the groups (Figure 2).

A comparison of amino acid and vitamin markers that exhibit significant differences across age groups is illustrated (Figure 2A). We evaluated the influence of age on the concentrations of these biomarkers. The results indicated that the concentrations of vitamins A, B1, B5, E, and L-cystine progressively increased with age, with the elderly showing the highest concentrations, particularly of L-cystine and vitamin B5. This indicated significant differences between the younger and senior groups ($P < 0.001$). Conversely, the concentrations of 1-methyl-L-histidine, L-aspartic acid, MK4, and L-serine decreased with age, reaching their lowest values in the senior group. In addition, through Kyoto Encyclopedia of Genes and Genomes (KEGG) pathway enrichment analysis, we found several significantly enriched metabolic pathways, such as the pantothenate and CoA biosynthesis pathway, the vitamin B1 (thiamine) metabolism pathway, and the cysteine and methionine metabolism pathway (Supplementary Figure 2B). These results suggest that significant changes in nutrition-related biomarkers are closely associated with age-related physiological changes. The relevant metabolic processes may play a crucial role in the construction of nutrition-related aging clocks, further supporting the significance of energy metabolism and oxidative stress in the aging process. The Kruskal-Wallis test and Dunn's *post hoc* test results (Figure 2B) showed that the ratios of 8-oxoGuo/Cre and 8-oxodGuo/Cre in the young group were significantly lower than those in the middle-aged and elderly groups, especially the 8-oxoGuo/Cre ratio, which showed a markedly reduced level ($P < 0.001$). In addition, significant differences were observed between the middle-aged and elderly cohorts, indicating that oxidative stress marker concentrations increase significantly with age, underscoring their importance in the aging processes.

3.3 Constructing a nutritional aging clock based on machine learning models of blood amino acids and vitamins

In this study, we constructed and validated a nutrition-related aging clock model based on amino acids and vitamins detected

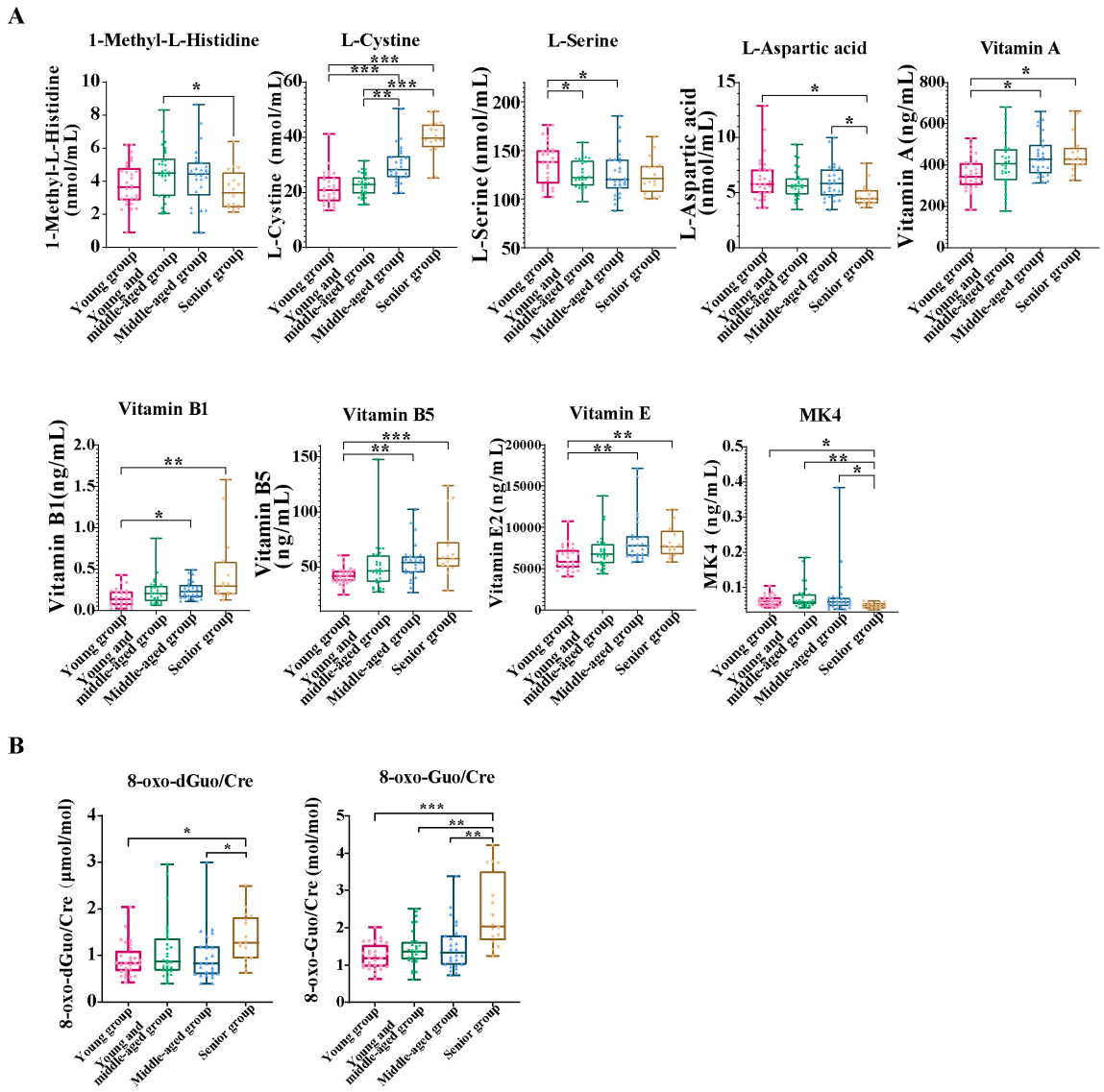

FIGURE 2
Analysis of biomarker differences in urine and blood samples across the four age groups. **(A)** This panel presents a comparative analysis of amino acid and vitamin biomarkers, with significant differences between age groups. **(B)** This box plot displays the change of urinary oxidative stress markers 8-oxodGuo/Cre and 8-oxoGuo/Cre ratios with age. Data are presented as median (interquartile range). For variables with normal distribution and homogeneity of variance, one-way analysis of variance (ANOVA) was performed, followed by Tukey's HSD test for *post hoc* comparisons. For variables that did not meet the assumptions of normality or homogeneity of variance, the Kruskal-Wallis test was used, followed by Dunn's test with Bonferroni correction for *post hoc* comparisons. A significance level of $P < 0.05$ was applied. All statistical analyses were conducted using SPSS version 23.0. Asterisks indicate statistical significance: ***$P < 0.001$, **$P < 0.01$, and *$P < 0.05$.

in plasma, using five machine learning algorithms: gradient boosting, LASSO, LightGBM, random forest, and XGBoost, to predict biological age and evaluate their predictive performance (Figure 3A). Each subplot depicts the predicted results of each individual algorithm, with blue dots representing the scatter distribution of projected ages vs. actual ages and the red line indicating the ideal prediction reference line. The LightGBM model demonstrated exceptional performance, with an R^2 of 0.8166 and MAE of 3.122 years, demonstrating high predictive accuracy and minimal error.

The LightGBM model proficiently predicts biological age, surpassing other models. Using the corrected age difference (cAgeDiff), we classified the study participants into three subgroups: accelerated aging, normal aging, and decelerated aging (Figure 3B), offering a novel perspective on understanding interindividual variations in aging and potentially facilitating the identification of relevant biomarkers. We then performed a feature significance analysis of the LightGBM model to identify the amino acids and vitamins that most significantly influence the prediction of biological age. The feature significance plot (Figure 3C) showed that L-cystine was the most significant feature, with a gain value of 0.46, emphasizing its crucial role in predicting biological age. The gain values for vitamin B1 and vitamin E were 0.12 and 0.09, respectively, while vitamins B3, MK4, and ethanolamine also had predictive value.

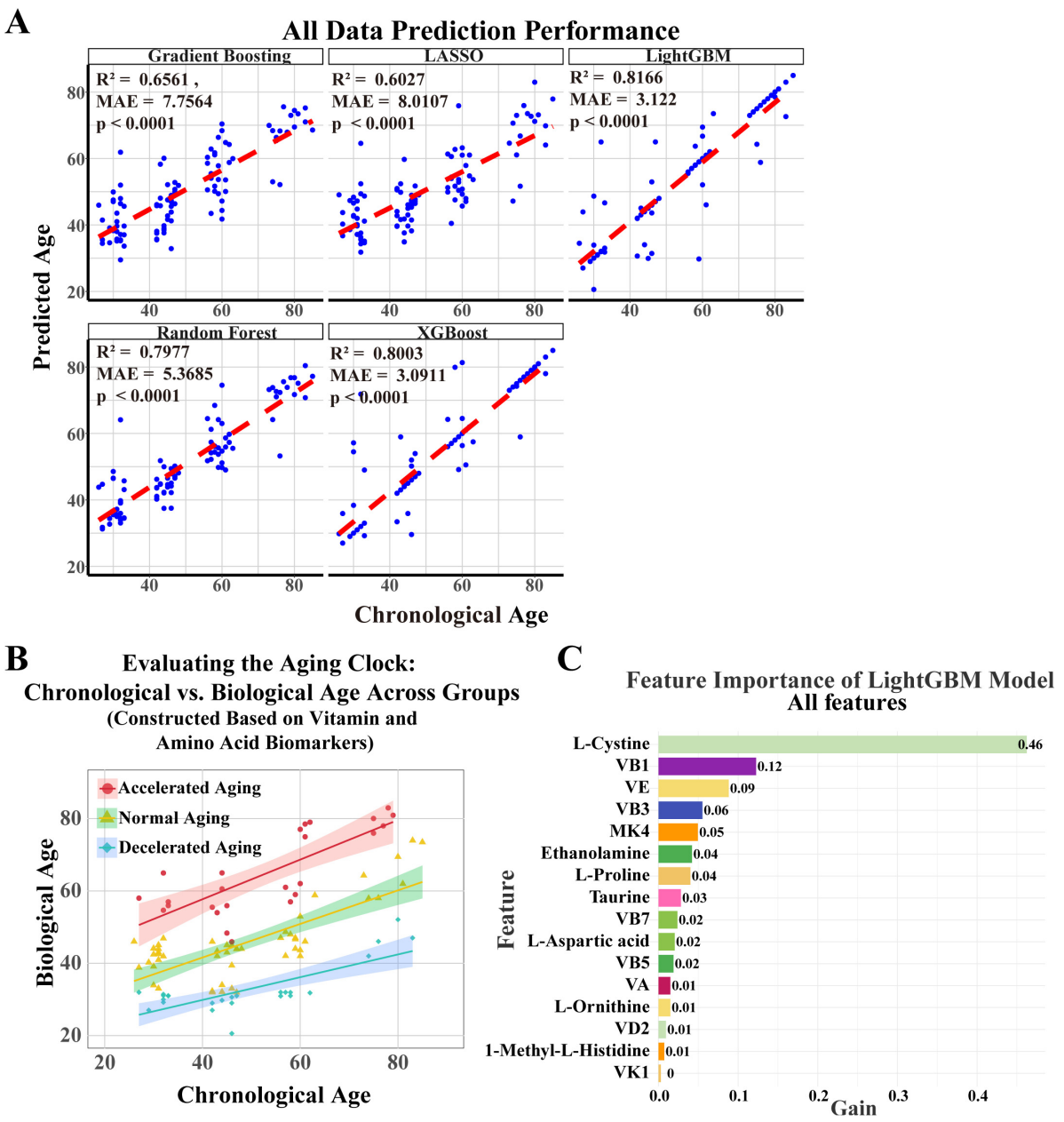

FIGURE 3
Establishment of an aging clock based on key vitamins and amino acids. **(A)** A nutritional aging clock model was developed using plasma amino acids and vitamins, along with five machine learning algorithms—gradient boosting, LASSO, LightGBM, random forest, and XGBoost—to forecast biological age and evaluate their predictive efficiency. Each subplot shows the algorithm's predicted results, with blue dots indicating the scatter distribution of projected ages against actual ages, and red lines representing the optimal prediction reference line. **(B)** Based on cAgeDiff, the study participants were divided into three subgroups: accelerated aging, normal aging, and decelerated aging. **(C)** The LightGBM model identified amino acids and vitamins that substantially affect biological age prediction through feature importance analysis.

3.4 Integration of blood amino acids and vitamins, body composition, and urinary oxidative stress biomarkers: Constructing a multidimensional nutrition-related aging clock

To improve the predictive accuracy of the model and gain a deeper understanding of the aging process, we comprehensively integrated plasma amino acids and vitamins, body composition (measured by BIA), and urinary oxidative stress markers (Figure 4). The predictive performance of each model is shown (Figures 4A, B). The LightGBM model performed the best, with an R^2 of 0.8807 and an MAE of 2.5877. The random forest model also performed well, with an R^2 of 0.8725 and an MAE of 4.3555. The gradient boosting model exhibited average predictive capability, with an R^2 of 0.7881 and an MAE of 5.4129. The XGBoost model demonstrated significantly lower prediction error than Gradient Boosting (MAE reduced from 5.4129 to 3.0842 years), with a comparable R^2 of 0.794. Although the LASSO model (Figure 4B)

demonstrated high accuracy (R^2 = 0.9360, MAE = 3.14 years), its feature sparsity may impact generalizability to diverse populations. Consequently, we determined that LightGBM is the most appropriate method for developing the nutritional aging clock.

A demographic categorization based on the comprehensive nutrition-related aging clock, revealing varying rates of aging, is presented (**Figure 4C**). This classification emphasizes the need to use multiple indicators in aging research and illustrates the diversity of aging among individuals. We then performed a thorough analysis of the importance of each characteristic in the LightGBM model to identify the parameters that most substantially affect the prediction of biological age. The gain values of various features are shown, with the basal metabolic rate at the top having a gain value of 0.52, indicating that it is the most important predictor in the model (**Figure 4D**). Next were vitamin B5, 8-oxoGuo/Cre, and L-cystine (with gain values of 0.13, 0.11, and 0.05, respectively), which also make significant contributions to the model's predictive ability. Moreover, features such as vitamin E and extracellular fluid showed certain predictive value, with a gain value of 0.04 each. In light of the substantial contributions of vitamin B5 and L-cystine to the model, yet their unclear biological underpinnings, we performed a systematic functional annotation and pathway-enrichment analysis using the CTD and Metascape databases (see **Supplementary Datasheets 1, 2**, **Supplementary Figures 4A–E** and **Supplementary Table 3** for full results). These results highlight key biomarkers strongly associated with aging phenotypes, whose predictive importance may reflect underlying biological pathways relevant to age-related decline.

Furthermore, we compared the differences in the model's important predictive factors—BMR, vitamin B5, 8-oxoGuo/Cre, and L-cystine—among populations with different aging rates (**Figure 4E**). We found that the BMR in the accelerated aging group was significantly lower than that in the normal and decelerated aging groups ($P < 0.01$). The levels of L-cystine and 8-oxoGuo/Cre were significantly higher in the accelerated aging group than in the normal aging group ($P < 0.001$) and the decelerated aging group ($P < 0.01$). Additionally, the level of vitamin B5 in the accelerated aging group was also higher than that in the decelerated aging group ($P < 0.05$).

3.5 Comparative analysis of biochemical indicators in populations with different aging rates

We performed a comparison of important biochemical markers across the three subgroups—accelerated aging, normal aging, and decelerated aging—based on the findings of the nutrition-related aging clock (**Figure 5**). The levels of free fatty acids (FFA) were significantly higher in the accelerated aging group than in the normal aging group ($P < 0.001$). Similarly, the levels of cystatin C (CysC) were much higher in the accelerated aging group than in the decelerated aging group ($P < 0.001$; **Figure 5A**). High-density lipoprotein cholesterol (HDL-C) levels were significantly elevated in the accelerated aging group compared with those in the normal aging group ($P < 0.05$). Furthermore, the levels of insulin-like growth factor (IGF) were much lower in the accelerated aging group than in the normal and decelerated aging groups ($P < 0.01$; **Figure 5A**).

The correlation strength between ΔAge (cAgeDiff) and various biochemical markers is depicted (**Figure 5B**). The correlation study used the Spearman correlation coefficient to evaluate the relationship between ΔAge and each biochemical parameter. Research on the vitamin and amino acid aging clock revealed a notable association between FFA and ΔAge (r = 0.39, $P < 0.01$), suggesting that FFA serves as a valuable biomarker for determining an individual's age. Further analysis of the aging clock found that low-density lipoprotein (LDL-C), glycated hemoglobin (HbA1c), and insulin (INS) all had strong relationships with ΔAge (r values of −0.34, −0.36, and −0.37, respectively; $P < 0.05$). LDL-C, HbA1c, and INS may therefore serve as valuable biomarkers for evaluating the aging process. Our findings reveal that FFA, LDL-C, HbA1c, and INS are biochemical markers most closely associated with ΔAge, suggesting their substantial involvement in the aging process.

To further explore the relationship between the comprehensive nutrition-related aging clock and the body's biochemical indicators, a correlation analysis was performed. The results show the correlation patterns (**Figure 5C** and **Supplementary Figure 5C**). The nutrition-related aging clock characteristics, including weight, lower limb muscle mass, extracellular fluid, muscle mass, standard weight, and BMR, exhibited significant positive correlations with biochemical markers such as prealbumin (PALB), IGF, serum creatinine (SCr), white blood cells (WBC), total bilirubin (TBIL), and serum uric acid (SUA), as indicated by the clustering analysis results. Conversely, substantial negative associations were noted between many indicators of the nutrition-related aging clock and markers such as IGF, HDL-C, WBC, total cholesterol (TC), FFA, and serum folate. These results underscore the significance of biochemical markers such as HDL-C, PALB, IGF, and SCr in evaluating an individual's nutritional status. The aging clock features did not exhibit significant correlations with other indicators, including cholinesterase (CHE) and TC. Overall, these findings highlight the complex interplay between the comprehensive nutrition-related aging clock and the body's biochemical profile.

3.6 Comparative analysis of physical examination indicators among populations with different aging rates

Physical examinations, which are crucial for assessing personal health as well as reflecting the aging process, have been included in our study. These measures objectively assess mobility decline, musculoskeletal integrity, and nutritional status, providing critical physiological context to complement molecular biomarker data.

The results of the daily 6 m walk test showed that the number of steps taken by individuals in the accelerated aging group was significantly higher than that taken by those in the normal ($P < 0.05$) and decelerated ($P < 0.01$) aging groups (**Figure 6A**). The results of the fastest 6 m walking test were similar, with the accelerated aging group showing significantly more steps than the normal and decelerated aging groups ($P < 0.05$ and $P < 0.01$), which indicates that walking ability declines with increasing aging

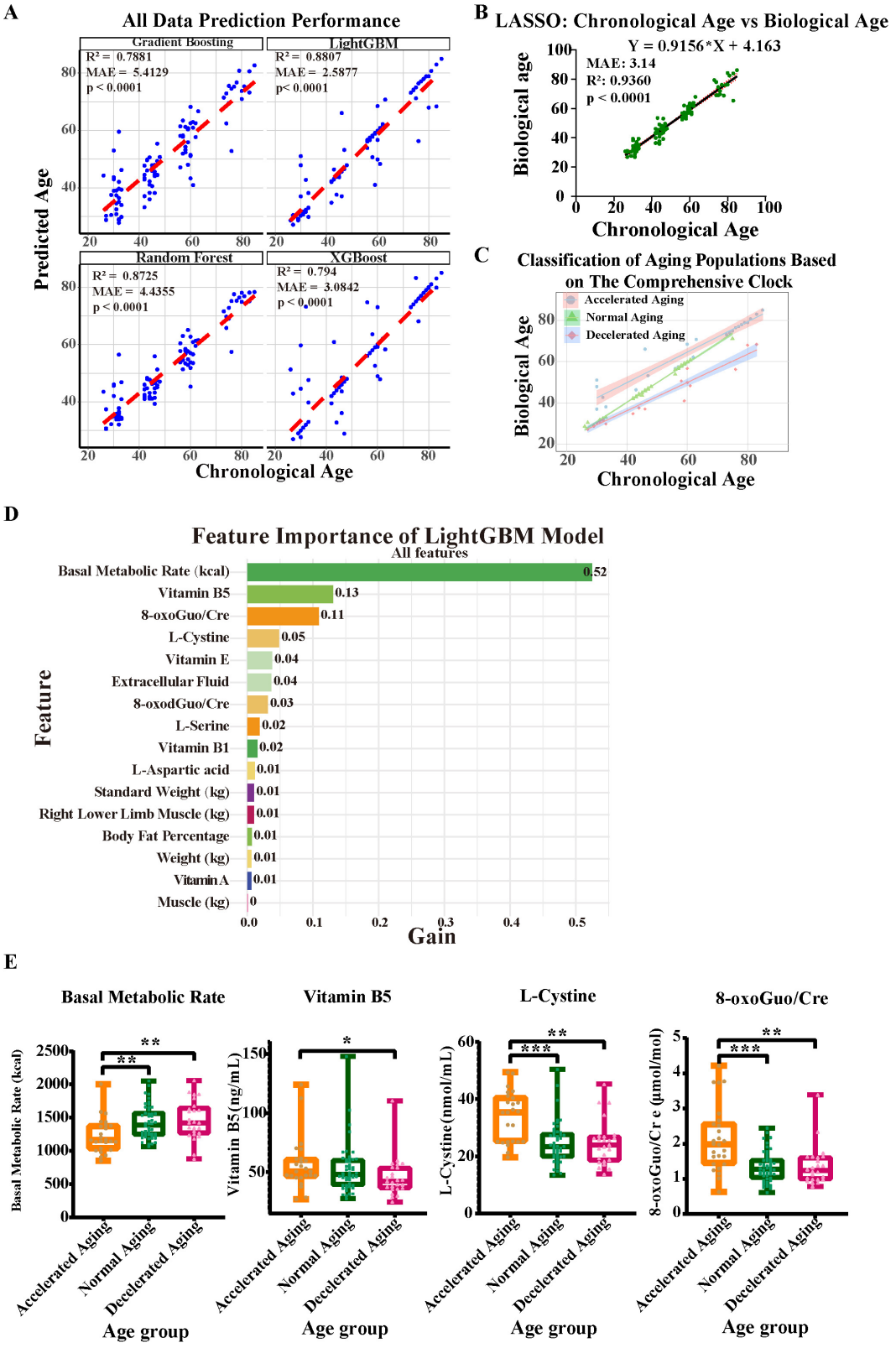

FIGURE 4
Construction of a comprehensive aging clock based on blood and urine biomarkers and bioelectrical impedance analysis results. **(A,B)** Considering body composition (assessed via BIA), plasma amino acids and vitamins, and urine oxidative stress indicators, five machine learning techniques were employed to develop an aging clock, with the prediction efficacy of each model shown. **(C)** The comprehensive nutritional aging clocks classify populations with different aging rates. **(D)** LightGBM feature-importance ranking (gain) for biological-age prediction. Basal metabolic rate, vitamin B5, 8-oxoGuo/Cre and L-cystine are the top contributors. **(E)** Comparative analysis of key feature factors across different aging groups. Asterisks indicate statistical significance: ***$P < 0.001$, **$P < 0.01$, and *$P < 0.05$.

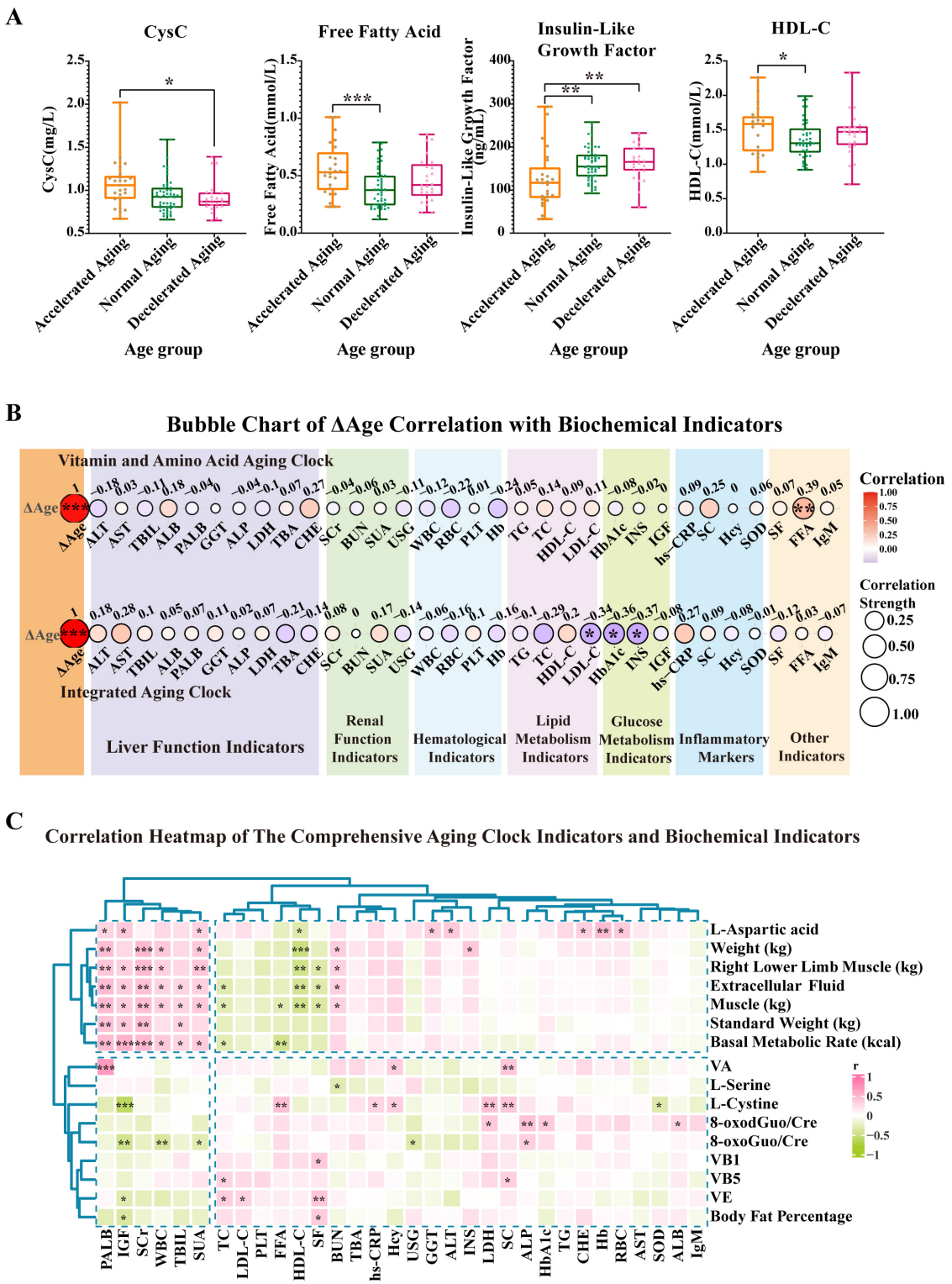

FIGURE 5
Prediction results of two aging clocks developed from the study population and differential analysis of populations stratified by cAgeDiff (ΔAge). Based on the results from the aging clock grouping, we conducted a comparative analysis of key biochemical indicators in the accelerated, normal, and decelerated aging subgroups. **(A)** This panel presents CysC, FFA, and HDL-C in the accelerated, normal, and decelerated aging groups, respectively. **(B)** This panel illustrates the strength of the association between ΔAge (cAgeDiff) and several biochemical markers. The correlation analysis uses the Spearman correlation coefficient to evaluate the relationship between ΔAge and each biochemical parameter. The two ΔAge values are derived from the vitamin and amino acid aging clock as well as the comprehensive aging clock. **(C)** The heatmap shows how biochemical indicators relate to the full nutritional aging clock markers. The vertical axis represents full nutritional aging clock markers, while the horizontal axis represents biochemical indicators. A color gradient indicates the strength of the correlation coefficient, with green representing a negative correlation and red representing a positive correlation. Asterisks indicate statistical significance: ***$P < 0.001$, **$P < 0.01$, and *$P < 0.05$.

rate (Figure 6B). The grip strength of the accelerated aging group was significantly lower than that of the normal and decelerated aging groups ($P < 0.01$ and $P < 0.05$), indicating a possible correlation with the deterioration of muscle mass and function, as illustrated in Figures 6C. The results of hand and foot reaction time tests showed that the reaction times of the accelerated aging group were significantly longer than those of the other two groups ($P < 0.01$ and $P < 0.05$; Figure 6D), possibly reflecting a decline in nervous system function with increasing aging rate. The height of the accelerated aging group was significantly lower than that of the other two groups ($P < 0.01$), possibly associated with spinal compression or other age-related physical changes (Figure 6E). The physiological subhealth score (PS) (ranging 0–100, higher values indicating better health status) results indicated that the PS score of the accelerated aging group was significantly lower than that of the decelerated aging group ($P < 0.05$; Figure 6F), suggesting a significant association between physiological subhealth status and aging rate. The ratio of 8-oxodGuo/Cre was significantly higher in the accelerated aging group than in the other two groups, indicating that oxidative stress levels increase with the aging rate (Figure 6G).

4 Discussion

This study reveals the trends in amino acid and vitamin levels, as well as oxidative stress markers, with age through a comprehensive analysis of plasma and urine samples from participants of different age groups. The results show that the levels of vitamins A, B1, B5, E, and L-cystine significantly increase with age; particularly, differences in L-cystine and vitamin B5 levels between the young and elderly groups are most pronounced, possibly reflecting a decline in metabolic and synthetic functions in the elderly, leading to the accumulation of these molecules in the body. In contrast, the levels of 1-methyl-L-histidine, L-aspartic acid, MK4, and L-serine decrease with age, reflecting a reduction in the activity of specific metabolic pathways (30, 31). These changes in biochemical indicators are closely related to the decline in physiological functions in the elderly population, such as reduced muscle mass and decreased immune function. In urine, 8-oxoGuo/Cre and 8-oxodGuo/Cre levels were significantly lower in the young group than in the middle-aged and senior groups, with significant differences also observed between the middle-aged and senior groups. This indicates that oxidative stress levels significantly increase with age, supporting the viewpoint that oxidative stress plays a key role in the process of aging and its related diseases (18, 19, 32).

In this study, the LightGBM model was the most accurate of the nutrition-related aging clock models created with different machine learning algorithms. Analysis of feature importance revealed that L-cystine, vitamin B1, and vitamin E are significant determinants in the prediction of biological age. These findings highlight the utility of integrating L-cystine, vitamins B1/B5/E, and oxidative stress markers as a novel multimodal panel for aging prediction, advancing our understanding of nutrient-metabolic interplay in aging. By adding BIA, plasma amino acids, vitamins, and urinary oxidative stress markers, the LightGBM model significantly improved its predictive capability ($R^2 = 0.8807$, MAE = 2.5877). In this study, BMR, vitamin B5 levels, 8-oxo-Guo/Cre ratio, and L-cystine were identified as key indicators of nutrition-related aging, highlighting the importance of energy metabolism and oxidative stress in aging (21, 33). These indicators may play complex roles in the aging process, with elevated levels potentially serving as biomarkers for the risk of age-related diseases. Changes in their levels not only serve as biomarkers for physiological aging but also associate with adverse health outcomes through pathways requiring further mechanistic investigation. Future research should further explore the specific roles of these biomarkers in the mechanisms of aging and their potential application value in the prevention and treatment of age-related diseases.

Our findings indicate that BMR was significantly lower in the accelerated aging group compared to the normal and decelerated aging groups, suggesting that the rate of decline in BMR may be related to an individual's aging speed and could serve as a marker to distinguish between different aging rate groups. Furthermore, a research study of senior male populations in southern China showed that an increase in BMR is independently associated with a reduction in all-cause mortality, while BMR decreases non-linearly with age, exhibiting an accelerated decline in older groups (34). BMR decreases with age and is closely related to the aging process. Kitazoe et al. found that mass-specific BMR (msBMR) and renormalized BMR (RmsBMR) can serve as new biomarkers for assessing aging, reflecting metabolic changes during the aging process (35). In summary, these results highlight the importance of basal metabolic rate (BMR) in the aging process. Changes in BMR not only reflect an individual's aging speed but may also provide clues for identifying different aging types. This finding offers new directions for understanding aging mechanisms and improving health management for the elderly.

Furthermore, our study found that vitamin B5 levels were higher in the accelerated aging group than in the decelerated aging group. Vitamin B5, also known as pantothenic acid, is an essential component for the synthesis of coenzyme A (CoA) and acyl carrier protein. CoA is not only a necessary cofactor for the synthesis of key biomolecules such as fatty acids, cholesterol, acetylcholine, and bile acids but also plays a central role in many metabolic pathways (36, 37). Since humans and animals cannot synthesize pantothenic acid, they must depend on food sources to meet their vitamin requirements. This external reliance emphasizes the importance of pantothenic acid in sustaining health and avoiding associated nutritional deficits (38). Additional studies have revealed that plasma vitamin B5 levels are associated with an increased risk of all-cause mortality, especially among hypertensive patients in China, with this connection being more prominent in the elderly and those with adequate folate levels (39). Regarding whether excessive intake of vitamin B5 can accelerate aging, current research findings are inconsistent. On the one hand, pantothenic acid, as a precursor to coenzyme A, is essential for cellular energy metabolism and antioxidant defense. In theory, having an appropriate quantity of pantothenic acid may help slow the aging process. On the other hand, excessive pantothenic acid consumption may disturb metabolic equilibrium inside cells, resulting in increased oxidative stress and potentially accelerating cellular aging. When examining the link between pantothenic acid consumption and aging, it is vital to compare the potential advantages in terms of health promotion and illness prevention with the potential adverse effects. Future studies should investigate the association between pantothenic acid consumption, metabolic state, and aging, as well as identify

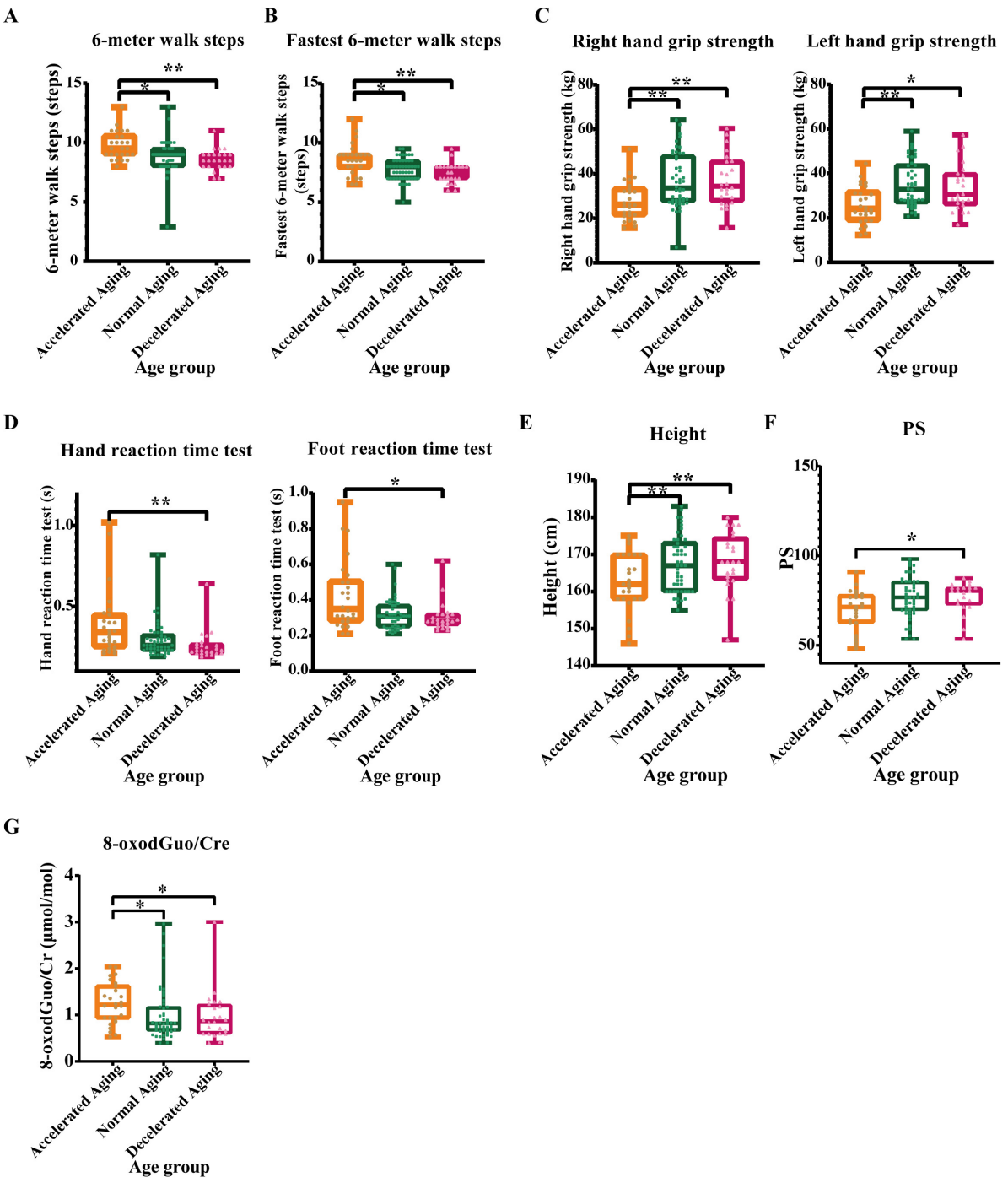

FIGURE 6
Comparative analysis of physical examination indicators in populations with different aging rates. **(A)** 6-meter walk steps, **(B)** Fastest 6-meter walk steps, **(C)** Grip strength, **(D)** Hand-foot reaction time, **(E)** Height, **(F)** Physiological subhealth score (PS), and **(G)** 8-oxodGuo/Cre (Oxidative stress marker). Physical exams, as a primary method for evaluating individual health status, may reveal physiological changes associated with aging. This study analyzed these physical examination metrics across rapid, normal, and slow aging subgroups. The accelerated aging group performed poorly on multiple physical examination indicators. Asterisks indicate statistical significance: $^{**}P < 0.01$ and $^{*}P < 0.05$.

strategies to maximize pantothenic acid intake through dietary or supplemental approaches to promote healthy aging.

We also found that the levels of L-cystine were significantly higher in the accelerated aging group than in the normal aging group. L-cystine is a specific amino acid formed by the linkage of two cysteine molecules through a disulfide bond. Lawrence C. Johnson and colleagues investigated the relationship between L-cystine and healthspan indicators related to aging using plasma metabolomics analysis, and discovered that the concentration of L-cystine in the elderly group was significantly higher than that in the young group, which is consistent with the findings of this study (40). Bramer et al. found that in the plasma of

patients with mild and severe COVID-19 infections, the levels of L-cystine were significantly elevated (41). Wang et al. by measuring the plasma levels of L-cystine in patients with Attention Deficit Hyperactivity Disorder (ADHD) and healthy control groups, found that the plasma levels of L-cystine in the ADHD group were significantly higher compared to the healthy control group (42). These studies collectively suggest that L-cystine may be related to the severity of the disease, and the increase in L-cystine may reflect the body's metabolic adaptation in response to oxidative stress and inflammatory responses. In accelerated aging individuals, the increase in L-cystine may be related to the decline in cellular antioxidant capacity and chronic inflammatory states, both of which are closely associated with the increased risk of age-related diseases. Future research should further explore the specific mechanisms of action of L-cystine under different physiological and pathological conditions, as well as its potential applications in aging and disease management.

We found that the ratio of the oxidative stress marker 8-oxoGuo/Cre was abnormally increased in the accelerated aging group. 8-oxo-Guo, indicative of RNA oxidative damage, correlates with elevated oxidative stress levels in several age-related disorders and serves as a crucial biomarker for evaluating oxidative stress status and disease risk (21). Moreover, our findings are consistent with Vatner et al.'s view that oxidative stress is a important mechanism limiting longevity and healthy aging (43).

Additionally, our study demonstrated a markedly increased amount of CysC in the accelerated aging group compared with that in the normal aging group, suggesting that CysC serves as a biomarker for declining renal function associated with accelerated aging. Recent investigations have demonstrated that heightened levels of CysC in individuals with metabolic syndrome correlate with a greater risk of all-cause mortality, including cardiovascular and cancer-related fatalities (44). This highlights the importance of CysC in assessing age-related physiological changes. The accelerated aging group showed markedly increased levels of FFA compared with both the normal and decelerated aging groups. This rise may indicate a disturbance in lipid metabolism, often seen in the elderly, with possible ramifications for the pathophysiology of age-related illnesses, such as type 2 diabetes and cardiovascular disorders (45). The concentration of IGF was much lower in the accelerated aging group than in the normal aging group, which may signify a disruption in growth signaling pathways crucial for maintaining tissue homeostasis and regeneration in older individuals (46, 47). Furthermore, HDL-C levels were markedly elevated in the accelerated aging group compared with those in the normal aging group, suggesting a correlation between HDL-C and accelerated aging. This discovery contradicts previous research, which indicated that elevated levels of HDL-C correlate with lifespan (48). Nevertheless, several studies have revealed that the inverse relationship between HDL-C and ASCVD stabilizes when HDL-C levels approach 40 mg/dL, and excessively elevated HDL-C levels may correlate with heightened risk, demonstrating a U-shaped curve (49, 50). Another study pointed out that higher levels of HDL-C are associated with an increased risk of fractures in healthy elderly individuals (51). Additionally, the SWAN HDL study found that women with midlife HDL-C > 80 mg/dL had 2.3-fold higher risk of cognitive decline over 20 years (52). Our data extend these findings to accelerated aging, where dysfunctional HDL likely promotes multisystem decline (e.g., bone loss, neuroinflammation). Future work should prioritize HDL functional assays over concentration alone.

Ultimately, by analyzing the physical examination metrics of various aging rate subgroups, we elucidated the relationship between aging rate and alterations in physiological function. The findings of the 6-m walking test demonstrated that walking ability diminishes with an increase in the rate of aging. The grip strength test findings indicated that the accelerated aging group had considerably reduced grip strength compared with both the normal and decelerated aging groups, indicating a reduction in muscle mass and function (53). Height measurements indicated that the accelerated aging group had a markedly reduced height compared with the other two groups, may reflect age-related physiological alterations such as spinal compression, rarefaction of bone (54, 55). The results of the response time test further confirmed that brain function declines with advancing age. PS scores were significantly increased in the accelerated aging cohort, and the ratio of oxidative stress markers 8-oxodGuo/Cre to 8-oxoGuo/Cre was disproportionately increased, indicating a decline in the individual's physiological subhealth status and elevated oxidative stress levels during the aging process (43, 56). The accelerated aging group had worse performance in many physical examination parameters, possibly associated with increased oxidative stress and reduced physiological function.

Physical examination indicators and biochemical markers are important tools for determining individual aging rates, and their patterns may suggest prospective targets for anti-aging therapies. Specific exercise programs may be created to enhance muscle strength and improve physical function in response to decreasing grip strength and walking ability; in response to increased oxidative stress, antioxidant treatment may be explored to slow the aging process (57, 58). Future research should delve deeper into the associations between these biomarkers and aging rates, evaluating corresponding intervention measures with the aim of developing more effective prevention and treatment strategies.

This study has limitations including its modest sample size (n = 100), limited elderly subgroup (n = 16), and restricted generalizability to chronic disease populations due to strict health screening. Findings are expressly applicable to demographically similar, strictly defined healthy populations and cannot be directly extrapolated to individuals with chronic diseases. while our feature selection approach identified biomarkers highly predictive of biological age, the cross-sectional design precludes causal inference. Despite this, our findings provide valuable baseline data on nutrition-related aging biomarkers in healthy adults. Future research should first validate these findings in larger cohorts with adequate elderly representation and chronic disease populations, before advancing to: mechanistic exploration of these biomarkers, personalized interventions, aging risk modeling, and novel anti-aging therapies. And longitudinal studies should validate whether these biomarkers modulate aging trajectories or primarily reflect age-related physiological changes. This progression will enable targeted strategies to improve healthy aging outcomes.

Data availability statement

The raw data supporting the conclusions of this article will be made available by the authors, without undue reservation.

Ethics statement

The studies involving humans were approved by the Ethics Committee of Beijing Hospital. The studies were conducted in accordance with the local legislation and institutional requirements. The participants provided their written informed consent to participate in this study.

Author contributions

Y-QM: Data curation, Formal analysis, Investigation, Methodology, Software, Validation, Visualization, Writing – original draft, Writing – review & editing. Y-MD: Investigation, Writing – review & editing. L-TZ: Investigation, Writing – review & editing. XG: Investigation, Writing – review & editing. S-JL: Investigation, Writing – review & editing. L-QZ: Investigation, Writing – review & editing. JL: Investigation, Writing – review & editing. X-YZ: Investigation, Writing – review & editing. S-SR: Writing – review & editing. H-LL: Formal analysis, Methodology, Writing – review & editing. R-MQ: Writing – review & editing. JP: Investigation, Writing – review & editing. JC: Investigation, Writing – review & editing. T-MZ: Writing – review & editing. J-PC: Conceptualization, Funding acquisition, Project administration, Resources, Supervision, Writing – review & editing.

Funding

The author(s) declare that financial support was received for the research and/or publication of this article. This research was supported by the National Key R&D Program of China (2024YFA1109102), National High Level Hospital Clinical Research Funding (BJ-2024-138), CAMS Innovation Fund for Medical Sciences (No. 2021-1-I2M-050), and National Natural Science Foundation of China (No. 82170856).

Acknowledgments

We express our sincere gratitude to Jian-Ping Cai for his invaluable guidance and meticulous proofreading of this manuscript. Additionally, we are deeply appreciative of the support and insightful advice provided by the esteemed members of the Institute of Geriatrics, Ministry of Health.

Conflict of interest

The authors declare that the research was conducted in the absence of any commercial or financial relationships that could be construed as a potential conflict of interest.

Generative AI statement

The authors declare that no Generative AI was used in the creation of this manuscript.

Any alternative text (alt text) provided alongside figures in this article has been generated by Frontiers with the support of artificial intelligence and reasonable efforts have been made to ensure accuracy, including review by the authors wherever possible. If you identify any issues, please contact us.

Publisher's note

Supplementary material

The Supplementary Material for this article can be found online at: https://www.frontiersin.org/articles/10.3389/fnut.2025.1563220/full#supplementary-material

References

1. Moqri M, Herzog C, Poganik J, Justice J, Belsky D, et al. Biomarkers of aging for the identification and evaluation of longevity interventions. *Cell.* (2023) 186:3758–75. doi: 10.1016/j.cell.2023.08.003

2. Duan R, Fu Q, Sun Y, Li Q. Epigenetic clock: a promising biomarker and practical tool in aging. *Ageing Res Rev.* (2022) 81:101743. doi: 10.1016/j.arr.2022.101743

3. Rentscher K, Klopack E, Crimmins E, Seeman T, Cole S, Carroll J. Social relationships and epigenetic aging in older adulthood: results from the health and retirement study. *Brain Behav Immun.* (2023) 114:349–59. doi: 10.1016/j.bbi.2023.09.001

4. Lehallier B, Shokhirev MN, Wyss-Coray T, Johnson AA. Data mining of human plasma proteins generates a multitude of highly predictive aging clocks that reflect different aspects of aging. *Aging Cell.* (2020) 19:e13256. doi: 10.1111/acel.13256

5. Shlisky J, Bloom D, Beaudreault A, Tucker K, Keller H, Freund-Levi Y, et al. Nutritional considerations for healthy aging and reduction in age-related chronic disease. *Adv Nutr.* (2017) 8:17–26. doi: 10.3945/an.116.013474

6. Tardy A, Pouteau E, Marquez D, Yilmaz C, Scholey A. Vitamins and minerals for energy, fatigue and cognition: a narrative review of the biochemical and clinical evidence. *Nutrients.* (2020) 12:228. doi: 10.3390/nu12010228

7. Field LB, Hand RK. Differentiating malnutrition screening and assessment: a nutrition care process perspective. *J Acad Nutr Dietetics.* (2015) 115:824–8. doi: 10.1016/j.jand.2014.11.010

8. Lin C-S, Liu L-K, Chen L-K, Fuh J-L. Association between masseter muscle volume, nutritional status, and cognitive status in older people. *Arch Gerontol Geriatr.* (2023) 113:105038. doi: 10.1016/j.archger.2023.105038

9. Freitas-Costa N, Andrade P, Normando P, Nunes K, Raymundo C, Castro I, et al. Association of development quotient with nutritional status of vitamins B6, B12, and folate in 6-59-month-old children: results from the Brazilian national survey on child nutrition (ENANI-2019). *Am J Clin Nutr.* (2023) 118:162–73. doi: 10.1016/j.ajcnut.2023.04.026

10. Michel J-P, Sadana R. "Healthy aging" concepts and measures. *J Am Med Dir Assoc.* (2017) 18:460–4. doi: 10.1016/j.jamda.2017.03.008

11. Roberts SB, Silver RE, Das SK, Fielding RA, Gilhooly CH, Jacques PF, et al. Healthy aging—nutrition matters: start early and screen often. *Adv Nutr.* (2021) 12:1438–48. doi: 10.1093/advances/nmab032

12. Melzer T, Manosso L, Yau S, Gil-Mohapel J, Brocardo P. In pursuit of healthy aging: effects of nutrition on brain function. *Int J Mol Sci.* (2021) 22:5026. doi: 10.3390/ijms22095026

13. Tappia PS, Shah AK, Dhalla NS. The efficacy of vitamins in the prevention and treatment of cardiovascular disease. *Int J Mol Sci.* (2024) 25:9761. doi: 10.3390/ijms25189761

14. Catapano A, Trinchese G, Cimmino F, Petrella L, D'Angelo M, Di Maio G, et al. Impedance analysis to evaluate nutritional status in physiological and pathological conditions. *Nutrients.* (2023) 15:2264. doi: 10.3390/nu15102264

15. Lee M, Jebb S, Oke J, Piernas C. Reference values for skeletal muscle mass and fat mass measured by bioelectrical impedance in 390 565 UK adults. *J Cachexia Sarcopenia Muscle.* (2020) 11:487–96. doi: 10.1002/jcsm.12523

16. Sohal RS, Weindruch R. Oxidative stress, caloric restriction, and aging. *Science.* (1996) 273:59–63. doi: 10.1126/science.273.5271.59

17. Ionescu-Tucker A, Cotman CW. Emerging roles of oxidative stress in brain aging and Alzheimer's disease. *Neurobiol Aging.* (2021) 107:86–95. doi: 10.1016/j.neurobiolaging.2021.07.014

18. Broedbaek K, Køster-Rasmussen R, Siersma V, Persson F, Poulsen H, de Fine Olivarius N. Urinary albumin and 8-oxo-7,8-dihydroguanosine as markers of mortality and cardiovascular disease during 19 years after diagnosis of type 2 diabetes - A comparative study of two markers to identify high risk patients. *Redox Biol.* (2017) 13:363–9. doi: 10.1016/j.redox.2017.06.005

19. Nie B, Gan W, Shi F, Hu G-X, Chen L-G, Hayakawa H, et al. Age-dependent accumulation of 8-oxoguanine in the DNA and RNA in various rat tissues. *Oxidative Med Cell Longev.* (2013) 2013:303181. doi: 10.1155/2013/303181

20. Chao M, Evans M, Hu C, Ji Y, Møller P, Rossner P, et al. Biomarkers of nucleic acid oxidation - A summary state-of-the-art. *Redox Biol.* (2021) 42:101872. doi: 10.1016/j.redox.2021.101872

21. Li L, Zhang X. The significance of 8-oxoGsn in aging-related diseases. *Aging Dis.* (2020) 11:1329–38. doi: 10.14336/AD.2019.1021

22. Gan W, Liu X-L, Yu T, Zou Y-G, Li T-T, Wang S, et al. Urinary 8-oxo-7,8-dihydroguanosine as a potential biomarker of aging. *Front Aging Neurosci.* (2018) 10:34. doi: 10.3389/fnagi.2018.00034

23. Maciejczyk M, Nesterowicz M, Szulimowska J, Zalewska A. Oxidation, glycation, and carbamylation of salivary biomolecules in healthy children, adults, and the elderly: can saliva be used in the assessment of aging? *J Inflamm Res.* (2022) 15:2051–73. doi: 10.2147/JIR.S356029

24. Canfield C-A, Bradshaw PC. Amino acids in the regulation of aging and aging-related diseases. *Transl Med Aging.* (2019) 3:70–89. doi: 10.1016/j.tma.2019.09.001

25. Ciancarelli I, Morone G, Iosa M, Cerasa A, Calabrò R, Iolascon G, et al. Influence of oxidative stress and inflammation on nutritional status and neural plasticity: new perspectives on post-stroke neurorehabilitative outcome. *Nutrients.* (2022) 15:108. doi: 10.3390/nu15010108

26. Cui J, Pang J, Zhang L, Li J, Wu X, Zhu X, et al. PENG ZU study on healthy aging in China (PENG ZU Cohort): design and goals. *China CDC Weekly.* (2024) 6:876–82. doi: 10.46234/ccdcw2024.187

27. Shih Y-M, Cooke MS, Pan C-H, Chao M-R, Hu C-W. Clinical relevance of guanine-derived urinary biomarkers of oxidative stress, determined by LC-MS/MS. *Redox Biol.* (2019) 20:556–65. doi: 10.1016/j.redox.2018.11.016

28. Xia X, Wang Y, Yu Z, Chen J, Han J-DJ. Assessing the rate of aging to monitor aging itself. *Ageing Res Rev.* (2021) 69:101350. doi: 10.1016/j.arr.2021.101350

29. Xia X, Chen X, Wu G, Li F, Wang Y, Chen Y, et al. Three-dimensional facial-image analysis to predict heterogeneity of the human ageing rate and the impact of lifestyle. *Nat Metab.* (2020) 2:946–57. doi: 10.1038/s42255-020-00270-x

30. Ducker GS, Rabinowitz JD. One-carbon metabolism in health and disease. *Cell Metab.* (2017) 25:27–42. doi: 10.1016/j.cmet.2016.08.009

31. Patel D, Lee T, Kumar S, Vyavahare S, Worth A, Hill W, et al. Alterations in bone metabolites with age in C57BL/6 mice model. *Biogerontology.* (2022) 23:629–40. doi: 10.1007/s10522-022-09986-7

32. Yu T, Slone J, Liu W, Barnes R, Opresko P, Wark L, et al. Premature aging is associated with higher levels of 8-oxoguanine and increased DNA damage in the Polg mutator mouse. *Aging Cell.* (2022) 21:e13669. doi: 10.1111/acel.13669

33. Bou Ghanem A, Hussayni Y, Kadbey R, Ratel Y, Yehya S, Khouzami L, et al. Exploring the complexities of 1C metabolism: implications in aging and neurodegenerative diseases. *Front Aging Neurosci.* (2024) 15:1322419. doi: 10.3389/fnagi.2023.1322419

34. Han F, Hu F, Wang T, Zhou W, Zhu L, Huang X, et al. Association between basal metabolic rate and all-cause mortality in a prospective cohort of southern chinese adults. *Front Physiol.* (2022) 12:790347. doi: 10.3389/fphys.2021.790347

35. Kitazoe Y, Kishino H, Tanisawa K, Udaka K, Tanaka M. Renormalized basal metabolic rate describes the human aging process and longevity. *Aging Cell.* (2019) 18:e12968. doi: 10.1111/acel.12968

36. Leonardi R, Jackowski S, Begley TJ. Biosynthesis of pantothenic acid and coenzyme a. *EcoSal Plus.* (2007) 2:1–18. doi: 10.1128/ecosalplus.3.6.3.4

37. Berger MM, Shenkin A, Schweinlin A, Amrein K, Augsburger M, Biesalski H-K, et al. ESPEN micronutrient guideline. *Clin Nut.* (2022) 41:1357–424. doi: 10.1016/j.clnu.2022.02.015

38. Hrubša M, Siatka T, Nejmanová I, Vopršalová M, Kujovská Krčmová L, Matoušová K, et al. Biological properties of vitamins of the B-complex, part 1: vitamins B1, B2, B3, and B5. *Nutrients.* (2022) 14:484. doi: 10.3390/nu14030484

39. Hong Y, Zhou Z, Zhang N, He Q, Guo Z, Liu L, et al. Association between plasma Vitamin B5 levels and all-cause mortality: a nested case-control study. *J Clin Hypertension.* (2022) 24:945–54. doi: 10.1111/jch.14516

40. Johnson L, Martens C, Santos-Parker J, Bassett C, Strahler T, Cruickshank-Quinn C, et al. Amino acid and lipid associated plasma metabolomic patterns are related to healthspan indicators with ageing. *Clin Sci.* (2018) 132:1765–77. doi: 10.1042/CS20180409

41. Bramer L, Hontz R, Eisfeld A, Sims A, Kim Y, Stratton K, et al. Multi-omics of NET formation and correlations with CNDP1, PSPB, and L-cystine levels in severe and mild COVID-19 infections. *Heliyon.* (2023) 9:e13795. doi: 10.1016/j.heliyon.2023.e13795

42. Wang L, Lin L, Lee S, Wu C, Chou W, Hsu C, et al. l-Cystine is associated with the dysconnectivity of the default-mode network and salience network in attention-deficit/hyperactivity disorder. *Psychoneuroendocrinology.* (2021) 125:105105. doi: 10.1016/j.psyneuen.2020.105105

43. Vatner S, Zhang J, Oydanich M, Berkman T, Naftalovich R, Vatner D. Healthful aging mediated by inhibition of oxidative stress. *Ageing Res Rev.* (2020) 64:101194. doi: 10.1016/j.arr.2020.101194

44. Song X, Xiong L, Guo T, Chen X, Zhang P, Zhang X, et al. Cystatin C is a predictor for long-term, all-cause, and cardiovascular mortality in US adults with metabolic syndrome. *J Clin Endocrinol Metab.* (2024) 109:2905–19. doi: 10.1210/clinem/dgae225

45. Henderson G. Plasma free fatty acid concentration as a modifiable risk factor for metabolic disease. *Nutrients.* (2021) 13:2590. doi: 10.3390/nu13082590

46. Tabibzadeh S. Signaling pathways and effectors of aging. *Front Biosci.* (2021) 26:50–96. doi: 10.2741/4889

47. Salminen A, Kaarniranta K, Kauppinen A. Insulin/IGF-1 signaling promotes immunosuppression via the STAT3 pathway: impact on the aging process and age-related diseases. *Inflammation Res.* (2021) 70:1043–61. doi: 10.1007/s00011-021-01498-3

48. Wang Y, Meng X, Wang A, Xie X, Pan Y, Johnston S, et al. Ticagrelor versus Clopidogrel in CYP2C19 loss-of-function carriers with stroke or TIA. *N Engl J Med.* (2018) 385:2520–30. doi: 10.1056/NEJMoa2111749

49. Casula M, Colpani O, Xie S, Catapano A, Baragetti A. HDL in atherosclerotic cardiovascular disease: in search of a role. *Cells.* (2021) 10:1869. doi: 10.3390/cells10081869

50. Singh K, Rohatgi A. Examining the paradox of high high-density lipoprotein and elevated cardiovascular risk. *J Thoracic Dis.* (2018) 10:109–12. doi: 10.21037/jtd.2017.12.97

51. Hussain S, Ebeling P, Barker A, Beilin L, Tonkin A, McNeil J. Association of plasma high-density lipoprotein cholesterol level with risk of fractures in healthy older adults. *JAMA Cardiol.* (2023) 8:268–72. doi: 10.1001/jamacardio.2022.5124

52. Qi M, Billheimer J, Chang C, Janssen I, Brooks M, Orchard T, et al. High-density lipoprotein over midlife and future cognition in women: the SWAN HDL ancillary study. *J Clin Endocrinol Metab.* (2025) 110:1980–8. doi: 10.1210/clinem/dgae697

53. Chen L. The grip on healthspan: handgrip strength as a vital sign of aging. *Arch Gerontol Geriatr.* (2024) 122:105436. doi: 10.1016/j.archger.2024.105436

54. Ghezelbash F, Shirazi-Adl A, Arjmand N, El-Ouaaid Z, Plamondon A, Meakin JR. Effects of sex, age, body height and body weight on spinal loads: sensitivity analyses in a subject-specific trunk musculoskeletal model. *J Biomech.* (2016) 49:3492–501. doi: 10.1016/j.jbiomech.2016.09.026

55. Ji S, Lee E, Kim BJ, Baek JY, Yi Y, Jang IY, et al. Height loss as an indicator of ageing through its association with frailty and sarcopenia: an observational cohort study. *Arch Gerontol Geriatr.* (2023) 110:104916. doi: 10.1016/j.archger.2022.104916

56. Jomova K, Raptova R, Alomar S, Alwasel S, Nepovimova E, Kuca K, et al. Reactive oxygen species, toxicity, oxidative stress, and antioxidants: chronic diseases and aging. *Arch Toxicol.* (2023) 97:2499–574. doi: 10.1007/s00204-023-03562-9

57. Ungvari Z, Fazekas-Pongor V, Csiszar A, Kunutsor SK. The multifaceted benefits of walking for healthy aging: from Blue zones to molecular mechanisms. *GeroScience.* (2023) 45:3211–39. doi: 10.1007/s11357-023-00873-8

58. Zhu J, Yang Y, Zeng Y, Han X, Chen W, Hu Y, et al. The association of physical activity behaviors and patterns with aging acceleration: evidence from the UK Biobank. *J Gerontol Ser A.* (2023) 78:753–61. doi: 10.1093/gerona/glad064

frontiers | Frontiers in Nutrition

TYPE Original Research
PUBLISHED 09 October 2025
DOI 10.3389/fnut.2025.1617256

OPEN ACCESS

EDITED BY
Qingyu Wang,
Capital Medical University, China

REVIEWED BY
Matteo Della Porta,
University of Milan, Italy
Mahdi Vajdi,
Isfahan University of Medical Sciences, Iran

*CORRESPONDENCE
Jinxi Zhao
✉ zhaojinximd@126.com
Yaofu Zhang
✉ zhangyftcm@mail.tsinghua.edu.cn

†These authors have contributed equally to this work and share first authorship

RECEIVED 24 April 2025
ACCEPTED 15 September 2025
PUBLISHED 09 October 2025

CITATION
Lin Y, Chen Y, Liu J, Li M, Tang Y, Zhao J and Zhang Y (2025) Iron status and dietary iron intake in relation to overweight/obesity in U.S. adults: a nationwide population-based study. *Front. Nutr.* 12:1617256.
doi: 10.3389/fnut.2025.1617256

Iron status and dietary iron intake in relation to overweight/obesity in U.S. adults: a nationwide population-based study

Yuanyuan Lin[1†], Yexin Chen[1†], Jiangteng Liu[1], Minghao Li[2], Ying Tang[1], Jinxi Zhao[1*] and Yaofu Zhang[3*]

[1]Dongzhimen Hospital, Beijing University of Chinese Medicine, Beijing, China, [2]Guanganmen Hospital, China Academy of Chinese Medical Sciences, Beijing, China, [3]Yuquan Hospital, Tsinghua University, Beijing, China

Background: Evidence on the associations between iron status biomarkers and both overweight/obesity prevalence and body mass index (BMI) is limited.
Methods: This cross-sectional analysis utilized data from 5,454 participants in the NHANES 2003–2006 and 2017–2020 cycles. Overweight and obesity were defined as BMI ≥ 25 kg/m^2 and ≥30 kg/m^2, respectively. Weighted multivariable logistic and linear regression models were used to assess associations between iron biomarkers, dietary iron intake, and overweight/obesity risk or BMI. Restricted cubic splines (RCS) were utilized to explore potential non-linear patterns. Furthermore, subgroup analyses stratified by categorical covariates were conducted.
Results: After adjusting for confounding variables, weighted logistic regression analysis identified reduced odds of overweight/obesity with higher dietary iron intake (OR = 0.98, p = 0.026), serum iron (SI; OR = 0.98, p = 0.004), and transferrin saturation (TSAT; OR = 0.98, p = 0.003). Weighted multivariable linear regression analysis demonstrated inverse associations of dietary iron intake (β = −0.06, p = 0.045), SI (β = −0.02, p < 0.001), and TSAT (β = −0.09, p < 0.001) with BMI. The total iron-binding capacity (TIBC) exhibited a marginal positive association with overweight/obesity risk and BMI. RCS analysis revealed non-linear dose–response relationships between SI, TSAT, TIBC, and overweight/obesity risk. After Bonferroni correction, no significant interaction effects were observed between iron biomarkers and stratified variables.
Conclusion: Elevated dietary iron intake, serum iron, and TSAT are inversely associated with overweight/obesity risk, highlighting the potential protective role of adequate iron status in preventing obesity.

KEYWORDS

iron, obesity, overweight, National Health and Nutrition Examination Survey (NHANES), transferrin saturation, cross-sectional study

Introduction

Overweight (defined as body mass index [BMI] ≥ 25 kg/m^2) and obesity (BMI ≥ 30 kg/m^2) affect over 2.11 billion adults globally, with U.S. age-standardized prevalence rates reaching 75.9% in men and 72.6% in women (1, 2). The disease burden linked to overweight and obesity is substantial, significantly elevating the risks of non-communicable diseases, including type 2 diabetes mellitus and cardiovascular disorders, as well as increasing susceptibility to over 13

types of cancer (3, 4). Most mortality related to non-communicable diseases, such as cancer, cardiovascular diseases, and respiratory diseases, reached its minimum within the BMI range of 21–25 kg/m^2 (5). Research indicates that sedentary lifestyles, genetic susceptibility, and the globally prevalent Western dietary pattern—characterized by high calories (mainly from sugar and fats) yet deficiencies in micronutrients and fiber—are well-established contributors to obesity and diabetes (6, 7). Additionally, emerging evidence underscores the interplay between micronutrient imbalances and obesity pathogenesis, offering novel avenues for prevention and therapy (8).

Iron, as an indispensable trace element, plays a pivotal role in modulating metabolic rate, gluconeogenesis, insulin sensitivity, and adipocyte phenotype (9). Approximately 90% of the daily iron needs come from endogenous sources rather than dietary intake (10). Multiple biomarkers serve as indicators of iron status in individuals. Serum iron (SI) reflects the amount of iron bound to transferrin in the circulation, which is crucial for diagnosing iron deficiency and iron-overload conditions (11). Total iron-binding capacity (TIBC) quantifies the maximum amount of iron that can be bound by transferrin in serum, reflecting the body's capacity to mobilize and deliver iron to tissues (12). Transferrin saturation (TSAT), calculated as the ratio of serum iron to TIBC, is a valuable indicator of iron availability for cells (12). Ferritin, the primary iron-storage protein in the body, functions as a key biomarker for assessing body iron reserves. It is critical to acknowledge, however, that ferritin serves as an acute-phase reactant, with its levels potentially elevated in inflammatory states, infections, or malignancies, irrespective of iron status (13). Iron status disorders may exacerbate obesity-related metabolic disorders by affecting mitochondrial function and cellular energy metabolism (14). Although a cross-sectional study of children aged 2 to 17 years suggested that higher dietary iron intake is associated with lower obesity risk (8), population-based evidence linking iron intake to adult obesity remains scarce. In addition, previous studies have reported conflicting findings regarding the association between iron status and overweight/obesity. A meta-analysis of 26 observational studies demonstrated lower serum iron and TSAT levels in overweight/obese individuals compared to normal-weight controls, with no significant difference in serum ferritin (15). In contrast, another study focusing on obese children found higher TIBC levels but no differences in serum iron or ferritin (16). Both studies were limited to group comparisons, and regression analyses to quantify associations, adjust for potential confounders, or explore dose–response relationships were lacking. Thus, the associations between dietary iron intake, iron status, and the risk of overweight/obesity in adults remain incompletely characterized.

Herein, utilizing data from the National Health and Nutrition Examination Survey (NHANES) database, this study simultaneously evaluated iron homeostasis biomarkers and dietary iron intake in relation to overweight/obesity risk and BMI, with the objective of providing evidence-based dietary insights for the prevention and management of adult obesity.

Materials and methods

Study population

This cross-sectional study used data derived from the NHANES. This nationally representative survey systematically collects comprehensive nutritional and health indicators of the American population through standardized physical examinations and interviews. The National Center for Health Statistics (NCHS) provides detailed documentation of NHANES study protocols, including standardized data collection manuals for questionnaires and laboratory tests, through its official portal at the Centers for Disease Control and Prevention.[1] Ethical clearance for the NHANES survey protocol was granted by the NCHS Research Ethics Review Board. Prior to enrollment, documented informed consent forms were voluntarily signed by participants or legally authorized representatives (17).

This study analyzed data from the NHANES 2003–2006 and 2017–2020 cycles. This selection was made to enhance the validity and generalizability of the statistical inferences, as these were the only cycles where data on both iron biomarkers and dietary iron intake were simultaneously available. The screening process is depicted in Figure 1. From an initial cohort of 36,030 participants, a total of 16,393 individuals with available data on at least one iron biomarker and BMI were enrolled. Subsequently, the study excluded 4,539 underage participants, 638 pregnant participants, and 5,762 participants with missing covariate data. As a result, a total of 5,454 participants were ultimately included in the final analysis. The complete-case analysis approach was adopted to avoid potential biases introduced by imputation methods.

Exposure and outcome definitions

Exposure variables were defined as dietary iron intake and indicators of iron status, including serum iron, TIBC, TSAT, and ferritin. Dietary iron intake was assessed using a 24-h dietary recall survey. The initial dietary recall interview was conducted in-person at the Mobile Examination Center, and the second occurred by telephone 3 to 10 days later, administered by trained interviewers. Dietary intakes were calculated using the standardized United States Department of Agriculture (USDA) Food and Nutrient Database for Dietary Studies. The average of the two 24-h dietary recall information was used for analysis. In cases where participants lacked the second dietary interview, data from the first dietary recall were utilized. Serum iron was measured via a meticulous three-step procedure using the ferrozine reagent on the Roche Cobas 6,000 analyzer series. In this process, Fe^{3+} was liberated from transferrin, reduced to Fe^{2+}, and complexed with ferrozine to form a colorimetric product, enabling its quantitative determination. TIBC was determined indirectly using measurements of serum iron and unsaturated iron-binding capacity obtained by the Roche method. TSAT was computed by dividing the measured value of frozen serum iron by the calculated TIBC and then multiplying the result by 100. Ferritin measurement was carried out using a sandwich immunoassay.

BMI was calculated as weight in kilograms divided by height in meters squared (kg/m^2). Both height and weight were measured using a calibrated weight scale and a stadiometer by trained examiners and recorders. Adult weight status was classified according to the World Health Organization (WHO) classification criteria, where

1 https://www.cdc.gov/nchs/nhanes/

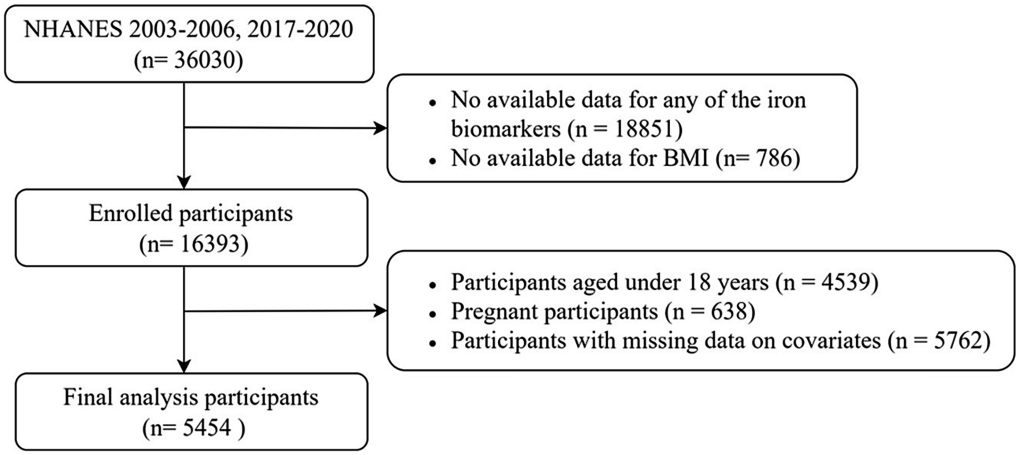

FIGURE 1
Flowchart of the study participants.

non-overweight/obesity was defined as a BMI of < 24.9 kg/m^2, overweight as a BMI of ≥ 25 kg/m^2, and obesity as a BMI of ≥ 30 kg/m^2 (18).

Covariates

Demographic and lifestyle factors used as covariates included age, sex, ethnicity, physical activity (PA), poverty–income ratio (PIR), and alcohol consumption. Physical activity was quantified as metabolic equivalent (MET) minutes of moderate-to-vigorous physical activity per week. Respondents were classified into three categories based on adult physical activity guidelines (19): highly active (≥1,200 MET-min/week, equivalent to ≥300 min/week of moderate-intensity or ≥150 min/week of vigorous-intensity activity), active (600–1,199 MET-min/week, equivalent to 150–299 min/week of moderate-intensity or 75–149 min/week of vigorous-intensity activity), and inactive (<600 MET-min/week). Poverty was measured using the PIR, which divided participants into low-income (PIR < 1.3) and high-income (PIR ≥ 1.3) categories. Alcohol consumption patterns were categorized into three distinct groups based on self-reported intake: non-drinkers were defined as individuals with no lifetime alcohol consumption; low-to-moderate drinkers, who consumed alcohol less than daily; and heavy drinkers, classified as individuals who consumed alcohol daily.

Clinical indicators linked to metabolic parameters were also included, such as diabetes status, total calorie intake, serum creatinine (SCR), alanine aminotransferase (ALT), aspartate aminotransferase (AST), total cholesterol (TC), and high-density lipoprotein cholesterol (HDL-C) (20–23). Diabetes mellitus was defined as a self-reported diagnosis via validated questionnaires or a glycosylated hemoglobin (HbA1c) level of ≥6.5%. The body roundness index (BRI), an indicator of visceral adiposity distribution, was calculated as: $BRI = 364.2 - 365.5 \times \sqrt{[1 - (\text{waist circumference}/(2\pi))^2 / (0.5 \times \text{height})^2]}$, where waist circumference and height are in centimeters (24).

Given the critical role of dietary vitamin C intake in enhancing non-heme iron absorption and influencing iron metabolism (25), it was also included as a nutritional covariate. Total calorie intake was adjusted for, as it is a major determinant of body weight and may confound the association between iron status and obesity. Dietary vitamin C and calorie intake were quantified using 24-h dietary recall surveys. The analysis incorporated the mean of two 24-h dietary assessments. When participants lacked a second dietary recall, data from the first recall were used.

Statistical analyses

To evaluate the differences in various variables across weight status groups, we employed the following statistical methods: continuous variables were presented as weighted median values with interquartile ranges (IQRs), while categorical variables were described using weighted frequencies and percentages. Group differences for continuous variables were assessed using the design-based Kruskal–Wallis test, which accounts for the complexities of the survey design and ensures the accuracy and reliability of the results. For categorical variables such as ethnicity, alcohol consumption, and physical activity, Pearson's chi-squared test with Rao–Scott adjustment was used. This adjustment is designed to address potential biases due to the survey design, thereby making the chi-squared test results more robust and reliable.

Associations between iron status, dietary iron intake, and BMI were evaluated using weighted linear regression models. Weighted logistic regression models were used to examine the relationship between iron status, dietary iron intake, and the risk of overweight/obesity. To explore potential non-linear relationships between iron status, dietary iron intake, and the risk of obesity/overweight, we used restricted cubic spline (RCS) models with four knots positioned at the 5th, 35th, 65th, and 95th percentiles of the exposure distribution. This configuration was selected to balance the smoothness of the fitted curve and avoid loss of precision due to overfitting (26).

Furthermore, stratified multivariate regression was utilized for subgroup analyses, adjusting for all covariates except the stratification variable. We performed subgroup analyses stratified by categorical variables, including sex, ethnicity, PIR, physical activity, alcohol use,

and diabetes status. To evaluate subgroup heterogeneity in associations, interaction terms were assessed via the likelihood ratio test (LRT). Specifically, LRT compared models with and without interaction terms (between exposure and stratifying covariates). A significant p-value for interaction indicated that the alternative model with interaction terms fitted the data better, confirming the presence of an interaction effect. All statistical tests were two-tailed, with statistical significance defined as a p-value of <0.05 for primary analyses (excluding subgroup analyses). For subgroup analyses involving multiple comparisons across stratified variables, the Bonferroni correction was applied to adjust the significance threshold: the original $\alpha = 0.05$ was divided by the total number of independent subgroup tests ($n = 6$), resulting in a corrected significance level of $\alpha' \approx 0.008$. All analyses were performed using R software (https://www.r-project.org/; version 4.4.2).

Results

Baseline characteristics of study participants

Among the 5,454 enrolled adults, 1,345 (25.51%) were categorized as non-overweight/non-obese, 1,655 (30.93%) as overweight, and 2,454 (43.56%) as obese. Table 1 presents the baseline characteristics and weighted estimates of adults with or without overweight/obesity in this study. Iron biomarkers differed significantly across weight categories: serum iron and TSAT decreased progressively with higher adiposity, from a median of 90.0 μg/dL and 29.00% in the non-overweight/obesity group to 79.0 μg/dL and 25.00% in the obesity group ($p < 0.001$), while ferritin increased from 80.20 ng/mL (IQR, 39.60–143.00) to 116.00 ng/mL (IQR, 57.00–198.00) ($p < 0.001$). TIBC, however, showed no statistically significant variation ($p = 0.204$). In addition, demographic and metabolic differences (sex, age, ethnicity, PIR, body roundness index, physical activity, and dietary vitamin C intake) were statistically significant across weight categories (All $p < 0.001$). Individuals with overweight/obesity exhibited a higher prevalence of diabetes, higher SCR, ALT, TC, and lower HDL-C. Nevertheless, no differences were observed in alcohol consumption, dietary iron intake, or caloric intake among these groups (all $p > 0.05$).

Associations of iron status and adults with overweight/obesity

Multivariable-adjusted logistic regression models assessed the odds of overweight or obesity (BMI ≥ 25 kg/m^2) in relation to iron biomarkers (Table 2). After completely adjusting for covariates, higher dietary iron intake was associated with 2% lower odds of overweight/obesity (OR = 0.98; 95% CI: 0.96–1.00; $p = 0.026$). Transferrin saturation demonstrated consistent inverse associations in three models, with each 1% increase corresponding to a 2% reduction in odds in model 3 (OR = 0.98; 95% CI: 0.96–0.99; $p = 0.003$). TIBC showed a marginal association (OR = 1.00; 95% CI: 0.99–1.00; $p = 0.003$), as the effect estimate and its confidence interval encompassed the null value. Serum iron also exhibited a non-significant inverse trend (OR = 1.00; 95% CI: 0.99–1.00; $P = 0.004$), while serum ferritin levels were unassociated with overweight/obesity ($P > 0.05$).

Associations between iron status and iron intake with BMI

Multivariable linear regression analyses (Table 3) revealed significant inverse associations between serum iron and TSAT with BMI across all models, whereas TIBC demonstrated a positive association. These relationships persisted in the fully adjusted model (model 3): each 1 μg/dL increase in serum iron was associated with a 0.02-unit decrease in BMI ($\beta = -0.02$; 95% CI: −0.03 to −0.02; $p < 0.001$), and each 1% increase in TSAT corresponded to a 0.09-unit reduction in BMI ($\beta = -0.09$; 95% CI: −0.11 to −0.06; $p < 0.001$). In the linear regression analysis examining the association between TIBC and BMI, a marginally statistically significant positive association was observed ($\beta = 0.01$, 95% CI: 0.00 to 0.02; $p = 0.022$). Higher dietary iron intake was also linked to lower BMI in model 3 ($\beta = -0.06$; 95% CI: −0.12 to 0.00; $p = 0.045$). In contrast, no significant association was observed between serum ferritin levels and BMI ($P > 0.05$).

The non-linear relationship between iron status and overweight/obesity

As illustrated in Figure 2, non-linear associations between iron status biomarkers and overweight/obesity risk were evaluated using RCS regression models adjusted for age, sex, ethnicity, PIR, PA, alcohol use, diabetes status, total calorie intake, and vitamin C intake, SCR, ALT, AST, TC, and HDL-C. Notably, a threshold-dependent effect was observed, with a significant reduction in obesity risks when TSAT values ranged between 16.76 and 39.81% (p-overall < 0.001; p-non-linear < 0.001). An inverted U-shaped relationship was identified between SI and obesity risks (p-overall < 0.001; p-non-linear = 0.011), with the OR peaking at a turning point of 57.39 μg/dL. Beyond this level, the OR declined with increasing SI concentrations. Similarly, TIBC showed a non-linear trend (p-overall < 0.001; p-non-linear = 0.002), with the highest OR observed at approximately 385.86 μg/dL and decreasing risks thereafter. In addition, a continuously decreasing linear trend between total dietary iron intake and the prevalence of overweight/obesity was observed (p-overall < 0.015; p-non-linear = 0.421). No significant relationship was observed between ferritin and overweight/obesity (p-overall = 0.021; p-non-linear = 0.212).

Subgroup analysis

Supplementary Tables 1, 2 present the results of subgroup analyses stratified by sex, ethnicity, PIR, PA, alcohol use, and diabetes status. After Bonferroni correction, no significant interaction effects were observed between iron biomarkers and stratified variables on either overweight/obesity risk or BMI in the multivariable-adjusted models (all interaction p-values > 0.008), indicating that the overall association pattern was consistent across the examined subgroups.

TABLE 1 Baseline characteristics of adults with or without overweight/obesity.

Characteristic	Non-obesity/ overweight	Overweight	Obesity	*p*-value
	N = 1,345 (25.51%)	*N* = 1,655 (30.93%)	*N* = 2,454 (43.56%)	
Sex				0.026*
Male	13,293,886 (57.66%)	12,828,603 (45.88%)	20,019,755 (50.84%)	
Female	9,761,824 (42.34%)	15,133,599 (54.12%)	19,354,349 (49.16%)	
Age (years)	40.00 (26.00, 58.00)	51.00 (36.00, 66.00)	49.00 (34.00, 62.00)	<0.001*
Age group				<0.001*
18–29 years	7,486,991 (32.47%)	4,033,748 (14.43%)	6,502,013 (16.51%)	
30–49 years	7,004,994 (30.38%)	9,295,246 (33.24%)	13,757,170 (34.94%)	
50–69 years	6,297,666 (27.31%)	9,773,849 (34.95%)	14,197,788 (36.06%)	
70 years above	2,266,059 (9.83%)	4,859,359 (17.38%)	4,917,134 (12.49%)	
Ethnicity				<0.001*
Non-Hispanic White	15,350,896 (66.58%)	18,012,626 (64.42%)	24,985,754 (63.46%)	
Mexican American	1,205,652 (5.23%)	2,425,757 (8.68%)	3,919,101 (9.95%)	
Non-Hispanic Black	2,171,324 (9.42%)	2,443,406 (8.74%)	4,645,418 (11.80%)	
Other Hispanic	1,407,558 (6.11%)	2,272,703 (8.13%)	2,875,460 (7.30%)	
Other/multi-ethnicities	2,920,281 (12.67%)	2,807,709 (10.04%)	2,948,371 (7.49%)	
PIR				0.002*
<1.3	5,248,152 (22.76%)	4,539,746 (16.24%)	7,599,285 (19.30%)	
≥1.3	17,807,558 (77.24%)	23,422,455 (83.76%)	31,774,819 (80.70%)	
BRI	3.09 (2.54, 3.73)	4.74 (4.19, 5.46)	7.02 (6.04, 8.53)	<0.001*
BMI	22.50 (20.70, 23.70)	27.20 (26.20, 28.40)	34.10 (31.70, 38.30)	<0.001*
Alcohol use				0.069
Heavy	920,827 (3.99%)	1,129,090 (4.04%)	901,382 (2.29%)	
Low-to-moderate	19,978,717 (86.65%)	24,941,741 (89.20%)	36,140,938 (91.79%)	
Non-drinker	2,156,165 (9.35%)	1,891,370 (6.76%)	2,331,784 (5.92%)	
PA				0.009*
Active	2,703,853 (11.73%)	3,377,098 (12.08%)	3,896,495 (9.90%)	
Highly active	15,193,918 (65.90%)	16,983,160 (60.74%)	22,424,348 (56.95%)	
Inactive	5,157,940 (22.37%)	7,601,943 (27.19%)	13,053,261 (33.15%)	
Diabetes				<0.001*
Yes	1,110,626 (4.82%)	3,217,449 (11.51%)	8,034,109 (20.40%)	
No	21,945,084 (95.18%)	24,744,752 (88.49%)	31,339,995 (79.60%)	
Dietary VC intake	60.35 (29.20, 114.35)	60.05 (28.85, 103.25)	49.25 (24.70, 96.95)	0.002*
Dietary iron intake	12.46 (9.15, 16.60)	12.46 (9.26, 17.73)	12.47 (9.27, 16.27)	0.356
Total calorie intake	1,863.00 (1,471.00, 2,476.50)	1,968.50 (1,503.00, 2,485.00)	1,962.50 (1,536.00, 2,566.00)	0.216
Serum iron (μg/dL)	90.00 (69.00, 113.00)	89.00 (68.00, 111.00)	79.00 (60.00, 99.00)	<0.001*
TIBC (μg/dL)	316.00 (289.00, 355.00)	324.00 (292.00, 353.00)	324.00 (295.00, 354.00)	0.204
TSAT (%)	29.00 (22.00, 36.00)	28.00 (22.00, 35.00)	25.00 (18.00, 31.00)	<0.001*
Ferritin (ng/mL)	80.20 (39.60, 143.00)	110.00 (56.60, 190.00)	116.00 (57.00, 198.00)	<0.001*
HbA1c (%)	5.30 (5.10, 5.50)	5.50 (5.20, 5.80)	5.60 (5.30, 6.00)	<0.001*
SCR (umol/L)	70.72 (61.88, 82.21)	76.91 (65.42, 89.28)	75.14 (64.53, 87.52)	<0.001*
ALT (U/L)	15.00 (12.00, 20.00)	18.00 (13.00, 25.00)	21.00 (15.00, 30.00)	<0.001*
AST (U/L)	19.00 (16.00, 23.00)	19.00 (16.00, 24.00)	19.00 (16.00, 24.00)	0.396

(Continued)

TABLE 1 (Continued)

Characteristic	Non-obesity/ overweight	Overweight	Obesity	*p*-value
	N = 1,345 (25.51%)	*N* = 1,655 (30.93%)	*N* = 2,454 (43.56%)	
TC (mmol/L)	4.55 (3.96, 5.22)	4.81 (4.19, 5.53)	4.78 (4.16, 5.51)	<0.001*
HDL-C (mmol/L)	1.55 (1.29, 1.81)	1.34 (1.11, 1.63)	1.19 (1.01, 1.42)	<0.001*

PIR, poverty–income ratio; BRI, body roundness index; BMI, body mass index; PA, physical activity; VC, vitamin C; TIBC, total iron-binding capacity; TSAT, transferrin saturation; SCR, serum creatinine; ALT, alanine aminotransferase; AST, aspartate aminotransferase; TC, total cholesterol; HDL-C, high-density lipoprotein cholesterol. * *p*-value < 0.05.

TABLE 2 Associations of iron status and dietary iron intake with the risk of overweight/obesity.

	Number	Model 1		Model 2		Model 3	
		OR (95%CI)	*p*-value	OR (95%CI)	*p*-value	OR (95%CI)	*p*-value
Iron intake (mg/ day)	5,454	0.99 (0.98, 1.01)	0.374	0.98 (0.97, 1.00)	0.028*	0.98 (0.96, 1.00)	0.026*
Serum iron (μg/dL)	5,454	0.99 (0.99, 1.00)	<0.001*	0.99 (0.99, 1.00)	<0.001*	0.99 (0.99, 1.00)	0.004*
Transferrin saturation (%)	5,444	0.98 (0.97, 0.99)	<0.001*	0.98 (0.97, 0.98)	<0.001*	0.98 (0.96, 0.99)	0.003*
TIBC (μg/dL)	5,444	1.00 (1.00, 1.00)	0.202	1.00 (1.00, 1.01)	0.004*	1.00 (1.00, 1.01)	0.003*
Ferritin (ng/mL)	5,437	1.00 (1.00, 1.00)	0.002*	1.00 (1.00, 1.00)	0.025*	1.00 (1.00, 1.00)	0.504

Model 1: Non-adjusted.
Model 2: Adjusted for age, sex, ethnicity, and PIR.
Model 3: Adjusted for age, sex, ethnicity, PIR, PA, alcohol use, diabetes status, total calorie intake, vitamin C intake, SCR, ALT, AST, TC, and HDL-C.
* *p*-value < 0.05.

TABLE 3 Associations of iron status and dietary iron intake with BMI.

	Number	Model 1		Model 2		Model 3	
		β (95%CI)	*p*-value	*β* (95%CI)	*p*-value	*β* (95%CI)	*p*-value
Iron intake (mg/ day)	5,454	−0.04 (−0.09, 0.01)	0.142	−0.03 (−0.08, 0.02)	0.215	−0.06 (−0.12, 0.00)	0.045*
Serum iron (μg/dL)	5,454	−0.04 (−0.04, −0.03)	<0.001*	−0.04 (−0.04, −0.03)	<0.001*	−0.02 (−0.03, −0.02)	<0.001*
Transferrin saturation (%)	5,444	−0.12 (−0.14, −0.10)	<0.001*	−0.12 (−0.14, −0.10)	<0.001*	−0.09 (−0.11, −0.06)	<0.001*
TIBC (μg/dL)	5,444	0.01 (0.00, 0.01)	0.013*	0.01 (0.00, 0.02)	0.008*	0.01 (0.00, 0.02)	0.022*
Ferritin (ng/mL)	5,437	0.00 (0.00, 0.00)	0.044*	0.00 (0.00, 0.01)	0.017*	0.00 (0.00, 0.00)	0.512

Model 1: Non-adjusted.
Model 2: Adjusted for age, sex, ethnicity, and PIR.
Model 3: Adjusted for age, sex, ethnicity, PIR, PA, alcohol use, diabetes status, total calorie intake, vitamin C intake, SCR, ALT, AST, TC, and HDL-C.
* *p*-value < 0.05.

Discussion

This study utilized data from the NHANES, a nationally representative cross-sectional dataset, to investigate the associations between iron status biomarkers and the risk of overweight/obesity, as well as BMI, among US adults. Specifically, overweight/obesity was negatively associated with dietary iron intake, serum iron levels, and transferrin saturation but positively associated with TIBC. Furthermore, these associations remained robust in the analysis of BMI: lower iron intake and transferrin saturation, alongside elevated TIBC, were significantly associated with higher BMI values.

Iron can alleviate obesity by regulating leptin levels and enhancing thermogenic capacity in adipose tissue. Serum leptin levels were observed to be 3.7-fold higher in obese individuals compared to their lean counterparts, while individuals with low iron status exhibited 3.2-fold higher serum leptin than those with high iron status (27). Hyperleptinemia-induced leptin resistance can contribute to obesity by disrupting hypothalamic satiety signaling (28). Mechanistically, iron has been shown to downregulate leptin transcription, with *in vitro* studies demonstrating iron-mediated suppression of leptin expression in adipocytes (27). Additionally, iron supplementation increased oxygen consumption and enhanced the thermogenic capacity of adipocytes, suggesting a promising approach to counteract obesity (29). Iron deficiency may also activate oxidative stress and elevate the expression of hypoxia-inducible factor 1 (HIF-1) (30). Overexpression of HIF-1α exacerbates adipose tissue dysfunction by inducing fibrosis and insulin resistance in white adipose tissue, thereby promoting obesity (31).

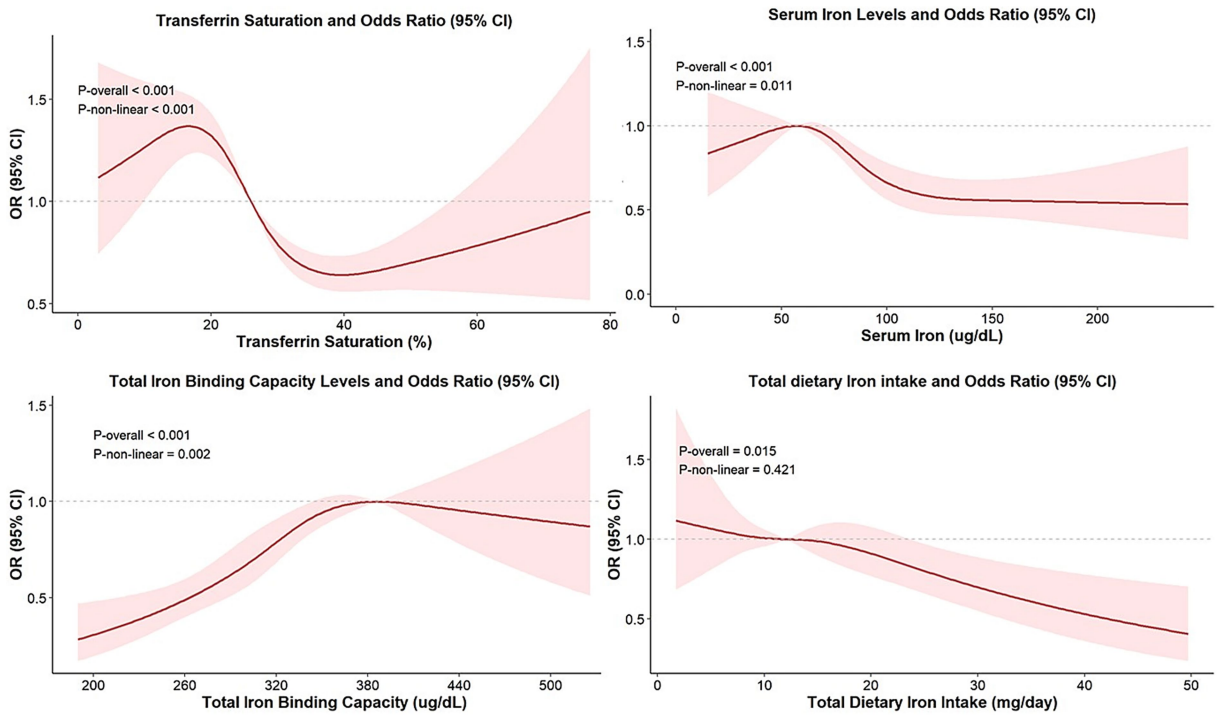

FIGURE 2
Non-linear relationship between iron status biomarkers and overweight/obesity. Models were adjusted for age, sex, ethnicity, PIR, PA, alcohol use, diabetes status, total calorie intake, vitamin C intake, SCR, ALT, AST, TC, and HDL-C.

There is a bidirectional interplay between obesity and iron deficiency, wherein iron deficiency reciprocally promotes adiposity via dysregulated leptin levels and impaired adipose tissue function, while obesity impairs iron absorption through chronic inflammation and hepcidin-mediated disruption of iron transport. In individuals with obesity, pro-inflammatory cytokines such as interleukin-6 (IL-6), IL-1β, and tumor necrosis factor-α (TNF-α) can upregulate hepcidin, a central regulator of iron homeostasis (32, 33). This peptide promotes the degradation of the iron exporter ferroportin in macrophages, hepatocytes, and the duodenum, thereby inhibiting iron flow into the plasma, reducing iron absorption, and decreasing circulating iron availability (34, 35). Moreover, chronic exposure to TNF-α in intestinal cells can downregulate the expression of iron transporters, thereby impairing iron absorption and leading to iron deficiency (36).

TIBC reflects the total capacity of transferrin to bind iron, with elevated TIBC typically indicating a state of functional iron deficiency, wherein iron availability is limited despite normal or low iron stores. In our analysis, the persistent positive association between TIBC and BMI/obesity risk aligns with this physiological role: during iron-restricted states, the liver upregulates transferrin synthesis to enhance iron uptake as a compensatory mechanism, leading to elevated TIBC (37).

Heightened dietary iron intake may mitigate the risk of overweight/obesity and decrease BMI, suggesting that maintaining sufficient iron intake may serve as a protective nutritional strategy against excessive adiposity. Similarly, previous studies observed that higher levels of dietary iron intake were linked to a lower prevalence of overweight/obesity and metabolic syndrome in adolescents (38, 39). In the *Vitamin and Mineral Requirements in Human Nutrition, Second Edition,* formulated by the World Health Organization, the recommended daily iron intake for adult women is between 19.6 mg and 58.8 mg, while the recommended range for adult males is 9.1 mg to 27.4 mg (40). Given the reduced rate of iron absorption in patients with obesity and the protective effect of iron on obesity, adequate iron consumption within this range is recommended.

Ferritin, a key protein responsible for iron storage, sequesters excess iron to prevent oxidative cellular damage (41). In this study, we found no significant relationship between serum ferritin levels and overweight/obesity prevalence. Although elevated ferritin can reflect iron storage overload in healthy individuals, it may be elevated in the absence of hepatic iron overload in patients with obesity, metabolic syndrome, and alcoholism (42, 43). In inflammatory states, macrophages can secrete proinflammatory cytokines that stimulate ferritin synthesis, potentially decoupling ferritin from its classical role as iron status biomarkers (44). Elevated ferritin levels observed in this context should not be interpreted in isolation as evidence of iron overload, as they may primarily reflect the levels of inflammation associated with obesity and concomitant diseases rather than true iron excess (32, 43).

This study has several limitations. First, its cross-sectional design does not allow for causal inference. Future longitudinal or interventional studies are needed to clarify the causal direction between iron metabolism and obesity. Second, dietary iron intake was assessed via interview recall, which is prone to recall bias. Third, defining obesity solely based on the BMI is inadequate (45). Due to the diversity of the included population, multidimensional indicators such as waist circumference and body fat percentage were not incorporated. Future research should take these indicators into

account to more precisely assess the individual health risks. Moreover, a potential limitation is that we were unable to uniformly include CRP or hsCRP as a covariate in sensitivity analyses across all cycles, due to methodological differences in the measurement of inflammatory markers. Although ferritin retains its core value as an indicator of iron stores, its interpretation may be influenced by inflammatory status (13). Thus, our analysis of ferritin's association with overweight/obesity could not fully account for potential confounding by inflammation. Future studies should aim to more accurately isolate the independent effects of iron metabolism from those of inflammation.

Conclusion

In conclusion, elevated levels of dietary iron intake, serum iron concentration, and transferrin saturation were linked to a lowered risk of overweight/obesity, suggesting that maintaining adequate iron status may play a crucial role in preventing and managing obesity. To further validate these associations, prospective cohort studies and mechanistic investigations are warranted to provide additional evidence and bolster this conclusion. Furthermore, evaluating iron deficiency in obese populations requires a comprehensive approach that incorporates multiple biomarkers to accurately assess iron status and inform targeted interventions.

Data availability statement

The original contributions presented in the study are included in the article/Supplementary material, further inquiries can be directed to the corresponding authors.

Ethics statement

The studies involving humans were approved by NCHS Research Ethics Review Board. The studies were conducted in accordance with the local legislation and institutional requirements. The participants provided their written informed consent to participate in this study.

Author contributions

YL: Writing – original draft, Formal analysis, Conceptualization, Methodology. YC: Writing – review & editing, Conceptualization, Formal analysis, Methodology, Data curation, Visualization. JL: Project administration, Writing – review & editing. ML: Writing – review & editing. YT: Writing – review & editing. JZ: Writing – review & editing, Supervision, Funding acquisition. YZ: Writing – review & editing, Supervision.

Funding

The author(s) declare that financial support was received for the research and/or publication of this article. This work was funded by the National Administration of Traditional Chinese Medicine High-Level Key Discipline: Traditional Chinese Medicine Endocrinology, 404053503; the Dongzhimen Hospital of Beijing University of Chinese Medicine High-Level Hospital Project — Leading Talent, DZMG-LJRC0001; the Beijing Natural Science Foundation General Program, No. 7222278; and the National Natural Science Foundation General Program, No. 82074354.

Conflict of interest

The authors declare that the research was conducted in the absence of any commercial or financial relationships that could be construed as a potential conflict of interest.

Generative AI statement

The authors declare that no Gen AI was used in the creation of this manuscript.

Any alternative text (alt text) provided alongside figures in this article has been generated by Frontiers with the support of artificial intelligence and reasonable efforts have been made to ensure accuracy, including review by the authors wherever possible. If you identify any issues, please contact us.

Publisher's note

Supplementary material

The Supplementary material for this article can be found online at: https://www.frontiersin.org/articles/10.3389/fnut.2025.1617256/full#supplementary-material

References

1. Ng M, Gakidou E, Lo J, Abate YH, Abbafati C, Abbas N, et al. Global, regional, and national prevalence of adult overweight and obesity, 1990–2021, with forecasts to 2050: a forecasting study for the global burden of disease study 2021. *Lancet*. (2025) 405:813–38. doi: 10.1016/S0140-6736(25)00355-1

2. GBD 2021 US Obesity Forecasting Collaborators. National-level and state-level prevalence of overweight and obesity among children, adolescents, and adults in the USA, 1990–2021, and forecasts up to 2050. *Lancet*. (2024) 404:2278–98. doi: 10.1016/S0140-6736(24)01548-4

3. Piché ME, Tchernof A, Després JP. Obesity phenotypes, diabetes, and cardiovascular diseases. *Circ Res*. (2020) 126:1477–500. doi: 10.1161/CIRCRESAHA.120.316101

4. Avgerinos KI, Spyrou N, Mantzoros CS, Dalamaga M. Obesity and cancer risk: emerging biological mechanisms and perspectives. *Metabolism*. (2019) 92:121–35. doi: 10.1016/j.metabol.2018.11.001

5. Bhaskaran K, Dos-Santos-Silva I, Leon DA, Douglas IJ, Smeeth L. Association of BMI with overall and cause-specific mortality: a population-based cohort study of 3·6

million adults in the UK. *Lancet Diabetes Endocrinol*. (2018) 6:944–53. doi: 10.1016/S2213-8587(18)30288-2

6. García-Montero C, Fraile-Martínez O, Gómez-Lahoz AM, Pekarek L, Castellanos AJ, Noguerales-Fraguas F, et al. Nutritional components in western diet versus mediterranean diet at the gut microbiota–immune system interplay. Implications for health and disease. *Nutrients*. (2021) 13:699. doi: 10.3390/nu13020699

7. Hu FB. Globalization of diabetes: the role of diet, lifestyle, and genes. *Diabetes Care*. (2011) 34:1249–57. doi: 10.2337/dc11-0442

8. Wang L, Liu W, Bi S, Zhou L, Li L. Association between minerals intake and childhood obesity: a cross-sectional study of the NHANES database in 2007-2014. *PLoS One*. (2023) 18:e0295765. doi: 10.1371/journal.pone.0295765

9. Harrison AV, Lorenzo FR, McClain DA. Iron and the pathophysiology of diabetes. *Annu Rev Physiol*. (2023) 85:339–62. doi: 10.1146/annurev-physiol-022522-102832

10. Hurrell R, Egli I. Iron bioavailability and dietary reference values. *Am J Clin Nutr*. (2010) 91:1461S–7S. doi: 10.3945/ajcn.2010.28674F

11. Camaschella C, Nai A, Silvestri L. Iron metabolism and iron disorders revisited in the hepcidin era. *Haematologica*. (2020) 105:260–72. doi: 10.3324/haematol.2019.232124

12. Peyrin-Biroulet L, Williet N, Cacoub P. Guidelines on the diagnosis and treatment of iron deficiency across indications: a systematic review1. *Am J Clin Nutr*. (2015) 102:1585–94. doi: 10.3945/ajcn.114.103366

13. Ma K, Ja S, Lg C, Sv T, Fm T. Ferritin for the clinician. *Blood Rev*. (2009) 23:95–104. doi: 10.1016/j.blre.2008.08.001

14. González-Domínguez Á, Visiedo-García FM, Domínguez-Riscart J, González-Domínguez R, Mateos RM, Lechuga-Sancho AM. Iron metabolism in obesity and metabolic syndrome. *Int J Mol Sci*. (2020) 21:5529. doi: 10.3390/ijms21155529

15. Zhao L, Zhang X, Shen Y, Fang X, Wang Y, Wang F. Obesity and iron deficiency: a quantitative meta-analysis. *Obes Rev*. (2015) 16:1081–93. doi: 10.1111/obr.12323

16. Sal E, Yenicesu I, Celik N, Pasaoglu H, Celik B, Pasaoglu OT, et al. Relationship between obesity and iron deficiency anemia: is there a role of hepcidin? *Hematology*. (2018) 23:542–8. doi: 10.1080/10245332.2018.1423671

17. CDC. Ethics review board approval. National Health and Nutrition Examination Survey. (2024). Available online at: https://www.cdc.gov/nchs/nhanes/about/erb.html (accessed March 23, 2025).

18. World Health Organization. Obesity and overweight. Available online at: https://www.who.int/zh/news-room/fact-sheets/detail/obesity-and-overweight (accessed March 27, 2025).

19. Piercy KL, Troiano RP, Ballard RM, Carlson SA, Fulton JE, Galuska DA, et al. The physical activity guidelines for americans. *JAMA*. (2018) 320:2020–8. doi: 10.1001/jama.2018.14854

20. Xu W, Dong Y, Liu S, Hu F, Cai Y. Association between organophosphorus pesticides and obesity among american adults. *Environ Health*. (2024) 23:65. doi: 10.1186/s12940-024-01104-z

21. Zhao L, Ogden CL, Yang Q, Jackson SL, Loria CM, Galuska DA, et al. Association of usual sodium intake with obesity among US children and adolescents, NHANES 2009-2016. *Obesity*. (2021) 29:587–94. doi: 10.1002/oby.23102

22. Liu M, Fang C, Mei K, Ling J, Fu W, Qi X, et al. Serum copper and obesity among healthy adults in the national health and nutrition examination survey. *PLoS One*. (2024) 19:e0300795. doi: 10.1371/journal.pone.0300795

23. Liu X, Zhang Y, Chai Y, Li Y, Yuan J, Zhang L, et al. Iron status correlates strongly to insulin resistance among U.S. adults: a nationwide population-base study. *J Clin Endocrinol Metab*. (2025) 110:677–684. doi: 10.1210/clinem/dgae558

24. Thomas DM, Bredlau C, Bosy-Westphal A, Mueller M, Shen W, Gallagher D, et al. Relationships between body roundness with body fat and visceral adipose tissue emerging from a new geometrical model. *Obesity*. (2013) 21:2264–71. doi: 10.1002/oby.20408

25. Lane DJR, Richardson DR. The active role of vitamin C in mammalian iron metabolism: much more than just enhanced iron absorption! *Free Radic Biol Med*. (2014) 75:69–83. doi: 10.1016/j.freeradbiomed.2014.07.007

26. Frank EH. Jr. Regression modeling strategies: With applications to linear models, logistic and ordinal regression, and survival analysis. SpringerLink. (2015). Available online at: https://link.springer.com/book/10.1007/978-3-319-19425-7 (accessed July 26, 2025).

27. Gao Y, Li Z, Gabrielsen JS, Simcox JA, Lee SH, Jones D, et al. Adipocyte iron regulates leptin and food intake. *J Clin Invest*. (2015) 125:3681–91. doi: 10.1172/JCI81860

28. Klok MD, Jakobsdottir S, Drent ML. The role of leptin and ghrelin in the regulation of food intake and body weight in humans: a review. *Obes Rev*. (2007) 8:21–34. doi: 10.1111/j.1467-789X.2006.00270.x

29. Mai X, Liu Y, Fan J, Xiao L, Liao M, Huang Z, et al. Iron supplementation and iron accumulation promote adipocyte thermogenesis through PGC1α-ATGL–mediated lipolysis. *J Biol Chem*. (2024) 300:107690. doi: 10.1016/j.jbc.2024.107690

30. Chen Y, Li X, Wang Z, Yuan S, Shen X, Xie X, et al. Iron deficiency affects oxygen transport and activates HIF1 signaling pathway to regulate phenotypic transformation of VSMC in aortic dissection. *Mol Med*. (2024) 30:90. doi: 10.1186/s10020-024-00859-y

31. Halberg N, Khan T, Trujillo ME, Wernstedt-Asterholm I, Attie AD, Sherwani S, et al. Hypoxia-inducible factor 1α induces fibrosis and insulin resistance in white adipose tissue. *Mol Cell Biol*. (2009) 29:4467–83. doi: 10.1128/MCB.00192-09

32. Cheng HL, Bryant C, Cook R, O'Connor H, Rooney K, Steinbeck K. The relationship between obesity and hypoferraemia in adults: a systematic review. *Obes Rev*. (2012) 13:150–61. doi: 10.1111/j.1467-789X.2011.00938.x

33. Qiu F, Wu L, Yang G, Zhang C, Liu X, Sun X, et al. The role of iron metabolism in chronic diseases related to obesity. *Mol Med*. (2022) 28:130. doi: 10.1186/s10020-022-00558-6

34. Ganz T, Nemeth E. Iron homeostasis in host defence and inflammation. *Nat Rev Immunol*. (2015) 15:500–10. doi: 10.1038/nri3863

35. Weiss G, Ganz T, Goodnough LT. Anemia of inflammation. *Blood*. (2019) 133:40–50. doi: 10.1182/blood-2018-06-856500

36. Sharma N, Laftah AH, Brookes MJ, Cooper B, Iqbal T, Tselepis C. A role for tumour necrosis factor α in human small bowel iron transport. *Biochem J*. (2005) 390:437–46. doi: 10.1042/BJ20050256

37. Frazer DM, Anderson GJ. The regulation of iron transport. *Biofactors*. (2014) 40:206–14. doi: 10.1002/biof.1148

38. Wang M, Chen Z, Zhang Y. Serum iron levels, dietary iron intake, and supplement use in relation to metabolic syndrome in adolescents: a cross-sectional study. *Biol Trace Elem Res*. (2025) 203:39–47. doi: 10.1007/s12011-024-04152-1

39. Zou Y, Huang L, Zhao D, He M, Han D, Su D, et al. Food and nutrient intake in children and adolescents with or without overweight/obesity. *Nutrients*. (2023) 15:4450. doi: 10.3390/nu15204450

40. World Health Organization. Vitamin and mineral requirements in human nutrition, 2nd edition. (2004). Available online at: https://www.who.int/publications/i/item/9241546123 (accessed April 7, 2025).

41. Lipschitz DA, Cook JD, Finch CA. A clinical evaluation of serum ferritin as an index of iron stores. *N Engl J Med*. (1974) 290:1213–6. doi: 10.1056/NEJM197405302902201

42. Lorcerie B, Audia S, Samson M, Millière A, Falvo N, Leguy-Seguin V, et al. Diagnosis of hyperferritinemia in routine clinical practice. *Presse Med*. (2017) 46:e329–38. doi: 10.1016/j.lpm.2017.09.028

43. Garcia-Casal MN, Pasricha SR, Martinez RX, Lopez-Perez L, Peña-Rosas JP. Are current serum and plasma ferritin cut-offs for iron deficiency and overload accurate and reflecting iron status? A systematic review. *Arch Med Res*. (2018) 49:405–17. doi: 10.1016/j.arcmed.2018.12.005

44. Kernan KF, Carcillo JA. Hyperferritinemia and inflammation. *Int Immunol*. (2017) 29:401–9. doi: 10.1093/intimm/dxx031

45. Rubino F, Cummings DE, Eckel RH, Cohen RV, Wilding JPH, Brown WA, et al. Definition and diagnostic criteria of clinical obesity. *Lancet Diabetes Endocrinol*. (2025) 13:221–62. doi: 10.1016/S2213-8587(24)00316-4

frontiers | Frontiers in Oncology

TYPE Original Research
PUBLISHED 04 November 2025
DOI 10.3389/fonc.2025.1614092

OPEN ACCESS

EDITED BY
Qingyu Wang,
Capital Medical University, China

REVIEWED BY
Yao Wei Zhang,
Southern Medical University, China
Ramkumar Katturajan,
Purdue University Indianapolis, United States

*CORRESPONDENCE
Youngwan Kim
youngwkim@yonsei.ac.kr

†These authors have contributed equally to this work

RECEIVED 18 April 2025
ACCEPTED 22 October 2025
PUBLISHED 04 November 2025

CITATION
An S, Kwon HY, Kim K, Kim S-K, Kim CS, Kim B, Do H and Kim Y (2025) Low expression of SOD and PRX4 as indicators of poor prognosis and systemic inflammation in colorectal cancer. *Front. Oncol.* 15:1614092. doi: 10.3389/fonc.2025.1614092

Low expression of SOD and PRX4 as indicators of poor prognosis and systemic inflammation in colorectal cancer

Sanghyun An[1,2†], Hye Youn Kwon[1,2†], Kwangmin Kim[1,2,3], Soo-Ki Kim[4], Cheol Su Kim[4], Bora Kim[5], Hyejin Do[6] and Youngwan Kim[1,2,7*]

[1]Department of Surgery, Yonsei University Wonju College of Medicine, Wonju, Republic of Korea, [2]Wonju Surgical Research Collaboration, Wonju, Republic of Korea, [3]Health Check-up Center, Wonju Severance Christian Hospital, Wonju, Republic of Korea, [4]Department of Microbiology, Yonsei University Wonju College of Medicine, South, Wonju, Republic of Korea, [5]Department of Internal Medicine, Yonsei University Wonju College of Medicine, Wonju, Republic of Korea, [6]Department of Anesthesiology, Chungju Medical Center, Chungju, Republic of Korea, [7]Graduate Medical Education, BayCare Health System, Riverview, FL, United States

Objectives: Oxidative stress, characterized by an imbalance between the levels of reactive oxygen species (ROS) and antioxidants, plays a critical role in cancer progression. However, the prognostic significance of antioxidant markers in colorectal cancer (CRC) remains unclear. This study aimed to evaluate the expression of antioxidant markers in tumor tissues and investigate their association with clinicopathological features, survival, and systemic inflammation.
Methods: We retrospectively analyzed 70 patients with CRC who underwent curative surgical resection. The tissue levels of superoxide dismutase (SOD), glutathione peroxidase (GPx), peroxiredoxin 4 (PRX4), and thioredoxin (Trx) were measured in freshly frozen tissues, and the patients were classified into high and low expression groups using the 1st quartile as the cutoff. Associations between antioxidant levels in tumor tissue using ELISA and clinicopathological characteristics, laboratory inflammatory markers, and survival outcomes were analyzed.
Results: Low SOD expression was significantly associated with a higher incidence of distant metastases. Similarly, low PRX4 expression was correlated with more aggressive tumor characteristics, including higher rates of distant metastasis, poor differentiation, and advanced T4 stage. Moreover, low PRX4 levels were linked to systemic inflammation, as reflected by increased neutrophil counts and neutrophil-lymphocyte ratio. Although not statistically significant, the low SOD and PRX4 groups exhibited worse 5-year disease-free survival.

Conclusions: Low SOD and PRX4 expression was associated with aggressive tumor features, poor survival, and heightened systemic inflammation in patients with CRC. Given their association with tumor aggressiveness and systemic inflammation, antioxidant markers such as SOD and PRX4 may serve as supportive prognostic biomarkers to help identify patients at risk of adverse clinical outcomes in CRC.

KEYWORDS

colorectal neoplasms, antioxidants, biomarkers, oxidative stress, prognosis

1 Introduction

Colorectal cancer (CRC) is the third most commonly diagnosed cancer and a leading cause of cancer-related deaths worldwide (1). Advances in surgical techniques, chemotherapy, radiotherapy, targeted therapy, and immunotherapy have significantly improved treatment outcomes. The development of these treatment strategies has significantly improved the overall survival (OS) of patients with CRC. However, the survival rate for advanced-stage CRC remains poor, with the global OS rate for stage IV metastatic CRC reported to be only 12% (2) and the overall recurrence rate of CRC reported to be 25% (3). These facts highlight the need for further investigation into factors influencing prognosis, disease progression, and novel treatments.

Oxidative stress, which is characterized by an imbalance between the levels of reactive oxygen species (ROS) and antioxidants, has been implicated in cancer development and progression (4–8). Antioxidants, including enzymatic systems such as superoxide dismutase (SOD) and catalase, and non-enzymatic molecules such as glutathione, are essential for neutralizing ROS, preserving cellular redox balance, and maintaining homeostasis (4, 9). Previous studies have suggested that specific antioxidants may be associated with CRC development and progression (10, 11).

Detoxification of ROS operates through a hierarchical system of antioxidant enzymes, each contributing at distinct stages to mitigate oxidative stress. SOD serves as the first line of defense by converting superoxide anions into hydrogen peroxide, which is subsequently neutralized by downstream enzymes such as glutathione peroxidase (GPx) or peroxiredoxins (PRX) to prevent cellular damage. Thioredoxin (Trx) plays a crucial role in this hierarchy by restoring the activity of oxidized antioxidants and ensuring that the system remains functional and efficient. Together, these enzymes maintain the redox balance and influence critical cellular processes, including proliferation, apoptosis, and metabolism, which are pivotal in cancer development (12). Despite their critical roles, comprehensive research investigating antioxidant levels in CRC tissues, particularly in relation to clinicopathological features, hematological markers, and prognosis, remains limited.

Based on these observations, we hypothesized that lower antioxidant levels lead to increased oxidative stress, contributing to more aggressive tumor features in CRC. The aim of this study was to explore the expression of antioxidant markers in fresh surgical specimens from patients with CRC and investigate the association between their expression levels and clinicopathological features, survival, and serological inflammatory markers. These findings can provide insights into their potential as prognostic biomarkers.

2 Methods

2.1 Population

We enrolled individuals diagnosed with stage I–III CRC according to the American Joint Committee on Cancer (AJCC) guidelines who underwent curative surgical resection between December 2013 and December 2017. To minimize potential sources of bias, we included consecutive patients who underwent curative resection for CRC during the study period and applied consistent inclusion and exclusion criteria. Patients who underwent palliative bypass surgery without radical resection, those with cancers in other organs, and those with a previous history of CRC were excluded. This study was approved by the Institutional Review Board of Wonju Severance Christian Hospital (approval number: CR:319147), and written informed consent was obtained from all participants. This study was conducted in accordance with the ethical principles of the Declaration of Helsinki. Clinical data were analyzed retrospectively using de-identified records; no direct identifiers were accessible to the investigators. The design, conduct, and reporting of this study adhered to the STROBE (Strengthening the Reporting of Observational Studies in Epidemiology) guidelines for observational studies and the REMARK (Reporting Recommendations for Tumor Marker Prognostic Studies) guidelines for biomarker research.

2.2 Data collection: clinicopathological data

Patients' clinical information, including age, sex, medical history, classification recommended by the American Society of Anesthesiologists (ASA), tumor location, tumor markers, pathologic information, and laboratory findings, were obtained from medical records. We defined well-differentiated and moderately differentiated tumors as having favorable differentiation and poorly differentiated and mucinous-type tumors as having poor differentiation. Disease-free survival (DFS) was defined as the period from the date of the index surgery to the date of tumor recurrence or death. OS was defined as the period from the date of index surgery to the date of death. Patient survival data were obtained from the colorectal cancer databases of Wonju Severance Christian Hospital and the Korean National Cancer Center.

2.3 Tissue sample preparation

Tumor and normal tissues were harvested and placed in ice-cold RIPA buffer (Pierce Biotechnology Inc., IL, U.S.A.) containing protease inhibitor cocktails (Sigma Chemical Co., St Louis, U.S.A.). The tissues were homogenized at 14000 rpm for 10 min and centrifuged for 5 min, and the supernatant was collected and stored at −80°C until further analysis.

2.4 Antioxidant assays

Levels of antioxidants, such as SOD, GPx, PRX, and Trx, in tumor and non-tumor tissues were measured according to the manufacturer's instructions. The levels of SOD and GPx in colon tumor and non-tumor lysates were measured using colorimetric methods with a Biovision kit (Milpitas, CA, USA), and the Trx level was measured using a fluorescent assay kit (Cayman Chemical Company, Ann Arbor, MI, USA). Protein concentrations were normalized using a Pierce BCA Assay Kit (Thermo Scientific, Rockford, IL, U.S.A.). Each antioxidant assay followed a preparation of standards and reaction processes. The absorbance to determine the concentration was read at the following wavelengths: SOD (450 nm), GPx (340 nm), and Trx (412 nm), using a SpectraMax ABS and ABS Plus Microplate Reader (Molecular Devices LLC, California, United States). An enzyme-linked immunosorbent assay specific for human cytokines was performed to determine the concentrations of peroxidase 4 (PRX4) (AbFrontier, Seoul, South Korea) in colon tumor and non-tumor tissues, according to the manufacturer's instructions. In brief, the standard stocks were serially diluted, and 100 uL final volumes of standards and samples were added to a 96-well plate. The plates were sealed, incubated, and washed with the washing buffer. The detection antibody was added (100 μL) to each well, and the plate was covered with a new adhesive strip and incubated at room temperature. After incubation and washing, streptavidin-HRP was added to each well (100 μL). Incubation was terminated after 20 min at room temperature, and the plates were kept away from direct light. A substrate solution was added to each well, and color development was terminated using the stop solution. The absorbance was read at 450 nm using a spectrophotometer.

2.5 Statistical analysis

We defined the 1st quartile value of each antioxidant marker as the cutoff value and classified patients into high- and low-expression groups. Cases with missing data for specific variables were excluded from the corresponding analyses. Differences in the clinicopathological features between the two groups were analyzed. Categorical variables were analyzed using the chi-square test and presented as frequencies and percentages. The Fisher exact test was performed if the frequency of the data was <5. The normality of all continuous data was tested using the Shapiro–Wilk test. Continuous variables were analyzed using the Student t-test and expressed as mean values and standard deviations. Non-normally distributed data were analyzed using the Mann–Whitney U test and are presented as medians and interquartile ranges. The Wilcoxon signed-rank test was performed to compare antioxidant levels between normal and tumor tissues for each patient. Survival analysis was performed using the Kaplan–Meier curve with a log-rank test. Cox proportional hazards regression model was performed to identify prognostic factors associated with DFS and OS. Variables with a p-value < 0.20 in univariate analysis were included in the multivariate model to adjust for potential confounders. Hazard ratios (HRs) and corresponding 95% confidence intervals (CIs) were calculated for each variable. All statistical analyses were performed using the R software (version 4.2.2; R Foundation for Statistical Computing, Vienna, Austria). Statistical significance was set at $p < 0.05$.

3 Results

3.1 Patient characteristics

Seventy patients were included, including 38 (54.3%) men, and the mean age was 69.6 years. The tumor was located in the right colon in 19 patients (27.1%); left colon, 27 (38.6%); and, rectum, 24 patients (34.3%). Fifty-five (78.6%) patients underwent minimally invasive surgery. Stage III and IV disease was observed in 31 (44.3%) and 13 patients (18.6%), respectively. Postoperative chemotherapy was administered to 46 patients (65.7%), whereas radiation therapy was administered to only 1 patient (1.4%). The median follow-up period was 59.5 months. During the follow-up period, tumor recurrence occurred in 17 patients (24.3%), and 5 patients (7.1%) died. Detailed patient characteristics are summarized in Table 1.

10.3389/fonc.2025.1614092

TABLE 1 Baseline characteristics.

Variable	Number of patients (n=70)	Percentage (%)
Age, mean ± SD	69.6 ± 10.8	
Gender		
Male	38	54.3
Female	32	45.7
Body mass index, mean ± SD	23.4 ± 3.5	
ASA score		
II	35	50.0
III	35	50.0
Medical history		
None	19	27.1
One	18	25.7
Two or more	33	47.1
Tumor location		
Right	19	27.1
Left	27	38.6
Rectum	24	34.3
CEA, median [IQR]	3.1 [2.0; 9.1]	
Operation method		
Open	15	21.4
MIS	55	78.6
T stage		
Tis	1	1.4
3	53	75.7
4	16	22.9
N stage		
0	28	40.0
1	28	40.0
2	14	20.0
M stage		
0	57	81.4
1	13	18.6
TNM stage		
0	1	1.4
2	25	35.7
3	31	44.3
4	13	18.6
TNM stage		
Metastatic lymph node, mean ± SD	2.2 ± 3.6	
Harvested lymph node, mean ± SD	24.8 ± 11.1	
Tumor differentiation		
Well-differentiated	13	18.8
Moderately differentiated	53	76.8
Poorly differentiated	1	1.4
Mucinous adenocarcinoma	2	2.9
Tumor size (cm), median [IQR]	4.5 [3.5; 6.0]	
Microsatellite status		
MSS	63	94.0
MSI-H	4	6.0
Chemotherapy		
No	24	34.3
Yes	46	65.7
Radiotherapy		
No	69	98.6
Yes	1	1.4
Recurrence		
No	42	60.0
Yes	17	24.3
Death		
No	45	64.3
Yes	5	7.1

SD, standard deviation; ASA, American Society of Anesthesiologists; CEA, carcinoembryonic antigen; IQR, interquartile range; MIS, minimally invasive surgery.

3.2 Antioxidant markers and their relationships with clinicopathologic features

Figure 1 shows the antioxidant levels detected in tumor tissue. The associations between each marker and the clinicopathological features are shown in Table 2.

3.2.1 SOD

The cutoff value for SOD was 54.81 (U/mL). Accordingly, 51 and 19 patients were classified into the high- and low expression

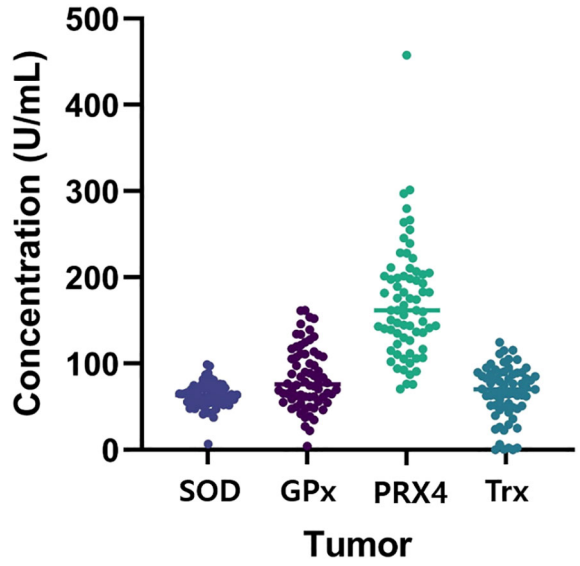

FIGURE 1
Antioxidant levels in tumor tissue.

groups, respectively. The baseline demographics did not differ significantly between the groups. Distant metastasis occurred in 36.8% of the low-SOD group compared with 11.8% of the high-SOD group (36.8% vs. 11.8%, p = 0.04).

3.2.2 GPx

The cut-off value for GPx was 65.89 (U/mL). Based on this value, 52 and 18 patients were categorized into the high- and low-expression groups, respectively. The baseline demographics did not differ significantly between the groups. However, KRAS mutations were identified in 50.0% of the high-GPx group compared with 17.6% of the low-GPx group (50.0% vs. 17.6%, p = 0.03).

3.2.3 PRX4

The cutoff value for PRX4 was 127.80 (U/mL). Accordingly, 52 and 18 patients were categorized into the high- and low-expression groups, respectively. The low-PRX4 group had a significantly higher proportion of T4 stage tumors (50.0% vs. 13.5%, p = 0.004), distant metastases (38.9% vs. 11.5%, p = 0.026), and poorly differentiated tumors (16.7% vs. 0%, p = 0.021) compared to high-PRX4 group. These findings indicate that reduced PRX4 expression may reflect a more malignant tumor biology.

3.2.4 Trx

The cutoff value for Trx was 39.08 (U/mL). Among the study population, 50 and 17 patients were in the high-and low-expression groups, respectively. There were no significant associations between Trx expression and the clinicopathological features.

3.3 Antioxidant markers and laboratory findings

Among the four antioxidant markers, PRX4 was significantly associated with hematological markers. Neutrophil count and neutrophil-lymphocyte ratio (NLR), both reflective of systemic inflammation, were significantly higher in the low-PRX4 group than those in the high-expression group (neutrophil count: 5.6 vs. 4.3, p = 0.027; NLR: 4.3 vs. 2.6, p = 0.003). No significant differences in laboratory findings were observed for the other antioxidant markers (Table 3).

3.4 The relationship between antioxidant markers and long-term prognosis

In the 5-year DFS analysis of SOD, no significant differences were observed between the high and low expression groups (76.8% vs. 63.3%, p = 0.48). Similarly, no significant differences in the 5-year OS were found between the groups (93.4% vs. 88.8%, p = 0.51). For PRX4, the low expression group showed a poorer 5-year DFS rate than the high expression group (54.1% vs. 79.3%), although this difference was not statistically significant (p = 0.11). Similarly, no significant differences were observed in the 5-year OS rates between the high- and low-PRX4 expression groups (94.4% vs. 91.4%, p = 0.48) (Figure 2). In the Cox regression analyses, CEA and poor tumor differentiation were identified as independent predictors of worse DFS (CEA: HR, 2.94; 95% CI, 1.02–8.51; p = 0.046; differentiation: HR, 14.71; 95% CI, 1.75–124.01; p = 0.013) (Table 4). For OS, poor differentiation remained the only significant prognostic factor (HR, 24.01; 95% CI, 1.50–384.9; p = 0.025). Antioxidant markers such as SOD and PRX4 showed no independent prognostic impact on DFS or OS in the multivariate models (Table 5).

4 Discussion

In line with our hypothesis, low antioxidant levels were associated with poor clinicopathological features, survival, and serological inflammatory markers in CRC. Low SOD expression was linked to a higher incidence of distant metastases. Similarly, low PRX4 expression was associated with more aggressive tumor characteristics, including a higher incidence of distant metastasis, poor differentiation, and advanced T4 stage. However, regarding survival outcomes, although Kaplan–Meier curves suggested a trend toward poorer 5-year DFS in the low SOD and PRX4 expression groups, Cox regression analysis did not confirm an independent association between these markers and survival outcomes. Additionally, the low PRX4 group showed elevated neutrophil

10.3389/fonc.2025.1614092

TABLE 2 Correlation of antioxidants with clinicopathologic features.

Variable	SOD			GPx			PRX4			Trx		
	Low (19)	High (51)	p	Low (n=18)	High (52)	p	Low (18)	High (52)	p	Low (17)	High (50)	p
Age	66.1 ± 13.3	71.0 ± 9.5	0.09	69.8 ± 11.6	69.6 ± 10.6	0.95	65.6 ± 14.6	71.1 ± 8.8	0.15	69.5 ± 13.0	69.5 ± 10.2	1.00
Gender			0.24			0.49			1.00			0.53
F	6 (31.6%)	26 (51.0%)		10 (55.6%)	22 (42.3%)		8 (44.4%)	24 (46.2%)		6 (35.3%)	24 (48.0%)	
M	13 (68.4%)	25 (49.0%)		8 (44.4%)	30 (57.7%)		10 (55.6%)	28 (53.8%)		11 (64.7%)	26 (52.0%)	
BMI	22.5 ± 4.0	23.7 ± 3.3	0.19	23.6 ± 3.6	23.3 ± 3.5	0.74	22.8 ± 4.2	23.6 ± 3.3	0.39	24.0 ± 3.8	23.1 ± 3.5	0.37
ASA classification			0.59			0.41			0.41			0.94
II	8 (42.1%)	27 (52.9%)		11 (61.1%)	24 (46.2%)		7 (38.9%)	28 (53.8%)		9 (52.9%)	24 (48.0%)	
III	11 (57.9%)	24 (47.1%)		7 (38.9%)	28 (53.8%)		11 (61.1%)	24 (46.2%)		8 (47.1%)	26 (52.0%)	
Medical History			0.57			0.50			0.32			0.57
none	6 (31.6%)	13 (25.5%)		3 (16.7%)	16 (30.8%)		7 (38.9%)	12 (23.1%)		6 (35.3%)	13 (26.0%)	
one	6 (31.6%)	12 (23.5%)		5 (27.8%)	13 (25.0%)		5 (27.8%)	13 (25.0%)		3 (17.6%)	15 (30.0%)	
≥2	7 (36.8%)	26 (51.0%)		10 (55.6%)	23 (44.2%)		6 (33.3%)	27 (51.9%)		8 (47.1%)	22 (44.0%)	
Tumor Location			0.27			1.00			0.77			0.35
Rt.	3 (15.8%)	16 (31.4%)		5 (27.8%)	14 (26.9%)		6 (33.3%)	13 (25.0%)		4 (23.5%)	15 (30.0%)	
Lt.	10 (52.6%)	17 (33.3%)		7 (38.9%)	20 (38.5%)		6 (33.3%)	21 (40.4%)		5 (29.4%)	21 (42.0%)	
Rectum	6 (31.6%)	18 (35.3%)		6 (33.3%)	18 (34.6%)		6 (33.3%)	18 (34.6%)		8 (47.1%)	14 (28.0%)	
CEA	3.8 [2.0;19.6]	2.7 [2.0; 7.5]	0.52	2.3 [2.0; 4.5]	3.8 [2.0;12.9]	0.13	3.4 [2.0;16.6]	2.9 [2.0; 7.1]	0.68	2.3 [2.0; 4.2]	3.9 [2.0; 9.1]	0.33
T stage			0.49			0.31			0.01			0.05
Tis	0 (0%)	1 (2%)		0 (0%)	1 (1.9%)		0 (0%)	1 (1.9%)		1 (5.9%)	0 (0%)	
3	13 (68.4%)	41 (78.4%)		16 (88.9%)	37 (71.2%)		9 (50.0%)	45 (86.5%)		16 (88.2%)	36 (72.0%)	
4	6 (31.6%)	10 (19.6%)		2 (11.1%)	14 (26.9%)		9 (50.0%)	7 (13.5%)		1 (5.9%)	14 (28.0%)	
N stage			0.95			0.20			0.60			0.54
0	7 (36.8%)	21 (41.2%)		8 (44.4%)	20 (38.5%)		6 (33.3%)	22 (42.3%)		9 (52.9%)	19 (38.0%)	
1	8 (42.1%)	20 (39.2%)		9 (50.0%)	19 (36.5%)		7 (38.9%)	21 (40.4%)		5 (29.4%)	21 (42.0%)	
2	4 (21.1%)	10 (19.6%)		1 (5.6%)	13 (25.0%)		5 (27.8%)	9 (17.3%)		3 (17.6%)	10 (20.0%)	
M stage			0.04			1.00			0.03			1.00
0	12 (63.2%)	45 (88.2%)		15 (83.3%)	42 (80.8%)		11 (61.1%)	46 (88.5%)		14 (82.4%)	40 (80.0%)	
1	7 (36.8%)	6 (11.8%)		3 (16.7%)	10 (19.2%)		7 (38.9%)	6 (11.5%)		3 (17.6%)	10 (20.0%)	
TNM Stage			0.11			0.89			0.08			0.35
0	0 (0.0%)	1 (2.0%)		0 (0.0%)	1 (1.9%)		0 (0.0%)	1 (1.9%)		1 (5.9%)	0 (0.0%)	
2	6 (31.6%)	19 (37.3%)		6 (33.3%)	19 (36.5%)		5 (27.8%)	20 (38.5%)		7 (41.2%)	18 (36.0%)	
3	6 (31.6%)	25 (49.0%)		9 (50.0%)	22 (42.3%)		6 (33.3%)	25 (48.1%)		6 (35.3%)	22 (44.0%)	
4	7 (36.8%)	6 (11.8%)		3 (16.7%)	10 (19.2%)		7 (38.9%)	6 (11.5%)		3 (17.6%)	10 (20.0%)	
Metastatic LNs	1.0 [0.0; 3.0]	1.0 [0.0; 3.0]	0.8	0.5 [0.0; 2.0]	1.0 [0.0; 3.5]	0.41	1.5 [0.0; 4.0]	1.0 [0.0; 3.0]	0.44	0.0 [0.0; 3.0]	1.0 [0.0; 3.0]	0.56
Harvested LNs	24.0 [19.0;29.0]	24.0 [16.5;30.0]	0.71	24.0 [19.0;32.0]	24.0 [16.5;30.0]	0.53	23.5 [19.0;26.0]	25.0 [17.0;31.0]	0.24	21.0 [14.0;26.0]	24.5 [18.0;33.0]	0.09
Differentiation			1.00			1.00			0.02			0.75

(Continued)

TABLE 2 Continued

Variable	SOD			GPx			PRX4			Trx		
	Low (19)	High (51)	p	Low (n=18)	High (52)	p	Low (18)	High (52)	p	Low (17)	High (50)	p
Good (wd/md)	18 (94.7%)	48 (96.0%)		17 (94.4%)	49 (96.1%)		15 (83.3%)	51 (100.0%)		16 (100.0%)	47 (94.0%)	
Poor (pd/ mucinous)	1 (5.3%)	2 (4.0%)		1 (5.6%)	2 (3.9%)		3 (16.7%)	0 (0.0%)		0 (0.0%)	3 (6.0%)	
Tumor size	5.3 [4.5; 6.1]	4.5 [3.2; 5.6]	0.14	4.5 [3.2; 6.5]	4.5 [4.0; 6.0]	0.85	4.8 [4.5; 6.2]	4.5 [3.1; 6.0]	0.40	4.6 [4.5; 5.5]	4.8 [3.2; 6.0]	0.80
Lymphatic invasion			0.24			0.34			0.21			0.72
0	13 (68.4%)	25 (49.0%)		12 (66.7%)	26 (50.0%)		7 (38.9%)	31 (59.6%)		8 (47.1%)	28 (56.0%)	
1	6 (31.6%)	26 (51.0%)		6 (33.3%)	26 (50.0%)		11 (61.1%)	21 (40.4%)		9 (52.9%)	22 (44.0%)	
Venous invasion			1			0.78			0.12			0.24
0	17 (89.5%)	46 (90.2%)		17 (94.4%)	46 (88.5%)		14 (77.8%)	49 (94.2%)		17 (100.0%)	43 (86.0%)	
1	2 (10.5%)	5 (9.8%)		1 (5.6%)	6 (11.5%)		4 (22.2%)	3 (5.8%)		0 (0.0%)	7 (14.0%)	
Perineural invasion			0.52			1.00			0.83			1.00
0	12 (63.2%)	38 (74.5%)		13 (72.2%)	37 (71.2%)		12 (66.7%)	38 (73.1%)		12 (70.6%)	37 (74.0%)	
1	7 (36.8%)	13 (25.5%)		5 (27.8%)	15 (28.8%)		6 (33.3%)	14 (26.9%)		5 (29.4%)	13 (26.0%)	
Microsatellite status			0.5			1.00			0.08			1.00
MSS	18 (100.0%)	45 (91.8%)		16 (94.1%)	47 (94.0%)		14 (82.4%)	49 (98.0%)		15 (93.8%)	45 (93.8%)	
MSI-H	0 (0.0%)	4 (8.2%)		1 (5.9%)	3 (6.0%)		3 (17.6%)	1 (2.0%)		1 (6.2%)	3 (6.2%)	
KRAS			0.26			0.04			0.49			0.73
Wild	13 (72.2%)	26 (53.1%)		14 (82.4%)	25 (50.0%)		11 (68.8%)	28 (54.9%)		9 (52.9%)	29 (61.7%)	
Mutant	5 (27.8%)	23 (46.9%)		3 (17.6%)	25 (50.0%)		5 (31.2%)	23 (45.1%)		8 (47.1%)	18 (38.3%)	
NRAS			1			1.00			1.00			1.00
Wild	12 (100.0%)	35 (94.6%)		10 (100.0%)	37 (94.9%)		9 (100.0%)	38 (95.0%)		11 (100.0%)	34 (94.4%)	
Mutant	0 (0.0%)	2 (5.4%)		0 (0.0%)	2 (5.1%)		0 (0.0%)	2 (5.0%)		0 (0.0%)	2 (5.6%)	
BRAF			0.66			1.00			1.00			1.00
Wild	18 (100.0%)	44 (93.6%)		16 (94.1%)	46 (95.8%)		15 (93.8%)	47 (95.9%)		16 (94.1%)	44 (97.8%)	
Mutant	0 (0.0%)	3 (6.4%)		1 (5.9%)	2 (4.2%)		1 (6.2%)	2 (4.1%)		1 (5.9%)	1 (2.2%)	
Chemotherapy			0.58			0.70			1.00			0.16
None	8 (42.1%)	16 (31.4%)		5 (27.8%)	19 (36.5%)		6 (33.3%)	18 (34.6%)		9 (52.9%)	15 (30.0%)	
Done	11 (57.9%)	35 (68.6%)		13 (72.2%)	33 (63.5%)		12 (66.7%)	34 (65.4%)		8 (47.1%)	35 (70.0%)	
Radiotherapy			1			0.58			1.00			1.00
None	19 (100.0%)	50 (98.0%)		17 (94.4%)	52 (100.0%)		18 (100.0%)	51 (98.1%)		17 (100.0%)	49 (98.0%)	
Done	0 (0.0%)	1 (2.0%)		1 (5.6%)	0 (0.0%)		0 (0.0%)	1 (1.9%)		0 (0.0%)	1 (2.0%)	

GPx, glutathione peroxidase; SOD, superoxide dismutase; Trx, thioredoxin; PRX4, peroxiredoxin 4; BMI, body mass index; ASA, American Society of Anesthesiologists; CEA, carcinoembryonic antigen; LNs, lymph node; WD, well-differentiated; MD, moderately differentiated; PD, poorly differentiated; MSS, microsatellite stable; MSI, microsatellite instability; MSI-H, microsatellite instability-high; KRAS, Kirsten rat sarcoma viral oncogene homolog; NRAS, Neuroblastoma RAS viral oncogene homolog; BRAF, B-Raf proto-oncogene, serine/threonine kinase.

counts and NLR, indicating a potential link between antioxidant depletion and the inflammatory tumor microenvironment.

SOD, a key enzymatic antioxidant, has been well-documented for its role in neutralizing ROS and maintaining cellular homeostasis. In our study, low SOD expression was associated with a higher rate of distant metastasis, supporting the hypothesis that reduced antioxidant defense contributes to cancer progression. This finding is consistent with previous studies showing that SOD dysregulation promotes oxidative stress, thereby facilitating the metastasis of various cancers. A study analyzing SOD levels in

10.3389/fonc.2025.1614092

TABLE 3 Correlation of antioxidants with laboratory features.

Variable	SOD			GPx			PRX4			Trx		
	Low (19)	High (51)	p	Low (n=18)	High (52)	p	Low (18)	High (52)	p	Low (17)	High (50)	p
WBC	7.5 [6.0; 9.4]	6.6 [5.7; 8.7]	0.23	7.1 [5.9;10.8]	6.9 [5.6; 9.1]	0.51	7.5 [6.4; 9.4]	6.6 [5.2; 9.1]	0.13	7.6 [6.9;10.1]	6.6 [5.5; 9.1]	0.07
Hb	11.9 [10.1;13.5]	12.4 [10.2;13.6]	0.88	12.6 [10.0;13.3]	12.1 [10.2;13.8]	0.93	11.8 [10.6;12.7]	12.4 [9.9;13.9]	0.66	12.6 [9.7;14.3]	11.8 [10.2;13.3]	0.67
PLT	294.0 [235.0;331.5]	259.0 [209.5;328.0]	0.22	269.5 [204.0;315.0]	259.0 [222.5;331.5]	0.6	253.5 [204.0;318.0]	275.5 [219.0;331.0]	0.43	259.0 [237.0;326.0]	269.5 [215.0;330.0]	0.91
Neutrophil	5.0 [3.9; 7.7]	4.7 [3.1; 6.4]	0.2	5.5 [3.1; 8.1]	4.7 [3.4; 6.0]	0.43	5.6 [4.8; 7.6]	4.3 [3.1; 6.4]	0.03	5.6 [4.6; 7.8]	4.8 [3.3; 6.8]	0.12
Lymphocyte	1.4 [1.2;1.7]	1.6 [1.1;1.9]	0.5	1.5 [1.0;1.9]	1.5 [1.2;1.9]	0.54	1.3 [1.0;1.8]	1.6 [1.3;1.9]	0.17	1.7 [1.3;1.9]	1.4 [1.1;1.8]	0.50
NLR	3.6 [2.5; 5.6]	2.8 [2.2; 4.4]	0.35	3.7 [2.1; 6.2]	2.9 [2.3; 4.3]	0.27	4.3 [3.6; 5.8]	2.6 [2.0; 4.1]	0.01	3.8 [2.6; 5.4]	3.0 [2.2; 4.5]	0.29
PLR	228.3 [153.2;268.9]	160.8 [132.7;269.7]	0.41	166.7 [131.3;335.4]	200.0 [132.7;269.1]	0.80	209.0 [149.4;270.2]	162.7 [128.9;273.6]	0.53	172.5 [140.5;263.8]	209.0 [134.7;278.0]	0.72
CRP	1.2 [0.5; 1.9]	0.4 [0.3; 1.2]	0.1	0.9 [0.3; 1.8]	0.4 [0.3; 1.5]	0.42	0.6 [0.3; 1.7]	0.7 [0.3; 1.7]	0.73	0.6 [0.3; 1.1]	0.7 [0.3; 1.8]	0.84
Albumin	3.9 [3.5;4.2]	3.8 [3.5;4.2]	0.89	3.8 [3.2;4.3]	3.9 [3.5;4.2]	0.69	3.8 [3.7;4.2]	3.9 [3.3;4.3]	0.37	4.2 [3.6;4.3]	3.8 [3.4;4.3]	0.57

GPx, glutathione peroxidase; SOD, superoxide dismutase; Trx, thioredoxin; PRX4, peroxiredoxin 4; WBC, white blood cell; Hb, hemoglobin; PLT, platelets; NLR, neutrophil-lymphocyte ratio; PLR, platelet-lymphocyte ratio; CRP, C-reactive protein.

hepatocellular carcinoma tissues reported that reduced SOD expression was associated with older age, larger tumor size, multiple tumor nodules, vascular emboli, poorer OS, and recurrence-free survival (13). In contrast, an observational study by Warsinggih et al. (14) reported that serum SOD levels in patients with CRC were elevated compared to normal reference values. Moreover, higher SOD levels were significantly associated with older age and advanced TNM stages in patients with CRC. Unlike our study, which measured antioxidant levels in tumor tissues, this study assessed antioxidant levels in blood samples. This methodological difference and timing of the measurements may account for these discrepant findings.

PRX4, a unique member of the peroxiredoxin family, is localized in the endoplasmic reticulum and plays a critical role in detoxifying hydrogen peroxide (15). Previous studies have investigated the role of PRX4 expression in tumor progression and the prognoses of various malignancies (15, 16). However, studies on PRX4 expression in CRC remain limited. A study by Yi et al. (17) analyzed PRX4 expression levels in tissue samples from 15 patients with CRC who underwent curative resection and divided the expression levels into four grades. They reported that higher levels of PRX4 expression were associated with unfavorable prognostic factors, including greater depth of invasion, lymph node metastasis, and advanced Dukes stage. In contrast, our study showed that a low PRX4 expression level is associated with aggressive tumor characteristics and increased systemic inflammation. According to the findings of Isohookana et al. (18), a study on patients with pancreatic cancer reported that low expression of peroxiredoxin in tissue samples was associated with unfavorable clinicopathologic features, including larger tumor size, nodal involvement, and poor differentiation. Similarly, another study on patients with hepatocellular carcinoma demonstrated that low PRX4 expression in tissue samples was related to increased tumor growth and invasion and reduced OS, and high PRX4 expression was found to decrease ROS levels in tumor tissue and was associated with better OS (19). However, a dual role of PRX4 was suggested in their study, which revealed that PRX4 knockdown led to a rapid increase in intracellular ROS levels, inducing cell death, and shed light on PRX4's complex role in cancer progression. Although PRX4's role is not fully understood, our findings and those of other studies suggest that PRX4 may act as a potential prognostic biomarker and therapeutic target in CRC, reflecting its complex role in tumor progression. Meanwhile, our study demonstrated that low PRX4 expression was associated with elevated inflammatory markers, including neutrophil count and NLR, reflecting an established link between oxidative stress and systemic inflammation (20). Recent research has provided deeper insights into the mechanistic link between low PRX4 expression and systemic inflammation. Specifically, PRX4 deficiency has been shown to potentiate NF-κB signaling and promote the transcription of pro-inflammatory chemokines, thereby facilitating neutrophil infiltration and amplifying inflammatory responses in affected tissues. Large-scale clinical studies further support an inverse association between circulating PRX4 levels and the risk of inflammatory disease, highlighting its potential utility as

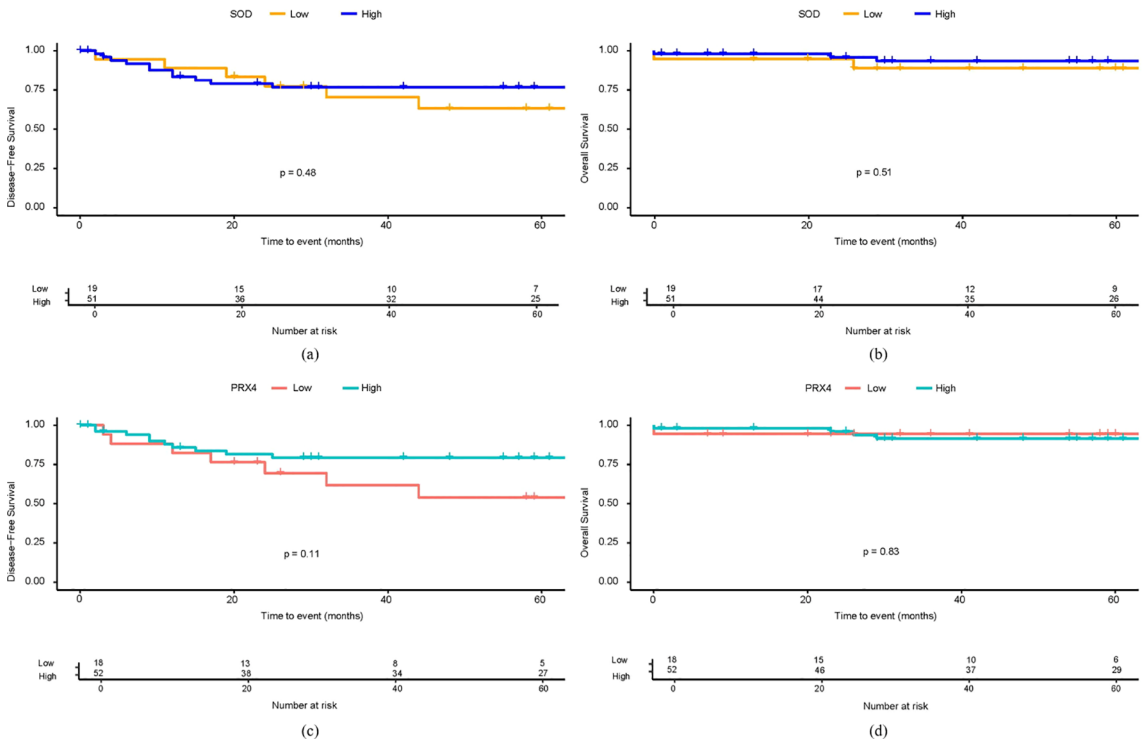

FIGURE 2
Survival analysis based on SOD and PRX4 expression levels. **(a)** 5-year DFS by SOD expression. **(b)** 5-year OS by SOD expression. **(c)** 5-year DFS by PRX4 expression. **(d)** 5-year OS by PRX4 expression.

a prognostic biomarker for systemic inflammation and adverse outcomes. These findings collectively suggest that reduced PRX4 expression may contribute to an inflammatory tumor microenvironment via the NF-κB–neutrophil axis in colorectal cancer (21, 22). However, given that tumor-associated inflammation is often chronic and multifaceted, the lack of association between other antioxidants and inflammatory markers in our study suggests that this relationship may not be directly reflected in all contexts. Further research is required to clarify the intricate interplay between antioxidants and systemic inflammation in patients with CRC.

These conflicting results on the relationship between antioxidants and tumors may be theoretically explained by the dual role of ROS in cancer. Reactive oxygen species are highly reactive molecules derived from oxygen and include superoxide anions (O_2^-), hydrogen peroxide (H_2O_2), and hydroxyl radicals (OH•). However, excess ROS levels can lead to alterations in the nuclear DNA, inducing mutations and genomic instability that promote cancer initiation. Furthermore, high ROS levels suppress the function of immune cells such as inhibitory T cells and natural killer cells, reducing the ability of the immune system to detect and eliminate early cancerous cells. Conversely, ROS can act as a double-edged sword by contributing to the elimination of cancer cells. Reactive oxygen species can inhibit cancer cell proliferation by suppressing proliferation-signaling pathways, cell cycle progression, and biosynthesis of nucleotides and ATP and by inducing cancer

TABLE 4 Cox regression analysis for DFS.

Variable	Category	Univariable HR (95% CI)	P-value	Multivariable HR (95% CI)	P-value
SOD	Low vs. High	0.70 (0.26–1.90)	0.488		
PRX4	Low vs. High	0.46 (0.18–1.21)	0.116	0.82 (0.27-2.46)	0.724
Age		1.02 (0.97–1.08)	0.359		
CEA (ng/mL)	≥5 vs. <5	4.21 (1.55–11.41)	0.005	2.94 (1.02-8.51)	0.046
Stage	III–IV vs. I–II	2.99 (1.47–6.09)	0.003	2.27 (0.62-8.28)	0.213
Differentiation	Poor vs. Well/ Moderate	37.07 (5.12–268.44)	<0.001	14.71 (1.75-124-01)	0.013
Adjuvant chemotherapy	Yes vs. No	2.22 (0.64–7.73)	0.21		

HR, hazard ratio; CI, confidence interval; SOD, superoxide dismutase; PRX4, peroxiredoxin 4; CEA, carcinoembryonic antigen.

TABLE 5 Cox regression analysis for OS.

Variable	Category	Univariate HR (95% CI)	P-value	Multivariate HR (95% CI)	P-value
SOD	Low vs. High	0.56 (0.09–3.33)	0.519	–	–
PRX4	Low vs. High	1.26 (0.14–11.30)	0.836	–	–
Age		1.03 (0.93–1.13)	0.6	–	–
CEA (ng/mL)	≥5 vs. <5	1.40 (0.23–8.40)	0.715	–	–
Stage	III–IV vs I–II	2.71 (0.30–24.28)	0.374	–	–
Differentiation	Poor vs Well/ Moderate	24.01 (1.50–384.9)	0.025	24.01 (1.50–384.9)	0.025
Adjuvant chemotherapy	Yes vs No	0.68 (0.11–4.07)	0.672	–	–

HR, hazard ratio; CI, confidence interval; SOD, superoxide dismutase; PRX4, peroxiredoxin 4; CEA, carcinoembryonic antigen.

cell death. This is achieved through the activation of stress-related pathways including endoplasmic reticulum stress, mitochondrial apoptotic pathways, p53-dependent apoptosis, and ferroptosis, a form of cell death triggered by iron-dependent lipid peroxidation (23, 24). In a similar context, antioxidants play a dual role in cancer, exhibiting both tumor-suppressive and tumor-promoting effects (25, 26). During the early stages of cancer, antioxidants mitigate ROS-induced DNA damage, protect cells from mutations, and induce genomic instability. However, during tumor progression, elevated antioxidant enzyme expression, as part of the hierarchical interaction of antioxidant systems, enables cancer cells to adapt to elevated ROS levels and promotes survival under oxidative stress. This duality reflects the complex role of antioxidants in cancer. Furthermore, differences in measurement methods and timing may have contributed to variability in the study results, highlighting the need for further research to achieve a more precise understanding of the role of antioxidants in cancer.

Given the critical roles of antioxidant systems in cancer initiation, progression, and therapeutic resistance, there has been growing interest in developing therapeutic approaches that target antioxidants (4, 27, 28). One such example is NOV-002, a glutathione disulfide mimic that modulates redox signaling; it improves response rates in patients with advanced HER2-negative breast cancer when combined with standard chemotherapy (29). Similarly, L-asparaginase, an enzyme that depletes asparagine and indirectly reduces glutathione levels, has demonstrated efficacy in treating acute lymphoblastic leukemia and advanced pancreatic cancer when used in combination with other treatments (30). These examples highlight how targeting the antioxidant system can enhance therapeutic outcomes. However, further studies are required to confirm their broader applicability. On the other hand, a randomized controlled trial of antioxidant supplements, including beta-carotene; vitamins A, C, and E; N-acetyl cysteine; and, selenium, was conducted to evaluate their cancer-preventive effects. A meta-analysis that pooled these studies reported no overall preventive effects of antioxidant supplements on cancer risk (31). Despite these efforts, robust evidence supporting the therapeutic effects of antioxidants is lacking, highlighting the need for further research to clarify their roles and potential in cancer treatment.

This study had several limitations. First, the relatively small sample size may limit the generalizability of the findings, and the retrospective nature of the analysis may have introduced a selection bias. Second, this study was conducted at a single institution, which may limit the generalizability of the findings to a broader population. Third, the study did not include all antioxidant systems, such as other key enzymes, for instance, catalase, which may also play significant roles in cancer progression and redox regulation. Additionally, this study analyzed antioxidant expression at a single time point without considering the dynamic changes in expression levels or temporal trends over the course of disease progression. Finally, this study was designed to examine associations between antioxidant marker expression and clinical prognostic factors rather than to elucidate the underlying biological mechanisms; further mechanistic studies are warranted to clarify these relationships. However, this study has some notable strengths. We utilized a well-defined cohort of patients with CRC who underwent curative resection to ensure consistency in clinical and pathological data. By directly measuring antioxidant markers in tumor and normal tissues, this study provides concrete data on how these markers are associated with cancer progression and prognosis. Furthermore, to our knowledge, this is the first study to analyze tissue-level antioxidant markers in relation to both clinical outcomes and systemic inflammation in patients with CRC.

In summary, the low expression levels of these antioxidants were associated with aggressive clinicopathological features. Furthermore, low antioxidant levels have been linked to high systemic inflammatory status, suggesting that antioxidant depletion may contribute to CRC progression through both tumor aggressiveness and inflammation, underscoring the need for further research to elucidate these mechanisms. These results highlight the potential of SOD and PRX4 as supportive biomarkers for predicting unfavorable clinical features, while further studies are warranted to establish their prognostic utility in CRC.

Data availability statement

The original contributions presented in the study are included in the article/supplementary material. Further inquiries can be directed to the corresponding author/s.

Ethics statement

The studies involving humans were approved by Institutional Review Board of Wonju Severance Christian Hospital. The studies were conducted in accordance with the local legislation and institutional requirements. The participants provided their written informed consent to participate in this study.

Author contributions

SA: Conceptualization, Methodology, Writing – review & editing, Data curation, Investigation, Validation, Formal Analysis, Writing – original draft, Software, Visualization. HK: Writing – original draft, Formal Analysis, Writing – review & editing, Data curation, Investigation, Conceptualization, Methodology, Validation. KK: Data curation, Conceptualization, Software, Visualization, Writing – review & editing, Formal Analysis. SK: Investigation, Writing – review & editing, Methodology, Validation. CK: Methodology, Validation, Investigation, Writing – review & editing. BK: Writing – review & editing, Validation, Data curation. HD: Validation, Writing – review & editing, Data curation. YK: Project administration, Data curation, Methodology, Conceptualization, Writing – original draft, Validation, Writing – review & editing, Investigation, Formal Analysis, Supervision.

Funding

The author(s) declare that no financial support was received for the research, and/or publication of this article.

Conflict of interest

The authors declare that the research was conducted in the absence of any commercial or financial relationships that could be construed as a potential conflict of interest.

Generative AI statement

The author(s) declare that no Generative AI was used in the creation of this manuscript.

Any alternative text (alt text) provided alongside figures in this article has been generated by Frontiers with the support of artificial intelligence and reasonable efforts have been made to ensure accuracy, including review by the authors wherever possible. If you identify any issues, please contact us.

Publisher's note

References

1. Siegel RL, Miller KD, Wagle NS, Jemal A. Cancer statistics, 2023. *CA Cancer J Clin*. (2023) 73:17–48. doi: 10.3322/caac.21763

2. Rawla P, Sunkara T, Barsouk A. Epidemiology of colorectal cancer: incidence, mortality, survival, and risk factors. *Prz Gastroenterol*. (2019) 14:89–103. doi: 10.5114/pg.2018.81072

3. Kunst N, Alarid-Escudero F, Aas E, Coupe VMH, Schrag D, Kuntz KM. Estimating population-based recurrence rates of colorectal cancer over time in the United States. *Cancer Epidemiol Biomarkers Prev*. (2020) 29:2710–8. doi: 10.1158/1055-9965.EPI-20-0490

4. Luo M, Zhou L, Huang Z, Li B, Nice EC, Xu J, et al. Antioxidant therapy in cancer: rationale and progress. *Antioxidants (Basel)*. (2022) 11:1128. doi: 10.3390/antiox11061128

5. Piskounova E, Agathocleous M, Murphy MM, Hu Z, Huddlestun SE, Zhao Z, et al. Oxidative stress inhibits distant metastasis by human melanoma cells. *Nature*. (2015) 527:186–91. doi: 10.1038/nature15726

6. Sayin VI, Ibrahim MX, Larsson E, Nilsson JA, Lindahl P, Bergo MO. Antioxidants accelerate lung cancer progression in mice. *Sci Transl Med*. (2014) 6:221ra15. doi: 10.1126/scitranslmed.3007653

7. Valko M, Leibfritz D, Moncol J, Cronin MT, Mazur M, Telser J. Free radicals and antioxidants in normal physiological functions and human disease. *Int J Biochem Cell Biol*. (2007) 39:44–84. doi: 10.1016/j.biocel.2006.07.001

8. Diplock AT, Charleux JL, Crozier-Willi G, Kok FJ, Rice-Evans C, Roberfroid M, et al. Functional food science and defence against reactive oxidative species. *Br J Nutr*. (1998) 80:S77–112. doi: 10.1079/bjn19980106

9. Che M, Wang R, Li X, Wang HY, Zheng XFS. Expanding roles of superoxide dismutases in cell regulation and cancer. *Drug Discov Today*. (2016) 21:143–9. doi: 10.1016/j.drudis.2015.10.001

10. Condello M, Meschini S. Role of natural antioxidant products in colorectal cancer disease: a focus on a natural compound derived from Prunus spinosa, Trigno ecotype. *Cells (Basel)*. (2021) 10:3326. doi: 10.3390/cells10123326

11. Stone WL, Krishnan K, Campbell SE, Palau VE. The role of antioxidants and pro-oxidants in colon cancer. *World J Gastrointest Oncol*. (2014) 6:55–66. doi: 10.4251/wjgo.v6.i3.55

12. Jomova K, Alomar SY, Alwasel SH, Nepovimova E, Kuca K, Valko M. Several lines of antioxidant defense against oxidative stress: antioxidant enzymes, nanomaterials with multiple enzyme-mimicking activities, and low-molecular-weight antioxidants. *Arch Toxicol*. (2024) 98:1323–67. doi: 10.1007/s00204-024-03696-4

13. Wang R, Yin C, Li XX, Yang XZ, Yang Y, Zhang MY, et al. Reduced SOD2 expression is associated with mortality of hepatocellular carcinoma patients in a mutant p53-dependent manner. *Aging (Albany NY)*. (2016) 8:1184–200. doi: 10.18632/aging.100967

14. Warsinggih, Irawan B, Labeda I, Lusikooy RE, Sampetoding S, Kusuma MI, et al. Association of superoxide dismutase enzyme with staging and grade of differentiation colorectal cancer: a cross-sectional study. *Ann Med Surg (Lond)*. (2020) 58:194–9. doi: 10.1016/j.amsu.2020.08.032

15. Thapa P, Ding N, Hao Y, Alshahrani A, Jiang H, Wei Q. Essential roles of peroxiredoxin IV in inflammation and cancer. *Molecules*. (2022) 27:6513. doi: 10.3390/molecules27196513

16. Ding N, Jiang H, Thapa P, Hao Y, Alshahrani A, Allison D, et al. Peroxiredoxin IV plays a critical role in cancer cell growth and radioresistance through the activation of the Akt/GSK3 signaling pathways. *J Biol Chem*. (2022) 298:102123. doi: 10.1016/j.jbc.2022.102123

17. Yi N, Xiao MB, Ni WK, Jiang F, Lu CH, Ni RZ. High expression of peroxiredoxin 4 affects the survival time of colorectal cancer patients, but is not an independent unfavorable prognostic factor. *Mol Clin Oncol*. (2014) 2:767–72. doi: 10.3892/mco.2014.317

18. Isohookana J, Haapasaari KM, Soini Y, Karihtala P. Loss of peroxiredoxin expression is associated with an aggressive phenotype in pancreatic adenocarcinoma. *Anticancer Res*. (2016) 36:427–33.

19. Guo X, Noguchi H, Ishii N, Homma T, Hamada T, Hiraki T, et al. The association of peroxiredoxin 4 with the initiation and progression of hepatocellular carcinoma. *Antioxid Redox Signal*. (2019) 30:1271–84. doi: 10.1089/ars.2017.7426

20. Bhol NK, Bhanjadeo MM, Singh AK, Dash UC, Ojha RR, Majhi S, et al. The interplay between cytokines, inflammation, and antioxidants: mechanistic insights and therapeutic potentials of various antioxidants and anti-cytokine compounds. *BioMed Pharmacother*. (2024) 178:117177. doi: 10.1016/j.biopha.2024.117177

21. Geertsema S, Geertsema P, Kieneker LM, Abdulle AE, la Bastide-van Gemert S, Bakker SJL, et al. Serum peroxiredoxin-4, a biomarker of oxidative stress, associates with new-onset chronic kidney disease: a population-based cohort study. *Redox Biol*. (2024) 77:103408. doi: 10.1016/j.redox.2024.103408

22. Suthahar N, Mourmans SGJ, Achten A, Aboumsallem JP, Meijers WC, Bomer N, et al. Peroxiredoxin-4, a marker of systemic oxidative stress, is associated with incident heart failure. *Eur J Heart Fail*. (2025) 27:905–11. doi: 10.1002/ejhf.3653

23. Huang R, Chen H, Liang J, Li Y, Yang J, Luo C, et al. Dual role of reactive oxygen species and their application in cancer therapy. *J Cancer*. (2021) 12:5543–61. doi: 10.7150/jca.54699

24. Kruk J, Aboul-Enein HY. Reactive oxygen and nitrogen species in carcinogenesis: implications of oxidative stress on the progression and development of several cancer types. *Mini Rev Med Chem*. (2017) 17:904–19. doi: 10.2174/1389557517666170228115324

25. Kim YS, Gupta Vallur P, Phaeton R, Mythreye K, Hempel N. Insights into the dichotomous regulation of SOD2 in cancer. *Antioxidants (Basel)*. (2017) 6:86. doi: 10.3390/antiox6040086

26. Walton EL. The dual role of ROS, antioxidants and autophagy in cancer. *BioMed J*. (2016) 39:89–92. doi: 10.1016/j.bj.2016.05.001

27. Gu X, Mu C, Zheng R, Zhang Z, Zhang Q, Liang T. The cancer antioxidant regulation system in therapeutic resistance. *Antioxidants (Basel)*. (2024) 13:778. doi: 10.3390/antiox13070778

28. Harris IS, DeNicola GM. The complex interplay between antioxidants and ROS in cancer. *Trends Cell Biol*. (2020) 30:440–51. doi: 10.1016/j.tcb.2020.03.002

29. Montero AJ, Diaz-Montero CM, Deutsch YE, Hurley J, Koniaris LG, Rumboldt T, et al. Phase 2 study of neoadjuvant treatment with NOV-002 in combination with doxorubicin and cyclophosphamide followed by docetaxel in patients with HER-2 negative clinical stage II-IIIc breast cancer. *Breast Cancer Res Treat*. (2012) 132:215–23. doi: 10.1007/s10549-011-1889-0

30. Bachet JB, Blons H, Hammel P, Hariry IE, Portales F, Mineur L, et al. Circulating tumor DNA is prognostic and potentially predictive of eryaspase efficacy in second-line in patients with advanced pancreatic adenocarcinoma. *Clin Cancer Res*. (2020) 26:5208–16. doi: 10.1158/1078-0432.CCR-20-0950

31. Myung SK, Kim Y, Ju W, Choi HJ, Bae WK. Effects of antioxidant supplements on cancer prevention: meta-analysis of randomized controlled trials. *Ann Oncol*. (2010) 21:166–79. doi: 10.1093/annonc/mdp286

Frontiers in Nutrition

Explores what and how we eat in the context of health, sustainability and 21st century food science

A multidisciplinary journal that integrates research on dietary behavior, agronomy and 21st century food science with a focus on human health.

Discover the latest Research Topics

See more →

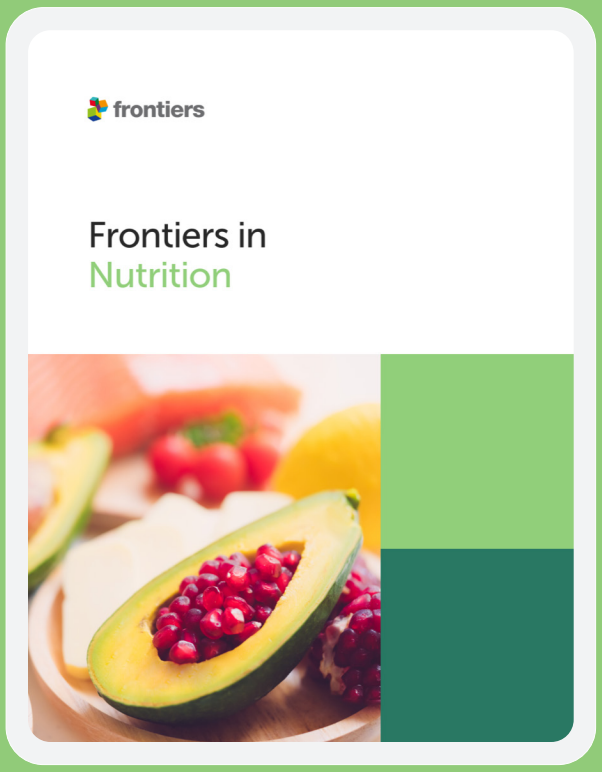

Frontiers

Avenue du Tribunal-Fédéral 34
1005 Lausanne, Switzerland
frontiersin.org

Contact us

+41 (0)21 510 17 00
frontiersin.org/about/contact